The neglected role of phytoplankton adaptation in marine ecosystem models

— *Implications for climate projections and future perspectives*

DISSERTATION
zur Erlangung des Doktorgrades
an der Fakultät für Mathematik, Informatik und Naturwissenschaften
Fachbereich Erdsystemwissenschaften
der Universität Hamburg

vorgelegt von
Isabell Hochfeld

Hamburg, 2024

Fachbereich Erdsystemwissenschaften

Datum der Disputation: 24.07.2024

Gutachter/innen der Dissertation: Prof. Dr. Inga Hense
Dr. Jana Hinners

Zusammensetzung der Prüfungskommission: Vorsitz Prof. Dr. Inga Hense
Dr. Jana Hinners
Prof. Dr. Matthias Hort
Prof. Dr. Johanna Baehr
Prof. Dr. Dirk Notz

Vorsitzender des Fach-Promotionsausschusses
Erdsystemwissenschaften: Prof. Dr. Hermann Held

Dekan der Fakultät MIN: Prof. Dr. Ing. Norbert Ritter

Acknowledgements

I would like to thank everyone who accompanied and supported me during this PhD project.

First, I want to thank Jana Hinners for all her time, support, advice, constructive feedback, and for having confidence in me during this journey. Thank you for always being there for me when I needed it, even out of working hours. I would also like to thank Milan for supporting us during our meetings :) Likewise, I am grateful to Inga Hense for giving me the opportunity to accomplish this PhD and to broaden my scientific horizon, for her help with the model design, and for her kind and warm-hearted supervision and support. The kind of comprehensive and warm-hearted supervision that I received is incredibly valuable, but hard to find. Many thanks to both of you.

Next, I would like to thank Matthias Hort for being my panel chair, for the constructive and interesting discussions we had during our panel meetings, and for his advice on my PhD project.

I would also like to thank Josefine Herrford for our mini group meetings, for our non-scientific chats in the office, and for the constrictive and helpful feedback that she gave me on parts of this thesis.

My next thanks go to the SICSS graduate school for organizing interesting workshops, retreats, and other non-scientific events. But most of all, I enjoyed meeting so many people from so many different scientific and cultural backgrounds!

Special thanks go to the other early-career scientists from the PhytoArk project, namely Alex, Juliane, and Sarah. Thank you for the nice days (and especially evenings) we had during project retreats and the Summer School, it wouldn't have been the same without you guys!

Finally, I would like to thank my friends and family. Thank you for reminding me that there is more to life than science, for protecting me from working too much, for being there for me when I needed a cheering up, and for always believing in me.

Thank you.
Isabell

ABSTRACT

Marine ecosystems fulfil functions that are vital for the global climate and human life, including the long-term storage of atmospheric carbon and food production. Despite their small size, phytoplankton are key players in marine ecosystem functioning. Phytoplankton are not only oxygen producers and the first link in the marine food chain, but also a crucial component of biogeochemical cycles and climate-relevant feedback loops. Global warming, however, leads to a rapid reorganization of phytoplankton communities, with severe consequences for ecosystem functioning. To reliably assess future changes in ecosystem functioning, we need robust approaches.

While sedimentary records and marine monitoring data provide information on the past to present state of an ecosystem, albeit on different temporal scales, laboratory and mesocosm experiments allow to study marine organisms and communities under future levels of warming. Still, experiments can neither replicate the complexity of real ecosystems nor provide realistic rates of environmental change. Ecosystem models can fill this gap and are therefore a very well-suited tool for estimating future species- to ecosystem-level changes. However, current model projections are inconsistent, which implies that the models are still neglecting crucial processes. Since model projections represent a valuable resource for political decision-making, improving their informative value is crucial. To improve model projections of future ecosystem changes, we first need to identify and implement all relevant processes, and test the models against long-term validation data afterwards. In this thesis, I evaluate the effect of a hitherto largely ignored process — phytoplankton adaptation — on simulated ecosystem dynamics and present a framework for long-term model validation.

Phytoplankton possess a high adaptive potential that can affect ecosystem responses to environmental changes on perennial time scales. To study how phytoplankton adaptation affects simulated ecosystem dynamics, I developed an innovative ecosystem model that combines competition between multiple phytoplankton functional groups and adaptation to global warming for the first time. I apply the model to the Baltic Sea, a temperate to subarctic coastal ecosystem that is impacted by above-average levels of warming. The simulations reveal that the effect of phytoplankton adaptation on the simulated ecosystem dynamics depends on environmental conditions. Under steady present-day conditions, adaptation allows for a more efficient use of resources through niche separation, which enhances primary production and associated ecosystem functions such as secondary production and carbon export. In a warming environment, on the contrary, adaptation increases the competitivity of inferior competitors, which can hence mitigate the dominance of preadapted superior competitors. Weaker dominance changes among functionally different taxa, in turn, mitigate changes in ecosystem functioning. Thus, until now, current ecosystem models may have systematically underestimated the resilience of marine communities against environmental changes, resulting in a systematic overestimation of phytoplankton and ecosystem responses to global warming.

Including evolutionary processes into ecosystem models is only the first step towards more reliable predictions of future ecosystem changes. Current predictive ecosystem models are usually developed for contemporary ecosystems and may no longer be applicable when ecosystem structure has changed in the future. Instead of being tailored to a specific ecosystem, models may represent fundamental processes so that they are equally applicable to past, present, and (by implication) future scenarios. To achieve this, we suggest testing models against major ecosystem changes in the past, which can be reconstructed from sedimentary records. Only when the same model can reproduce the current state of an ecosystem and its major changes in the past, we may have some confidence in the model's predictions of the future. Most likely, several iterations will be required to revise the model structure until the same model can reproduce both contemporary observations and validation data from the past. This process may uncover other relevant processes that have been ignored in ecosystem models so far.

This thesis demonstrates that while ecosystem models are a promising tool for assessing future ecosystem changes, there is still much room for improvement. First, I show that phytoplankton adaptation can significantly change simulated ecosystem dynamics. Second, I present a framework for the long-term validation of evolutionary ecosystem models to increase their general applicability and hence the informative value of their predictions. My work not only emphasizes the need to revise current ecosystem models, especially those relevant for political decisions, but also provides approaches for solutions.

ZUSAMMENFASSUNG

Marine Ökosysteme erfüllen Funktionen, die für das globale Klima und uns Menschen essenziell sind, zum Beispiel die Langzeitspeicherung von atmosphärischem Kohlenstoff und die Produktion von Nahrungsmitteln. Trotz ihrer geringen Größe spielen Phytoplanktonorganismen eine Schlüsselrolle für die Funktionen mariner Ökosysteme. Phytoplanktonorganismen produzieren nicht nur Sauerstoff und stellen das erste Glied der marinen Nahrungskette dar, sondern sind auch für biogeochemische Kreisläufe und klimarelevante Rückkopplungsschleifen von wesentlicher Bedeutung. Die globale Erwärmung führt allerdings zu einer raschen Umstrukturierung von Phytoplanktongemeinschaften, mit schwerwiegenden Konsequenzen für marine Ökosystemfunktionen. Es werden robuste Ansätze benötigt, um künftige Veränderungen von Ökosystemfunktionen zuverlässig abzuschätzen.

Während Sedimentkerne und Beobachtungen Informationen über den vergangenen bis gegenwärtigen Zustand eines Ökosystems liefern, wenn auch auf unterschiedlichen Zeitskalen, erlauben Labor- und Mesokosmosexperimente die Untersuchung von Meeresorganismen und -gemeinschaften unter zukünftigen Klimabedingungen. Dennoch können Experimente weder die Komplexität realer Ökosysteme noch realistische Erwärmungsraten widerspiegeln. Ökosystemmodelle können diese Wissenslücke schließen und sind daher sehr gut geeignet, um künftige Veränderungen von Spezies und Ökosystemen abzuschätzen. Die bisherigen Modellvorhersagen sind jedoch widersprüchlich, was darauf hindeutet, dass aktuelle Modelle immer noch entscheidende Prozesse vernachlässigen. Da Modellprojektionen eine wertvolle Ressource für die politische Entscheidungsfindung darstellen, ist es essenziell, ihre Aussagekraft zu verbessern. Um die Aussagekraft von Modellprojektionen zu erhöhen, müssen zunächst alle relevanten Prozesse identifiziert und implementiert werden, und anschließend müssen die Modelle mit Langzeitdaten validiert werden. In dieser Dissertation bewerte ich die Auswirkungen eines bisher größtenteils vernachlässigten Prozesses — der evolutionären Anpassung von Phytoplankton — auf simulierte Ökosystemprozesse und stelle ein Konzept für die Langzeitvalidierung von Ökosystemmodellen vor.

Phytoplanktonpopulationen besitzen ein großes Anpassungspotential, welches klimabedingte Ökosystemveränderungen auf mehrjährigen Zeitskalen beeinflussen kann. Um zu untersuchen, wie sich die Anpassung von Phytoplankton auf simulierte Ökosystemprozesse auswirkt, habe ich ein innovatives Ökosystemmodell entwickelt, das zum ersten Mal den Wettbewerb zwischen mehreren funktionellen Phytoplanktongruppen und deren Anpassung an die globale Erwärmung kombiniert. Ich wende das Modell auf die Ostsee an, ein gemäßigt bis subarktisches Küstenökosystem, welches von einer überdurchschnittlichen Erwärmung betroffen ist. Die Simulationen zeigen, dass sich die Anpassung je nach Umweltbedingungen unterschiedlich auf die simulierten Ökosystemprozesse auswirkt. Unter stabilen heutigen Bedingungen erlaubt die Anpassung eine effizientere Nutzung von Ressourcen durch Nischentrennung, was die Primärproduktion und die damit verbundenen Ökosystemfunktionen, beispielsweise die Sekundärproduktion und den Kohlenstoffexport, erhöht. Unter sich erwärmenden Bedingungen erhöht die Anpassung dagegen die Wettbe-

werbsfähigkeit von unterlegenen Konkurrenten, welche folglich die Dominanz von vorangepassten überlegenen Konkurrenten abschwächen können. Geringere Dominanzverschiebungen zwischen funktionell unterschiedlichen Taxa reduzieren wiederum Veränderungen der Ökosystemfunktionen. Folglich könnten bisherige Ökosystemmodelle die Widerstandsfähigkeit von marinen Gemeinschaften gegenüber Umweltveränderungen systematisch unterschätzt haben, was in einer systematischen Überschätzung der klimabedingten Phytoplankton- und Ökosystemveränderungen resultieren würde.

Die Einbeziehung von evolutionären Prozessen in Ökosystemmodelle ist allerdings nur der erste Schritt, um die Vorhersagen von künftigen Ökosystemveränderungen zuverlässiger zu machen. Aktuelle Vorhersagemodelle werden meist für heutige Ökosysteme entwickelt und sind möglicherweise nicht mehr anwendbar, wenn sich die Struktur des Ökosystems in der Zukunft verändert hat. Anstatt auf ein spezifisches Ökosystem zugeschnitten zu sein, könnten Modelle grundlegende Prozesse repräsentieren, damit sie gleichermaßen auf vergangene, gegenwärtige und (im Umkehrschluss) zukünftige Szenarien anwendbar sind. Um dies zu erreichen, empfehlen wir, Modelle anhand vergangener Ökosystemveränderungen zu testen, welche aus Sedimentkernen rekonstruiert werden können. Nur wenn dasselbe Modell sowohl den heutigen Zustand eines Ökosystems als auch seine wesentlichen Veränderungen in der Vergangenheit reproduzieren kann, können wir den Vorhersagen des Modells für die Zukunft ein gewisses Vertrauen entgegenbringen. Es wird wahrscheinlich einige Iterationen erfordern, die Modellstruktur so zu überarbeiten, dass das Modell sowohl die heutigen Beobachtungen als auch die Validierungsdaten aus der Vergangenheit reproduzieren kann. Durch diesen Prozess könnten möglicherweise auch weitere essenzielle Prozesse identifiziert werden, die bisher in Ökosystemmodellen vernachlässigt wurden.

Diese Dissertation demonstriert, dass Ökosystemmodelle zwar ein vielversprechendes Werkzeug zur Abschätzung künftiger Ökosystemveränderungen darstellen, aber noch viel Raum für Verbesserungen besteht. Erstens zeige ich, dass sich die Anpassung von Phytoplankton erheblich auf die simulierten Ökosystemprozesse auswirken kann. Zweitens stelle ich ein Konzept zur Langzeitvalidierung von evolutionären Ökosystemmodellen vor, welches ihre allgemeine Anwendbarkeit und damit auch die Aussagekraft ihrer Vorhersagen erhöhen kann. Meine Arbeit macht nicht nur deutlich, dass derzeitige Ökosystemmodelle überarbeitet werden müssen, insbesondere diejenigen, die für die Politikgestaltung relevant sind, sondern liefert auch Lösungsansätze.

Contents

Chapter 1

INTRODUCTION

Marine ecosystems and their functioning have a direct impact on the global climate and on us humans (Weatherdon et al., 2016; Hain et al., 2014). However, global warming leads to a rapid reorganization of marine communities (Pecl et al., 2017), meaning that future changes in ecosystem functioning are inevitable (Hoegh-Guldberg and Bruno, 2010). Ecosystem models are increasingly used to assess future changes in ecosystem functions like net primary production and carbon export, but their projections differ not only in magnitude but also in the direction of change (Laufkötter et al., 2015, 2016). Since model projections are a valuable resource for political decision-making (Intergovernmental Panel on Climate Change (IPCC), 2022; Meier et al., 2014), improving their informative value is vital.

In this thesis, I contribute to the improvement of model projections of future ecosystem changes by addressing two major uncertainties in current ecosystem models. First, most ecosystem models ignore the high evolutionary potential of phytoplankton, which are key players in marine ecosystems. To fill this gap, I have developed an innovative evolutionary ecosystem model that I apply to the Baltic Sea — a temperate to subarctic, semi-enclosed brackish ecosystem affected by above-average levels of multiple stressors (Reusch et al., 2018). Second, most ecosystem models are developed for ecosystems in their current state, so that they may no longer be applicable when ecosystem structure has changed in the future. I present a conceptual framework that makes use of data from sediment archives to develop evolutionary ecosystem models that are equally applicable to the past, the present, and, by implication, the future.

In the following, I explain the role of phytoplankton in marine ecosystems, how phytoplankton are responding to global warming, and what these responses may imply for ecosystem functioning. I continue by describing the importance of ecosystem models for assessing future changes in marine ecosystems, and point out remaining limitations in their predictive ability. Finally, I identify two major uncertainties in current ecosystem models that may explain the aforementioned limitations and briefly explain how I address these uncertainties in this thesis.

The crucial role of phytoplankton in marine ecosystems — an uncertain future

Numerous economic sectors directly depend on healthy marine environments, including recreation, tourism, and fisheries (Weatherdon et al., 2016). Fisheries, in turn, add substantially to food security (Weatherdon et al., 2016). In addition, marine ecosystems contribute to the long-term storage of atmospheric CO_2 through the biological carbon pump (Hain et al., 2014). The biological carbon pump is responsible for $60 - 70\,\%$ of the oceanic surface-to-depth carbon gradient (Toggweiler et al., 2003), and has sequestered about $20\,\%$ of the anthropogenic CO_2 emissions released since 1750 (Khatiwala et al., 2013). Marine organisms are also involved in other climate-relevant feedback mechanisms, for example, by promoting cloud formation through the production of dimethyl sulfide (DMS) (Simó, 2001; Wingenter et al., 2007; Clarke et al., 1998) and by influencing the physical properties of the ocean, such as viscosity (Hutchinson and Webster, 1994) and water temperature (Sathyendranath et al., 1991; Hense, 2007).

Despite being small in size, phytoplankton play key roles in the functioning of marine ecosystems (Fig. 1.1). Phytoplankton contribute about half of the world's photosynthesis (Field et al., 1998), form the basis of the marine food web (Fenchel, 1988), and are a essential component of biogeochemical cycles (Hutchins and Fu, 2017). Considering the carbon cycle, for example, phytoplankton drive the biological carbon pump by fixing CO_2 using solar energy (Basu and Mackey, 2018). Phytoplankton can further affect the climate by producing dimethylsulfoniopropionate (DMSP), which is converted into dimethyl sulfide (DMS) by marine ecosystem processes and released into the atmosphere where it seeds cloud formation (Simó, 2001; Clarke et al., 1998). In addition, phytoplankton blooms can increase the temperature of the sea surface through light absorption and cool the water masses below through shading (Sathyendranath et al., 1991; Hense, 2007). Buoyant phytoplankton taxa floating on the surface can furthermore change the viscosity of the water and inhibit wind-driven surface mixing (Hutchinson and Webster, 1994), which enhances the effects of light absorption and shading (Sonntag and Hense, 2011) and can even affect large-scale ocean circulation (Jung and Moon, 2019). The contribution to ecosystem functioning varies among phytoplankton functional groups, which may differ in their quality as food/susceptibility to predation, their sinking speed, their production of DMSP, and their buoyancy (Litchman et al., 2015; Keller et al., 1989; Moreno-Ostos et al., 2009). As a consequence of global warming, phytoplankton communities are changing, and so are the ecosystem functions associated with them.

Phytoplankton respond to global warming by changing their phenology. On global average, the phytoplankton spring bloom advances at a rate of 6 d per decade (Poloczanska et al., 2013), while regional rates may be notably higher. In the Baltic Sea, for example, the spring bloom advances more than twice as fast (14 d per decade), and the autumn bloom is delayed even faster (31 d per decade, Wasmund et al., 2019). These exceptional phenological changes can be attributed to exceptional warming (Reusch et al., 2018), with the Baltic Sea warming about 3 times faster than the global average (Rutgersson et al., 2014). This exceptional warming is also the reason why the Baltic Sea is the focus of this thesis. Overall, phenological changes in phytoplankton lead to temporal mismatches with the growth of higher trophic levels like zooplankton and fish (Asch et al., 2019; Edwards and Richardson, 2004; Winder and Schindler, 2004a), which affects the energy flow to top predators (Frederiksen et al., 2011).

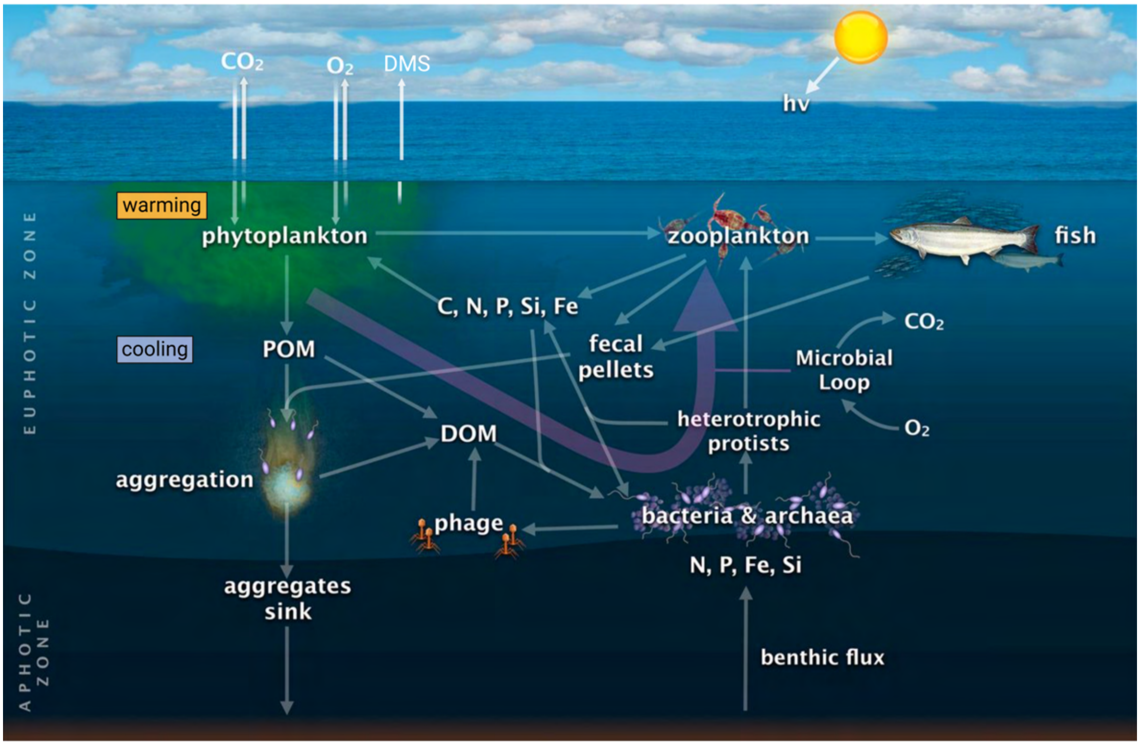

Figure 1.1: A schematic showing the role of phytoplankton in marine ecosystems. Phytoplankton grow close to the water surface, producing biomass and O_2 via photosynthesis under the consumption of CO_2 and nutrients. In addition, many phytoplankton taxa synthesize dimethylsulfoniopropionate (DMSP), which is transformed into dimethyl sulfide (DMS) by ecosystem processes and released into the atmosphere where it seeds cloud formation (Simó, 2001; Clarke et al., 1998). Due to light absorption, the phytoplankton bloom warms the water surface and simultaneously cools the water masses below the bloom through shading (Sathyendranath et al., 1991; Hense, 2007). Phytoplankton biomass is consumed by higher trophic levels, for example, zooplankton and fish, or released into the water column as dissolved or particulate organic matter (DOM and POM, respectively). DOM and POM are decomposed by bacteria and archaea under the consumption of oxygen and the release of CO_2, while bacteria and archaea are consumed by zooplankton (microbial loop, violet arrow). A fraction of the organic matter aggregates and sinks into deeper water layers, where it is stored for centuries to millennia (DeVries et al., 2012). Modified from Worden et al. (2015) and Azam and Malfatti (2007); use permitted by AAAS and Springer Nature.

In addition to phenological changes, global warming causes changes in species distribution. Marine organisms move poleward at a rate of 72 km per decade, with the fastest leading-edge expansion for phytoplankton ($\sim$470 km per decade, Poloczanska et al., 2013). The resulting changes in phytoplankton species composition and abundance may lead to strong regional changes in the DMS flux to the atmosphere, which may have significant impacts on regional temperature and precipitation patterns (Bopp et al., 2003). In addition, the altered prey availability may further impact zooplankton and fish stocks (Heneghan et al., 2023). For example, a decline in Antarctic sea ice and sea ice algae has led to a decrease in the density of Antarctic krill (Atkinson et al., 2004), which supports commercial fisheries (Everson, 2000). The decrease in krill density, in turn, has caused a decline in the population sizes of top predators, including penguins, seals, and albatrosses (Reid and Croxall, 2001). All in all, altered food web structures resulting from changes in phytoplankton phenology, species composition, and abundance eventually lead to climate-relevant ecosystem changes, e.g., by changing the amount of atmospheric carbon that is exported to deeper water layers.

Changes in carbon export, however, may also be directly caused by dominance shifts among functionally different phytoplankton taxa. For example, a decrease in diatom biomass and a simultaneous increase in dinoflagellate biomass were observed in the North Atlantic, the North Sea, and the Baltic Sea (Leterme et al., 2005; Klais et al., 2011). Diatoms are characterized by higher sinking rates than dinoflagellates (Heiskanen, 1998), meaning that a shift from diatom to dinoflagellate dominance could decrease the downward transport of organic matter. Some of the dominant dinoflagellate species in the Baltic Sea, however, produce large numbers of resting stages that sink to the sea floor and have a low germination success in the next season (Spilling et al., 2018). Consequently, a shift from diatom to dinoflagellate dominance could also enhance the long-term burial of organic matter, including carbon and especially nutrients, which are more concentrated in dinoflagellate than diatom sinking material (Spilling et al., 2014, 2018). The long-term burial of nutrients could contribute to diminishing the advanced eutrophication of the Baltic Sea (Spilling et al., 2018), which has turned the Baltic Sea into one of the most hypoxic ocean areas in the world (Breitburg et al., 2018).

As global warming progresses, nutrient loading is becoming increasingly problematic since the combination of warming and nutrient loading promotes harmful algal blooms (Paerl and Paul, 2012; Glibert et al., 2014; Gobler et al., 2017). Harmful algal blooms, which can be formed by poisonous diatoms, dinoflagellates, and cyanobacteria, can disrupt food webs, affect fisheries, and pose a risk to wildlife and human health (Heil et al., 2005; Backer and McGillicuddy, 2006; Brand et al., 2012; Glibert et al., 2012). Cyanobacteria, however, are not only problematic due to their toxicity but also due to their ability to fix atmospheric nitrogen. Cyanobacterial nitrogen fixation contributes to eutrophication and therefore promotes ocean deoxygenation (Long et al., 2021; Vahtera et al., 2007). In the highly eutrophic and hypoxic Baltic Sea, an increase in nitrogen-fixing cyanobacteria over the past decades has mitigated the success of nitrogen-related nutrient management by $\sim 66\,\%$ (Gustafsson et al., 2017). The role of nitrogen fixation for nutrient management in the Baltic Sea is expected to increase even further in the future (Hense et al., 2013). In addition to nitrogen fixation, cyanobacteria are characterized by their buoyancy (Walsby et al., 1995). An increase in cyanobacteria could therefore increase the importance of biogeophysical feedbacks such as light absorption, increased surface albedo (shading), and reduced wind stress (Sonntag and Hense, 2011).

In conclusion, the multitude of phytoplankton responses to global warming is already affecting marine ecosystems and their functioning. The phytoplankton and ecosystem responses we observe today are underlain by an increase in global surface temperature of $\sim 1.25\,^{\circ}\mathrm{C}$ since the period $1850-1900$, and an additional increase of up to $\sim 3.5\,^{\circ}\mathrm{C}$ is expected by the end of the century under the most extreme emission scenario (IPCC scenario SSP5-8.5, Allan et al., 2021). Future consequences for marine ecosystems are largely unknown, and there is a potential for synergisms and antagonisms among stressors, as well as a growing risk of exceeding irreversible tipping points, which may trigger amplifying feedback loops and domino effects (Rockström et al., 2009; Hoegh-Guldberg and Bruno, 2010). Predicting future ecosystem changes is of great importance, but remains a major challenge.

Ecosystem modeling — a tool for assessing future ecosystem changes

Marine monitoring data and sedimentary records can provide trends for future ecosystem changes based on the past (Suikkanen et al., 2007; Poutanen and Nikkilä, 2001). In addition, “futuristic ecosystems” like the Baltic Sea that are impacted by above-average levels of anthropogenic stressors can serve as a “time machine” for other ecosystems and provide direct insights into possible future changes (Reusch et al., 2018). The problem with monitoring data and sedimentary records, however, is that they are temporarily and spatially limited in their coverage and/or resolution (van Beusekom et al., 2009; Hjerne et al., 2019; Abrantes et al., 2005; Maslin et al., 2005). Laboratory and mesocosm experiments, on the contrary, allow us to study how marine organisms and communities respond to future levels of warming on a daily basis (Sommer et al., 2015; Yvon-Durocher et al., 2015; Jin and Agustí, 2018). So far, however, no long-term experiments exist that simulate species or community responses to realistic rates of environmental change. Furthermore, experiments cannot account for complex feedbacks between organisms and their environment. Ecosystem models (Box 1.1) can fill the aforementioned knowledge gaps and therefore currently represent the best tool for estimating future species- to ecosystem-level changes.

Box 1.1: Ecosystem models — an overview

Ecosystem models make use of mathematical formulations to describe interactions between different components of the ecosystem, including organic matter (living organisms, detritus), as well as chemical substances (nutrients, toxins, carbon, oxygen, etc.). Each component of the model ecosystem, such as nutrients, phytoplankton, zooplankton, and detritus, is represented by a model state variable. Model state variables are linked by source and sink processes such as nutrient uptake, grazing, mortality, and remineralization. Source and sink processes are described with differential equations and may depend on environmental conditions, for example, salinity, temperature, and light. Ecosystem models can be applied as 0-dimensional box models or coupled to a 1D or 3D physical environment.

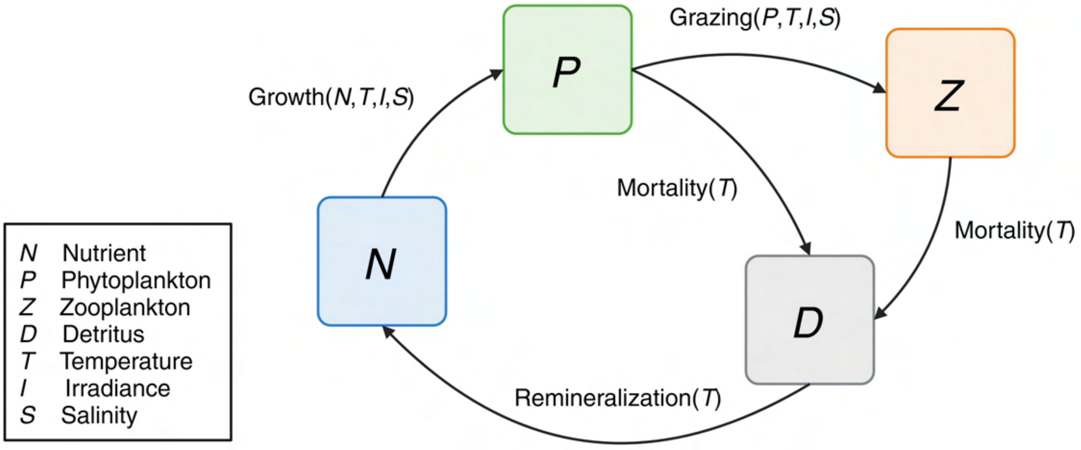

Figure 1.2: Example for a simple 0-dimensional box model that simulates the dynamics between a nutrient N, a phytoplankton population P, a zooplankton population Z, and detritus D. Both phytoplankton growth and zooplankton grazing are assumed to depend on temperature T, irradiance I, salinity S, and nutrient availability N/phytoplankton concentration P. Mortality and remineralization are implemented temperature-dependent. The figure was created with BioRender.com.

Ecosystem models provide a wide range of applicability. For example, ecosystem models can be used to study the temporal and spatial patterns of phytoplankton community composition (Bruggeman and Kooijman, 2007; Follows et al., 2007; Ward et al., 2012; Dutkiewicz et al., 2020). In addition, ecosystem models allow to identify potential trade-offs, for example between phytoplankton diversity and different ecosystem functions such as primary production and export production (Smith et al., 2016; Acevedo-Trejos et al., 2018). Furthermore, potential feedback loops can be identified and studied, e.g., between phytoplankton and water temperature (phytoplankton light absorption) (Manizza et al., 2005, 2008; Park et al., 2015), phytoplankton and cloud formation (planktonic DMSP/DMS production) (Cropp et al., 2007), or cyanobacteria and their biotic and abiotic environment (Hense, 2007). Finally, ecosystem models can simulate the responses of phytoplankton (or higher trophic levels) to biotic and abiotic factors, including viruses (Weitz et al., 2015; Krishna et al., 2024), eutrophication (Gustafsson et al., 2012), ocean acidification (Dutkiewicz et al., 2015), and temperature changes (Elliott et al., 2005; Lee et al., 2018). Embedded into regional or global coupled Earth system models, ecosystem models are increasingly used to assess future ecosystem changes on regional to global scale, including oxygen conditions, net primary production, and carbon export (Meier et al., 2011, 2012b; Séférian et al., 2014; Laufkötter et al., 2015, 2016).

Future projections of marine biogeochemistry, however, are inconsistent across models. For example, global models project small to moderate decreases in carbon export that differ by up to an order of magnitude, and for net primary production, the models even disagree on the direction of change (Laufkötter et al., 2015, 2016). Therefore, it is not surprising that the latest generation of CMIP models (Coupled Model Intercomparison Project Phase 6, Eyring et al., 2016) cannot reproduce observations of open ocean surface chlorophyll (see Fig. 1.3 and Séférian et al., 2020). As shown in Fig. 1.3, current CMIP models both underestimate (blue) and overestimate (red) chlorophyll in the open ocean depending on the geographic location, with the patterns of mismatch being largely inconsistent across models. This demonstrates that these global Earth system models, and especially their ecosystem components, do not include or resolve fundamental biogeochemical processes, which adds to the uncertainty of their simulations. Since CMIP model projections, among others, form the base of political decision-making (Intergovernmental Panel on Climate Change (IPCC), 2022; Meier et al., 2014), improving their informative value is vital.

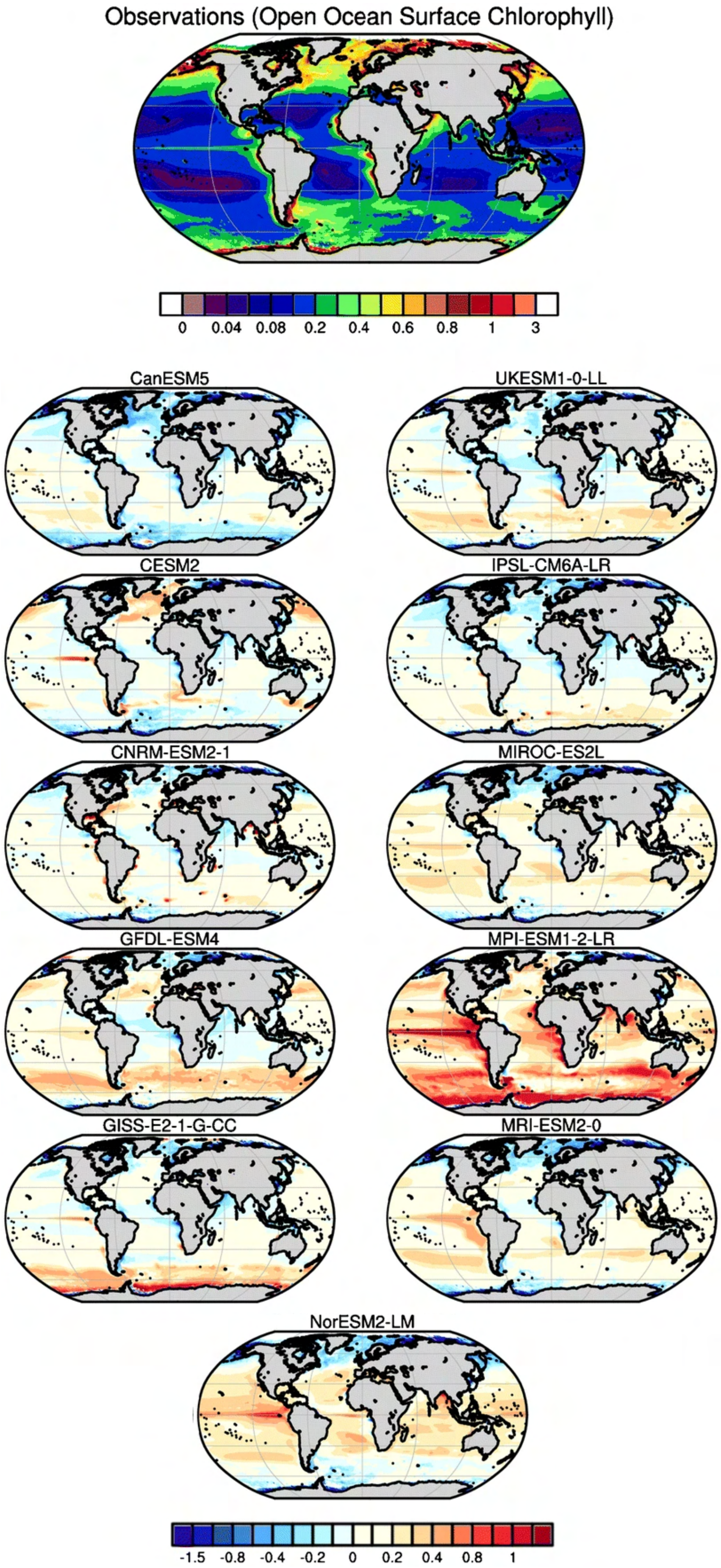

Figure 1.3: Comparison between data and CMIP6 models. The top panel shows satellite data on surface chlorophyll in the open ocean $\left(\mathrm{Chl}, \left[\mathrm{mg\,Chl\,m^{-3}}\right]\right)$ (Valente et al., 2016) averaged over the period 1998 – 2014. The other panels show the difference between the data and simulations by ocean biogeochemical models embedded within CMIP6 Earth system models for the same period. The red color indicates that the models overestimate open ocean surface chlorophyll, while the blue color indicates an underestimation. Modified from Séférian et al. (2020); the material is available under a Creative Commons Attribution 4.0 International License (https://creativecommons.org/licenses/by/4.0/).

Aim and outline of this thesis

In in this thesis, I identify and address two major uncertainties in current ecosystem models. First, current ecosystem models largely ignore a fundamental process, namely the high evolutionary potential of phytoplankton, which results from their large population sizes and short generation times. Laboratory experiments showed that phytoplankton can adapt to environmental changes within 200 – 600 generations (Schaum and Collins, 2014; Jin and Agustí, 2018; O'Donnell et al., 2018). In nature, phytoplankton adaptation can be relevant on perennial time scales and thus, adaptive responses to global warming have already occurred (Irwin et al., 2015; Hinners et al., 2017; Hattich et al., 2024). Adaptation is therefore important for phytoplankton responses and ultimately ecosystem responses to global warming, and may alter model projections of the former notably (Ward et al., 2019). Some ecosystem models already account for the high adaptive potential of phytoplankton (Clark et al., 2013; Sauterey et al., 2017; Beckmann et al., 2019; Le Gland et al., 2021), but so far, no evolutionary ecosystem model has considered phytoplankton adaptation to global warming and competition between multiple functional groups simultaneously. Since different phytoplankton functional groups fulfil different functions in the ecosystem, for example, through nitrogen fixation and/or toxicity, their individual responses to global warming will affect ecosystem functioning and need to be considered when assessing future ecosystem changes.

Here, I present results from an innovative ecosystem model that combines the competition between multiple phytoplankton functional groups and their adaptation to global warming for the first time. In **Study I**, me and my co-author apply the model to the Baltic Sea, which is affected by above-average levels of warming, nutrient load, and deoxygenation (Reusch et al., 2018), and perform simulations for present-day and future climate scenarios. For each climate scenario, we run (a) simulations without phytoplankton adaptation and (b) simulations with mutations in the optimum temperature for growth. With these simulations, we aim to study the interplay between phytoplankton competition and adaptation and disentangle their separate effects on simulated phytoplankton dynamics under contemporary and future climates. Specifically, we want to answer the following research question:

How does the interplay between competition and adaptation affect simulated phytoplankton responses to global warming?

Although adaptation can be affected by the resuspension of resting cells that were buried in the sediment (Rengefors et al., 2017), this process is largely ignored in evolutionary ecosystem models. In addition, there is no consensus about the effect of resuspension on adaptation since both a slowdown and an enhancement were suggested (Ribeiro et al., 2013; Kremp et al., 2016; Hairston Jr and De Stasio Jr, 1988). To fill these knowledge gaps, we perform additional simulations for present-day and future climate scenarios, which consider both adaptation and resuspension. We aim to further understand:

How does resting cell resuspension affect adaptation to global warming?

In **Study II**, we build on **Study I** and use an extended version of the model that allows for the calculation of different ecosystem functions, including nitrogen fixation and carbon export. A few evolutionary ecosystem models have already addressed questions related to ecosystem functioning, including the effect of phytoplankton size diversity on productivity (Smith et al., 2016), drivers on phytoplankton C:N stoichiometry, which can affect the biological carbon pump (Sauterey and Ward, 2022), and the impact of bacterial adaptation to global warming on the microbial loop and primary production (Cherabier and Ferrière, 2022). So far, however, no model has explicitly asked the question of how phytoplankton adaptation to global warming could affect ecosystem functioning. Thus, we use our extended model to investigate:

How does phytoplankton adaptation affect simulated ecosystem dynamics and future changes in ecosystem functioning?

Apart from the lack of adaptation, another major uncertainty in current ecosystem models is that they are usually developed for the contemporary state of an ecosystem. Thus, models may be no longer applicable when ecosystem structure has changed in the future. To study future ecosystem and climate changes, models should consider general mechanisms instead of being tailored to the ecosystem of interest at a specific time.

In **Study III**, my co-authors and I design a conceptual framework for developing evolutionary ecosystem models that are equally applicable to past, present, and (by implication) future scenarios. In our framework, we suggest calibrating ecosystem models to reproduce contemporary observations and then testing them against long-term validation data from the past. Only if a model can reproduce both calibration and validation data, which may require several iterations to adjust the model structure, it should be used predictively.

We present sediment archives as valuable source of long-term validation data. Natural sediments archive past ecosystem changes, including information on environmental conditions (Hillaire-Marcel and De Vernal, 2007), biodiversity and relative taxa abundances (Alsos et al., 2022; Monchamp et al., 2016; Zimmermann et al., 2023), as well as trait adaptation (Bennington et al., 1991; Hinners et al., 2017; Isanta-Navarro et al., 2021). In the manuscript for **Study III**, we discuss the advantages of using data from sediment archives for validation instead of data from monitoring or experiments, and answer the following research question:

How can data from sediment archives improve evolutionary ecosystem models and their projections of future ecosystem changes?

Since we are presenting a novel approach that has not yet been implemented in practice, we also discuss:

What are the remaining challenges and what is the potential of our approach?

Chapter 2

STUDIES OF THIS THESIS

Contribution to the studies of this thesis

Study I

Hochfeld, I. and Hinners, J. (2024): Evolutionary adaptation to steady or changing environments affects competitive outcomes in marine phytoplankton. (Published in Limnology and Oceanography, 69, 1172 – 1186, https://doi.org/10.1002/lno.12559)

My contribution: I co-designed the study, implemented the model, performed the model simulations, analyzed the model output, and was mainly responsible for writing the manuscript, handling the submission, and coordinating the review process.

Study II

Hochfeld, I. and Hinners, J. (2024): Phytoplankton adaptation to steady or changing environments affects marine ecosystem functioning. (Submitted to Biogeosciences, https://doi.org/10.5194/egusphere-2024-1246)

My contribution: I co-designed the study, implemented the model, performed the model simulations, analyzed the model output, and was mainly responsible for writing the manuscript and handling the submission.

Study III

Hochfeld, I., Arz, H., Bálint, M., Becks, L., Bolius, S., Epp, L. S., Kaiser, J., Klausmeier, C., Kremp, A., Litchman, E., Pfenninger, M., Romahn, J., Schmidt, A., Ward, B. A., and Hinners, J. (2024): How sediment archives can improve model projections of future marine ecosystem changes. (Manuscript, submission planned to Global Change Biology)

My contribution: I co-designed the study, participated in the discussion, and was largely involved in writing the manuscript.

2.1 Study I: The interplay between competition & adaptation

Evolutionary adaptation to steady or changing environments affects competitive outcomes in marine phytoplankton

Isabell Hochfeld & Jana Hinners

The interplay of phytoplankton competition and adaptation affects how phytoplankton, and ultimately marine ecosystems, respond to global warming. However, current ecosystem models that are run under global warming scenarios do not include both processes simultaneously. To fill this gap, we developed an innovative ecosystem model for the Baltic Sea that simulates competition between three phytoplankton functional groups and allows for adaptation to changing temperatures. As adaptation can be affected by the resuspension of dormant resting cells from the sediment, we explicitly implemented this mechanism. We found that resuspension tends to slow down adaptation, and that competition and adaptation influence each other. The outcome of the competition-adaptation interplay depends on environmental conditions. In a steady environment, competition drives adaptation to individual temperature niches to reduce competition pressure. In a changing environment, adaptation allows inferior competitors to mitigate the dominance of preadapted superior competitors. Our results demonstrate that by neglecting adaptation, models can systematically overestimate warming-related changes in taxa dominance. Ecosystem models should include both competition and adaptation to accurately simulate phytoplankton responses to global warming. Our model is ideally suited to integrate emerging evolutionary data based on long-term data series (e.g., from sediment archives) to further improve projections of future ecosystem change.

Published in Limnology and Oceanography

Introduction

The functioning of marine ecosystems is affected by the dominant phytoplankton taxa and the functional traits that these taxa express (Litchman et al., 2015). Due to global warming, both taxa dominances and functional traits are changing (Klais et al., 2011; Irwin et al., 2015). Even though competition between phytoplankton taxa and adaptive trait changes affect phytoplankton responses, and ultimately ecosystem responses to global warming (Litchman et al., 2015), current ecosystem models do not consider both processes simultaneously (Laufkötter et al., 2015; Munkes et al., 2021). To study how the interplay of competition and adaptation influences community, population, and trait changes of phytoplankton in response to global warming, we developed an ecosystem model for the Baltic Sea that includes three competing phytoplankton functional groups and allows for adaptation to changing temperatures.

Global warming has already caused ecological responses of phytoplankton, which include shifts in bloom timing and changes in species dominance (Winder and Sommer, 2012). As phytoplankton form the base of the marine food web (Fenchel, 1988), these responses can alter food web structures and eventually lead to ecosystem-level changes (Edwards and Richardson, 2004). In the Baltic Sea, an extension of the phytoplankton growing season (Wasmund et al., 2019), a shift from diatom to dinoflagellate dominance during spring bloom (Klais et al., 2011), as well as an increase in cyanobacterial summer biomass (Suikkanen et al., 2007) have been observed over the past 50 yr. Especially the increasing cyanobacteria represent a threat for the Baltic Sea ecosystem due to their toxicity for higher trophic levels (Chorus and Welker, 2021) and their contribution to ocean deoxygenation (Long et al., 2021; Munkes et al., 2021). Cyanobacteria enhance primary production through nitrogen fixation (Hense, 2007) and hence promote hypoxia by increasing the microbial oxygen demand in bottom waters as dead biomass is decomposed. In turn, spreading hypoxia enhances the release of iron-bound phosphate from sediments (Conley et al., 2002), promoting cyanobacterial summer blooms and creating a positive feedback mechanism that maintains hypoxia (Vahtera et al., 2007).

Changes in phytoplankton phenology and species dominance do not necessarily result from ecological processes alone but can also be affected by evolutionary adaptation. Owing to their large population sizes and short generation times, phytoplankton possess a high potential to adapt to new environments through mutation and selection. Laboratory experiments demonstrated that phytoplankton can adapt to environmental changes within $200-600$ generations, corresponding to a few years in nature (Jin and Agustí, 2018). Consequently, phytoplankton already show adaptive changes in temperature-dependent functional traits in response to global warming (Irwin et al., 2015; Hinners et al., 2017).

Both competition and adaptation shape phytoplankton community composition and influence each other. Experiments with bacteria (Lawrence et al., 2012) and phytoplankton (Collins, 2011) demonstrated that interspecific competition has a major impact on adaptation to a novel environment. Likewise, a competition-evolution experiment with coccolithophores and diatoms revealed that strong selection pressures affect competitivity and species dominance (Listmann et al., 2020). Thus, to realistically estimate phytoplankton responses to global warming, we need to understand how competition and adaptation influence each other in different environments.

So far, no long-term experiments exist that allow us to study the interplay between phytoplankton competition and adaptation under global warming on realistic time scales. Numerical models can bridge this knowledge gap by simulating species- and ecosystem-level responses to global warming at realistic rates of environmental change.

In the Baltic Sea, ecosystem models are used to perform both hindcasts and future climate projections. Prominent examples include ERGOM (Neumann et al., 2002), SCOBI (Eilola et al., 2009), BALTSEM (Savchuk, 2002), BFM (Fransner et al., 2018), and ERSEM (Vichi et al., 2004). While all these biogeochemical models consider physical processes, only ERGOM, SCOBI, and BFM are coupled to full ocean circulation models. The Baltic Sea ecosystem is represented by three to four phytoplankton functional groups, which compete for three to four different nutrients, and are grazed by one to four zooplankton groups. While hindcasts were performed with all models presented here, a multimodel ensemble of ERGOM, SCOBI, and BALTSEM was used for climate projections (Meier et al., 2014). Even if the results of climate projections are relevant for stakeholders, neither the models presented here nor similar models like CEMBS (Dzierzbicka-Głowacka et al., 2013) or ECOSMO (Daewel and Schrum, 2013) consider evolutionary adaptation of phytoplankton. Instead of adaptation, however, BFM, ERSEM, and an updated version of ERGOM (Neumann et al., 2022) allow for variable nutrient stoichiometry. Whether variable stoichiometry or the interplay of competition and adaptation is more important for realistic climate projections is beyond the scope of this article. Nonetheless, the absence of adaptation in the above models remains a major uncertainty factor that calls into question the validity of their climate projections.

Contrary to the models presented above, there are ecosystem models that consider adaptation. Phytoplankton cell size is frequently used as adaptive master trait, including size-related physiological cell properties and trade-offs (Daines et al., 2014; Sauterey and Ward, 2022). Other ecosystem models simulate adaptive changes in the optimum growth temperature (Beckmann et al., 2019), the encystment rate (Hinners et al., 2019), two different functional traits (Le Gland et al., 2021), or overall fitness (Walworth et al., 2020). However, none of the previously mentioned ecosystem models considers competition between different functional groups and adaptation to global warming simultaneously. Current eco-evolutionary models that do so, in turn, lack ecosystem dynamics (De Mazancourt et al., 2008; Northfield and Ives, 2013; Barabás and D'Andrea, 2016).

Although adaptation can be affected by the resuspension of dormant resting cells from the sediment (Rengefors et al., 2017), current ecosystem models largely ignore this process. So far, resuspension has either been represented in a simplified manner, e.g., by disabling the background mortality of resting cells (Daines et al., 2014), or in a completely conceptual framework (Sundqvist et al., 2018).

Here, we present for the first time an ecosystem model that simultaneously considers competition and adaptation of three major phytoplankton functional groups (dinoflagellates, diatoms, and diazotrophic cyanobacteria) in a global warming scenario, including an explicit representation of resuspension. We apply our model to the Baltic Sea, an ecosystem that is heavily influenced by anthropogenic activities, including above-average levels of warming (Reusch et al., 2018). For each phytoplankton functional group, we simulate the life cycle of one representative species or of a complex that contains multiple species. In addition, our model allows for two flexible temperature-dependent traits: cell size, which responds plastically to changing temperatures, and optimum growth temperature, which can adapt through mutation and selection. We assess future climate-driven community, population, and trait changes, and disentangle to which degree these changes result from competition or adaptation. Taking advantage of our detailed representation of phytoplankton life cycles, we explicitly simulate the resuspension of dormant resting cells from the sediment and study potential effects of resuspension on adaptive changes in the optimum temperature.

Materials and methods

Model concept

Our model uses a 0-dimensional agent-based approach (Appendix A.1) to simulate the life cycles of three major phytoplankton functional groups (dinoflagellates, diatoms, and diazotrophic cyanobacteria). Compartments for bulk zooplankton, nutrients, and detritus complete the ecosystem (Fig. 2.1.1). We simulate only one nutrient, nitrogen, which represents the most limiting nutrient in coastal ecosystems (Howarth and Marino, 2006). Being the first to disentangle the separate effects of competition and adaptation on warming-related phytoplankton responses, we decided to restrict competition to a single nutrient, which produces clear results that are straightforward to interpret. Including more nutrients (e.g., phosphorus and silica) would unnecessarily increase the complexity of our model without helping us to answer our research question.

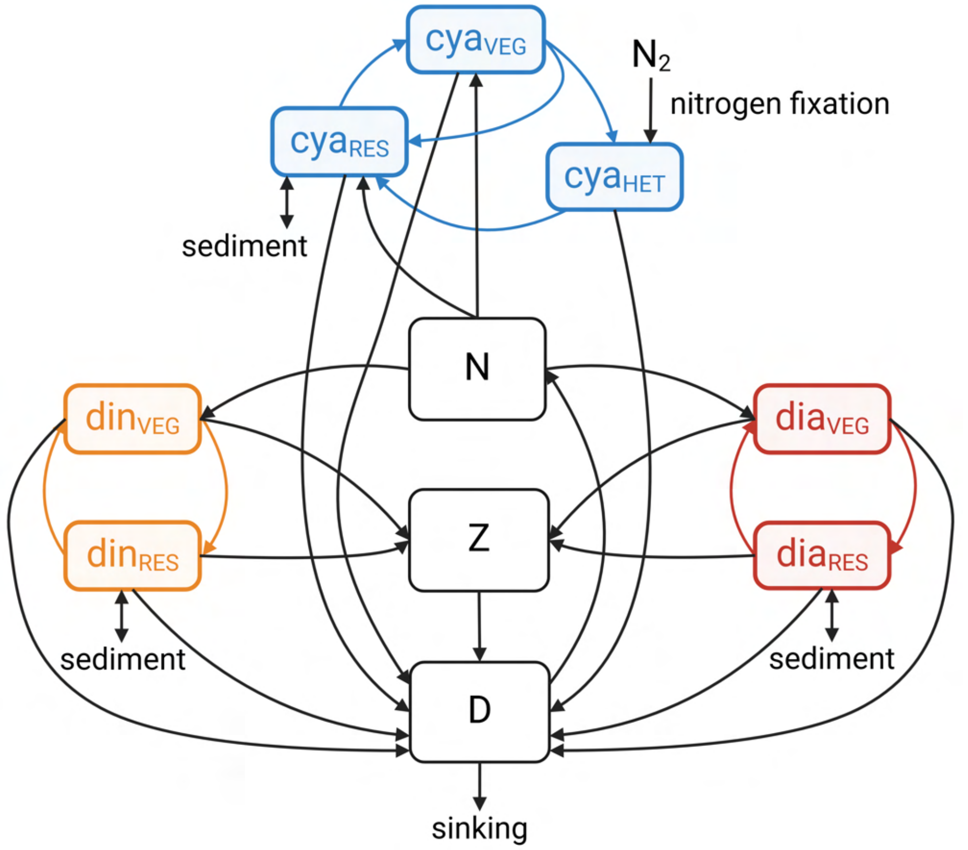

Figure 2.1.1: Ecosystem components of our model including compartments for nitrogen (N), detritus (D), and zooplankton (Z), as well as agent-based life cycles of dinoflagellates (din), diatoms (dia), and cyanobacteria (cya). Each life cycle comprises a resting (RES) and a growing stage (VEG cells). For cyanobacteria, we consider a second, nitrogen-fixing growing stage (VEG cells with heterocysts, HET). Also shown are the nitrogen fluxes between the different ecosystem components, and the sources and sinks of nitrogen (cyanobacterial nitrogen fixation, resuspension and burial of resting cells, and sinking of detritus). The figure was created with BioRender.com.

In addition to nitrogen, phytoplankton growth depends on photosynthetically available radiation and temperature. Dissolved inorganic nitrogen is taken up by all actively growing phytoplankton cells except for vegetative cyanobacteria cells that grow in filaments with nitrogen-fixing heterocysts. The nitrogen content of all dead phytoplankton and zooplankton cells is added to the detritus pool, which is remineralized back into bioavailable nitrogen at a constant rate. Due to constant sinking of detritus and stochastic burial of phytoplankton resting cells, nitrogen is lost from the system. Nitrogen loss is counteracted by the resuspension of previously buried resting cells and cyanobacterial nitrogen fixation. The probability of buried resting cells to be resuspended from the sediment decreases exponentially with time and is only possible between September and April due to vertical mixing. Thus, the nitrogen cycle in our model system is open, meaning that the amount of nitrogen in the system can change over time. All sources and sinks of nitrogen, as well as the nitrogen fluxes between the different ecosystem components, are shown in Fig. 2.1.1. A detailed model description is available in Appendix A.2.

Our model simulates the dynamics of three important phytoplankton functional groups in the Baltic Sea, each represented by one common taxon or by a complex of common taxa. Following Hinners et al. (2019), we model the life cycle of a cold-water dinoflagellate species of the genus *Apocalathium*. We distinguish between two different life cycle stages, actively growing vegetative (VEG) cells and resting cysts. Resting cysts germinate after a dormancy period of several months (Kremp, 2000); we simplify this process by prescribing germination to a certain period in early spring (between day 44 and day 60). The transfer from VEG cells back to cysts depends on temperature, with the encystment rate increasing strongly around a temperature threshold of 6 °C. For diatoms, we chose a cold-water species of the genus *Thalassiosira*. Again, we distinguish between a resting stage (RES; spores) and a growing stage (VEG cells). Like Warns (2013), we assume that the transfer between stages depends on the actual growth conditions, i.e., the realized growth rate. For cyanobacteria, we consider a complex that represents the dominant nitrogen-fixing genera in the Baltic Sea, *Nodularia*, *Aphanizomenon*, and *Anabaena* (Karlsson et al., 2005). The cyanobacteria life cycle comprises three different stages given by VEG cells without heterocysts (nitrogen-limited), VEG cells with heterocysts (not nitrogen-limited), and resting cells (akinetes). We parameterize the transfer between the cyanobacteria life cycle stages by combining two modeling approaches (Hense and Beckmann, 2006, 2010): Similar to diatoms, the transfer between stages depends on the actual growth conditions, which are either measured by the realized growth rate or by the severity of different growth-limiting factors. For VEG cells, we separate growth conditions into nitrogen limitation and limitation by temperature and light. While nitrogen limitation leads to heterocyst formation, unfavorable temperature and light conditions initiate the transfer from VEG cells to resting cells. Following other models (Hense and Beckmann, 2006; Lee et al., 2018), we assume that cyanobacteria are non-grazeable due to toxicity, while dinoflagellates and diatoms are equally grazed by zooplankton. Further details on the simulated taxa and their life cycles can be found in Appendix A.2.

In addition to phytoplankton life cycle dynamics, we consider two flexible temperature-dependent phytoplankton traits. The first flexible trait is the optimum temperature, which determines temperature limitation of growth. The optimum temperature is subject to random mutations, which we implement using an agent-based modeling approach (Appendix A.1). In our model, each agent represents the same amount of biomass. As the three functional groups differ in their cell sizes (Table A1 in Appendix A.3), the number of cells per agent, i.e., resolution, differs among groups. Based on Beckmann et al. (2019), we assume that resolution affects the probability that a mutation occurs when an agent divides. We calculate the mutation probability for one agent by multiplying the number of cells within the agent by the mutation probability for one cell, for which we use an experimentally derived value of $2.5{\times}10^{-3}$ (Lenski and Travisano, 1994). As our agents combine more than $2.5{\times}10^{3}$ cells, mutations occur at every division, with the number of mutations being proportional to the number of cells within the agent. Thus, an agent combining more cells experiences more mutations per division. However, due to the larger number of cells within the agent, these mutations require the same time to be fixed as in smaller agents with less cells and less mutations. For this reason, we use the same mutational standard deviation (or mutational step size) for all agents independent of their resolution (0.1 °C, Beckmann et al., 2019). These assumptions are similar to a modeling study by Merico et al. (2014), which uses a fixed mutational step size independent of population size, with larger populations having more mutations in total.

The second flexible trait, the cell size, responds plastically to temperature. The relation between cell size and temperature is inversely proportional, meaning that a temperature increase of 1 °C causes a cell size decrease of ∼ 2.5 % (Atkinson et al., 2003). In our model, plastic responses occur during cell division and affect the newly produced daughter cell. Following Beckmann et al. (2019), we assume that a cell divides after having grown to a critical size. As Beckmann et al. (2019) do not consider cell size plasticity, they use the same critical size of $2b_0$ for all cells, with b_0 being the initial cell size right after division. To account for cell size plasticity, we calculate the critical size of the newly produced daughter cell depending on environmental temperature. We assume that the daughter cell divides after having grown to $2b_{0,\mathrm{T}}$, with $b_{0,\mathrm{T}}$ being the initial size that the daughter cell would have if cell size responded instantaneously to temperature. We calculate $b_{0,\mathrm{T}}$ for the temperature during daughter cell production after Atkinson et al. (2003). In this way, an increase in temperature leads to a decrease in the daughter's critical size, reducing the initial size of the following generation. In addition, we consider that changes in cell size affect metabolic cell properties including maximum nitrogen uptake rate (Ward et al., 2017), half saturation constant for nitrogen (Litchman et al., 2007), basal cellular nitrogen requirement (Ward et al., 2017), maximum nitrogen storage capacity (Marañón et al., 2013), and theoretical maximum metabolic rate (Ward et al., 2017). In our model, cell size thus determines the nitrogen-limited growth rate, which we calculate from internal nitrogen quotas using a variable-internal-stores model by Grover (1991) (Appendix A.2.2).

Model setup and environmental forcing

For our simulations, we use a 0-dimensional model setup, which corresponds to a well-mixed tank. We assume that the sides of the tank are closed, while both top and bottom are open. This means that we neglect immigration and emigration of phytoplankton and zooplankton but still allow for changes in total mass due to interactions with the atmosphere (nitrogen fixation) and the benthic zone (sinking of detritus, burial of resting cells, and resuspension of resting cells).

At the beginning of a simulation, we initialize each phytoplankton functional group with the same biomass and overlapping generations. To create overlapping generations, we sample the biomass of each cell randomly from a uniform distribution between minimum cell biomass right after division ($b_{0,\mathrm{T}}$, Table A1 in Appendix A.3) and maximum cell biomass right before division ($2b_{0,\mathrm{T}}$). In contrast to cell biomass, optimum temperature is initially the same for all individuals of a functional group. In this way, we ensure that the observed adaptation results from mutations alone and not from initial intraspecific diversity.

Following other models (Hense and Beckmann, 2006; Hinners et al., 2019), we simulate 12 equal months for each year (30 d per month) with a time step of 1 h. For a steady seasonal forcing, the model requires a spin-up period of ∼ 65 yr until phenology, taxa abundance, and mean traits have largely stabilized (Figs. A1 and A2 in Appendix A.4). The steady seasonal forcing used for spin-up represents present-day conditions in the Gulf of Finland. For the seasonal variation of irradiance, we use the same function as Hinners et al. (2019), which was originally adapted from Stramska and Zuzewicz (2013). The function provides higher irradiance levels during summer and lower irradiance levels during winter. For the seasonal temperature forcing, we use a sinusoidal fit to sea surface temperature data from the Gulf of Finland. Prior to fitting, we averaged the data over the whole gulf area and over the last 10 yr (2011 – 2021) to compensate for regional differences and special temperature events such as heat waves. Sea surface temperature data were downloaded from the Copernicus database (https://resources.marine.copernicus.eu/products). The seasonal temperature and irradiance forcings are visualized in Fig. A3a in Appendix A.4; the corresponding equations are available in Appendix A.2.4.

Model scenarios

To disentangle the separate effects of competition and adaptation on climate-driven phytoplankton responses, we simulate six different model scenarios (Table 2.1.1).

Table 2.1.1: Overview of the six model scenarios that we analyze in this study. We perform seven different simulations for each scenario, with each simulation being run over 100 yr. "Control" corresponds to a present-day seasonal temperature forcing for the Gulf of Finland, to which "warming" adds a steady temperature increase of 0.3 °C per decade (IPCC scenario SSP3-7.0, Allan et al., 2021).

	No adaptation	Adaptation	Adaptation and resuspension
Control	C	CA	CAR
Warming	W	WA	WAR

The first two model scenarios represent control scenarios (C: control; CA: control and adaptation), which we force with the present-day seasonal forcing for the Gulf of Finland over 100 yr. Both C and CA serve as spin-up for two global warming scenarios W (warming) and WA (warming and adaptation). To simulate global warming, we add a continuous temperature increase of 0.3 °C per decade to the seasonal temperature forcing, which corresponds to the IPCC scenario SSP3-7.0 (Allan et al., 2021). This configuration is run for further 100 yr to simulate global warming during the next century (see Fig. A3b in Appendix A.4). While adaptation in the optimum temperature is disabled in C and W, it is enabled in CA and WA. This means that in C and W, we simulate ecological phytoplankton responses only, with competition (i.e., selection) as the single controlling factor. In CA and WA, on the contrary, phytoplankton responses to global warming are controlled by the combined effects of competition and adaptation (i.e., mutation and selection), meaning that they are eco-evolutionary.

To add further complexity to the representation of evolutionary processes in our model, we consider another essential mechanism that can both enhance and slow down adaptation (Rengefors et al., 2017): the resuspension of resting cells from previous blooms that were buried in the sediment. To study potential effects of resuspension on our model phytoplankton community, we simulate two additional scenarios termed CAR (control and adaptation and resuspension) and WAR (warming and adaptation and resuspension), where both adaptation and resuspension are enabled. For each of the six model scenarios (Table 2.1.1), we perform seven different simulations and average the output to ensure robust results.

Results

Model validation for present-day conditions

To validate our model for present-day conditions, we use the two control scenarios C and CA; CAR is evaluated in a separate section ("Effects of RES resuspension"). Both C and CA produce the same seasonal succession of functional groups (Fig. 2.1.2): The blooming season starts with the spring bloom of dinoflagellates and diatoms, which reach maximum abundances in March and May, respectively. The spring bloom is followed by a summer bloom of cyanobacteria, which are most abundant in July. In autumn, diatoms form a second but weaker bloom with maximum abundances at the beginning of November. Our simulated seasonal succession of functional groups results from their individual responses to environmental growth conditions, including nitrogen concentration, temperature, and irradiance (Appendix A.2.2 and Figs. A4, A5, and A6 in Appendix A.4).

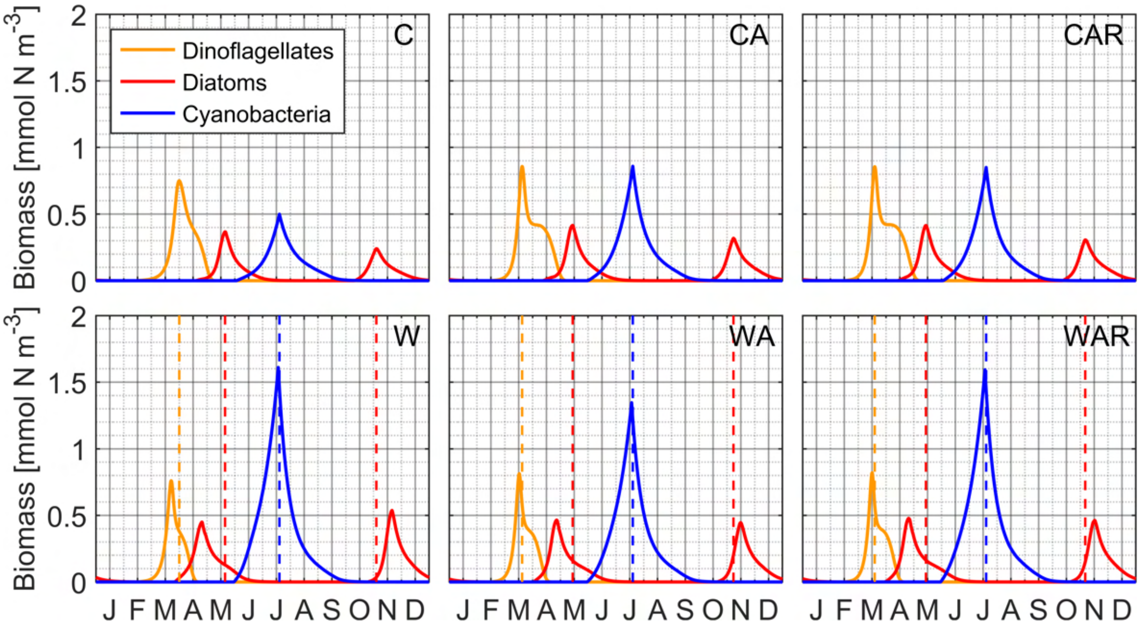

Figure 2.1.2: Biomass of phytoplankton growing stages during the last simulation year for all six model scenarios (C: control; W: warming; CA: control and adaptation; WA: warming and adaptation; CAR: control and adaptation and resuspension; WAR: warming and adaptation and resuspension). For each model scenario, seven different simulations were averaged. The dashed lines in each warming scenario indicate the timing of the bloom peaks in the corresponding control scenario. Please note that the biomass of both cyanobacteria growing stages (VEG cells without heterocysts and VEG cells with heterocysts) is summarized.

However, even if C and CA produce the same seasonal succession of functional groups, the timing of the individual blooms may differ by several days. Bloom timing, in this context, refers to the time when the bloom reaches its peak. In C, the spring bloom occurs later than in CA, with dinoflagellates and diatoms peaking ~ 11 d and ~ 6 d later, respectively (Table 2.1.2). The diatom autumn bloom, on the contrary, occurs ~ 4 d earlier in C than in CA. In addition, C shows lower bloom amplitudes, especially for cyanobacteria, which produce a $\sim 42\,\%$ weaker summer bloom. According to a *t*-test, the mentioned differences between C and CA are statistically significant (we use a significance level of 0.05 for *t*-tests, Table A2 in Appendix A.3). Despite these differences, the two control scenarios C and CA agree reasonably well with recent monitoring data from the Baltic Sea (Hjerne et al., 2019), except for slight deviations in spring bloom timing (see section "Deviations in spring bloom timing").

Table 2.1.2: Average bloom timing, peak abundance, and optimum temperature (T_{opt}) of all taxa for the three control scenarios C (control), CA (control and adaptation), and CAR (control and adaptation and resuspension), including standard deviations. For each scenario, averages were calculated from the last simulation year of seven different simulations.

		C	CA	CAR
Timing [d]	Dinoflagellates	89.93 ± 0.78	78.71 ± 0.73	77.90 ± 0.79
	Diatoms spring	139.96 ± 0.45	133.60 ± 0.79	133.77 ± 0.88
	Diatoms autumn	303.13 ± 0.83	307.25 ± 0.67	305.57 ± 0.84
	Cyanobacteria	198.29 ± 0.00	198.29 ± 0.00	198.29 ± 0.00
Abundance $\left[\text{mmol N m}^{-3}\right]$	Dinoflagellates	0.76 ± 0.01	0.87 ± 0.03	0.88 ± 0.02
	Diatoms spring	0.37 ± 0.00	0.42 ± 0.01	0.43 ± 0.01
	Diatoms autumn	0.25 ± 0.01	0.33 ± 0.02	0.32 ± 0.02
	Cyanobacteria	0.50 ± 0.02	0.86 ± 0.09	0.85 ± 0.08
T_{opt} [°C]	Dinoflagellates	10.80 ± 0.00	5.03 ± 0.29	5.22 ± 0.19
	Diatoms	12.00 ± 0.00	11.25 ± 0.18	11.39 ± 0.14
	Cyanobacteria	28.50 ± 0.00	27.83 ± 0.32	28.22 ± 0.15

Moreover, we find that in CA, the optimum temperatures of both dinoflagellates and diatoms track seasonal changes in environmental temperature following an initial acclimation period after germination (Fig. A7 in Appendix A.4). Dinoflagellates show the highest adaptation rate with a change in mean optimum temperature of ∼ 0.18 °C within 1 month. This simulated adaptation rate agrees well with observed adaptation rates for *Chaetoceros tenuissimus* (Jin and Agustí, 2018).

Ecological phytoplankton responses to global warming

In the two warming scenarios W and WA, our phytoplankton community shows different ecological responses to global warming, including shifts in bloom timing and changes in bloom amplitude (Fig. 2.1.2). Shifts in bloom timing are only notable for dinoflagellates and diatoms but not for cyanobacteria. For dinoflagellates and diatoms, blooms are shifted towards the winter period, with the shift being stronger in W than in WA. Dinoflagellates bloom ∼ 8 d earlier in W compared with C, while the shift between WA and CA only amounts to ∼ 3 d (Table 2.1.3). Diatoms show an even stronger shift in bloom timing than dinoflagellates: while the spring bloom is shifted by ∼ 25 d and ∼ 17 d, the autumn bloom is shifted by ∼ 17 d and ∼ 8 d in W and WA, respectively.

Apart from shifts in bloom timing, W and WA produce increasing bloom amplitudes for all functional groups, except for dinoflagellates. Again, the observed changes are stronger in W than in WA. Cyanobacteria show the strongest amplitude increase with ∼ 223 % in W and ∼ 57 % in WA, followed by diatoms. For diatoms, the autumn bloom increases more than the spring bloom. Dinoflagellates, however, increase only slightly in W, while they decrease in WA; this is in line with the overall stronger amplitude increase in W.

According to a t-test, bloom timing and bloom amplitudes differ significantly between W and WA for all functional groups; the only exception is the timing of the cyanobacterial summer bloom (Table A3 in Appendix A.3).

Table 2.1.3: Average warming-related changes in bloom timing, peak abundance, and optimum temperature (T_{opt}) for all taxa and model scenarios, including propagated errors. Scenario abbreviations: C = control; W = warming; CA = control and adaptation; WA = warming and adaptation; CAR = control and adaptation and resuspension; WAR = warming and adaptation and resuspension. Negative changes in bloom timing indicate a shift towards earlier in the year. Please note that changes in taxa abundance are not given as absolute values like in Table 2.1.2 but as relative changes. According to a *t*-test, all changes are statistically significant at the 0.05 level. For details, see Table A4 in Appendix A.3.

		W vs. C	WA vs. CA	WAR vs. CAR
Timing [d]	Dinoflagellates	-8.45 ± 1.05	-2.97 ± 1.06	-2.77 ± 0.96
	Diatoms spring	-25.13 ± 0.53	-17.08 ± 1.05	-18.53 ± 1.08
	Diatoms autumn	$+16.92 \pm 0.94$	$+7.83 \pm 1.20$	$+9.78 \pm 1.53$
	Cyanobacteria	-1.25 ± 0.00	-1.25 ± 0.00	-1.25 ± 0.00
Abundance [%]	Dinoflagellates	$+2.63 \pm 1.29$	-4.33 ± 4.00	-5.37 ± 3.01
	Diatoms spring	$+21.40 \pm 1.59$	$+10.47 \pm 3.12$	$+13.07 \pm 2.09$
	Diatoms autumn	$+118.81 \pm 3.92$	$+41.52 \pm 5.39$	$+52.64 \pm 6.89$
	Cyanobacteria	$+222.68 \pm 4.37$	$+56.69 \pm 11.17$	$+87.38 \pm 10.66$
T_{opt} [°C]	Dinoflagellates	0.00 ± 0.00	$+1.41 \pm 0.41$	$+0.89 \pm 0.24$
	Diatoms	0.00 ± 0.00	$+1.49 \pm 0.21$	$+1.30 \pm 0.20$
	Cyanobacteria	0.00 ± 0.00	$+1.23 \pm 0.52$	$+0.69 \pm 0.21$

Adaptive phytoplankton responses to global warming

Already in the control scenario CA, we observe notable adaptation of all functional groups. Dinoflagellates adapt to notably lower temperatures in CA (Fig. 2.1.3), with most of the adaptation occurring within the first ~ 60 yr of the simulation period (Fig. A2 in Appendix A.4). Throughout the entire CA simulation period of 100 yr, dinoflagellates decrease their mean optimum temperature (T_{opt}) by 5.8 °C, from an initial T_{opt} of 10.8 °C (Hinners et al., 2017) to a new T_{opt} of 5.0 °C (Table 2.1.2). Diatoms and cyanobacteria also show a tendency towards lower temperatures; this tendency is considerably weaker than for dinoflagellates, though. Both diatoms and cyanobacteria reduce their initial optimum temperatures of 12 °C (Spilling, 2011) and 28.5 °C (Collins and Boylen, 1982; Lehtimäki et al., 1997) by 0.7 °C throughout CA. At the end of CA, diatoms and cyanobacteria thus grow at new optimum temperatures of 11.3 °C and 27.8 °C, respectively. While most of the adaptation of diatoms occurs during the first ~ 65 yr of the simulation period, which is similar to dinoflagellates, cyanobacteria show steady adaptation over the 100 yr of simulation (Fig. A2 in Appendix A.4). Overall, adaptive trait changes in CA correlate temporally with ecological changes in bloom timing and taxa abundance (Figs. A1 and A2 in Appendix A.4).

In the warming scenario WA, we observe notable adaptation of all functional groups to the increasing temperatures. Dinoflagellates increase their mean T_{opt} by 1.4 °C throughout WA (Table 2.1.3). The resulting T_{opt} of 6.4 °C is still notably lower than the initial T_{opt} of dinoflagellates at the beginning of CA (10.8 °C, Table 2.1.2). Diatoms and cyanobacteria, on the contrary, increase their mean T_{opt} above their initial optimum temperatures. Throughout WA, the mean T_{opt} of diatoms and cyanobacteria increases by 1.5 °C and 1.2 °C, respectively, giving final optimum temperatures of 12.7 °C and 29.1 °C. Thus, the final optimum temperatures of diatoms and cyanobacteria at the end of WA are by ~ 0.7 °C and ~ 0.6 °C higher than their initial optimum temperatures at the beginning of CA, respectively.

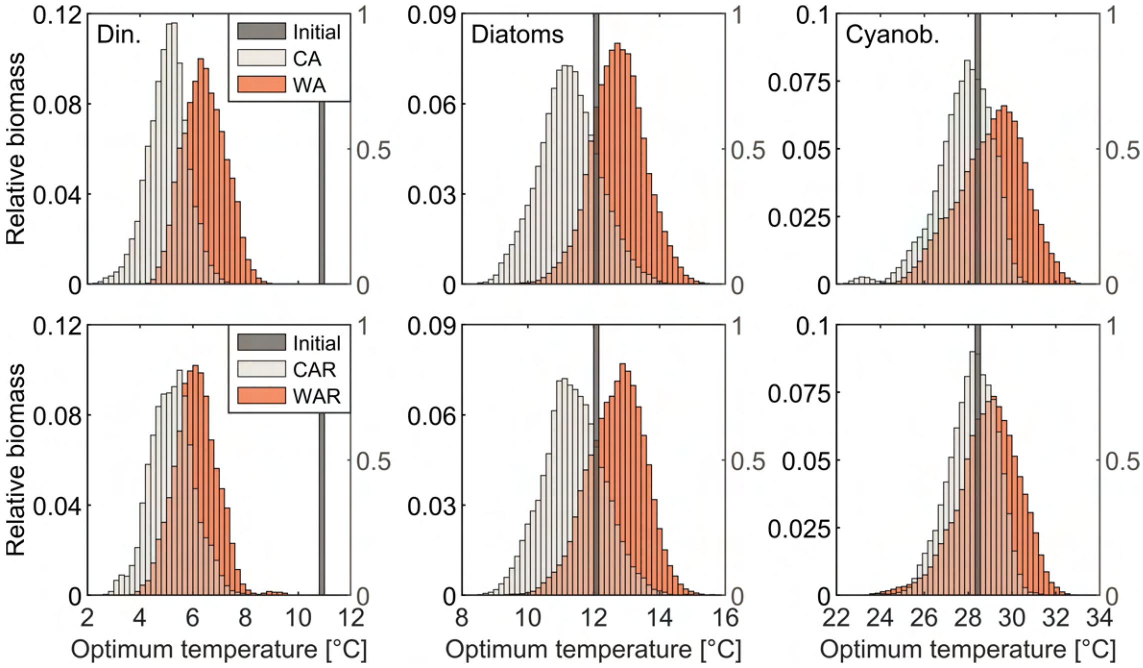

Figure 2.1.3: Evolution of the optimum temperature through mutation and selection. Shown are the initial value, the preliminary trait distribution after 100 yr of present-day seasonal forcing, and the final trait distribution after 100 yr of warming. Upper panels: adaptation only, i.e., CA (control and adaptation) and WA (warming and adaptation); lower panels: adaptation plus resuspension, i.e., CAR (control and adaptation and resuspension) and WAR (warming and adaptation and resuspension). For each model scenario, trait distributions were merged from monthly histograms of the last simulation year of seven different simulations. Please note that the temperature range on the x-axis differs between functional groups.

Effects of RES resuspension

When we enable the resuspension of resting cells from the sediment, we observe only slight phenological changes in the control scenario CAR compared with CA (Fig. 2.1.2 and Table 2.1.2). While taxa abundances are comparable, autumn diatoms bloom ~ 2 d earlier in CAR; this shift in bloom timing is statistically significant according to a t-test (Table A2 in Appendix A.3). Similarly, we found autumn diatoms to bloom ~ 4 d earlier in the control scenario without adaptation C when compared with CA (see section “Model validation for present-day conditions”).

The slight phenological changes in CAR are accompanied by reduced thermal adaptation. While in both CA and CAR, optimum temperatures evolve towards lower values, the final optimum temperatures at the end of CAR are between 0.14 °C and 0.39 °C higher than at the end of CA (Table 2.1.2). Changes in adaptation are, however, only statistically significant for cyanobacteria, for which adaptation is reduced the most (Table A2 in Appendix A.3).

Under warming conditions, we observe stronger phenological effects of resuspension as part of a general weakening of adaptation-related effects. The results of the WAR scenario resemble more closely the results of the W than the WA scenario (Fig. 2.1.2). While the two diatom blooms tend to be shifted $\sim 1-2$ d more towards the winter period, the cyanobacterial summer bloom is by $\sim 18\,\%$ stronger in WAR than in WA. The difference in cyanobacteria biomass is statistically significant (Table A3 in Appendix A.3).

The stronger effects of resuspension under warming conditions are accompanied by a greater slowdown of adaptation (Fig. 2.1.3 and Table 2.1.3). In WAR, the three functional groups increase their mean optimum temperatures between 0.20 °C and 0.54 °C less than in WA. The resulting differences in optimum temperature are, however, only statistically significant for dinoflagellates (Table A3 in Appendix A.3). In addition, we observe a slight narrowing of the T_{opt} trait distribution in WAR for both dinoflagellates and cyanobacteria, for which adaptation is slowed more than for diatoms.

Discussion

In this study, we investigated the interplay between phytoplankton competition and adaptation under global warming using an eco-evolutionary ecosystem model. We found that adaptation reduces warming-related ecological phytoplankton responses in terms of changes in bloom timing and amplitude. Resuspension of resting cells can slow down adaptation and hence enhance changes in bloom timing and amplitude. To the best of our knowledge, this is the first ecosystem model that simulates competition and adaptation of multiple phytoplankton functional groups under global warming, allowing us to disentangle how the interplay of both processes affects warming-related phytoplankton responses on realistic time scales. Due to the simplicity of the model design, we will not discuss exact magnitudes in detail but focus on qualitative differences.

Deviations in spring bloom timing

Contrary to recent monitoring data from the Baltic Sea (Hjerne et al., 2019), dinoflagellates bloom earlier in spring than diatoms in our simulations. One possible explanation for this could be that our model does not consider re-stratification during spring, which plays an important role during spring bloom formation in the Baltic Sea (Klais et al., 2011). While motile dinoflagellates require stratified conditions to form a bloom (Margalef et al., 1979), nonmotile diatoms are favored under turbulent mixing (María Trigueros and Orive, 2001). In addition, the monitoring data do not distinguish between species but only functional groups, while we simulate a single species from each functional group (except for cyanobacteria). The traits of our chosen species do not necessarily coincide with the bulk traits of the functional group that the species belongs to. Consequently, the species we chose may not bloom at the same time as the bulk of species in the corresponding functional group. Indeed, lower optimum temperatures were measured for the cold-water dinoflagellate *Apocalathium malmogiense* than for the cold-water diatom *Thalassiosira baltica* (Spilling, 2011; Hinners et al., 2017). As we simulate a dinoflagellate species of the genus *Apocalathium* and a diatom species of the genus *Thalassiosira*, we use these optimum temperatures to initialize our model. The earlier bloom of dinoflagellates in our simulations is hence a result of the physiological properties of *Apocalathium*, including the initial optimum temperature and in particular the strong increase in encystment at low temperatures ($\sim 6\,^{\circ}\mathrm{C}$). Thus, we can conclude that for our chosen phytoplankton species, our model produces a realistic seasonal cycle.

Eco-evolutionary dynamics in a steady environment

The results of control scenario C differ notably from the two control scenarios CA and CAR, which themselves are comparable. Contrary to C, both CA and CAR include adaptation, meaning that the observed differences must result from adaptation-related effects. In comparison to C, CA and CAR show slightly shifted blooms of higher amplitude. Adaptation in CA and CAR allows each functional group to improve its growth conditions by utilizing its niche more efficiently.

Dinoflagellates improve their growth conditions by adapting to lower temperatures. Additional CA simulations using only dinoflagellates reveal that this adaptation pattern is not driven by interspecific competition with diatoms but by intraspecific competition for nitrogen, which selects for early bloomers (Fig. A8 in Appendix A.4). Even in the absence of interspecific competition, dinoflagellates do not extend their niche towards higher temperatures due to restrictions in their life cycle. Resurrection experiments demonstrated that the temperature threshold for encystment of *A. malmogiense* remained constant at around 6 °C over the last century of global warming (Hinners et al., 2017), prohibiting a shift towards later blooming. As our simulations cover a similar time span, we implemented the encystment threshold as a fixed trait.

Contrary to dinoflagellates, adaptation of diatoms is controlled by interspecific competition with cyanobacteria. As inferior competitors under warm, nitrogen-limited conditions, diatoms lower their optimum temperature to avoid competition for nitrogen. This hypothesis is confirmed by additional CA simulations using only diatoms. These simulations show that without interspecific competition, diatoms adapt to higher temperatures in a steady environment to merge their spring and autumn blooms (Fig. A9 in Appendix A.4). Thus, we can conclude that interspecific competition between diatoms and cyanobacteria drives niche separation. This finding goes in line with a modeling study by Barabás and D'Andrea (2016), who found that competing species place themselves more evenly across the trait axis if they can adapt.

Contrary to dinoflagellates and diatoms, adaptation of cyanobacteria is neither driven by intra- nor by interspecific competition for nitrogen, which is not surprising given their ability to fix atmospheric nitrogen. Instead, the difference between environmental and optimum temperature is the driving factor, with the initial T_{opt} of cyanobacteria being almost 9 °C higher than maximum environmental temperature in summer. Despite the large temperature difference, cyanobacteria reduce their mean optimum temperature by only 0.7 °C throughout CA. This is most likely caused by the wide, plateau-shaped thermal reaction norm of cyanobacteria (Fig. A4 in Appendix A.4), which does not lead to a strong selection pressure on the optimum temperature even if environmental temperature differs notably from the optimum. Indeed, the growth rate of initial genotypes is only 17 % lower than the growth rate of genotypes that are adapted optimally to environmental temperature. Our hypothesis is further supported by the T_{opt} trait distribution of cyanobacteria, which is the broadest among the functional groups in our model (Fig. A10 in Appendix A.4). Simulations by Beckmann et al. (2019) showed that trait diversity is reduced under strong selection pressure. Thus, in our simulations, selection pressure indeed seems to be weaker for cyanobacteria than for dinoflagellates and diatoms. The weak selection pressure on cyanobacteria prevents them from completing adaptation to control conditions within the 100 yr of simulation, meaning that we still observe transient trait dynamics at the end of CA. Dinoflagellates and diatoms, on the contrary, complete adaptation in CA within less than 100 yr. As neither dinoflagellates nor diatoms are implemented with larger mutation rates or larger mutational step sizes than cyanobacteria, their faster adaptation must result from the stronger selection pressure they experience. We propose that the stronger selection pressure on dinoflagellates and diatoms results from their narrower thermal reaction norms (Fig. A4 in Appendix A.4). For comparison, cyanobacteria can reach 90 % of their maximum growth rate over a temperature range of 9.4 °C. For dinoflagellates and diatoms, this range is considerably narrower with 4.7 °C and 4.2 °C, respectively. To conclude, selection pressure and adaptation speed are not only affected by the difference between optimum and environmental temperature but also by the width and shape of the thermal reaction norm.

From the above discussion, we can conclude that adaptation allows all functional groups to improve their individual growth conditions to a certain degree, with the drivers of adaptation differing among groups. However, adaptation of one group may also affect the other groups through changes in competition. For example, diatom adaptation reduces competition with cyanobacteria, which is beneficial for both sides. Reduced competition with diatoms leaves more nitrogen for the nitrogen-limited vegetative cyanobacteria life cycle stage, which can hence initiate a larger summer bloom. Indeed, additional CA simulations without cyanobacterial adaptation reveal that reduced competition with diatoms causes 71 % of the amplitude increase in CA compared with C, while only the remaining 29 % result from adaptation of cyanobacteria to colder temperatures. As a result, reduced competition with diatoms indirectly enhances the bloom of vegetative cyanobacteria with heterocysts and thus increases the amount of fixed atmospheric nitrogen. The higher nitrogen input into the system in summer allows for stronger blooms of dinoflagellates and especially diatoms, which can directly take up the newly available nitrogen in autumn. In conclusion, adaptation in a steady environment induces positive feedback in our simulations: While diatoms actively improve their growth conditions through niche separation, cyanobacteria benefit passively from reduced competition with diatoms. The higher nitrogen availability due to enhanced cyanobacterial nitrogen fixation feeds back positively on both diatoms and dinoflagellates.

Eco-evolutionary dynamics in a changing environment

The two warming scenarios with and without adaptation WA and W produce ecological phytoplankton responses of notably different intensity, which nevertheless follow the same trends. Both scenarios show a shift of dinoflagellates and diatoms towards the winter period, as well as a notable increase in cyanobacteria biomass in summer. As these findings are consistent with trends observed over the past 50 yr of global warming in the Baltic Sea (Suikkanen et al., 2007; Wasmund et al., 2019), we believe them to be realistic.

By comparing the relative magnitude of warming-related changes between W and WA, we can disentangle the effects of competition and adaptation in a warming environment. In a steady environment, we found adaptation to enhance bloom amplitudes; in a warming environment, however, adaptation has the opposite effect. For increasing temperatures, amplitudes are lower in WA, where adaptation is enabled, especially for cyanobacteria. To understand if the weaker cyanobacteria bloom in WA is mainly caused by cyanobacterial thermal adaptation or adaptation-related differences in competition, we performed additional simulations in which we disabled the thermal adaptation of cyanobacteria. The simulations reveal that cyanobacterial thermal adaptation leads to an increase in bloom amplitude of 2 % and hence only has a minor effect. Thus, the observed differences in cyanobacterial bloom amplitude must result from adaptation-related differences in competition with diatoms. Due to lacking adaptation in W, diatoms (and dinoflagellates) can only compensate the increase in temperature by shifting their blooms towards the winter period, when temperatures are closer to their fixed optimum temperature. Thus, diatoms are less abundant and less competitive in late spring and leave more nitrogen for the nitrogen-limited vegetative cyanobacteria, which can initiate a larger summer bloom. In WA, on the contrary, diatoms increase their optimum temperature above their fixed T_{opt} in W. However, this shift is lower than the shift in environmental temperature. In the absence of interspecific competition, diatoms track changes in environmental temperature more closely as confirmed by additional WA simulations using only diatoms (Fig. A9 in Appendix A.4). This suggests that cyanobacteria restrict diatom adaptation to increasing temperatures, which matches findings from a modeling study by De Mazancourt et al. (2008). De Mazancourt et al. (2008) showed that the presence of preadapted species (in our case cyanobacteria) restricts adaptation of other species. Even if cyanobacteria restrict diatom adaptation in WA, diatoms manage to increase their optimum temperature above their fixed T_{opt} in W, which reduces the shift in bloom timing, and increases the abundance and competitivity of diatoms in late spring. The enhanced competition with diatoms reduces nitrogen availability for nitrogen-limited vegetative cyanobacteria and leads to a weaker cyanobacterial summer bloom.

In conclusion, our warming simulations reveal that adaptation reduces ecological phytoplankton responses to global warming in terms of changes in bloom timing and amplitude. This finding matches findings from previous theoretical modeling studies. For example, Barabás and D'Andrea (2016) found that communities that can evolve are much more robust against environmental change. Similarly, Northfield and Ives (2013) found that if global warming leads to conflicting interests between species (i.e., stronger competition), coevolution reduces warming-related effects and hence changes in species abundance.

Effects of RES resuspension

In our simulations, the resuspension of resting cells (or propagules) tends to slow down adaptation to global warming, which is expressed by slightly stronger shifts in bloom timing and a stronger cyanobacterial summer bloom. We can explain the observed slowing effect of resuspension by the re-introduction of past-adapted resting cells to the actively growing population. A similar slowing effect was observed for lake copepods (Hairston Jr and De Stasio Jr, 1988). However, some studies suggest that propagule banks can aid phytoplankton to cope with environmental change as they contain a high diversity of genotypes (Ribeiro et al., 2013; Kremp et al., 2016). The effect of resuspension on adaptation seems to depend on whether the resuspended genotypes are a random or nonrandom sample of the total gene pool (Hairston Jr and De Stasio Jr, 1988; Rengefors et al., 2017). For layered sediments, this suggests that the resuspended sample of the total gene pool, and hence the effect of resuspension on adaptation, are affected by the adaptation history of the population.

In our study, propagule banks are formed in an initially steady environment that transforms into a steadily warming environment. Under steady conditions, all taxa adapt to lower temperatures, with adaptation being weakened by resuspension. Thus, when temperatures begin to increase, initial optimum temperatures are higher in the warming scenario with resuspension WAR than in the warming scenario without resuspension WA. Due to the previous adaptation to colder temperatures, the sediment additionally contains genotypes that are adapted to even higher temperatures than the actively growing population at the beginning of WAR. This raises the question of why resuspension slows down adaptation to higher temperatures instead of enhancing it. During the 100 yr of steady environmental conditions in CAR, most adaptation to colder temperatures occurs during the first ~ 70 yr (Fig. A11 in Appendix A.4), meaning that warm-adapted genotypes are buried deep in the sediment. As resuspension probability decreases exponentially with time in our model, the number of resuspended warm-adapted genotypes is negligible compared with the number of cold-adapted genotypes that are resuspended. Thus, the slowing effect of resuspension dominates in our warming simulations. Indeed, the higher optimum temperatures in the beginning of WAR are outpaced after $\sim 60-80$ yr by the faster adaptation in WA, leading to the lag in adaptation that we observe after 100 yr of warming (Fig. A11 in Appendix A.4). The lag in adaptation in WAR leads to a stronger shift of the two diatom blooms towards winter, which reduces the competition between spring diatoms and cyanobacteria and hence allows for a stronger cyanobacterial summer bloom.

In addition, resuspension narrows the T_{opt} trait distributions of both dinoflagellates and cyanobacteria, which are much more affected by slowed adaptation than diatoms. We suggest that the lesser effect of resuspension on diatoms results from the two diatom blooms per year, which may allow for faster adaptation. Indeed, a comparison of the additional CA simulations using only dinoflagellates with those using only diatoms reveals that diatoms have the potential to adapt much faster than dinoflagellates when not restricted by interspecific competition (Fig. A12 in Appendix A.4). During the first 4 yr of simulation, when the diatom spring and autumn blooms have not merged yet, diatoms adapt more than 2 times faster than dinoflagellates.

To conclude, our results show that resuspension of resting cells tends to slow down adaptation. Our results, however, strongly depend on adaptation history. We suggest for future work to further investigate the effect of adaptation history on resuspension.

Model biases and suggestions for future work

Below, we describe the major assumptions and simplifications that we made in our model and discuss which model biases they may imply. In addition, we give suggestions for future work.

It is a major challenge to parameterize the transfer between different life cycle stages, for which we need information on triggers and rates of transition. As both parameters are poorly constrained, we must estimate them though model calibration. However, the parameters estimated for present-day conditions may not be applicable to a global warming scenario. As revealed by resurrection experiments, the cold-water dinoflagellate *A. malmogiense* showed a decrease in the encystment rate over the past century of global warming, while the temperature threshold for encystment remained unchanged (Hinners et al., 2017). Consequently, different life cycle traits seem to respond differently to environmental change, meaning that further experimental research is needed to improve the model parameterization of phytoplankton life cycles.

Another potential model bias affects our mutational algorithm. We simulate trait changes due to random mutations (and sexual recombination) by randomly sampling the modified trait value from a Gaussian distribution centered at the original trait value. The width of this distribution, i.e., the standard deviation of mutations, cannot be measured directly in the laboratory and must hence be estimated through model calibration. For our simulations, we used the same value as (Beckmann et al., 2019) (see section "Model concept"). In our warming scenario WA, dinoflagellates, diatoms, and cyanobacteria show an average increase in T_{opt} of $\sim 0.14\,^{\circ}\mathrm{C}$ per decade for a steady temperature increase of 0.3 °C per decade. As evolution experiments can neither replicate the complexity of marine ecosystems nor the time scales of global warming, we compare our simulated adaptation rates to observations. Evaluating 15 yr of observational data for 67 species, Irwin et al. (2015) found a mean increase in the realized niche of 0.45 °C for a mean temperature increase of 0.73 °C, giving an average adaptation rate of 0.3 °C per decade. Thus, our simulations show adaptation rates of the same order of magnitude. The slightly slower adaptation in our simulations may result from the slower temperature increase (0.3 °C per decade vs. 0.45 °C per decade), leading to a lower selection pressure. For higher selection pressures, e.g., over the course of the seasonal cycle, we observe higher adaptation rates in the range of $\sim 0.18\,^{\circ}\mathrm{C}$ within 1 month for dinoflagellates (Fig. A7 in Appendix A.4), which suggests that our chosen mutational standard deviations are not artificially limiting adaptation to temperature changes.

Being the focus of our study, phytoplankton adaptation is simulated with a high degree of complexity, while adaptation of zooplankton is not taken into account. As we consider zooplankton merely for the sake of grazing mortality, we use a simplistic representation, where we ignore potential zooplankton adaptation, life cycle dynamics, and effects of irradiance and temperature on grazing. Thus, the zooplankton in our model is entirely controlled by phytoplankton, which leads to comparable responses to global warming in terms of increasing abundances and shifts in bloom timing. Observations showed that the abundance of herbivorous zooplankton is strongly controlled by their phytoplankton prey (Richardson and Schoeman, 2004), while phenological shifts synchronized with phytoplankton are mainly associated with fast-growing zooplankton (Adrian et al., 2006; Dam, 2013). This suggests that our representation of zooplankton may be reasonable for fast-growing taxa like *Daphnia*, while our model is inappropriate to represent slow-growing taxa with more complex life cycles like copepods (Adrian et al., 2006). We expect that an explicit simulation of the adaptation of fast-growing zooplankton would not change our results notably. Adaptation of slow-growing zooplankton, however, may have a larger effect, but we still do not expect qualitative changes. Future work can expand on our model and include a more complex representation of zooplankton, including light- and temperature-dependent grazing, life cycle dynamics, and adaptation.

Another bias is that our model cannot capture the functional diversity of the real-world Baltic Sea phytoplankton community. Our model community consists of three major functional groups (dinoflagellates, diatoms, and cyanobacteria), each represented by one taxon or by an averaged complex. Thus, we do not account for other important groups such as ciliates or other flagellates (Thamm et al., 2004) and for the functional diversity within each group. Most likely, across-species functional diversity within a functional group greatly enhances the group's potential to adapt to environmental changes (Litchman et al., 2015). With that in mind, we might be missing other key competitors like summer-blooming dinoflagellate or diatom species. Based on our own findings, the absence of these competitors most likely influences both phenology and adaptation of our focal phytoplankton taxa. For the above reasons, we do not interpret our results quantitatively but focus on analyzing qualitative differences between scenarios and identifying general eco-evolutionary mechanisms. We suggest that future work builds on our findings and investigates which role diversity within functional groups plays in the Baltic Sea phytoplankton community regarding both competition and adaptive potential.

Finally, as mentioned in section "Deviations in spring bloom timing", our model is currently not coupled to a physical ocean model. Thus, we ignore physical processes like vertical mixing and stratification, which may, e.g., affect our simulated species succession during phytoplankton spring bloom. In addition, our 0-dimensional model setup leads to an unrealistic adaptation pattern of cyanobacteria. Under warming conditions, preadapted cyanobacteria adapt to even higher temperatures and hence evolve away from environmental temperature. We can explain this apparent maladaptation by our 0-dimensional representation of competition. Nitrogen concentration is low at the end of the diatom spring bloom when vegetative cyanobacteria start to grow. As warm conditions are favorable for cyanobacteria, they grow faster and become nitrogen-limited more quickly than under control conditions. With nitrogen recovering over time due to nitrogen fixation and remineralization, the environment selects for later-blooming vegetative cyanobacteria with higher optimum temperatures. We expect that by resolving the spatial distribution of nitrogen in a 1D or 3D physical environment, our model would simulate a more realistic adaptation pattern of cyanobacteria. Previous 1D models showed that diatoms may shift their spring bloom to deeper water layers when nitrogen gets depleted at the surface (Warns, 2013; Lee et al., 2018). As cyanobacteria can grow more efficiently than diatoms on low nitrogen due to their smaller size (Litchman et al., 2007), they could take over growth at the surface on the remaining nitrogen without competing directly with diatoms. As a result, cyanobacteria would no longer experience an unrealistic selection pressure towards higher temperatures. Still, we think that the coupling to a physical model would not change our main results and conclusions.

Based on the above discussion, we can conclude that a physical environment would make our model more realistic. In turn, however, our model would also be a valuable addition to existing coupled biological-physical models. Existing models for the Baltic Sea project a notable increase in cyanobacteria biomass in the future if nutrient loads are not reduced (Meier et al., 2012a; Hense et al., 2013). As these models ignore phytoplankton adaptation, they may systematically overestimate warming-related changes in cyanobacteria biomass. Integrating our model into a coupled biological-physical model could hence notably improve climate projections. As long-term evolutionary data (e.g., from sediment archives) become available, these will moreover represent a valuable source for model calibration. As improving climate projections is relevant for political decision-making, we suggest for future work to test our or a similar approach in a coupled biological-physical environment.

Conclusions

Our modeling study demonstrates that the combined effects of phytoplankton competition and adaptation may differ from their separate effects. Both processes influence each other and shape phytoplankton communities through their interplay. The outcome of this interplay depends on environmental conditions.

In a steady environment, each functional group occupies a fixed niche in which it can improve its growth conditions through adaptation. The main driver of adaptation is given by the most limiting factor for growth. For nitrogen fixers, temperature appears to be the main driver, while it is nitrogen for nitrogen-limited groups. Nitrogen-limited groups maximize their growth rate by adapting to the temperature that coincides with the highest nitrogen concentration within their niche. If groups are inferior competitors, they adapt to avoid interspecific competition for nitrogen. If groups are superior competitors or if no competitor is present, adaptation is driven by intraspecific competition for nitrogen. In a changing environment, however, niches are no longer fixed and thus, groups can no longer avoid competition. Adaptation allows inferior competitors to increase their competitivity and hence to mitigate the dominance of superior competitors.

In conclusion, the role of adaptation cannot be neglected in changing environments, otherwise warming-related changes in taxa dominance (and bloom timing) can be systematically overestimated. To realistically simulate phytoplankton responses to environmental changes, future ecosystem models must consider both competition and adaptation. Moreover, our results demonstrate that adaptation can be affected by dormant resting cells that are resuspended from the sediment. Our study highlights that eco-evolutionary ecosystem models represent a powerful tool to estimate phytoplankton responses and even ecosystem responses to global warming. Future work can build on our model and expand on our representation of competition, e.g., by including multiple limiting nutrients and/or a physical environment. In addition, future models can integrate emerging evolutionary data based on long-term data series (e.g., from sediment archives). The integration of such data will allow us to further improve projections of future ecosystem changes in response to anthropogenic environmental change.

2.2 Study II: The effect of adaptation on ecosystem functioning

Phytoplankton adaptation to steady or changing environments affects marine ecosystem functioning

Isabell Hochfeld & Jana Hinners

Global warming poses a major threat to marine ecosystems, which fulfill important functions for humans and the climate. Ecosystem models are therefore increasingly used to estimate future changes in the functioning of marine ecosystems. However, projections differ notably between models. We propose that a major uncertainty factor in current models is that they ignore the high adaptive potential of phytoplankton, key players in marine ecosystems. Here, we use a 0-dimensional evolutionary ecosystem model to study how phytoplankton adaptation can affect estimations of future ecosystem-level changes. We found that phytoplankton adaptation can notably change simulated ecosystem dynamics, with the effect depending on environmental conditions. In a steady environment, adaptation allows for a more efficient use of resources, which enhances primary production and related ecosystem functions. In a warming environment, on the contrary, adaptation mitigates dominance changes among functionally different taxa and consequently leads to weaker changes in related ecosystem functions. Our results demonstrate that by neglecting phytoplankton adaptation, models may systematically overestimate future changes in the functioning of marine ecosystems. Future work can build on our results and include evolutionary processes into more complex model environments.

Submitted to Biogeosciences

Introduction

Global warming leads to a rapid reorganization of marine ecosystems, which poses a major threat to their functioning (Pecl et al., 2017). Since changes in the functioning of marine ecosystems directly impact humans and even feed back on the climate, understanding them is crucial (Pecl et al., 2017; Prentice et al., 2015). Ecosystem models have proven a valuable tool in this regard, but projections differ notably between models (Laufkötter et al., 2015, 2016). Current models largely ignore the high adaptive potential of phytoplankton (Laufkötter et al., 2015, 2016; Munkes et al., 2021), which are key players in marine ecosystems (Litchman et al., 2015). Here, we fill this gap by using an evolutionary ecosystem model to study the effect of phytoplankton adaptation to global warming on projected changes in ecosystem functioning. We apply the model to the Baltic Sea, which is impacted by above-average levels of multiple stressors (Reusch et al., 2018).

Phytoplankton contribute about half of global photosynthesis (Field et al., 1998), are the foundation of the marine food web (Fenchel, 1988), drive biogeochemical cycles (Hutchins and Fu, 2017), and even feed back on the physical properties of the ocean (Hense, 2007; Sathyendranath et al., 1991). Furthermore, phytoplankton-related ecosystem functioning feeds back on the climate, e.g., through changes in the export of atmospheric carbon into deeper water layers (biological carbon pump) (Basu and Mackey, 2018) or the planktonic production of dimethyl sulfide, which seeds cloud formation (Wingenter et al., 2007). However, due to global warming, the role of phytoplankton in marine ecosystems is changing.

Phytoplankton respond to global warming through changes in phenology, which are expressed, for example, in an earlier and prolonged blooming season in the Baltic Sea (Wasmund et al., 2019). The resulting mismatches with higher trophic levels like zooplankton and fish alter food web structures and may eventually lead to ecosystem-level changes (Asch et al., 2019; Edwards and Richardson, 2004; Winder and Schindler, 2004a). In addition, the poleward migration of phytoplankton causes changes in species composition and abundance (Poloczanska et al., 2013), which may additionally affect zooplankton and fish stocks (Fossheim et al., 2015). Indeed, fisheries are already impacted by warming-related changes (Peterson et al., 2017). Finally, warming and eutrophication promote harmful algal blooms, which pose a threat to animal and human health (Gobler et al., 2017; Paerl et al., 2015; Glibert et al., 2014). To conclude, ongoing global warming will lead to changes in phytoplankton and consequently, to changes in the functioning of marine ecosystems. Since these changes are expected to have a direct impact on human well-being and the climate (Pecl et al., 2017; Prentice et al., 2015), predicting them is of great importance.

Ecosystem models offer the possibility to assess future changes in ecosystem functioning. For example, ecosystem models can be integrated into global ocean circulation models to simulate future changes in net primary production on global scale, but models do not even agree on the direction of change (Laufkötter et al., 2015). Similarly, regional models for the Baltic Sea cannot agree on the future development of cyanobacteria blooms regarding timing, concentrations, and nitrogen fixation (Hense et al., 2013; Meier et al., 2011; Neumann, 2010). These uncertainties can notably affect estimations of future ocean deoxygenation (Long et al., 2021), nutrient load (Reusch et al., 2018; Wasmund et al., 2001), and harmful algal bloom dynamics (Hallegraeff, 2010; Paerl et al., 2015). To conclude, the validity of current model projections remains questionable. Since model projections form the base of political decision-making (Intergovernmental Panel on Climate Change (IPCC), 2022; Meier et al., 2014), there is an urgent need to improve their informative value. A first step could be to identify the key processes that affect ecosystem functioning. One key process that is lacking in all models above and similar models (Daewel and Schrum, 2013;

Dzierzbicka-Głowacka et al., 2013; Savchuk, 2002) is the evolutionary adaptation of phytoplankton.

Their large population sizes and short generation times allow phytoplankton to adapt quickly to environmental changes. Evolution experiments, observations, and resurrection experiments showed that phytoplankton adaptation can be relevant on perennial or even shorter time scales (Jin and Agustí, 2018; Irwin et al., 2015; Hattich et al., 2024). Due to the crucial role of phytoplankton in marine ecosystems, considering phytoplankton adaptation in models may notably change projected changes in ecosystem functioning (Ward et al., 2019).

Some ecosystem models already consider the evolutionary adaptation of phytoplankton. So far, evolutionary ecosystem models have generally been used to study the spatial distribution and/or temporal evolution of different functional traits (Le Gland et al., 2021; Beckmann et al., 2019; Sauterey et al., 2017). Only a few evolutionary ecosystem models have already addressed questions related to ecosystem functioning. For example, Smith et al. (2016) identified a trade-off between phytoplankton size diversity and productivity depending on the frequency of environmental disturbance. Sauterey and Ward (2022) investigated drivers of phytoplankton C:N stoichiometry, which affects the efficiency of the biological carbon pump. Finally, Cherabier and Ferrière (2022) studied the effect of bacterial adaptation to global warming on the microbial loop and the resulting impact on primary production.

So far, however, no model has explicitly addressed the question of how phytoplankton adaptation to global warming could affect the functioning of a marine ecosystem. A first step might be to estimate the effect of adaptation on warming-related changes in phytoplankton community composition. Different phytoplankton functional groups fulfill different functions in the ecosystem, for example, by contributing differently to the biological carbon pump (sinking speed), the nitrogen cycle (nitrogen fixation), and the energy transfer to higher trophic levels (food quality, susceptibility to predation) (Litchman et al., 2015). To our knowledge, there is only one model to date that considers competition between multiple phytoplankton functional groups and their adaptation to global warming simultaneously (Hochfeld and Hinners, 2024). Using this model, Hochfeld and Hinners (2024) demonstrated that adaptation can significantly reduce simulated phytoplankton responses to global warming in terms of changes in bloom timing and relative taxa abundance. However, it has not been studied yet how adaptation-related changes in phytoplankton responses may affect ecosystem functioning.

Here, we use a slightly modified version of the Hochfeld and Hinners (2024) model to estimate for the first time how phytoplankton adaptation may affect warming-related changes in different ecosystem functions, including primary production, secondary production, carbon export, nitrogen fixation, and resource use efficiency (RUE). We apply the model to the Baltic Sea, which is already impacted by above-average levels of warming, nutrient load, and deoxygenation (Reusch et al., 2018). Due to the 0-dimensional setup of the model, we do not evaluate absolute changes in ecosystem functions. Instead, we focus on how phytoplankton adaptation may change the future contribution of primary production to these ecosystem functions. Our study is a first step to improve model projections of future ecosystem-level changes that future work can build upon.

Materials and Methods

Model description

To study how phytoplankton adaptation to global warming may affect simulated future changes in ecosystem functioning, we slightly extended the model from Hochfeld and Hinners (2024). A more detailed description of the model is available in Hochfeld and Hinners (2024) and the associated supplementary material. The model simulates the dynamics of phytoplankton, zooplankton, dissolved inorganic nitrogen, and dead organic matter (detritus) in a 0-dimensional framework (Fig. 2.2.1). Since we focus on phytoplankton and their functions in the marine ecosystem, we resolve three different phytoplankton functional groups. Like Hochfeld and Hinners (2024), we chose three of the most common functional groups in the Baltic Sea, dinoflagellates, diatoms, and diazotrophic cyanobacteria, and represent each group by a common taxon or by a complex of common taxa. For dinoflagellates and diatoms, we simulate two cold-water species of the genera *Apocalathium* and *Thalassiosira*, respectively. For cyanobacteria, we simulate a complex that includes the most abundant nitrogen-fixing genera in the Baltic Sea, *Nodularia*, *Aphanizomenon*, and *Anabaena* (Karlsson et al., 2005; Stal et al., 2003). Since we assume that the cyanobacteria complex produces toxins, the cyanobacteria in our model are not grazed by zooplankton, which is consistent with other modeling studies (Hense and Beckmann, 2006; Hinners et al., 2015; Lee et al., 2018). Dinoflagellates and diatoms, on the contrary, are grazed equally by zooplankton.

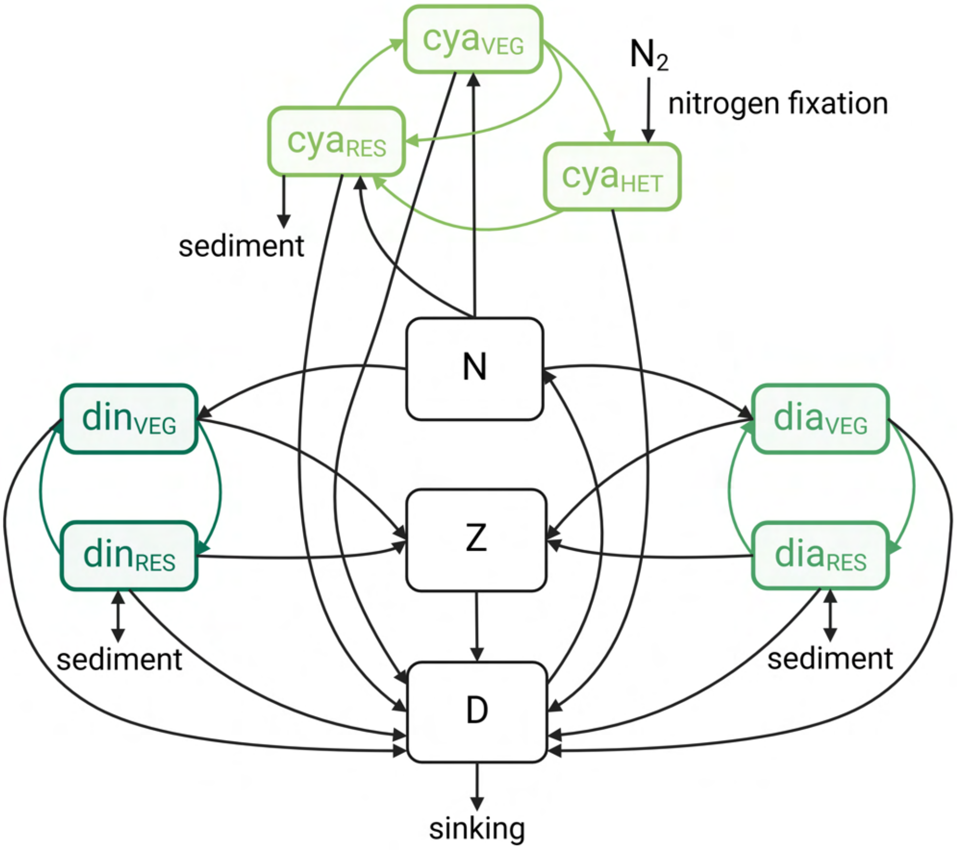

Figure 2.2.1: Components of the ecosystem model including compartments for dissolved inorganic nitrogen (N), detritus (D), and zooplankton (Z), along with agent-based life cycles of dinoflagellates (din), diatoms (dia), and cyanobacteria (cya). Each life cycle is represented by a resting stage (RES) and a vegetative growing stage (vegetative cells, VEG). For cyanobacteria, the model simulates a second, nitrogen-fixing growing stage (vegetative cells with heterocysts, HET). The figure additionally shows the nitrogen fluxes between the different ecosystem components, and the sinks and sources of nitrogen (sinking of detritus, burial of phytoplankton resting cells and resuspension of phytoplankton resting cells, cyanobacterial nitrogen fixation). The figure was adapted from Hochfeld and Hinners (2024) and created with BioRender.com.

To ensure an accurate representation of phytoplankton phenology under warming conditions, the model explicitly resolves phytoplankton life cycle dynamics. For all functional groups, the model differentiates between a resting stage and a vegetative growing stage, with growth being limited by light, temperature, and dissolved inorganic nitrogen. The cyanobacteria life cycle additionally includes a diazotrophic growing stage, which can fix atmospheric nitrogen (N_2) and is therefore not limited by dissolved inorganic nitrogen. The diazotrophic growing stage of cyanobacteria is hence the only phytoplankton growing stage in the model that does not take up dissolved inorganic nitrogen. The nitrogen content of the dead phytoplankton and zooplankton biomass fills the detritus pool, which is constantly remineralized back into bioavailable nitrogen. Nitrogen is lost from the system through sinking of detritus and stochastic burial of phytoplankton resting cells, and can be replenished through the resuspension of previously buried resting cells and cyanobacterial nitrogen fixation.

The model does not only consider competition for nitrogen between different phytoplankton taxa, but also changes in two temperature-dependent functional traits. The first flexible trait, the optimum temperature for growth, adapts through random mutations. Cell size, on the contrary, responds plastically to temperature, with the cell size decreasing linearly with increasing temperature (Atkinson et al., 2003). For further details on the implementation of mutations and plasticity, see Hochfeld and Hinners (2024). The model also takes into account that changes in cell size influence metabolic cell properties (Litchman et al., 2007; Marañón et al., 2013; Ward et al., 2017), which in turn determine the nitrogen-limited growth rate (Grover, 1991). Since trait changes such as those described above affect individual cells, the model uses an agent-based approach after Beckmann et al. (2019) to simulate the dynamics of agents (super-individuals) with their individual phenotypic trait values. Zooplankton, dissolved inorganic nitrogen, and detritus, on the contrary, are represented by compartments, i.e., collections of cells or molecules described by their averaged properties and their concentration.

Ecosystem functions

Our extended version of the Hochfeld and Hinners (2024) model allows us to analyze different ecosystem functions, including carbon export, cyanobacterial nitrogen fixation, and resource use efficiency (RUE).

We calculate carbon export from the carbon content of buried phytoplankton resting cells and the carbon that is exported through sinking of detritus. Detritus contains the dead phytoplankton and zooplankton cells, as well as the remains from unassimilated feeding. Following Ward et al. (2012), we divide detritus into dissolved inorganic matter (DOM) and particulate organic matter (POM), of which only POM is exported into deeper water layers. For the taxonomic groups in our model, we divide detritus 50:50 between POM and DOM (Ward et al., 2012). Since the model calculates in nitrogen units, we use the Redfield ratio to convert nitrogen into carbon (Redfield, 1934).

To determine the amount of fixed atmospheric nitrogen, we assume that all the fixed nitrogen is converted into biomass. Thus, we define nitrogen fixation as the biomass built up by the diazotrophic cyanobacteria life cycle stage during each time step.

Following Ptacnik et al. (2008), we calculate resource use efficiency (RUE) as the ratio of phytoplankton biomass and dissolved inorganic nitrogen. Since the cyanobacteria in our model can fix atmospheric nitrogen, we use simulations without cyanobacteria to derive RUE. Hence, we only consider the RUE of dinoflagellates and diatoms. Both dinoflagellates and diatoms are grazed by zooplankton; to avoid grazing-related biases in RUE, we additionally exclude zooplankton from RUE simulations.

Model scenarios

To understand how the adaptation of phytoplankton to different environments affects model estimations of related ecosystem functions, we implement four different model scenarios based on Hochfeld and Hinners (2024) (Table 2.2.1). We perform seven simulations for each scenario and average the output to ensure robust results. Each simulation is run over 100 yr.

Table 2.2.1: Overview of the four model scenarios that we evaluate in this article. For each scenario, we run seven different simulations over 100 yr and average the output. "Control" represents a present-day seasonal temperature forcing for the Gulf of Finland. "Warming" adds a constant temperature increase of 0.3 °C per decade to the control forcing (IPCC scenario SSP3-7.0, Allan et al., 2021).

	No adaptation	Adaptation
Control	C	CA
Warming	W	WA

The first two model scenarios, C (control) and CA (control and adaptation), are control scenarios that use a steady seasonal temperature and irradiance forcing for present-day conditions in the Gulf of Finland. The forcing is the same as in Hochfeld and Hinners (2024). The two control scenarios C and CA serve as spin up for two global warming scenarios W (warming) and WA (warming and adaptation). We simulate global warming by adding a steady temperature increase of 0.3 °C per decade to the seasonal temperature forcing, which is equivalent to the IPCC scenario SSP3-7.0 (Allan et al., 2021). Adaptation in the optimum temperature is disabled for C and W but enabled for CA and WA. In this way, we can study how the (in)ability of phytoplankton to adapt to their environment may affect ecosystem functioning.

In the four model scenarios presented above, the resuspension of phytoplankton resting cells from the sediment is disabled. Hochfeld and Hinners (2024) found that resuspension tends to slow down adaptation to global warming and can hence weaken adaptation-related effects. For completeness, we performed additional control and warming simulations in which we enabled resuspension (CAR: control and adaptation and resuspension; WAR: warming and adaptation and resuspension) and observed a similar effect. Thus, we do not explicitly analyze and discuss these simulations here; an example is shown in Fig. B1 in Appendix B.2.

Results

Seasonal phytoplankton dynamics

The seasonal phytoplankton dynamics and the reasons for differences between scenarios are described in detail in Hochfeld and Hinners (2024). In summary, the two control scenarios C and CA produce a realistic seasonal cycle for the focal phytoplankton taxa, including a spring bloom of dinoflagellates and diatoms, a summer bloom of cyanobacteria, and a second but weaker bloom of diatoms in autumn (Fig. 2.2.2). In CA, where phytoplankton can adapt, competition for nitrogen drives adaptation to individual temperature niches, which reduces competition pressure. Due to reduced competition with diatoms, cyanobacteria can initiate a stronger summer bloom, which increases the amount of nitrogen in the system through nitrogen fixation. The higher concentration of nitrogen, in turn, allows for stronger blooms of dinoflagellates and diatoms.

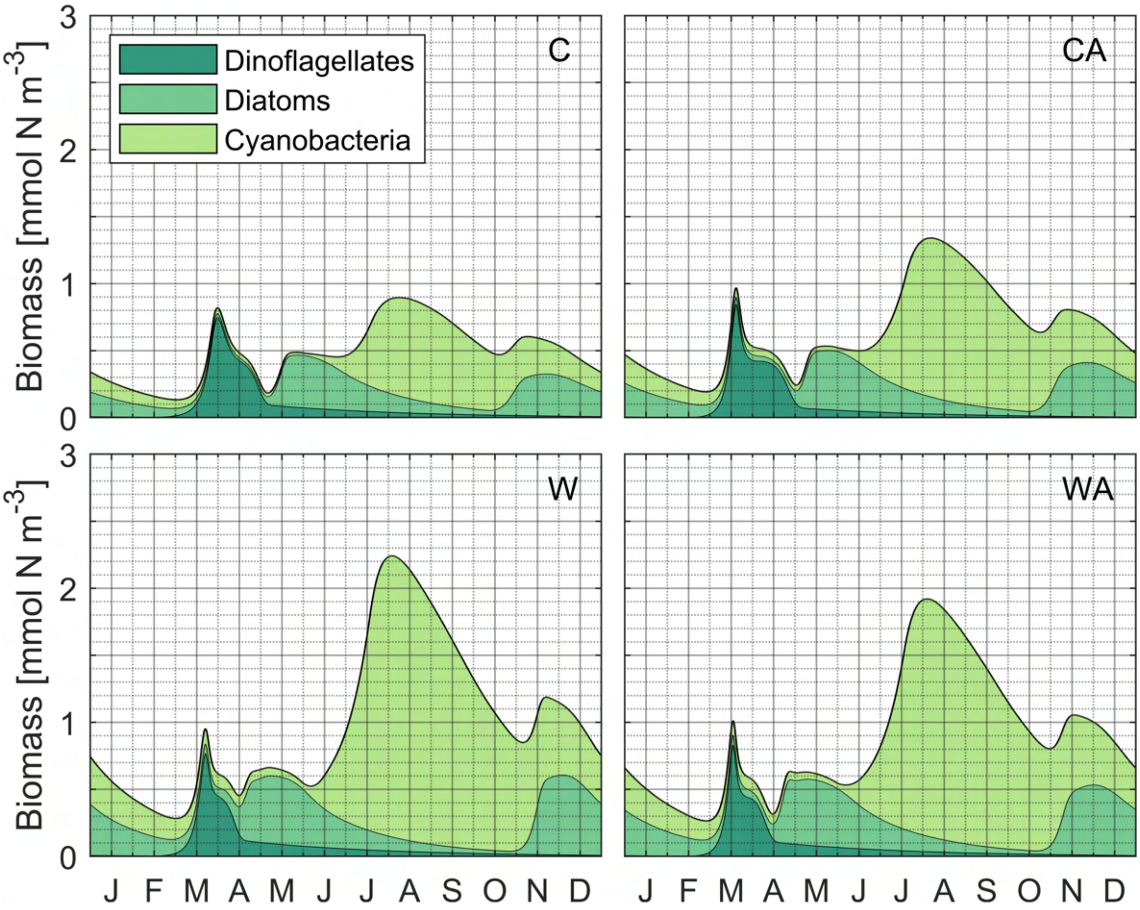

Figure 2.2.2: Accumulated phytoplankton biomass during the last simulation year of the four different model scenarios (C: control; CA: control and adaptation; W: warming; WA: warming and adaptation). For each scenario, the output of seven different simulations was averaged. The colors indicate the share of dinoflagellates, diatoms, and cyanobacteria in the total phytoplankton biomass.

The two warming scenarios W and WA were found to reproduce trends that have been observed in the Baltic Sea over the past decades (Hochfeld and Hinners, 2024), including an earlier and prolonged phytoplankton blooming season (Wasmund et al., 2019) as well as an increase in cyanobacteria biomass in summer (Suikkanen et al., 2007). The warming-related changes in bloom timing and cyanobacteria biomass were shown to be weaker in the presence of adaptation by up to $\sim 9\,\mathrm{d}$ and $56\,\%$, respectively (Hochfeld and Hinners, 2024). Adaptation to the increasing temperatures in WA enhances the competitivity of non-preadapted taxa. Thus, non-preadapted diatoms can compete more strongly with preadapted cyanobacteria, which leads to a weaker cyanobacterial summer bloom (Hochfeld and Hinners, 2024).

Seasonal zooplankton dynamics

For all model scenarios, zooplankton biomass peaks during phytoplankton spring bloom following the peak in phytoplankton biomass; remember that we simulate cyanobacteria as single summer-blooming phytoplankton taxon, which we assume to be non-grazeable due to toxicity. Despite these simplifications in the model, the simulated seasonal pattern is indeed reasonable for some of the common zooplankton taxa in the Baltic Sea (Feike et al., 2007; Dutz et al., 2010). Although all four model scenarios agree on a general seasonal pattern, both bloom timing and amplitude differ notably between them (Fig. 2.2.3 and Table 2.2.2), with the differences being statistically significant according to a t-test (Table B1 in Appendix B.1).

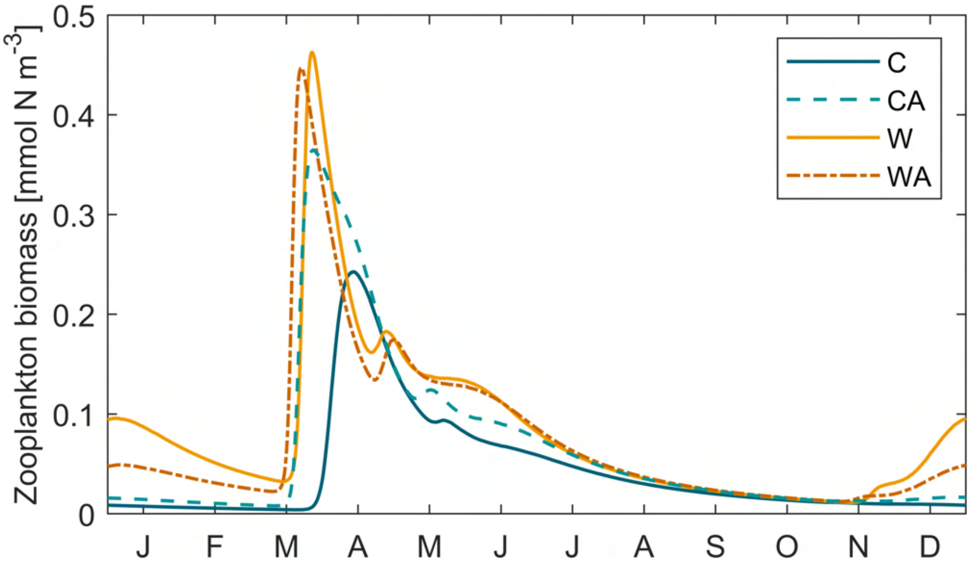

Figure 2.2.3: Zooplankton biomass during the last simulation year of the four different model scenarios (C: control; CA: control and adaptation; W: warming; WA: warming and adaptation). For each scenario, we averaged the output of seven different simulations.

Table 2.2.2: Average zooplankton timing, peak abundance, and time lag to the phytoplankton peak in spring for the two control scenarios C (control) and CA (control and adaptation), along with the associated standard deviations. Also shown are the corresponding average warming-related changes in W (warming) and WA (warming and adaptation), including propagated errors. For each scenario, we calculated average values from the last simulation year of seven different simulations. Please note that warming-related changes in zooplankton peak abundance are not presented as absolute values but as relative changes. A series of t-tests revealed that the differences between all four scenarios are statistically significant at the 0.05 level; see Table B1 in Appendix B.1 for details.

	C	CA	W	WA
Timing [d]	102.4 ± 2.0	86.5 ± 2.4	-16.9 ± 2.3	-5.5 ± 2.6
Abundance $\left[\mu\mathrm{mol\,N\,m^{-3}}\right]$	244.8 ± 17.2	373.0 ± 46.0	$+92.4\,\% \pm 7.4\,\%$	$+21.2\,\% \pm 13.0\,\%$
Time lag [d]	12.9 ± 2.4	8.0 ± 2.5	-8.7 ± 2.8	-3.5 ± 2.8

In the control scenario with phytoplankton adaptation, CA, we observe an earlier and stronger zooplankton bloom than in the control scenario without phytoplankton adaptation, C (Fig. 2.2.3). In CA, zooplankton peak ~ 16 d earlier than in C with a ~ 52 % higher peak amplitude (Table 2.2.2). These findings resemble the dynamics of phytoplankton under control conditions, which develop an earlier and stronger spring bloom if they can adapt (Fig. 2.2.2).

Likewise, zooplankton show similar responses as phytoplankton to global warming, including a shift in bloom timing towards winter and an increase in peak amplitude, with the responses being weaker when phytoplankton adaptation is enabled (Fig. 2.2.3). While the zooplankton spring bloom peaks ~ 17 d and ~ 5 d earlier in W and WA, bloom amplitude increases by ~ 92 % and ~ 21 %, respectively (Table 2.2.2). In conclusion, zooplankton strongly resemble the dynamics of phytoplankton in all four model scenarios.

Irrespective of these similarities between phytoplankton and zooplankton, however, the time lag between their bloom peaks differs notably between the four model scenarios. Under control conditions, we observe a time lag of ~ 13 d and ~ 8 d in C and CA, respectively (Table 2.2.2).

The two warming scenarios W and WA, on the contrary, produce a comparable and notably shorter time lag of only ~4 d. Thus, in our simulations, warming seems to reduce the time lag between phytoplankton and zooplankton blooms. In addition, we find that the time lag correlates negatively with the peak amplitudes of both phytoplankton and zooplankton, meaning that the higher the amplitude, the shorter the time lag (Fig. B2 in Appendix B.2). While both correlations are significant, the time lag correlates notably stronger with zooplankton peak amplitude than with phytoplankton peak amplitude ($r\,(26) = -0.99$, $p = 2.05 \times 10^{-21}$ for zooplankton and $r\,(26) = -0.81$, $p = 2.41 \times 10^{-7}$ for phytoplankton).

Annual balances

The annual balances of different ecosystem functions are shown in Fig. 2.2.4 for the last simulation year of all model scenarios. Figure 2.2.4 reveals that phytoplankton produce ~10 times more biomass than zooplankton per year and hence dominate biomass production in our simulations. Primary production, in turn, is dominated by cyanobacteria, while dinoflagellates account for the smallest amount of primary production per year.

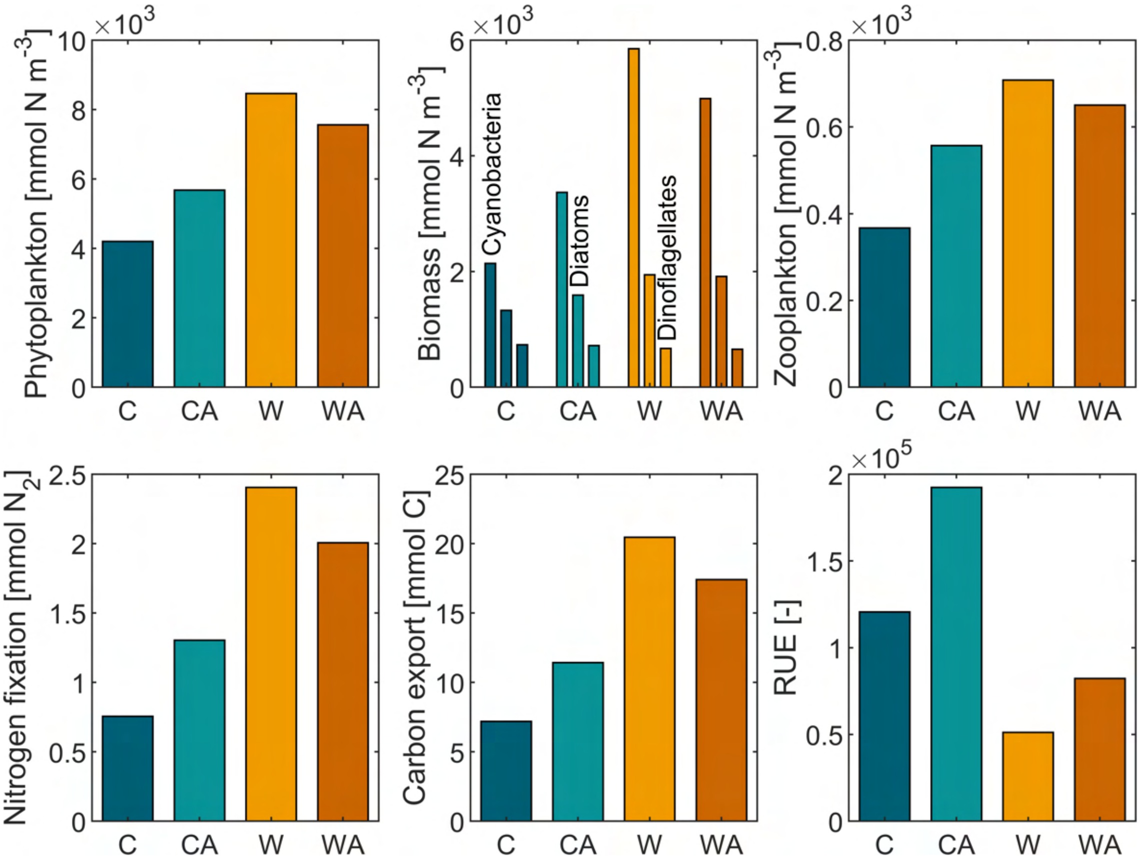

Figure 2.2.4: Annual balances of different ecosystem functions for the last simulation year of the four model scenarios (C: control; CA: control and adaptation; W: warming; WA: warming and adaptation). For each scenario, annual balances were averaged from seven different simulations.

For cyanobacteria, annual biomass increases under global warming, with the increase being by ~56 % weaker if thermal adaptation is enabled (Table 2.2.3). Under control conditions, on the contrary, cyanobacteria biomass is by ~52 % higher with thermal adaptation. While diatoms follow a similar trend, however with smaller differences between the scenarios, dinoflagellates show a contrasting development. Dinoflagellate annual biomass decreases slightly under global warming and is comparable between C and CA as well as W and WA, respectively. Thus, thermal adaptation does not seem to have a notable effect on the biomass production of dinoflagellates. Despite the contrasting development of dinoflagellates, total phytoplankton biomass follows the same trend as cyanobacteria and diatoms. This finding is underlined by strong positive correlations between total phytoplankton biomass, cyanobacteria, and diatoms, while dinoflagellates correlate negatively with all three (Fig. 2.2.5). In all four model scenarios, total phytoplankton biomass correlates strongest with cyanobacteria ($0.98 \leq r \leq 1$) and weakest with dinoflagellates ($-0.73 \leq r \leq -0.07$).

Table 2.2.3: Average annual balances for the two control scenarios C (control) and CA (control and adaptation), along with the associated standard deviations. Additionally shown are the corresponding average warming-related changes in W (warming) and WA (warming and adaptation), including propagated errors. For each scenario, we calculated average values from the last simulation year of seven different simulations. Please note that the warming-related changes in W and WA are not presented as absolute values but as relative changes. A series of *t*-tests demonstrated that the differences between all four model scenarios are statistically significant at the 0.05 level with only one exception (dinoflagellates in W and WA). See Table B2 in Appendix B.1 for details.

	C	CA	W [%]	WA [%]
Dinoflagellates $\left[\mathrm{mmol\,N\,m^{-3}}\right]$	732.7 ± 9.2	718.1 ± 15.1	-8.6 ± 2.4	-8.8 ± 3.0
Diatoms $\left[\mathrm{mmol\,N\,m^{-3}}\right]$	1327.6 ± 44.0	1591.8 ± 78.5	$+46.3 \pm 3.4$	$+20.2 \pm 5.1$
Cyanobacteria $\left[\mathrm{mmol\,N\,m^{-3}}\right]$	2140.8 ± 80.9	3367.2 ± 524.8	$+173.3 \pm 3.9$	$+48.2 \pm 15.9$
Phytoplankton $\left[\mathrm{mmol\,N\,m^{-3}}\right]$	4201.1 ± 121.9	5677.0 ± 597.2	$+101.4 \pm 3.0$	$+33.2 \pm 10.8$
Zooplankton $\left[\mathrm{mmol\,N\,m^{-3}}\right]$	366.9 ± 19.7	556.7 ± 51.0	$+92.9 \pm 5.5$	$+16.8 \pm 9.6$
N_2 fixation $\left[\mu\mathrm{mol\,N_2\,m^{-3}}\right]$	755.6 ± 40.3	1303.3 ± 246.3	$+218.1 \pm 5.4$	$+53.8 \pm 19.4$
Carbon export $\left[\mu\mathrm{mol\,C\,m^{-3}}\right]$	7194.9 ± 356.3	11429.0 ± 1868.9	$+184.1 \pm 5.0$	$+52.3 \pm 16.7$
RUE $\left[10^3\right]$	120.6 ± 3.7	192.3 ± 5.9	-57.6 ± 4.1	-57.2 ± 4.7

Zooplankton annual biomass also correlates positively with the annual biomasses of diatoms, cyanobacteria, and total phytoplankton. Under control conditions, correlation is strongest with diatoms ($r \geq 0.81$), while under global warming, zooplankton biomass correlates strongest with total phytoplankton biomass ($r \geq 0.60$). In addition, zooplankton biomass production is notably affected by phytoplankton adaptation, which is consistent with our findings from the previous section. Under control conditions, zooplankton produce by $\sim 52\,\%$ more biomass if phytoplankton can adapt. Under global warming, zooplankton biomass increases, with the increase being by $\sim 73\,\%$ weaker when phytoplankton adaptation is enabled.

The annual amount of fixed atmospheric nitrogen mirrors the annual biomass of cyanobacteria, which is confirmed by a strong positive correlation in all four model scenarios with $r \geq 0.99$. Under control conditions, cyanobacteria fix $\sim 72\,\%$ more nitrogen when adaptation is enabled. Global warming leads to an increase in nitrogen fixation, and hence the nitrogen input into the system, by $\sim 218\,\%$ in W and $\sim 54\,\%$ in WA, respectively.

Carbon export correlates positively with both phytoplankton and zooplankton biomass, with the correlation being stronger with phytoplankton, which dominate biomass production ($r \geq 0.90$ vs. $r \geq 0.69$). Among phytoplankton, carbon export correlates strongest with cyanobacteria, which dominate primary production ($r \geq 0.85$). In addition, carbon export is notably affected by phytoplankton adaptation. Under present-day conditions, carbon export is by $\sim 59\,\%$ higher in CA than in C. Global warming leads to an increase in carbon export by $\sim 184\,\%$ in W and $\sim 52\,\%$ in WA, respectively.

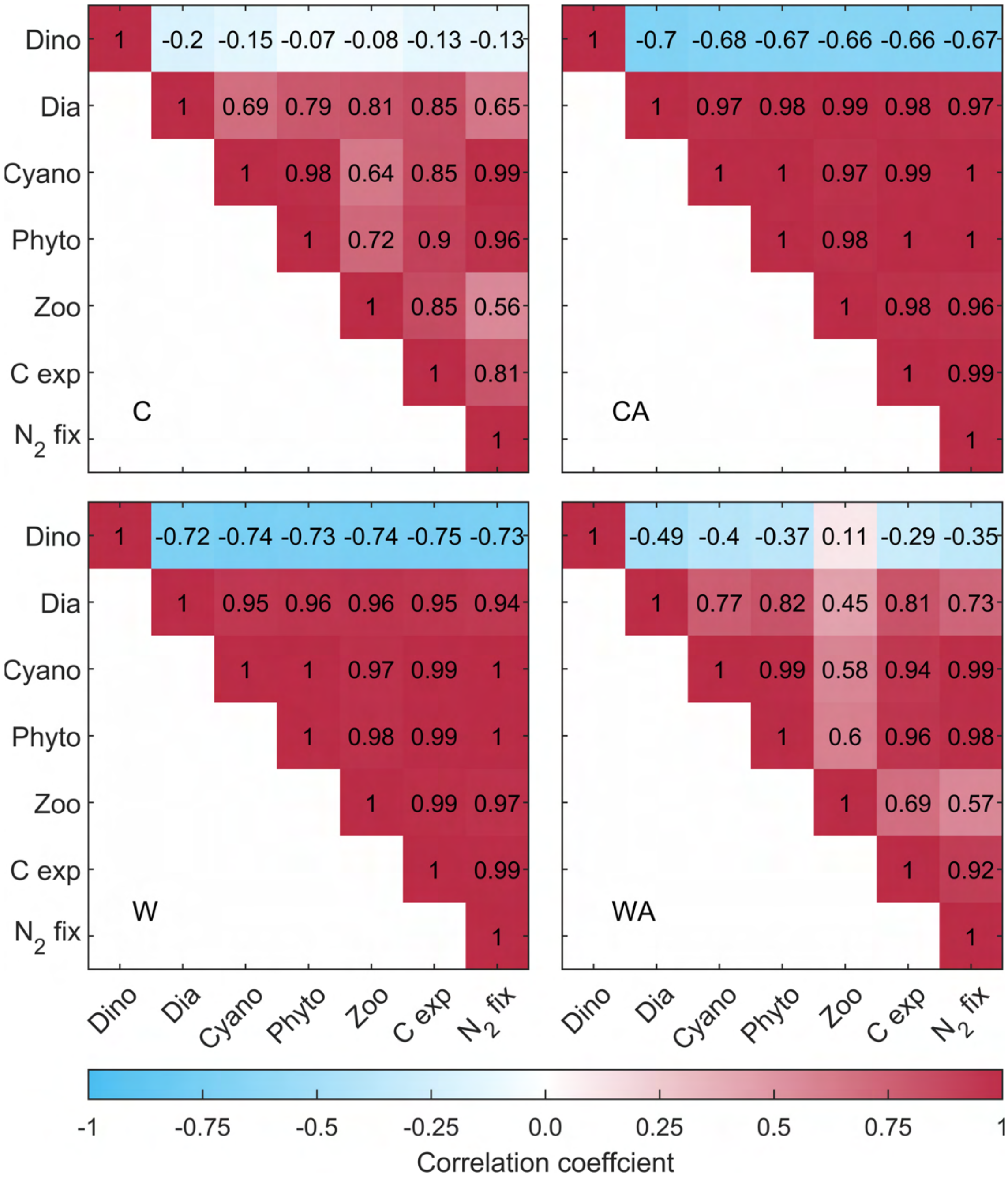

Figure 2.2.5: Correlation matrices showing the correlation coefficients between different ecosystem functions for the four different model scenarios (C: control; CA: control and adaptation; W: warming; WA: warming and adaptation). For C and CA, we calculated correlation coefficients using the annual balances from the last 95 yr of seven different simulations. For W and WA, however, we only used the last 40 yr to capture warming-related changes. All correlations shown here, except for those with dinoflagellates, are significant at the 0.05 level according to a *t*-test (see Fig. B3 in Appendix B.2). Please note that resource use efficiency (RUE) is not included since we derived RUE from simulations without cyanobacteria and zooplankton.

Finally, resource use efficiency (RUE) decreases under global warming in our simulations, with the decrease being similar with and without phytoplankton adaptation ($\sim 57\,\%$ and $\sim 58\,\%$, respectively). Independent of the climate scenario, RUE is always higher if phytoplankton can adapt. Phytoplankton adaptation leads to an increase in RUE by $\sim 59\,\%$ and $\sim 61\,\%$ under control and warming conditions, respectively.

In conclusion, all ecosystem functions that we investigate in this study, except for dinoflagellates, show similar developments in the four model scenarios. This is underlined by strong positive correlations, which are significant at the 0.05 level (Fig. B3 in Appendix B.2). Dinoflagellates, on the contrary, correlate (mostly) negatively with all other ecosystem functions; correlations with dinoflagellates are only partly significant, though. Independent of their direction, all correlations notably change their strength between the four model scenarios. Under control conditions, all correlations are stronger if phytoplankton adaptation is enabled. This pattern reverses under global warming, where correlations are weaker with adaptation. This weakening is particularly strong for zooplankton, for which the negative correlation with dinoflagellates turns slightly positive in WA.

Discussion

In this study, we used an evolutionary ecosystem model to investigate how ecosystem functioning may change in response to global warming, and how these changes may be affected by phytoplankton adaptation. We found that phytoplankton and zooplankton respond similarly to global warming, with the responses being weaker in the presence of phytoplankton adaptation. Likewise, warming-induced changes in associated ecosystem functions are generally less pronounced if phytoplankton adaptation is enabled in our simulations.

Phytoplankton

The model projects an increase in total phytoplankton biomass in response to global warming. This increase is predominantly driven by cyanobacteria, which are preadapted to high temperatures (Collins and Boylen, 1982; Lehtimäki et al., 1997; Nalewajko and Murphy, 2001). This finding agrees with observations, which have revealed a strong increase in cyanobacterial summer biomass in the Baltic Sea over the past decades (Suikkanen et al., 2007). A further increase in cyanobacteria in the future can have severe consequences for the ecosystem, for example, due to their toxicity for higher trophic levels (Repavich et al., 1990; Quesada et al., 2006; Chorus and Welker, 2021) and their ability to fix atmospheric nitrogen. We discuss potential impacts of increasing nitrogen fixation in section "Nitrogen fixation". Future work can build on our results by including an explicit representation of cyanotoxin production and its effects on higher trophic levels.

While diatoms also increase under global warming, dinoflagellates show a slight warming-related decrease in annual biomass. This finding disagrees with observations reporting a shift from diatom to dinoflagellate dominance during spring bloom over the past decades in several areas of the Baltic Sea (Klais et al., 2011). These observations, however, are on functional group level, while we simulate one focal species per group. Resurrection experiments with our focal cold-water dinoflagellate of the genus *Apocalathium* revealed that encystment strongly depends on temperature, and that the temperature threshold for encystment remained constant over the past century of global warming at around 6 °C (Hinners et al., 2017). However, experiments by Kremp et al. (2009) showed that encystment strategies vary among Baltic cold-water dinoflagellates, with temperature not always being the main trigger mechanism. Thus, our model may not be appropriate for estimating future changes in overall spring bloom dynamics but only changes in our focal species.

Considering the dinoflagellate *Apocalathium* specifically, warming leads to an earlier onset of encystment and hence an earlier termination of the spring bloom. As a result, less cysts are produced and the inoculum decreases, weakening the spring bloom of *Apocalathium* over the years as global warming progresses. Consequently, our simulations suggest that warming induces negative feedback in the life cycle of *Apocalathium*. However, Hinners et al. (2017) found that *Apocalathium* has decreased its encystment rate over the past century of global warming, which prevents an abrupt bloom termination at temperatures around 6 °C. To test if a decrease in the encystment rate could weaken the negative feedback in our simulations, we performed additional simulations in which we artificially decreased *Apocalathium*'s encystment rate at the rate measured by Hinners et al. (2017). The simulations reveal that a corresponding decrease in the encystment rate leads to an even stronger decrease in the biomass of *Apocalathium* under global warming (Fig. B4 in Appendix B.2). This suggests that the encystment rate of *Apocalathium* may respond differently to future global warming than to past global warming, or that we are missing another crucial factor. Further research is needed, for example in the form of evolution experiments. In addition, future work can build on our model and include an explicit representation of adaptation in the encystment rate of *Apocalathium*.

On the contrary to *Apocalathium*, our focal cold-water diatom of the genus *Thalassiosira* benefits indirectly from warming due to the increase in cyanobacterial nitrogen fixation. The more nitrogen is fixed in summer, the stronger is the bloom of *Thalassiosira* in autumn. A stronger autumn bloom adds more spores to the inoculum, and a larger inoculum allows for a stronger bloom of *Thalassiosira* in spring, which is further promoted by the weaker bloom of *Apocalathium*. The stronger spring bloom of *Thalassiosira* further increases the inoculum pool, which, in turn, further enhances the autumn bloom. Thus, on the contrary to *Apocalathium*, warming indirectly induces positive feedback in the life cycle of *Thalassiosira*, which is mainly driven by the response of cyanobacteria and, to a lesser extent, by that of *Apocalathium*.

To conclude, our results demonstrate that the responses of different phytoplankton taxa affect each other due to differences in their physiology and function. Thus, when simulating ecosystem-level responses to changing environments, it is crucial for models to include functionally different taxa with their individual physiologies (e.g., life cycle dynamics) to account for feedback and competition. As already demonstrated by Hochfeld and Hinners (2024), an adequate representation of competition also requires an explicit simulation of evolutionary adaptation.

Zooplankton

Our simulated zooplankton responses to global warming qualitatively agree with our simulated responses of phytoplankton; in both cases, responses are weaker if phytoplankton adaptation is enabled. In our warming scenarios, both phytoplankton and zooplankton increase in abundance. A study by Richardson and Schoeman (2004) demonstrated that the abundance of herbivorous zooplankton significantly depends on their phytoplankton prey (bottom-up control), meaning that a warming-related increase in phytoplankton will most likely lead to an increase in zooplankton abundance.

In addition, our simulations show a warming-related shift in bloom timing towards winter for both phytoplankton and zooplankton, with the shift being stronger for zooplankton. Hence, our model does not produce a warming-related increase in the time lag between phytoplankton and zooplankton blooms as suggested by several studies (Edwards and Richardson, 2004; Winder and Schindler, 2004a,b; Adrian et al., 2006). Instead, the time lag between phytoplankton and zooplankton tends to decrease in our warming scenarios compared to the corresponding control scenarios. This decrease in the time lag is strongly connected to zooplankton peak amplitude, with higher peak amplitudes coinciding with shorter time lags. Higher zooplankton peak amplitudes indicate stronger grazing on phytoplankton, and hence stronger top-down control. This means that the time lag between phytoplankton and zooplankton seems to decrease when top-down control increases.

The decreasing time lag in our simulations may result from our simplistic representation of zooplankton. We assume that zooplankton grazing depends exclusively on phytoplankton biomass and do not consider potential effects of irradiance and temperature. Moreover, we neglect both zooplankton life cycle dynamics and adaptation. However, observations show that several zooplankton taxa peak earlier in the season in response to global warming (Richardson, 2008). Dam (2013) interprets the observed phenological shifts in zooplankton as a combination of ecological and evolutionary responses. For example, Dam (2013) argues that zooplankton do not only respond to changes in temperature itself but also to phenological changes in prey, which select for fast-growing zooplankton. Indeed, some phytoplankton and zooplankton taxa show synchronous shifts in bloom timing, for example diatoms and *Daphnia* (Adrian et al., 2006). Some studies even suggest a warming-related decrease in the time lag between phytoplankton and zooplankton (Aberle et al., 2012; Almén and Tamelander, 2020). Consequently, the reduced time lag produced by our model indeed seems realistic for fast-growing zooplankton taxa like *Daphnia*, which are “selected” in our global warming simulations by the earlier and stronger phytoplankton spring bloom. However, our model is not suitable for simulating slow-growing zooplankton with longer and more complex life cycles such as copepods or larvae of the mussel *Dreissena polymorpha* (Adrian et al., 2006).

In conclusion, our results suggest that warming-related responses of fast-growing zooplankton may be closely related to responses of their phytoplankton prey. Thus, phytoplankton adaptation may indeed reduce zooplankton responses to global warming, and the effects of phytoplankton adaptation may even propagate further up the food chain. Future work can build on our model and study how a more complex representation of zooplankton, including both fast- and slow-growing taxa, and higher trophic levels may be affected by phytoplankton adaptation.

Carbon export

Our simulations project a warming-related increase in carbon export in the future, which is more than halved if phytoplankton adaptation is enabled. The projected changes in carbon export correlate significantly with projected changes in biomass production, which are dominated by a strong increase in cyanobacterial summer biomass. In the Baltic Sea, cyanobacteria blooms have intensified over the last century of global warming (Finni et al., 2001), especially during the last decades (Suikkanen et al., 2007). This development is reflected by sediment records, which show a simultaneous increase in cyanobacteria pigments and carbon content during the same period (Poutanen and Nikkilä, 2001). In the future, warming is expected to further increase summer primary production with a positive feedback on carbon export in several areas of the Baltic Sea (Tamelander et al., 2017).

Even if our model results are consistent with these findings, we need to keep in mind that we use a 0-dimensional model setup, which cannot represent certain mechanisms that are crucial for carbon export. For example, we cannot explicitly simulate physical processes in the ocean like vertical mixing, including seasonal changes in stratification and mixed layer depth. In addition, crucial processes like gravitational particle sinking and fragmentation are only included implicitly in our model, while we neglect vertical migration of zooplankton and nekton (Henson et al., 2022). Finally, in semi-enclosed ecosystems like the Baltic Sea, carbon export is not predominantly fueled by phytoplankton primary production but also by benthic primary production and riverine and terrestrial inputs (Goñi et al., 2000; Renaud et al., 2015; Tallberg and Heiskanen, 1998). Since these key processes (and maybe others) are lacking in our model, we cannot interpret our results as projections of future carbon export. Instead, we interpret them as projections of the future contribution of primary production to carbon export. Our results reveal that the contribution of primary production to carbon export may increase in the Baltic Sea in the future and that phytoplankton adaptation may notably weaken this increase.

Nitrogen fixation

Our model results suggest a strong warming-related increase in nitrogen fixation in the future, which is a direct result of the projected increase in cyanobacterial summer biomass. Today, the Baltic Sea is already impacted by above-average levels of nutrient load (Reusch et al., 2018). For example, nitrogen-driven eutrophication turned the Baltic Sea into one of the most hypoxic ocean areas worldwide, with severe consequences for productivity, biodiversity, and biogeochemical cycling (Breitburg et al., 2018). In the future, global warming is expected to further increase the vulnerability of coastal systems to nutrient loading as harmful algal bloom events become more likely and pose an increasing threat to animal and human health (Gobler et al., 2017; Paerl et al., 2015; Glibert et al., 2014).

Since the 1970s, nutrient management strategies have been applied to the Baltic Sea catchment area, resulting in a reduction of anthropogenic nitrogen load by $\sim 25\,\%$ (Reusch et al., 2018). At the same time, however, nitrogen load by fixation increased notably (Gustafsson et al., 2017). Model simulations demonstrated that the contribution of nitrogen fixation to the total nitrogen load to the Baltic Sea increased from almost 20 % in the 1980s to almost 35 % in the 2000s, so that the total nitrogen load decreased by only $\sim 9\,\%$ (Gustafsson et al., 2017). For the future, our results suggest that the importance of cyanobacterial nitrogen fixation for the nitrogen budget of the Baltic Sea will most likely continue to increase and further mitigate the success of nutrient management strategies. Therefore, nutrient management strategies urgently need to account for nitrogen load by fixation to be successful in the future. Since our projected increase in nitrogen fixation is more than halved if we consider phytoplankton adaptation, we strongly recommend that models used for assessment consider phytoplankton adaptation to realistically estimate future nitrogen load by fixation.

Resource use efficiency (RUE)

Since we had to exclude nitrogen-fixing cyanobacteria from RUE simulations, our assessed potential effects of warming and adaptation on RUE are only valid for a two-species ecosystem including a cold-water dinoflagellate of the genus *Apocalathium* and a cold-water diatom of the genus *Thalassiosira*. For this species configuration, we found that adaptation increases resource use efficiency under both control and warming conditions. In both climate scenarios, adaptation is driven by competition for nitrogen, allowing *Apocalathium* and *Thalassiosira* to use the available nitrogen optimally within their means.

Apocalathium can only grow within a specific temperature niche, with the freezing point of sea water at the lower end and the fixed temperature threshold of encystment (6 °C) at the upper end (see Hinners et al., 2019, and section "Phytoplankton"). Within this fixed niche, *Apocalathium* adapts to lower temperatures under control conditions due to intraspecific competition for nitrogen. Since nitrogen concentration is highest during the initial phase of the bloom (Fig. B5 in Appendix B.2), the environment selects for early bloomers with comparatively low optimum temperatures, which grow first and leave less nitrogen for individuals with higher optimum temperatures. Selection for early bloomers advances the bloom peak by more than 1 week compared to the control scenario without adaptation, which extends the bloom duration by a few days. Bloom duration, in this context, refers to the time during which growing stages reach a minimum concentration of $0.05\,\mathrm{mmol\,N\,m^{-3}}$.

On the contrary to *Apocalathium*, *Thalassiosira* is not restricted by its life cycle and can therefore occupy its optimal niche more flexibly. Under control conditions, *Thalassiosira* adapts to higher temperatures to (I) delay its bloom by $\sim 18\,\mathrm{d}$ to reduce competition with *Apocalathium*, and (II) merge its spring and autumn blooms into a single bloom, which persists from June until December (Fig. B5 in Appendix B.2). In this way, *Thalassiosira* can continuously take up nitrogen for 5 months in a row until light becomes limiting in winter.

When temperatures increase under global warming, RUE decreases but remains at a higher level when adaptation is enabled. Without adaptation, the spring bloom of *Apocalathium* is shifted by $\sim 7\,\mathrm{d}$ towards winter, with the peak amplitude decreasing by $\sim 18\,\%$ (Fig. B5 in Appendix B.2). These warming-related changes lead to a decrease in bloom duration of more than 2 weeks. The spring and autumn blooms of *Thalassiosira* are shifted towards winter as well, and even more than the spring bloom of *Apocalathium* ($\sim 26\,\mathrm{d}$ and $\sim 24\,\mathrm{d}$, respectively). However, both *Thalassiosira* blooms only show minor changes in peak amplitude and duration.

With adaptation, *Thalassiosira* does not show notable warming-related changes in bloom timing, duration, or amplitude. The spring bloom of *Apocalathium*, on the contrary, is again by more than 2 weeks shorter, meaning that the shortening is not caused by lacking adaptation but by the fixed temperature threshold of encystment. Still, with adaptation, we observe a slightly smaller shift in bloom timing of *Apocalathium* with $\sim 5\,\mathrm{d}$ instead of $\sim 7\,\mathrm{d}$, and a $\sim 16\,\%$ higher peak amplitude.

To conclude, our simulations show that adaptation generally allows for a more efficient use of resources and thus higher RUE. Models that ignore adaptation may hence systematically underestimate RUE under both present-day and future conditions. However, our projected warming-related decrease in RUE only applies to the species configuration in our model. We cannot make statements about future changes in RUE in other ecosystems with a different set of species. Future work can build on our results and investigate RUE in more complex ecosystems to make more general statements about future warming-related changes. Our results demonstrate that future models should consider not only adaptation, but also possible species-specific constraints on adaptation, such as life cycle dynamics.

Control factors and feedbacks in our model ecosystem

We found that all ecosystem functions are positively correlated in our simulations, with dinoflagellate annual biomass being the only exception. Under control conditions, all correlations (regardless of their direction) are stronger with phytoplankton adaptation, when niche separation allows for a stronger cyanobacterial summer bloom (see section “Seasonal phytoplankton dynamics”). Due to the stronger cyanobacterial summer bloom, more atmospheric nitrogen is fixed. The increase in nitrogen fixation is beneficial especially for diatoms, which can immediately take up the newly available nitrogen in autumn. Dinoflagellates, however, do not benefit from increased nitrogen fixation. During spring bloom, dinoflagellates reach a higher maximum concentration than diatoms. Since we assume that zooplankton grazing depends on phytoplankton biomass only (see section “Zooplankton”), grazing is stronger on dinoflagellates than on diatoms. Indeed, zooplankton peak during dinoflagellate spring bloom, meaning that dinoflagellates constitute the main food source for zooplankton. Hence, the stronger dinoflagellates grow due to increased nitrogen fixation, the more they are grazed by zooplankton, and increased nitrogen fixation has no positive impact on dinoflagellate biomass. Zooplankton, on the contrary, benefit indirectly from increased nitrogen fixation. To conclude, adaptation induces positive feedback in our control simulations: Dinoflagellates and diatoms adapt to individual temperature niches to reduce competition for nitrogen, with the reduced competition between diatoms and cyanobacteria allowing for a stronger cyanobacterial summer bloom. While the increased cyanobacterial nitrogen fixation has a direct positive effect on diatoms, zooplankton benefit indirectly through stronger grazing on dinoflagellates. The result is an overall increase in biomass production, which, in turn, increases carbon export.

Under global warming, we observe a similar positive feedback mechanism for W, where phytoplankton adaptation is disabled. For WA, on the contrary, we find an overall weakening of correlations, even if cyanobacteria are stronger in WA than in CA. Correlations in WA are weaker especially for dinoflagellates and zooplankton, with the negative correlation between them turning slightly positive. Correlations for diatoms are weakened as well but to a lesser extent. Due to the stronger cyanobacterial summer bloom, nitrogen fixation increases in WA compared to CA, which is again beneficial for diatoms. As a result, grazing pressure on diatoms increases and weakens the positive correlation between diatoms and zooplankton. In addition to the enhanced grazing pressure, there is another factor that reduces the benefit of the increasing cyanobacteria for diatoms. As demonstrated by Hochfeld and Hinners (2024), cyanobacteria restrict diatom adaptation to the increasing temperatures in WA due to their presence in summer, leading to a stronger shift of the two diatom blooms towards winter. While this is not necessarily problematic for the diatom autumn bloom if sufficient light is available, it is for the spring bloom since dinoflagellates are present at lower temperatures. Thus, we observe a weaker positive correlation between diatoms and cyanobacteria in WA than in CA. Due to the stronger grazing on diatoms, zooplankton are also less positively impacted by cyanobacteria. The weaker positive effect of cyanobacteria on diatoms and zooplankton is reflected in a slight weakening of the remaining positive correlations, and a notable weakening of the negative correlations with dinoflagellates. Furthermore, the reduced relative grazing pressure on dinoflagellates reverses the negative correlation with zooplankton, meaning that an increase in zooplankton biomass no longer implies a decrease in dinoflagellate biomass.

To conclude, cyanobacteria are the most important control factor in our model ecosystem, which is also confirmed by a principal component analysis (Fig. B6 in Appendix B.2). First, cyanobacteria produce the highest amount of biomass per year. Second, due to their ability to fix atmospheric nitrogen, they directly control the biomass production of dinoflagellates and diatoms, and indirectly of zooplankton. Cyanobacteria are therefore the main factor for carbon export in our simulations, which also agrees with observations as discussed above (see section “Carbon export”). However, the interdependencies between cyanobacteria and the other taxa may change depending on the climate scenario and the presence or absence of phytoplankton adaptation. Under control conditions and in W, there are clear losers and winners of increased nitrogen fixation among the phytoplankton, with dinoflagellates being the losers and diatoms being the winners. In WA, these dynamics begin to reverse slightly since cyanobacteria restrict diatoms in their adaptation to higher temperatures. These results demonstrate that by neglecting adaptation, we may be missing adaptation-related changes in taxa interactions, especially in changing environments, which can affect the entire ecosystem and hence its functioning.

Conclusions

Our study demonstrates that phytoplankton adaptation does not only affect simulated phytoplankton dynamics themselves but also simulated ecosystem functions through bottom-up control. The effect of phytoplankton adaptation on simulated ecosystem functions depends on environmental conditions.

In a steady environment, phytoplankton adaptation allows for a more efficient use of resources through niche separation, which, in turn, increases primary production. An increase in primary production may enhance secondary production, nitrogen fixation, and carbon export, and maybe even other ecosystem functions not included in this study. Thus, by neglecting adaptation, models can systematically underestimate resource use efficiency in a steady environment and hence ecosystem functions that are directly related to primary production. In a warming environment, however, adaptation has the opposite effect. With the ability to adapt to the increasing temperatures, non-preadapted taxa can mitigate the dominance of superior preadapted taxa. Since different taxa fulfill different functions in the ecosystem, weaker changes in their abundance lead to weaker changes in related ecosystem functions. By neglecting phytoplankton adaptation, models may therefore systematically overestimate warming-related changes in ecosystem functioning. To realistically simulate ecosystem functioning in both steady and changing environments, future models should not only consider multiple phytoplankton functional groups due to their different roles in the ecosystem but also their potential to adapt to their environment. Our study furthermore suggests that models without adaptation may miss adaptation-related interdependencies between taxa that may play out differently in steady and changing environments and can hence lead to changes in ecosystem dynamics and functioning. In addition, our study highlights the importance of life cycle dynamics for phytoplankton responses to global warming due to potential feedback mechanisms and/or adaptation constraints.

Our study is a first step to improve model projections of future ecosystem-level changes. Future work can build on our results, for example by expanding our model ecosystem to include multiple nutrients, a higher diversity of phytoplankton functional groups, a more complex representation of zooplankton, and higher trophic levels. Another next step would be to couple our or a similar evolutionary ecosystem model to a 1D or 3D physical environment to allow for a more realistic representation of physically driven processes, e.g., biogeochemical cycling. The performance of such an evolutionary biogeochemical-physical model could then be tested against long-term evolutionary data (e.g., from sediment archives). Using such a validated model for climate projections could notably improve estimations of future ecosystem-level changes.

2.3 Study III: From past ecosystem changes to future projections

How sediment archives can improve model projections of future marine ecosystem changes

Isabell Hochfeld, Helge Arz, Miklós Bálint, Lutz Becks, Sarah Bolius, Laura S. Epp, Jérôme Kaiser, Christopher Klausmeier, Anke Kremp, Elena Litchman, Markus Pfenninger, Juliane Romahn, Alexandra Schmidt, Ben A. Ward, and Jana Hinners

Global warming is a major threat to marine biodiversity and ecosystem functioning, with consequences that are yet largely unknown. To frame these consequences, we need to understand how marine ecosystems respond to warming and related environmental changes. Ecosystem models have proven a valuable tool in this regard, but their projections differ notably. A major limitation in current models may be that they largely ignore evolutionary dynamics, which nonetheless can be relevant on the simulated time scales. In addition, models are usually fit to contemporary data and used predictively afterwards, without further validation that they are equally applicable to past (and by inference, future) scenarios. A promising approach to validate ecosystem models are biological archives such as natural sediments, which "collect" and archive long-term ecosystem changes. Sediment archives provide a variety of information on past ecosystem status, including environmental conditions, biodiversity, relative abundances of taxa, and (functional) traits of living and extinct organisms and communities. We present a framework to make use of such information to validate evolutionary ecosystem models and improve model predictions of future ecosystem changes. Using the example of phytoplankton, key players in marine systems, we review existing literature and discuss (I) which data can be derived from ancient sedimentary archives, (II) how we can integrate these data into evolutionary ecosystem models to improve model projections of climate-driven ecosystem changes, and (III) future perspectives and aspects that remain challenging.

Submission planned to Global Change Biology

Introduction

Driven by the reality of global warming as a major threat to marine biodiversity and ecosystem functioning, ecosystem models are increasingly used to estimate future changes in marine ecosystems. However, projected changes differ notably between models (Laufkötter et al., 2015, 2016). Moreover, models largely ignore evolutionary processes (Laufkötter et al., 2015, 2016; Munkes et al., 2021) that can be highly relevant on the simulated time scales (Jin and Agustí, 2018; Irwin et al., 2015). The reliability of current model projections therefore remains questionable. Here, we propose to use data from sediment archives to validate ecosystem models before using them predictively, and discuss how this approach can improve model projections.

Compared to the period 1850 – 1900, global mean surface temperature has already increased by ~1.25 °C and is expected to increase by up to a further ~3.5 °C until the end of the century under the most extreme emission scenario (IPCC scenario SSP5-8.5, Allan et al., 2021). Marine organisms are responding to global warming, for example, through changes in phenology and seasonal migration (Peer and Miller, 2014; Wasmund et al., 2019), populations moving poleward (Fossheim et al., 2015; Poloczanska et al., 2013), and increased harmful algal blooms (Anderson et al., 2012; Hallegraeff, 2010). Marine communities perform ecosystem functions that are vital to human societies, including food production (Hollowed et al., 2013) and carbon sequestration (Hain et al., 2014). The response of these ecosystem services under ongoing global warming remains subject to great uncertainty, and there is a real but unknown risk of positive feedbacks, irreversible tipping points, and ecosystem collapse (Lenton et al., 2008). Predicting future changes in marine ecosystem functioning is hence of great importance but remains a major challenge.

Dynamic ecosystem models currently represent the best tool to understand complex feedbacks between evolving ecosystems and their environment, but it is a considerable challenge to develop models that would apply equally well to past, present, and future scenarios. Despite their great potential, current models predict diverging changes in ecosystem functions like carbon cycling and net primary production (Laufkötter et al., 2015, 2016). Since models hardly agree on the direction of change, the validity of current model projections remains questionable.

To improve model projections, we need (I) to verify that all relevant processes are considered and (II) to validate projections with long-term data. In terms of (I), current ecosystem models largely ignore a crucial process that can influence ecosystem responses to environmental changes on perennial time scales — evolutionary adaptation (Irwin et al., 2015; O'Donnell et al., 2018; Hattich et al., 2024). Some models already consider adaptation (Beckmann et al., 2019; Sauterey et al., 2017; Le Gland et al., 2021), but only a small number have been compared to empirical data, both from experiments (Denman, 2017) and from sediment archives (Gibbs et al., 2020; Hinners et al., 2019). So far, however, testing against data has not been used as a tool to improve model projections. With respect to (II), both experiments and marine monitoring studies cannot account for long-term environmental changes, while experiments hardly capture the complexity of real ecosystems. Natural archives such as sediments, however, allow reconstructing long-term ecosystem responses to past environmental changes (Capo et al., 2021; Ellegaard et al., 2020). Sediments preserve environmental proxies (Hillaire-Marcel and De Vernal, 2007), organismal remains such as DNA (Alsos et al., 2022; Monchamp et al., 2016; Zimmermann et al., 2023), and dormant resting cells and seeds that can be resurrected and used for experiments (Bennington et al., 1991; Hinners et al., 2017; Isanta-Navarro et al., 2021). Since sediments can be dated, we can use the preserved information to derive long-term time series on past environmental conditions, biodiversity, relative taxa abundance, and adaptive changes in (functional) traits.

Here, we discuss how we can use data from sediment archives to improve marine ecosystem models and their projections of future ecosystem-level changes. Our approach focuses on phytoplankton, key players in marine ecosystems and respective models. Phytoplankton account for about half of global photosynthesis (Field et al., 1998), are the basis of the marine food web (Fenchel, 1988), represent an important component of biogeochemical cycles (Hutchins and Fu, 2017), and can even influence ocean physics (Hense, 2007; Sathyendranath et al., 1991). In addition, the large population sizes and short generation times of phytoplankton allow them to adapt quickly to changing environmental conditions (Aranguren-Gassis et al., 2019; Irwin et al., 2015; O'Donnell et al., 2018; Hattich et al., 2024). All these factors, together with their long-lived dormant resting stages (Delebecq et al., 2020; Sanyal et al., 2022), make phytoplankton ideal model organisms for the approach that we present here. Based on existing literature, we discuss which data we can obtain from sediment archives, how we can use these data to improve ecosystem models and their projections, and remaining challenges and future perspectives.

Sediment archives — understanding phytoplankton responses to environmental change

Sediment archives provide information on past ecosystem status, including environmental conditions, biodiversity, relative abundances of taxa, and (functional) traits of living and extinct organisms and communities (Fig. 2.3.1). Such data can be used to constrain ecosystem models.

Dating sediment archives

Before working with sediment archives, the sediments must be dated accurately to obtain a well-constrained relationship between age and sediment depth, a so-called age model. Common sediment dating methods include radiocarbon dating, lead isotope dating, and event stratigraphy. Radiocarbon (^{14}C) dating is based on ^{14}C half-life. Determining the amount of radioactive ^{14}C relative to the ^{12}C stable isotope allows estimating age ca. 50,000 yr back in time (Hajdas et al., 2021). After 1950, radiocarbon dating is not applicable anymore due to the radiocarbon added artificially to the atmosphere by atmospheric nuclear bomb tests. Therefore, sediments deposited after 1950 are dated using different methods such as lead isotope (^{210}Pb) dating and event stratigraphy. While the ^{210}Pb dating approach is based on the half-life of atmospheric ^{210}Pb (Appleby, 2001), event stratigraphy is based on the detection of particular events registered in, e.g., chemical parameters of the sediments. A classic example is the detection of the appearance and maximum content of ^{137}Cs, ^{241}Am, or $^{239+240}$Pu artificial radionuclides corresponding to the beginning of the global atmospheric nuclear bomb tests in 1953 and their maximum in 1963 (Appleby, 2001; Hancock et al., 2011). Another example is the identification of volcanic ash layers in the sediment cores, which originate from well-dated volcanic eruptions (Lowe and Alloway, 2015). By combining all the dating methods mentioned above, it is possible to obtain robust age models of sediment cores over the last ca. 50,000 yr, knowing that dating uncertainties increase with age. Other stratigraphic methods such as oxygen isotope stratigraphy, biostratigraphy, or paleomagnetic stratigraphy are applied to date older sediments (Bradley, 2015).

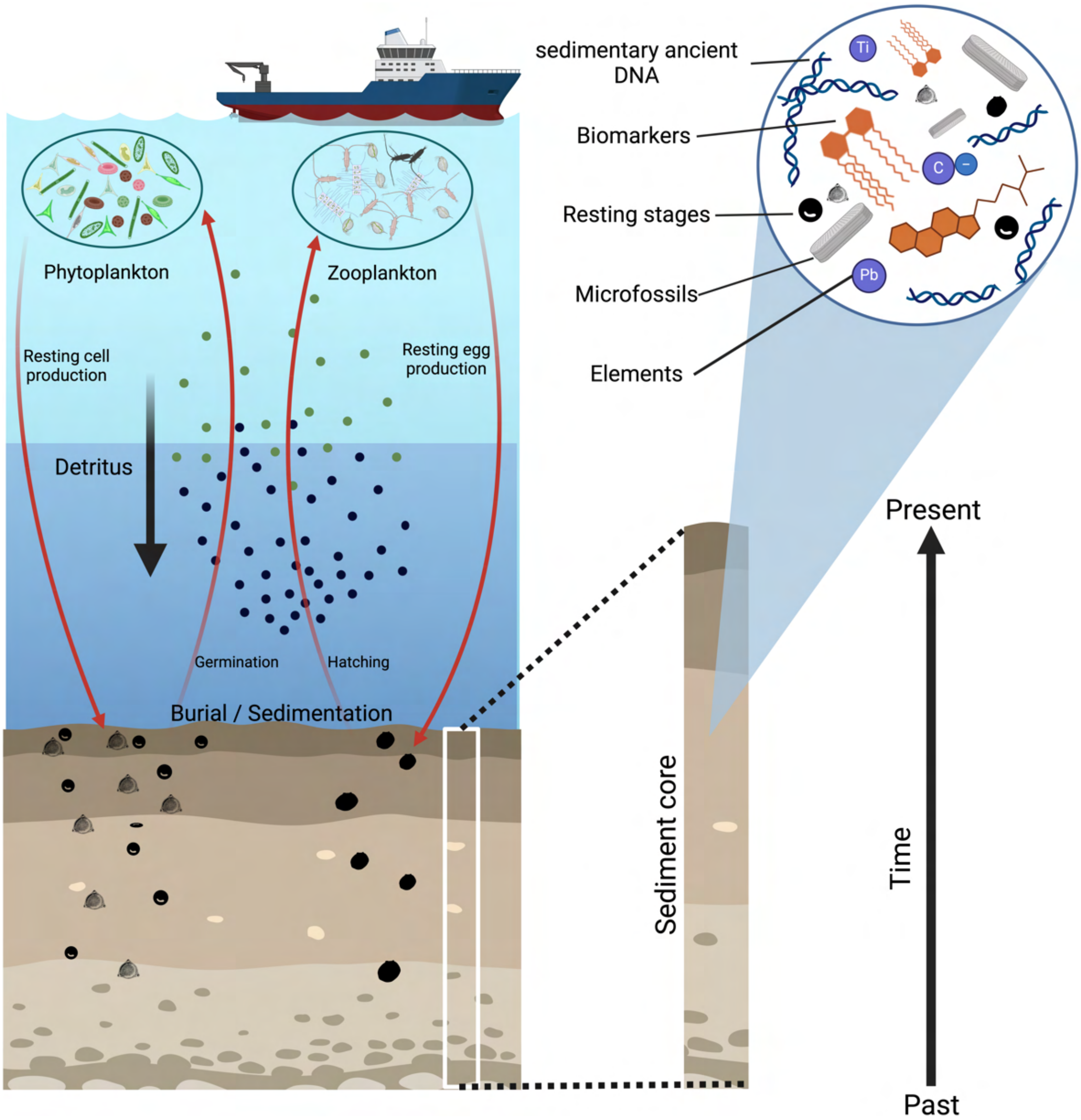

Figure 2.3.1: Overview of different types of data (environmental and biological) that can be obtained from sediment archives. **Left:** Schematic showing the deposition of organismal remains in the sediment. Green dots represent active plankton cells, while black dots indicate planktonic resting stages. The red arrows show resting stage production and deposition in the sediment, as well as germination and hatching of planktonic resting stages from the sediment. The black arrow represents sinking of dead organic matter (detritus) to the seafloor. Preserved organismal remains are shown in the sediment. **Right:** Zoom into the sediment core showing different types of data that can be obtained. The figure was created with BioRender.com.

Environmental data

Abiotic and biotic proxies, or indicators, preserved in sediment archives allow reconstructing physicochemical characteristics of past marine and limnic environments. For example, surface salinity can be estimated using lipids (alkenones) produced by micro-phytoplankton species of the order Isochrysidales (Medlin et al., 2008; Rosell-Melé, 1998; Kaiser et al., 2017). Trace metals and their isotopes such as Mo, U, or W represent indicators for past suboxic to euxinic conditions in the water column and/or the sediments (Brumsack, 2006; Dellwig et al., 2019). Relative assemblages of microfossils (e.g., resting stages of dinoflagellates, silica frustules of diatoms, calcareous shells of foraminifera) preserved in sediments provide important information not only on salinity, but also on pH, trophic state, and temperature, and are therefore powerful proxies (Hillaire-Marcel and De Vernal, 2007). In terms of water temperature proxies, the Mg/Ca and Sr/Ca ratios of foraminifera reflect temperature changes at different depths of the water column, depending on the thriving depth of foraminiferal species (Lear et al., 2002; Cléroux et al., 2008). Indexes based on alkenones (U_{37}^{K}, Prahl et al., 1988) as well as other membrane lipids derived from archaea (TEX_{86}, Schouten et al., 2013) can be used to reconstruct surface and subsurface temperature. These, and many other physical methods, biological proxies, and geochemical tracers find their diverse application in paleoceanography (Hillaire-Marcel and De Vernal, 2007).

Proxy-based reconstructions have to be considered carefully as they may be biased due to preservation/degradation and influenced by local-to-regional environments. Using a multiproxy approach and calibration depending on the environment are important for reliable reconstructions. Reconstructed environmental conditions of the past can then be used as environmental forcing for ecosystem models.

Biological data

Apart from information on environmental conditions, sediment archives provide a wide variety of biological information, such as biodiversity, relative taxa abundance, and trait adaptation.

Microfossils

Traditionally, the focus of research on sediment archives has been on fossilized plankton remains. Fossil phytoplankton communities only represent species that consist of stable mineral structures (e.g., of silica), or contain specific fossilizable molecules such as sporopollenin. Among dinoflagellates, only a fraction of the community produces resting cysts (Limoges et al., 2020; Van Nieuwenhove et al., 2020), which are preserved over time and can be used for quantitative paleoecological reconstructions and biostratigraphy. Diatoms, on the other hand, are well-represented in the fossil record due to their resistant silica frustules with their diverse species-specific structures (Weckström, 2006). Also some filamentous cyanobacteria produce resistant resting stages, akinetes, constituting long-term records in brackish-marine and lake sediments (Wood et al., 2021). In lakes, chrysophyte cysts can build up long-term records providing information on group-specific phytoplankton dynamics over long time scales (Korkonen et al., 2017). Typically, the generated microfossil data are quantitative; analyses provide data on relative abundances of taxa through "time". Such data will, to some extent, allow estimating relative biomasses of the represented taxa and larger taxonomic groups, e.g., cyanobacteria, diatoms, and dinoflagellates. While microfossils provide continuous (semi-)quantitative long-term records of fossilizable phytoplankton taxa over geological time scales, their biodiversity information is limited. Only a fraction of taxa within the phytoplankton community is usually represented in the fossil record, and therefore, respective data are likely biased (Bálint et al., 2018). Nevertheless, for those taxa that are suitable and sufficiently represented, highly informative demographic data can be generated from microfossil and resting stage records (Cermeño et al., 2012; Matul et al., 2018; Kremp et al., 2018). Furthermore, data on the temporal distribution of larger taxonomic groups as obtained from microfossil records can provide general information on trait composition and function of phytoplankton communities (Blank and Sánchez-Baracalco, 2010). Such data can serve as validation for ecosystem modeling studies.

Sedimentary ancient DNA

To capture biodiversity dynamics of phytoplankton through time, recent advances in ancient DNA approaches can increase taxonomic coverage and resolution. DNA can be preserved for thousands of years in natural biological archives, such as freshwater sediments (Clarke et al., 2019; Capo et al., 2021), marine sediments (Coolen et al., 2009, 2013; Armbrecht et al., 2022), and permafrost (Willerslev et al., 2003; Kjær et al., 2022). Compared to microfossils, a distinctive characteristic of ancient DNA data lies in their capability for broad taxonomic coverage. Because every organism contains DNA and the differences between species are defined by their DNA, in theory, DNA could be used to identify any organism that has been left in sediment deposits (Bálint et al., 2018). Establishing relative abundances of organisms from their DNA record is challenging though. While fossilized remains of certain phytoplankton taxa can inform us about cell counts, DNA records can be informative about copy numbers of particular genes (Mejbel et al., 2021). Since gene copy numbers can vary by orders of magnitude among species, inferences about abundance can be challenging with methods that target many taxa at once (Vasselon et al., 2018). If the focus is on a narrow set of taxa, gene copy number information provided by quantitative analyses (qPCR or ddPCR) might be more readily translated into abundance information, especially if the range of gene copy numbers per cell can be estimated for the focal species (Godhe et al., 2008). This approach potentially allows to obtain demographic information on a targeted taxon in specific sediment horizons. The recovered genetic diversity can furthermore inform on the effective population size of a population, which influences the population's evolvability (Charlesworth, 2009). Thus, changes in the effective population size can be qualitatively compared to changes in the number of different agents in agent-based ecosystem models. In addition, under stable, non-selective environmental conditions, effective population size should be positively correlated with a population's trait variance.

Resurrection experiments

Living sediment archives are represented by temporal deposits of living dormant resting stages, which can be obtained from organisms that produce long-lived dormant resting cells/seeds such as specific plants (McGraw et al., 1991; Sallon et al., 2008), zooplankton (Kerfoot and Weider, 2004; Pauwels et al., 2010), and phytoplankton (Härnström et al., 2011; Hinners et al., 2017). Laminated sediments, which form under anoxic conditions due to the absence of mixing by benthic fauna, therefore contain distinct age cohorts of dormant or quiescent phytoplankton (Ellegaard et al., 2017). Such resting stages can germinate when exposed to oxygen, and cells start growing when suitable temperature, light, and nutrient conditions are provided. A number of studies have demonstrated the "resurrection" potential of different phytoplankton taxa after extended periods of resting, ranging from decades to millennia (Härnström et al., 2011; Kremp et al., 2018; Sanyal et al., 2022).

Phytoplankton strains that have been re-established from germinated resting stages of different temporal sediment layers can be characterized pheno- and genotypically (Hinners et al., 2017; Härnström et al., 2011). Comparison of trait values among temporal cohorts will provide information on trait changes, their rates of change, and the mechanisms behind (Hattich et al., 2024). Different traits, e.g., temperature-dependent growth and nutrient uptake (Hattich et al., 2024), photosynthesis-related traits (Medwed et al., unpublished), resting stage formation (Hinners et al., 2017), and toxicity (Wood et al., 2021) have been measured in laboratory experiments on resurrected strains and resulting data have been used in ecosystem models (Hinners et al., 2019). Traits that are of particular interest for ecosystem modeling include growth characteristics depending on environmental conditions (reaction norms), cell size, mortality rates, grazing rates (of zooplankton), toxicity, as well as triggers and rates of transition between life cycle stages. While trait data of revived cultures from uppermost contemporary sediment layers can be used for the calibration of ecosystem models, trait time-series of deeper, older sediment layers provide data for ecosystem model validation, as described in more detail in the following section “Implementing data from sediment archives into (evolutionary) ecosystem models”. Emerging high-throughput phenotyping methods allow for extensive trait measurements even for large sets of cultures (Argyle et al., 2021).

Phenotypic trait data from resurrected cultures can be linked to their genetic traits. A common method for this is represented by Genome-Wide Association Studies (GWAS) (Visscher et al., 2017; Uffelmann et al., 2021; Hirschhorn and Daly, 2005). GWAS connect variations in the DNA sequence, known as Single Nucleotide Polymorphisms (SNPs), to a specific trait. This is done by using statistical methods to find a correlation between each SNP and the trait. The strength of this correlation is represented by a p-value. GWAS approaches can help to determine if certain functional groups of genes (e.g., those involved in oxidation or CO_2 fixation) were selected for or lost over time. In addition, GWAS approaches can help to determine whether the traits of interest are polygenic and can thus be adequately modeled as continuous quantitative traits. The success of this method depends on several factors, including the quality of the phenotypic data and the accuracy of the genetic data.

Implementing data from sediment archives into (evolutionary) ecosystem models

Ecosystem models provide a powerful tool to study the functioning of ecosystems and their responses to environmental changes. For example, marine ecosystem models can be used to understand global patterns of phytoplankton diversity (Dutkiewicz et al., 2020; Ward et al., 2012). In addition, they can help to identify potential feedback loops (e.g., between cyanobacteria and their environment, Hense, 2007) and trade-offs (e.g., between phytoplankton diversity and productivity, Smith et al., 2016). Finally, marine ecosystem models can simulate how phytoplankton (and zooplankton) respond to different biotic and abiotic factors, including viruses (Krishna et al., 2024; Weitz et al., 2015), eutrophication (Gustafsson et al., 2012), ocean acidification (Dutkiewicz et al., 2015), and temperature changes (Lee et al., 2018; Elliott et al., 2005).

The neglected role of evolutionary adaptation in ecosystem models

Over the past few years, ecosystem models have been increasingly used to estimate the impact of global warming on marine ecosystems and their functioning. Although the results of climate projection studies are relevant for stakeholders (Intergovernmental Panel on Climate Change (IPCC), 2022), current models differ notably in their formulations and predictions, with some models even disagreeing on the direction of change (Laufkötter et al., 2015, 2016). We argue that a major source of uncertainty in current models is that they do not account for the high adaptive potential of phytoplankton.

Experiments and observations demonstrated that phytoplankton adaptation can be important on perennial time scales (Hattich et al., 2024; Irwin et al., 2015; O'Donnell et al., 2018; Aranguren-Gassis et al., 2019) and may hence alter predicted ecosystem changes notably (Ward et al., 2019). Indeed, a recent modeling study revealed that adaptation can significantly reduce simulated warming-related changes in phytoplankton phenology and relative taxa abundance (Hochfeld and Hinners, 2024). Changes in phenology and relative taxa abundance, in turn, may have a direct impact on ecosystem functioning (Litchman et al., 2015; Edwards and Richardson, 2004). To conclude, it is becoming increasingly clear that evolutionary adaptation cannot be neglected in climate projection studies, putting current models and their ability to predict future ecosystem changes into question.

Evolutionary adaptation can be integrated into ecosystem models by allowing for one or more phytoplankton traits to change on intergenerational time scales. In case of changing temperature, for example, phytoplankton thermal adaptation can be represented with an evolvable optimum temperature for growth (Kremer and Klausmeier, 2017; Beckmann et al., 2019). Different approaches exist to integrate adaptation into ecosystem models, with the most suitable approach depending on the research question. Overviews can be found in Beckmann et al. (2019) and Klausmeier et al. (2020a). However, integrating adaptation into ecosystem models brings new challenges, such as identifying the relevant traits and the associated limits and trade-offs (O'Donnell et al., 2018; Ward et al., 2019). One approach to obtain the necessary evolutionary information is represented by evolution experiments (Ward et al., 2019; Hinners et al., 2024). Since such experiments can neither replicate the complexity of real ecosystems nor long-term environmental changes, we argue that sediment archives as “natural evolution experiments” represent a valuable complementary source of information, which we explain further below.

Building an (evolutionary) ecosystem model including data from sediment archives

It is a considerable challenge to develop ecosystem models that can be applied equally well to past, present, and future scenarios. Most state-of-the-art models are developed in a two-step process that comprises the definition of prior estimates of parameter values (initialization) and the iterative fit to contemporary observations through parameter adjustment (calibration). We argue that this approach relies too heavily on how an ecosystem is structured in the present, so that models may no longer be applicable when ecosystem structure has changed in the future. To avoid these problems, models should represent fundamental processes that apply more generally instead of being tailored to a specific ecosystem. The general applicability of a model can be tested with an additional step during model development, validation, which makes use of data from sediment archives. A recent study presented such an approach for non-evolutionary terrestrial models, which is mainly based on plant remains (Alsos et al., 2024). Our approach focuses on phytoplankton, key players in marine ecosystems and respective models. Due to the high evolutionary potential of phytoplankton, we additionally consider evolutionary processes.

The model development approach that we propose here comprises three different steps: initialization, calibration, and validation (Fig. 2.3.2). Both initialization and calibration are performed using contemporary data, while validation requires data from sediment archives. Only when all three steps of model development have been completed should a model be used to simulate future ecosystem changes.

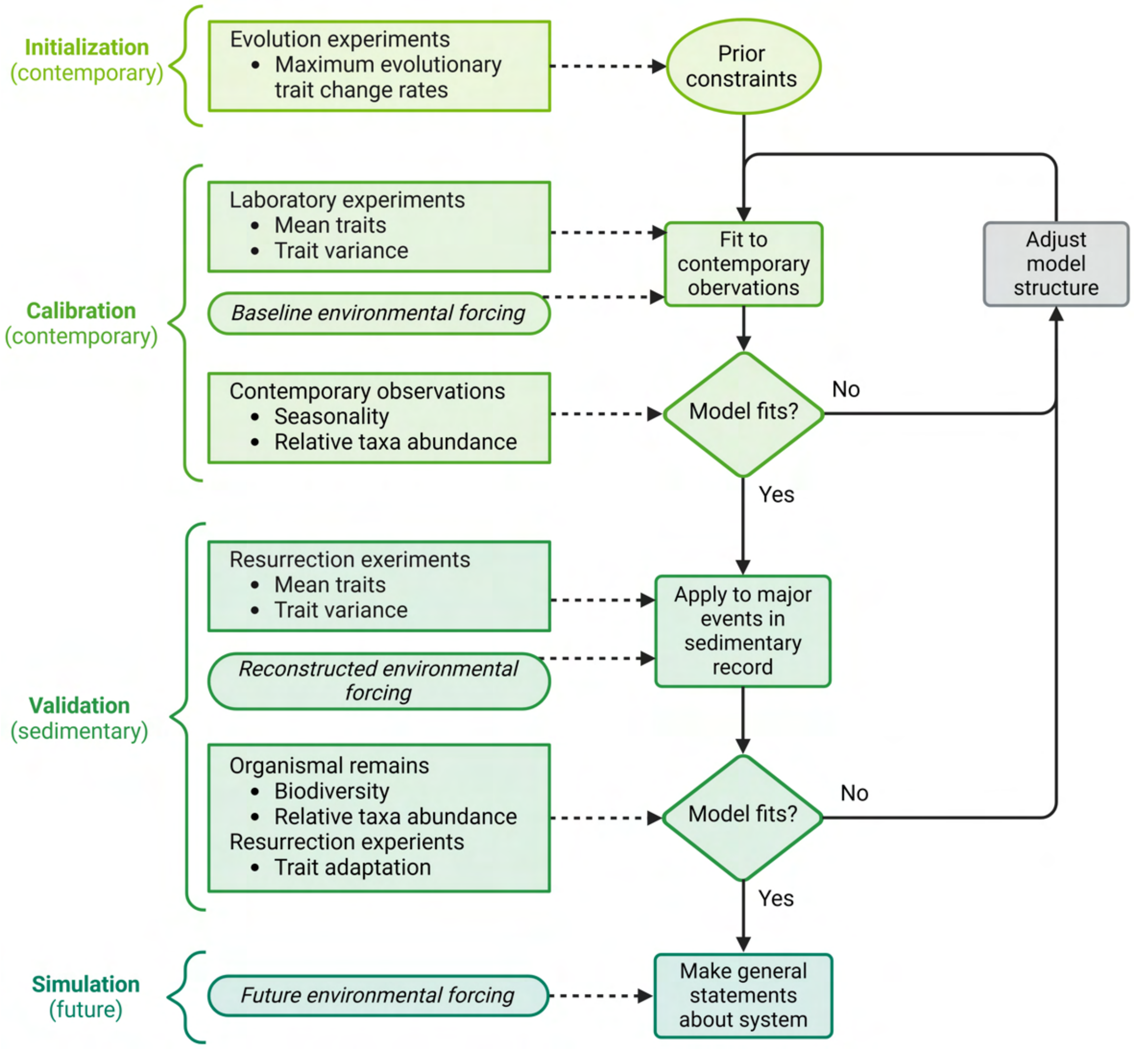

Figure 2.3.2: Conceptual framework for the development of an (evolutionary) ecosystem model that can be applied equally well to past, present, and future scenarios. Shown are the three different steps of model development (initialization, calibration, validation), the following application of the model (simulation), and the data required for each step.

Initialization requires prior estimates of parameter values that need to be valid regardless of the simulated environmental scenario. Such parameters include constraints on adaptation, such as maximum evolutionary trait change rates, which are, however, difficult to assess. For example, evolutionary trait change rates can be assessed by comparing ancestral trait values to those from populations evolved in a new environment for a specific time after accounting for plastic responses (Collins and Bell, 2004; Hutchins et al., 2015; Listmann et al., 2016). In addition, it is possible to measure changes in fitness proxies, most commonly population growth rate or lineage competitive ability (Elena and Lenski, 2003). However, interpretation is not straightforward since the relationship between fitness and proxy may change over time (Collins et al., 2020). Finally, genetic mutation rates can be estimated via genome sequencing (e.g., Krasovec et al., 2019), but genetic mutation does not necessarily translate into trait changes. While functional traits may depend on multiple genes (epistasis), one gene may affect multiple traits (pleiotropy) (Lässig et al., 2017; Østman et al., 2012; Tyler et al., 2009). To conclude, evolutionary trait change rates can only be assessed roughly and need to be further adjusted in the next steps of model development.

The goal of model calibration is to fine tune the model parameters and the model structure until the model reproduces contemporary observations. To do so, initial values for mean traits and trait variance are required (Fig. 2.3.2). These parameters can be measured in the laboratory for recently sampled organisms (Lehtimäki et al., 1997; Vincent and Silvester, 1979). The model is then forced with a baseline environmental forcing, usually a steady seasonal forcing that represents present-day conditions. Using this forcing, the model is run until it reaches a steady state, where phenology and relative taxa abundances repeat each season. Simulated phenology and relative taxa abundances are then compared to contemporary observations from seagoing research and remote sensing. If the model does not reproduce the observations, model parameters and structure are adjusted iteratively until model output and observations match.

As the final step, model validation aims to test if the model is equally applicable to past, present, and (by implication) future scenarios by comparing the model output to independent validation data. We argue that data from sediment archives are ideally suited for validation, with a contemporarily calibrated model being successfully validated if it can represent major shifts in community structure and/or function that are present in the sedimentary record. As a first step, validation needs initial values for the mean and variance of the relevant traits. These parameters can be measured in the laboratory for resurrected organisms sampled from the sediment layer that corresponds to the beginning of the validation period. In addition, environmental conditions during the validation period must be reconstructed to create a forcing for the model. The simulated biodiversity and relative taxa abundances can then be compared to organismal remains from different sediment layers throughout the validation period. Similarly, simulated trait changes can be compared to results from resurrection experiments, which are performed with organisms from different sediment layers of the validation period. If the contemporarily calibrated model cannot reproduce major events in the sediment record, this implies that the model's structure and parameterization are not general to both contemporary and past systems and should therefore not be used to make predictions.

For example, Gibbs et al. (2020) used an evolutionary ecosystem model that was parameterized in accordance with contemporary laboratory measurements to reproduce an observed shift in the trophic status of coccolithophores after the end-Cretaceous mass extinction. However, while the model produced an evolutionary response that was qualitatively consistent with the sedimentary record, the simulated evolutionary response progressed at a rate that was orders of magnitude too fast. This indicates that the model structure would require further adjustments until both contemporary and sedimentary data are reproduced before the model could be used predictively.

While such a model could be recalibrated to fit the past data, we do not recommend this approach, because the ad hoc adjustment of the model parameters does not fix the underlying problem. In addition, calibration is not possible when making predictions. Therefore, instead of recalibrating the model to past data, we advocate refining the model structure to better represent processes that do apply generally, across past, present, and future systems. After recalibration to contemporary data, the refined model could be tested again against past data. Repeating this process iteratively until both contemporary and past data can be reproduced with the same model assures that the model can produce meaningful statements about an ecosystem's possible response to future climate changes.

Challenges and potential of using data from sediment archives for ecosystem modeling

Our approach has the potential to increase the informative value of model projections of future changes in marine ecosystems. However, there are still some challenges associated with it.

One major challenge comprises the low temporal resolution of sedimentary records, which can range from multi-centennial to annual depending on the sedimentation rate (Abrantes et al., 2005; Maslin et al., 2005). Thus, phenological information is missing even in high-resolution records, meaning that simulated phenology cannot be validated using data from sediment archives. Instead, simulated phenology can be validated using monitoring data, which may go back several decades (Catlett et al., 2021; Edwards et al., 2010; Hjerne et al., 2019; Wasmund et al., 2019). Simulated longer-term ecosystem changes on perennial time scales, however, can still be validated using sediment archives. In addition, preservation issues can lead to sediment horizons being lost for analysis due to low concentrations of total organic carbon. Biotic proxies for the reconstruction of environmental conditions and DNA also suffer from preservation/degradation biases and are therefore not independent from each other (Wakeham and Canuel, 2006; Zonneveld et al., 2010; Dommain et al., 2020; Mitchell et al., 2005). Preservation/degradation biases in biological data may lead to incomplete information on mean traits and trait variance. Resting stages that have been preserved in the sedimentary record and could be revived for experiments may not be representative of the entire population at the time of deposition, and therefore may not be representative of its traits. However, assuming that the fittest individuals of a population were most abundant in the past and hence are most abundant in the sediment, we should be able to measure representative mean trait values for the population. To obtain reliable estimates of trait variance, experimental studies on phytoplankton traits should aim to characterize as many strains as possible, e.g., using high-throughput methods (Argyle et al., 2021).

Evolutionary models require knowledge of how rapidly and how far the aforementioned traits can change from generation to generation, as well as of the trade-offs between traits (Levins, 1962; Litchman et al., 2007) and ultimate constraints on adaptation (Klausmeier et al., 2020b). Such information is available from evolutionary experiments, but it is still unclear how applicable such information will be when moving from a highly simplified evolutionary experiment to a more complex community context. A major challenge in this regard is to link trait changes to changes in fitness. While the relationship between a fitness proxy and actual fitness may change over time (Collins et al., 2020), fitness is largely determined by species interactions (Schabhüttl et al., 2013). Based on the assumption that the most competitive phytoplankton taxa are also the most abundant in the sediment, sediment archives make it possible to estimate the relative fitness of different taxa.

Despite limitations and knowledge gaps, sediment archives represent a valuable source of information that has the potential to advance ecosystem model development and hence model predictions of future ecosystem-level changes. As pointed out above, a crucial step in ecosystem model development is to make sure that models are equally applicable to past, present, and future scenarios before using them predictively. This requires validation data that must be independent from the data used for calibration. Moreover, validation data need to cover the complexity of marine ecosystems and long-term environmental changes over hundreds to thousands of years. While data from laboratory, mesocosm, or marine monitoring studies only partly fulfill these criteria, sediment archives fulfill all of them. Furthermore, the approach presented here is not limited to phytoplankton, but can be applied to other organisms that are well-represented in the sediment record, such as zooplankton (Isanta-Navarro et al., 2021; Wersebe and Weider, 2023), viruses (Coolen, 2011), and terrestrial plants (Alsos et al., 2024).

Conclusions

Marine communities perform ecosystem functions that are essential for the environment and for humans. However, it is largely unknown how these ecosystem functions will change under global warming, and the possibility of positive feedbacks, irreversible tipping points, and ecosystem collapse must be considered. It is therefore crucial to develop tools that provide reliable estimates of future changes in marine ecosystems.

Ecosystem models represent a promising tool in this regard, but they largely disagree on future ecosystem changes. Here, we present an auspicious approach that can improve future model predictions. We argue that ecosystem models must account for evolutionary processes, which are largely ignored by current models but can be highly relevant on perennial time scales. In addition, models must represent fundamental processes instead of being tailored to a specific ecosystem. To achieve this, it must be validated that ecosystem models are equally applicable to past and present scenarios before they can be used predictively. However, independent validation is largely missing from current ecosystem modeling studies. We suggest calibrating ecosystem models using contemporary observations, and validating the calibrated models against major ecosystem changes that are present in sedimentary records. Compared to data from conventional experiments and marine monitoring, sediment archives make it possible to map the complexity of real ecosystems and long-term environmental changes. Only if a contemporarily calibrated ecosystem model can reproduce observations from sedimentary records, we can have some confidence in its predictions of future ecosystem changes.

Some challenges remain, especially regarding the low temporal resolution of sediment archives and their partly biased information. Nevertheless, data from sediment archives provide a unique opportunity to learn from the past and hence have the potential to take ecosystem models and their predictions of future ecosystem changes a crucial step forward. The approach that we present here is not restricted to phytoplankton but can be applied to other organisms and ecosystems as well.

Chapter 3

SUMMARY & CONCLUSIONS

This PhD thesis contributes to improving predictions of future changes in marine ecosystems by addressing two major uncertainties in current marine ecosystem models, namely the neglect of phytoplankton adaptation and the predictive use of models tailored to contemporary ecosystems.

Study I: The interplay between competition & adaptation

Until now, no ecosystem modeling study has investigated how the simulated response of a phytoplankton community with multiple competing functional groups to global warming changes when evolutionary adaptation is considered. Likewise, other important processes that can influence adaptation, such as resting cell resuspension, have been largely ignored in ecosystem models. In the first study of this thesis, my co-author and I filled these gaps by developing an innovative ecosystem model that for the first time combines the competition between multiple phytoplankton functional groups, their adaptation to global warming, and resting cell resuspension. We applied the model to the Baltic Sea, which is impacted by above-average levels of warming, and performed simulations for present-day and future climate scenarios. For each climate scenario, we ran three different types of simulations: (a) simulations without phytoplankton adaptation, (b) simulations with mutations in the optimum temperature for growth, and (c) simulations with mutations and resting cell resuspension from the sediment. With these simulations, we can now answer our initial research questions:

How does the interplay between competition and adaptation affect simulated phytoplankton responses to global warming?

How does resting cell resuspension affect adaptation to global warming?

We found that simulations that consider both competition and adaptation produce different results than simulations in which only one of the two processes is included. Both processes influence each other, with the outcome of their interplay depending on environmental conditions. In a steady environment, competition for resources leads to adaptation to individual temperature niches (niche separation). In a warming environment, adaptation allows inferior competitors to increase their competitivity, which in turn allows them to mitigate the dominance of preadapted superior competitors. Thus, by neglecting adaptation, models may systematically overestimate phytoplankton responses to global warming in terms of changes in relative taxa abundances and bloom timing.

In our simulations, resting cell resuspension tends to slow down adaptation to global warming since past-adapted resting cells are re-introduced to the actively growing population.

To conclude, **Study I** demonstrates that adaptation increases the resilience of marine communities to environmental change and reduces dominance changes among taxa, which is in agreement with previous theoretical models (Barabás and D'Andrea, 2016; Northfield and Ives, 2013). Our study extends the previous findings by showing that they do not only apply in a theoretical framework but also in an ecosystem context. Thus, future ecosystem models should no longer ignore evolutionary processes, especially those used for climate projections. Instead, future ecosystem models should consider both competition and adaptation simultaneously to realistically simulate phytoplankton responses to global warming.

Study II: The effect of adaptation on ecosystem functioning

So far, no modeling study has investigated how phytoplankton adaptation to global warming could affect the functioning of a marine ecosystem. In **Study II**, we filled this gap by extending the model developed in **Study I** to explicitly calculate different ecosystem functions, including nitrogen fixation and carbon export. Using the extended version of the model, we again performed simulations for present-day and future climate conditions, in each case with and without phytoplankton adaptation in the optimum temperature. These simulations now allow us to answer our initial research question:

How does phytoplankton adaptation affect simulated ecosystem dynamics and future changes in ecosystem functioning?

The simulations show that phytoplankton adaptation affects not only the simulated phytoplankton dynamics themselves, but also the simulated ecosystem dynamics, as phytoplankton are key players in marine ecosystems. Similar to **Study I**, the effect of phytoplankton adaptation on the simulated ecosystem dynamics depends on environmental conditions. In a steady environment, adaptations allows for a more efficient usage of the limiting resources through niche separation. Enhanced resource use efficiency, in turn, increases primary production and associated ecosystem functions such as secondary production and carbon export. In a warming environment, adaptation reduces dominance changes among functionally different taxa and hence mitigates changes in ecosystem functioning. Thus, by neglecting phytoplankton adaptation, models may systematically underestimate resource use efficiency and associated ecosystem functions in a steady environment, and systematically overestimate their changes in a warming environment.

In agreement with models and observations, **Study II** predicts an increase in nitrogen fixation and cyanobacteria-related carbon export in the Baltic Sea over the next century of global warming (Hense et al., 2013; Poutanen and Nikkilä, 2001; Tamelander et al., 2017). However, the simulated increase is more than halved if phytoplankton adaptation is considered. These results demonstrate that phytoplankton adaptation is not only relevant to accurately simulate phytoplankton responses to global warming, but in a much broader context. With phytoplankton as key players in marine ecosystems, the accurate simulation of their responses to global warming is a prerequisite for realistic estimates of future changes in ecosystem functioning. Thus, ecosystem models to date may have substantially overestimated future changes in marine ecosystems. To avoid these uncertainties in the future, evolutionary processes need to become a common feature in predictive marine ecosystem models.

Study III: From past ecosystem changes to future projections

In the third study of this thesis, we addressed the second major uncertainty in current marine ecosystem models, namely that predictive models are tailored to the current state of an ecosystem and may therefore not be applicable to the future. We argue that models should only be used predictively if they represent fundamental processes that apply equally to the past, present, and future state of an ecosystem. Based on the idea that we can learn about these fundamental processes from past ecosystem changes present in sedimentary records, we designed a conceptual framework for developing evolutionary ecosystem models that are equally applicable to past, present, and future scenarios. Using this framework, we can now answer our initial research questions:

How can data from sediment archives improve evolutionary ecosystem models and their projections of future ecosystem changes?

What are the remaining challenges and what is the potential of our approach?

Our framework suggests calibrating evolutionary ecosystem models using contemporary observations, e.g., from seagoing research and/or satellite data, and testing the calibrated models against major ecosystem changes that are present in sedimentary records (validation). Abiotic and biotic proxies archived in sedimentary records provide information about past environmental conditions, including salinity, oxygen conditions, pH, trophic state, and temperature, which can be used as forcing for models. The model output can then be compared to biological information on biodiversity, relative taxa abundances, and trait adaptation derived from microfossils, sedimentary ancient DNA, and resurrectable resting stages present in the sediment. Only when the same model can reproduce both contemporary observations and major events in the sedimentary record, which may require several iterations to refine the model structure, should the model be used predictively.

Despite its great potential, there are still some challenges associated with our approach. These include the low temporal resolution of sedimentary records without seasonality information and degradation/preservation biases in both environmental and biological data. In addition, evolutionary ecosystem models require information on maximum adaption rates, limits and ultimate constraints on adaptation, as well as trade-offs between traits, which cannot be obtained from sediment archives but from evolution experiments. It is unknown, however, how applicable such information will be when moving from an idealized experiment to a complex ecosystem.

Even if some challenges remain, data from sediment archives allow for long-term validation over millennia, are independent from the calibration data, and capture the complexity of real ecosystems. These crucial requirements for validation data are only partly fulfilled by laboratory experiments, mesocosm experiments, or marine monitoring studies. In addition, our approach is not limited to phytoplankton but can be applied to other organisms that are well-represented in the sedimentary record, for example, zooplankton and terrestrial plants.

While the validation of predictive models is already common for atmosphere and ocean circulation models (Tonani et al., 2015; Hollingsworth, 1994), this procedure is largely ignored by the ecosystem modeling community. Although some ecosystem models have already been used for both hindcast simulations and future projections, the hindcasts were only used to estimate model biases (Meier et al., 2014; Eilola et al., 2011; Meier et al., 2011). As previously shown for ocean circulation models, validation can significantly improve model performance, with the improvement depending on the quality of the validation data (Oke et al., 2015a,b). With our validation concept for ecosystem models specifically, it may be possible to improve their performance not only by refining the representation of existing processes, but also by identifying other relevant processes that have been ignored so far. Since our approach is based on sedimentary records, which provide higher quality validation data than both observations and experiments, it has the potential to take the development of predictive ecosystem models a crucial step forward and should be adopted by the ecosystem modeling community.

However, our approach may not only be valuable for modeling studies but also for experimental research. In nature, multiple environmental factors change simultaneously (Allan et al., 2021). Identifying the main driver(s) responsible for the ecosystem changes present in sedimentary records can therefore be challenging. Iteratively refining the structure of an ecosystem model until the model can reproduce both contemporary and sedimentary data can help to understand the observed ecosystem changes and their drivers.

General conclusions and perspectives for future research

Providing reliable estimates of future changes in marine ecosystems is crucial. Marine communities fulfil vital functions for the global climate and us humans (Hain et al., 2014; Weatherdon et al., 2016), which are threatened by ongoing global warming (Pecl et al., 2017; Hoegh-Guldberg and Bruno, 2010). Ecosystem models currently represent the best tool for assessing future ecosystem changes and are therefore a valuable resource for political decision-making (Intergovernmental Panel on Climate Change (IPCC), 2022; Meier et al., 2014). However, existing models predict diverging changes in ecosystem functions like net primary production and carbon export (Laufkötter et al., 2015, 2016), which implies that they are still neglecting fundamental processes. This PhD thesis demonstrates that phytoplankton adaptation, a fundamental process that is largely ignored in existing ecosystem models, can significantly change simulated phytoplankton and ecosystem dynamics under both present-day and future climate conditions. My results show that adaptation increases the resilience of marine communities to environmental change and thus reduces changes in phytoplankton taxa abundances and ecosystem functions like nitrogen fixation and carbon export by a multitude. Therefore, it seems highly questionable to implement phytoplankton with fixed traits, which is common in existing ecosystem models. Until now, ecosystem models may have systematically underestimated the resilience of marine communities to environmental change, which may have led to a systematic overestimation of phytoplankton and ecosystem responses to global warming. Adaptation should become a common feature in future ecosystem models, especially those used for climate projections.

Incorporating evolutionary processes into marine ecosystem models is only a first step towards more reliable predictions of future ecosystem changes, and much potential remains for future research efforts. Considering this work specifically, the next logical step would be to test my model against data from sediment archives and revise the model structure until both contemporary observations and sediment data are reproduced. Afterwards, the model could be used for climate projections again, and the results could be compared to the unvalidated climate projections from **Study I** and **Study II**. The comparison of climate projections before and after validation would allow to investigate how validation affects model projections of future ecosystem changes and provide further insight into the true potential of this approach.

Even if validated, the model presented in this thesis will not be suitable to provide quantitative estimates of future changes in marine ecosystems due to its simplistic design. Thus, model complexity will need to be increased, or evolutionary processes will need to be integrated into existing, more complex ecosystem models. Considering the model presented here specifically, the potentially most important addition would be the coupling to a 1D or 3D physical environment due to the importance of physical processes for biogeochemical cycling. Integrating evolutionary processes into existing global coupled Earth system models, such as the CMIP models, could potentially reduce their disagreement about future changes in ecosystem functioning.

In conclusion, evolutionary processes should no longer be neglected by the marine ecosystem modeling community. Instead, they should be integrated into policy-relevant Earth system models, e.g., the CMIP models, using computationally efficient evolutionary algorithms such as continuous trait diffusion (Le Gland et al., 2021; Chen and Smith, 2018). If validated against data from sediment archives, such models could eventually provide reliable estimates of future ecosystem changes, maybe even quantitatively. While a lot of work remains to be done to achieve this goal, my work is a first crucial step. By addressing two major uncertainties in current ecosystem models, I was able not only to emphasize the need to revise these models, especially when used for climate projections, but also to provide approaches to solutions. Future work can build on my results and bring the modeling community closer to reliable estimates of future ecosystem changes.

Appendix A

APPENDICES FOR STUDY I

A.1 Evolution in ecosystem models

Ecosystem models use mathematical formulations to conceptualize the dynamics of living and non-living organic matter (organisms, e.g., phytoplankton, and detritus), as well as other ecosystem components (nutrients, chemicals, toxins). All ecosystem components are represented by model state variables, which are linked by sink and source processes like nutrient uptake, growth, mortality, and remineralization. Processes are formulated as differential equations and may depend on environmental conditions such as temperature, salinity, and light. For example, phytoplankton growth may depend on environmental temperature, which can be parameterized with a thermal limitation function.

To simulate phytoplankton adaptation to changing temperatures, the thermal limitation function can be implemented with evolvable parameters (e.g., optimum temperature). The most suitable strategy to integrate evolutionary processes into ecosystem models depends on the complexity of the ecosystem model itself. Global circulation models, for instance, require a computationally efficient and thus simplified implementation of evolutionary processes. Zero-dimensional box models, on the contrary, allow for a computationally more demanding and hence more complex representation of evolution.

Individual-based models (IBMs), which simulate individual phytoplankton cells with their individual phenotypic trait values, provide the most realistic and thus most complex representation of evolutionary processes. One prominent approach that simulates trait value changes in response to environmental changes was developed by Beckmann et al. (2019). In their model, Beckmann et al. (2019) assume that cells take up nutrients, grow, divide, and die. However, cells are also affected by stochastic processes, e.g., during mortality or due to random mutations. A random mutation in a daughter cell's trait occurs every several hundred cell divisions (Lenski and Travisano, 1994). The daughter cell's trait is sampled randomly from a Gaussian distribution centered at the parent's trait value with a prescribed standard deviation. In this way, small step mutations are much more likely than large step mutations, while it is equally likely that mutations decrease or increase the daughter's competitivity. Over time, natural selection acts and the most competitive cells that need the lowest time to divide again become dominant. Maladapted cells, on the contrary, become extinct if their doubling rate is lower than stochastic loss processes like mortality and grazing. In this manner, the entire population adapts progressively.

Since simulating the evolution of natural populations with millions of individuals would take a lot of computational time, identical individuals are often grouped into one model variable, a so-called agent. Due to the larger number of cells within one agent, mutations are expected to occur more frequently but with a smaller standard deviation. Here, we use such an agent-based approach to simulate the interplay of competition and adaptation in Baltic Sea phytoplankton in response to warming.

A.2 Towards an agent-based adaptive phytoplankton community model with life cycle dynamics

Local contents

A.2.1 Model concept

Basic compartment-based NPZD-type model

Our 0-dimensional agent-based adaptive phytoplankton community model with life cycle dynamics is based upon a simple compartment-based NPZD-type model that simulates a closed element cycle with four state variables: a nutrient N, a phytoplankton population P, a zooplankton population Z, and detritus D. The four state variables are represented by their concentration. Since nitrogen is the most limiting nutrient in marine ecosystems, the concentration is usually given in mmol nitrogen per m^3 (Table A.2.1). Source and sink processes, like growth and mortality, lead to changes in concentration over time. These concentration changes can be calculated with the following system of equations:

$$\frac{\mathrm{d}P}{\mathrm{d}t} = \underbrace{\mu P}_{\text{P growth}} - \underbrace{\gamma P}_{\text{P mortality}} - \underbrace{g(P)\, Z}_{\text{Z grazing}} \tag{A.1}$$

$$\frac{\mathrm{d}Z}{\mathrm{d}t} = \underbrace{\beta\, g(P)\, Z}_{\text{Z grazing}} - \underbrace{\epsilon Z}_{\text{Z excretion}} - \underbrace{\psi Z^2}_{\text{Z mortality}} \tag{A.2}$$

$$\frac{\mathrm{d}N}{\mathrm{d}t} = \underbrace{\epsilon Z}_{\text{Z excretion}} + \underbrace{rD}_{\text{remin.}} - \underbrace{\mu P}_{\text{P growth}} \tag{A.3}$$

$$\frac{\mathrm{d}D}{\mathrm{d}t} = \underbrace{\gamma P}_{\text{P mortality}} + \underbrace{\psi Z^2}_{\text{Z mortality}} + \underbrace{(1-\beta)\, g(P)\, Z}_{\text{Z unassimilated prey}} - \underbrace{rD}_{\text{remin.}} \tag{A.4}$$

Compartment-based NPPPZD-type life cycle model

The above Equations (A.1)-(A.4) describe an ecosystem with only one phytoplankton population and ignore phytoplankton life cycle processes. Since our model considers three different phytoplankton functional groups including their life cycles, we need more than one phytoplankton state variable to describe the dynamics of our ecosystem. In particular, we need one state variable for each life cycle stage of each functional group, i. e., three state variables for cyanobacteria, as well as

Symbol	Description	Unit
P	Phytoplankton concentration	$\mathrm{mmol\,N\,m^{-3}}$
Z	Zooplankton concentration	$\mathrm{mmol\,N\,m^{-3}}$
N	Concentration of dissolved inorganic nitrogen	$\mathrm{mmol\,N\,m^{-3}}$
D	Concentration of detritus	$\mathrm{mmol\,N\,m^{-3}}$
μ	Growth rate of phytoplankton	$\mathrm{d^{-1}}$
γ	Mortality rate of phytoplankton	$\mathrm{d^{-1}}$
g	Grazing rate of zooplankton	$\mathrm{d^{-1}}$
β	Assimilation efficiency of zooplankton	–
ϵ	Excretion rate of zooplankton	$\mathrm{d^{-1}}$
ψ	Mortality rate of zooplankton	$\mathrm{d^{-1}}$
r	Remineralization rate of detritus	$\mathrm{d^{-1}}$

Table A.2.1: Description of the different variables used in the basic compartment-based NPZD-type ecosystem model (Equations (A.1)-(A.4)).

two state variables for dinoflagellates and diatoms, respectively. Because one of the three simulated cyanobacterial life cycle stages is able to fix atmospheric nitrogen (N_2), our model comprises an open element cycle. Moreover, our model includes a sinking term for the detritus compartment, as well as terms for burial and resuspension of phytoplankton resting cells. The following Equations (A.5)-(A.11) describe the resulting concentration changes of our seven phytoplankton state variables; the corresponding parameters are given in Table A.2.2.

Dinoflagellates

We simulate the life cycle of a cold-water dinoflagellate species of the genus *Apocalathium.* We use the parameterization from Hinners et al. (2019), with the exception that we neglect the gametes, which we assume to play a minor role in the life cycle of our chosen *Apocalathium* species. Thus, we consider two life cycle stages in total, a growing stage (vegetative cells P_1^1, Equation (A.5)) and a resting stage (cysts P_2^1, Equation (A.6)). We assume that growth of vegetative cells depends on nitrogen concentration N, environmental temperature T, and irradiance I:

$$\frac{\mathrm{d}P_1^1}{\mathrm{d}t} = \underbrace{\mu_1(N,T,I)P_1^1}_{\text{growth}} + \underbrace{\tau_{P_2^1 P_1^1} P_2^1}_{\text{transfer from } P_2^1} - \underbrace{\gamma_{11} P_1^1}_{\text{mortality}} - \underbrace{g(P_1^1)\,Z}_{\text{grazing}} - \underbrace{\tau_{P_1^1 P_2^1} P_1^1}_{\text{transfer to } P_2^1} \tag{A.5}$$

$$\frac{\mathrm{d}P_2^1}{\mathrm{d}t} = \underbrace{\eta_1 P_{2,\mathrm{b}}^1}_{\text{resuspension}} + \underbrace{\tau_{P_1^1 P_2^1} P_1^1}_{\text{transfer from } P_1^1} - \underbrace{\delta_1 P_2^1}_{\text{burial}} - \underbrace{\gamma_{12} P_2^1}_{\text{mortality}} - \underbrace{g(P_2^1)\,Z}_{\text{grazing}} - \underbrace{\tau_{P_2^1 P_1^1} P_2^1}_{\text{transfer to } P_1^1} \tag{A.6}$$

The transition rates τ are explained in section "Life cycle transitions" for all phytoplankton functional groups and life cycle stages. The index "b" in the resuspension term denotes cells that are buried in the sediment.

Diatoms

For diatoms, we simulate the life cycle of a cold-water species of the genus *Thalassiosira* following Warns (2013). Like for dinoflagellates, we consider a growing stage (vegetative cells P_1^2, Equation (A.7)) and a resting stage (spores P_2^2, Equation (A.8)); both diatom life cycle stages are parameterized similarly to the two dinoflagellate life cycle stages (see Equations (A.5) and (A.6)):

$$\frac{\mathrm{d}P_1^2}{\mathrm{d}t} = \underbrace{\mu_2(N,T,I)P_1^2}_{\text{growth}} + \underbrace{\tau_{P_2^2P_1^2}P_2^2}_{\text{transfer from } P_2^2} - \underbrace{\gamma_{21}P_1^2}_{\text{mortality}} - \underbrace{g(P_1^2)\,Z}_{\text{grazing}} - \underbrace{\tau_{P_1^2P_2^2}P_1^2}_{\text{transfer to } P_2^2} \tag{A.7}$$

$$\frac{\mathrm{d}P_2^2}{\mathrm{d}t} = \underbrace{\eta_2P_{2,\mathrm{b}}^2}_{\text{resuspension}} + \underbrace{\tau_{P_1^2P_2^2}P_1^2}_{\text{transfer from } P_1^2} - \underbrace{\delta_2P_2^2}_{\text{burial}} - \underbrace{\gamma_{22}P_2^2}_{\text{mortality}} - \underbrace{g(P_2^2)\,Z}_{\text{grazing}} - \underbrace{\tau_{P_2^2P_1^2}P_2^2}_{\text{transfer to } P_1^2} \tag{A.8}$$

Cyanobacteria

The most complex life cycle in our model is the life cycle of N_2-fixing cyanobacteria of the order Nostocales. Instead of a single species, we consider a cyanobacteria complex that represents the dominant N_2-fixing genera in the Baltic Sea, *Nodularia*, *Aphanizomenon*, and *Anabaena* (Stal et al., 2003; Karlsson et al., 2005). By combining two modeling approaches (Hense and Beckmann, 2006, 2010), we simulate three life cycle stages in total, two growing stages and one resting stage.

The first growing stage represents vegetative cells (P_1^3), which occur in chain-like colonies, so-called filaments. Similar to vegetative dinoflagellates and diatoms, the growth of vegetative cyanobacteria depends on temperature, light, and dissolved inorganic nitrogen (Equation (A.9)). Nitrogen depletion leads to differentiation of some vegetative cells into so-called heterocysts, which fix N_2 for the entire filament. However, we do not simulate heterocysts explicitly but only their effect on vegetative growth. Consequently, the second growing stage represents filaments of vegetative cells where heterocysts are present (P_2^3). Contrary to vegetative cells without heterocysts, the growth of vegetative cells with heterocysts is not limited by dissolved inorganic nitrogen but by temperature, light, and an internal energy quota E (Equation (A.10)). Nitrogen fixation requires far more energy than nitrogen uptake, leading to significantly reduced growth rates (Stephens et al., 2003). Therefore, we follow Hense and Beckmann (2010) and assume that growth of vegetative cells with heterocysts is limited by the internally stored energy E and ceases when E is exhausted. While E is consumed by nitrogen fixation and growth, it can be refilled by light capture (see Equation (A.15) in the next section). We only calculate changes in E during the N_2-fixing stage and assume that the two other stages are not limited by energy. Thus, we initialize the N_2-fixing stage with a full energy quota. The cyanobacterial resting stage P_3^3 is parameterized similarly to the resting stages of dinoflagellates and diatoms (Equation (A.11)).

Apart from N_2 fixation, cyanobacteria are the only algae in our model that are able to produce toxins. Consequently, we follow other models (Hense and Beckmann, 2006; Lee et al., 2018; Hinners et al., 2015) and assume that cyanobacteria are not grazed by zooplankton; the following equations do hence not contain any grazing terms:

$$\frac{\mathrm{d}P_1^3}{\mathrm{d}t} = \underbrace{\mu_{31}(N,T,I)P_1^3}_{\text{growth}} + \underbrace{\tau_{P_3^3P_1^3}P_3^3}_{\text{transfer from } P_3^3} - \underbrace{\gamma_{31}P_1^3}_{\text{mortality}} - \underbrace{\tau_{P_1^3P_2^3}P_1^3}_{\text{transfer to } P_2^3} - \underbrace{\tau_{P_1^3P_3^3}P_1^3}_{\text{transfer to } P_3^3} \tag{A.9}$$

$$\frac{\mathrm{d}P_2^3}{\mathrm{d}t} = \underbrace{\mu_{32}(T,I,E)P_2^3}_{\text{growth}} + \underbrace{\tau_{P_1^3P_2^3}P_1^3}_{\text{transfer from } P_1^3} - \underbrace{\gamma_{32}P_2^3}_{\text{mortality}} - \underbrace{\tau_{P_2^3P_3^3}P_2^3}_{\text{transfer to } P_3^3} \tag{A.10}$$

$$\frac{\mathrm{d}P_3^3}{\mathrm{d}t} = \underbrace{\eta_3P_{3,\mathrm{b}}^3}_{\text{resuspension}} + \underbrace{\tau_{P_1^3P_3^3}P_1^3}_{\text{transfer from } P_1^3} + \underbrace{\tau_{P_2^3P_3^3}P_2^3}_{\text{transfer from } P_2^3} - \underbrace{\delta_3P_3^3}_{\text{burial}} - \underbrace{\gamma_{33}P_3^3}_{\text{mortality}} - \underbrace{\tau_{P_3^3P_1^3}P_1^3}_{\text{transfer to } P_1^3} \tag{A.11}$$

Agent-based adaptive phytoplankton community model with life cycle dynamics

The seven phytoplankton equations presented above (Equations (A.5)-(A.11)) describe each life cycle stage as a so-called compartment, i. e., a collection of cells. Each compartment is defined by a single parameter set that represents the averaged properties of all cells within the compartment. However, we aim to simulate both ecological and evolutionary phytoplankton responses to global warming. Since mutations occur on the level of the individual, it is more natural to treat a phytoplankton population as a collective of individual cells. Simulating the evolution of natural populations with millions of individuals would need a lot of computational time, though. To reduce computational time, identical individuals can be grouped into one model variable, a so-called agent. Due to the larger number of cells within one agent, smaller mutations are assumed to occur more frequently.

Due to the reasons stated above, we replace all phytoplankton compartments of the NPPPZD-type life cycle model by a collective of agents. Prior to each simulation, each agent is initialized with a specific parameter set that consists of fixed and flexible traits. Fixed traits are passed unalteredly to the offspring and may differ between functional groups and life cycle stages. Flexible traits, on the contrary, can change due to phenotypic plasticity (maximum cell size) or mutation (optimum temperature); see “Model concept” in **Study I** (section 2.1). Both fixed and flexible traits determine the individual growth rate μ_i of the i^{th} cell, with μ_i changing the cell’s biomass b_i according to Equation (A.12):

$$\frac{\mathrm{d}b_i}{\mathrm{d}t} = \mu_i \tag{A.12}$$

As stated in the previous section, we assume that vegetative growth is limited by dissolved inorganic nitrogen, temperature, and light. We calculate the nitrogen-limited growth rate $\mu_{\lim_N}$ from cell biomass b_i, the internal nitrogen quota Q_i, and nitrogen concentration N (see section “Nitrogen limitation”). By multiplying the nitrogen-limited growth rate with limitation functions for temperature and light, we obtain the individual growth rate μ_i^{veg} of the i^{th} vegetative cell (Equation (A.13)). For each functional group, we use a different temperature limitation function $\lim_T$, with the function’s value depending on environmental temperature T, group-specific traits, and the cell-specific optimum temperature T_i^{opt} (see section “Temperature limitation”). Light limitation $\lim_L$ is determined by irradiance I, group-specific traits, and cell-specific metabolic rates φ_i (see section “Light limitation”).

$$\mu_i^{\text{veg}} = b_i^{0,T} \times \mu_{\lim_N}(b_i, Q_i, N) \times \lim_T(T, T_i^{\text{opt}}) \times \lim_L(I, \varphi_i) \tag{A.13}$$

with the cell-specific theoretical minimum cell biomass $b_i^{0,T}$, which we derive from environmental temperature T during cell production (see “Model concept” in **Study I** (section 2.1)).

To calculate the growth rate of the i^{th} vegetative cell within a N_2-fixing filament μ_i^{het} (Equation (A.14)), we replace the nitrogen-limited growth rate $\mu_{\lim_N}$ in Equation (A.13) by the saturated growth rate μ_{sat}, which assumes that the cell-internal nitrogen storage is completely filled. In addition, we replace light limitation $\lim_L$ by energy limitation $\lim_E$ after Hense and Beckmann (2006):

$$\mu_i^{\text{het}} = b_i^{0,T} \times \zeta \times \mu_{\text{sat}}(b_i) \times \lim_T(T, T_i^{\text{opt}}) \times \lim_E(E_i), \text{ with } \lim_E = 1 - \left(\frac{E_i}{E_{\max}} - 1\right)^n \tag{A.14}$$

As explained for the "compartment-based life cycle model", vegetative cells with heterocysts show lower growth rates than vegetative cells without heterocysts. Following Hense and Beckmann (2006), we assume that growth rates of vegetative cells with heterocysts are reduced by a factor of 4. Therefore, we scale the saturated growth rate in Equation (A.14) with a factor of $\zeta = 0.25$.

Following Hense and Beckmann (2006), we choose n to be large and even and $E_{\max} = 1$, meaning that we assume the internal energy storage to be as large as the energy stored in the organic material. The form of $\lim_E$ furthermore assumes that growth does not slow down before the energy quota E_i is almost exhausted.

To calculate temporal changes of E_i, we modify Equation (1) in Hense and Beckmann (2006) to Equation (A.15):

$$\frac{\mathrm{d}E_i}{\mathrm{d}t} = \underbrace{b_i^{0,T} \times \lim_L(I, \varphi_i) \times \left(1 - \left(\frac{E_i}{E_{\max}}\right)^n\right) \times (\omega_{lc0} + E_{\text{perc}} \times (\omega_{lc} - \omega_{lc0}))}_{\text{light capture}} - \underbrace{m \times \mu_i^{\text{het}}}_{\text{N}_2\text{ fixation}} - \underbrace{\mu_i^{\text{het}}}_{\text{growth}} \tag{A.15}$$

As shown in Equation (A.15), we assume that E_i is refilled by light capture and consumed by nitrogen fixation and growth. The amount of energy that is refilled depends on a constant light capture rate ω_{lc0} (Table A.2.2) and a growth rate-dependent light capture rate ω_{lc} (see Table A.2.5 in section "Light limitation"). We express the scale of growth rate-dependence of light capture by a factor E_{perc} (Table A.2.2). Similar to Hense and Beckmann (2006), we account for the higher energy consumption of nitrogen fixation compared to growth by multiplying the fixation term with a factor $m = 3$.

Following Beckmann et al. (2019), we assume that the i^{th} cell divides when $b_i \geq 2b_i^{0,T}$, increasing the number of live cells by one. To conserve total living biomass, we assign half of the parental biomass to each daughter cell. We then calculate the phytoplankton concentration diagnostically from Equation (A.16):

$$P = \frac{1}{V} \sum_{i=1}^{M} b_i \tag{A.16}$$

with the volume of the considered domain V and the number of live cells M.

An agent-based model treats life cycle transitions, mortality, burial, resuspension, and zooplankton grazing as stochastic processes; we describe them mathematically by Equations (A.17)-(A.20). In our model, a cell transfers to another life cycle stage if

$$X_{(0,1)} < \tau_{\text{crit}} \tag{A.17}$$

where $X_{(0,1)}$ is a random number between 0 and 1. To calculate the non-dimensional transition threshold τ_{crit}, we combine the time step Δt with the transition rate τ:

$$\tau_{\text{crit}} = \Delta t\ \tau, \text{ with the requirement that } \tau \leq \Delta t^{-1} \tag{A.18}$$

For instance, we use a germination rate of $\tau = 0.1\,\mathrm{d}^{-1} = 1.1574 \times 10^{-6}\mathrm{s}^{-1}$ to simulate the transfer from dinoflagellate cysts to vegetative dinoflagellates (see Table A.2.6 in section "Life cycle transitions"). By combining the germination rate τ with the time step $\Delta t = 3600\,\mathrm{s}$ according to Equation (A.18), we obtain a transition threshold of $\tau_{\text{crit}} = 0.0042$. Following Equation (A.17), a dinoflagellate cyst then transfers to the vegetative stage if

$$X_{(0,1)} < \tau_{\mathrm{crit}} = 3600\,\mathrm{s} \times 1.1574 \times 10^{-6}\,\mathrm{s}^{-1} = 0.0042$$

Mortality and burial are simulated similarly. The corresponding rates are given in Table A.2.2. Resuspension, however, requires a more complex representation. The probability for a cell to be resuspended from the sediment decreases exponentially with the time since burial ϑ_i, which is cell-specific. A cell is resuspended from the sediment if Equation (A.19) is fulfilled:

$$X_{(0,1)} < \eta_{\mathrm{crit}}, \text{ with } \eta_{\mathrm{crit}} = \Delta t\ \eta\ \mathrm{e}^{-\vartheta_i/\tau_C} \tag{A.19}$$

with the non-dimensional resuspension threshold η_{crit}, the basic resuspension rate η, and the characteristic time $\tau_C = 10\,\mathrm{yr}$. Due to the exponentially decreasing resuspension probability, we do not explicitly consider additional loss processes like mortality and grazing for dormant resting cells in the sediment.

Zooplankton grazing is a stochastic process as well, a phytoplankton cell is grazed if

$$X_{(0,1)} < g_{\mathrm{crit}}, \text{ with } g_{\mathrm{crit}} = \Delta t\ g_{\mathrm{pref}}\ Z\ g_{\mathrm{H}} \tag{A.20}$$

The non-dimensional grazing threshold g_{crit} is the product of the time step Δt, the grazing preference g_{pref}, zooplankton concentration Z, and a Holling-type grazing function g_{H} evaluated at the current time step. The grazing preference is a group-specific number between 0 and 1. Since we assume that dinoflagellates and diatoms are equally grazed by zooplankton, we set $g_{\mathrm{pref}} = 1$ for both of them. The grazing function g_{H} is the same for all functional groups. The model allows to choose between Holling-type functions I to IV; we use type III in our simulations (Equation (A.21)). The parameters for Holling-type III are given in Table A.2.2.

$$g_H = g_{\max}\ \frac{P^v}{P^v + k_P^v} \tag{A.21}$$

We represent zooplankton, dissolved inorganic nitrogen, and detritus by compartments; the coupling between compartments and agents is described by Equations (A.22)-(A.24). For the coupling to the detritus compartment (Equation (A.4) with sinking of detritus s_D as additional sink), we have to collect the biomass of all phytoplankton cells that died during the current time step:

$$\gamma P = \frac{1}{V\Delta t}\sum_{i=1}^{M}\begin{cases} b_i, & X_{(0,1)} < \gamma_{crit} \\ 0, & X_{(0,1)} \geq \gamma_{crit}\end{cases} \tag{A.22}$$

Similarly, for the coupling to the zooplankton compartment (Equation (A.2)), we have to collect the biomass of all phytoplankton cells that were grazed during the current time step:

$$gZ = \frac{1}{V\Delta t}\sum_{i=1}^{M}\begin{cases} b_i, & X_{(0,1)} < g_{\mathrm{crit}} \\ 0, & X_{(0,1)} \geq g_{\mathrm{crit}}\end{cases} \tag{A.23}$$

The coupling to the nitrogen compartment is more complicated since we calculate uptake depending on internal nitrogen quotas (see section "Nitrogen limitation"). Thus, uptake is not directly coupled to growth and we cannot simply sum up all growth terms of the current time step as suggested by Equation (A.3). Instead, we have to sum up all uptake terms ρ_i of the current time step, meaning that we replace μP in Equation (A.3) by ρP. The calculation of nitrogen uptake ρ is explained in the next section.

$$\rho P = \frac{1}{V}\sum_{i=1}^{M}\rho_i \tag{A.24}$$

Table A.2.2: Parameters for our agent-based adaptive phytoplankton community model with life cycle dynamics. Parameter values were extracted from the following references: Dinoflagellates: Hinners et al. (2019); diatoms: Warns (2013); cyanobacteria: Hense and Beckmann (2006, 2010); zooplankton: Schartau and Oschlies (2003), except for $g_{\max}$ (Merico et al., 2009) and k_P (Fasham et al., 1990); detritus: Hinners et al. (2019). Adjusted and newly defined parameters are indicated by *. Please note that the mortality rates of resting stages were adjusted to our burial rate so that loss is equal to the corresponding reference.

	Symbol	Parameter	Value	Unit
Dinoflagellates	γ_{11}	Mortality rate P_1^1	0.005	d^{-1}
	γ_{12}	Mortality rate P_2^1	0.0091*	d^{-1}
	δ_1	Burial rate P_2^1	0.2*	yr^{-1}
	η_1	Resuspension rate P_2^1	0.06*	yr^{-1}
Diatoms	γ_{21}	Mortality rate P_1^2	0.02	d^{-1}
	γ_{22}	Mortality rate P_2^2	0.0195*	d^{-1}
	δ_2	Burial rate P_2^2	0.2*	yr^{-1}
	η_2	Resuspension rate P_2^2	0.06*	yr^{-1}
Cyanobacteria	γ_{31}	Mortality rate P_1^3	0.013	d^{-1}
	γ_{32}	Mortality rate P_2^3	0.013	d^{-1}
	γ_{33}	Mortality rate P_3^3	0.0136*	d^{-1}
	δ_3	Burial rate P_3^3	0.2*	yr^{-1}
	η_3	Resuspension rate P_3^3	0.06*	yr^{-1}
	ζ	Growth rate factor P_2^3 vs. P_1^3	0.25	–
	ω_{lc0}	Constant light capture rate P_2^3	0.537*	d^{-1}
	n	Exponent in Equation (A.14)	100*	–
	$E_{\max}$	Maximum energy quota	1	–
	E_{perc}	Factor growth rate dependence	$1.1574\times10^{-7*}$	–
	m	Factor N_2 fixation	3	–
Zooplankton	$g_{\max}$	Maximum grazing rate	2.25	d^{-1}
	γ_Z	Mortality rate	0.2	$\mathrm{d}^{-1}\,(\mathrm{mmol\,N\,m^{-3}})^{-1}$
	ϵ	Excretion rate	0.009	d^{-1}
	β	Assimilation efficiency	0.75	–
	k_P	Half saturation constant	1.0	$\mathrm{mmol\,N\,m^{-3}}$
	v	Exponent in Holling type III	3	–
Detritus	r_D	Remineralization rate	0.1	d^{-1}
	s_D	Sinking rate	0.097*	d^{-1}
Resuspension	τ_C	Characteristic time	10*	yr

A.2.2 Limitation of growth

Nitrogen limitation

We calculate the nitrogen-limited growth rate based on internal nitrogen quotas, which in turn depend on cell size. A laboratory study by Marañón et al. (2013) revealed that the relationship between cell size and maximum growth rate (i. e., saturated growth rate) is taxon-independent and unimodal, with a peak at intermediate cell sizes ($\sim 100\,\mu\text{m}^3$). Ward et al. (2017) explain this finding as a trade-off between nutrient uptake and the potential rate of internal metabolism. While the ability of cells to replenish their internal quota increases with size, their ability to synthesize new biomass decreases with size. Here, we consider this trade-off by combining a variable-internal-stores (VIS) model (Grover, 1991) with experimentally-derived allometric relations between cell volume and metabolic cell properties (Litchman et al., 2007; Marañón et al., 2013; Ward et al., 2017, see Table A.2.3). The reference cell volumes for each functional group, which we allow to change due to temperature-dependent plasticity, are given in Table A1 in Appendix A.3. The general nitrogen affinity of the different functional groups, i.e., nitrogen limitation after Monod (1949), is visualized in the top panel of Fig. A5 in Appendix A.4 for cell volumes at 15 °C.

The VIS model that we use for our calculations (Grover, 1991) follows Droop (1973) by assuming that the nutrient-limited growth rate $\mu_{\lim_N}$ is a hyperbolic function of the cell quota Q. Growth is only possible if the cell quota Q exceeds the basal nutrient requirement $Q_{\min}$. Growth increases with increasing Q towards a theoretical maximum growth rate μ_∞, which assumes an infinite and thus unobtainable cell quota:

$$\mu_{\lim_N} = \begin{cases} \mu_\infty \left(1 - \dfrac{Q_{\min}}{Q}\right), Q > Q_{\min} \\ 0, \qquad\qquad\qquad Q \leq Q_{\min} \end{cases} \tag{A.25}$$

The allometric relations for μ_∞ and $Q_{\min}$ for nitrogen-limited phytoplankton are given in Table A.2.3. The cell quota Q decreases due to growth until growth ceases at $Q_{\min}$; when a cell divides, Q is partitioned between the two daughter cells. Q is refilled by nutrient uptake ρ until the maximum nutrient storage capacity $Q_{\max}$ is reached (Droop, 1973):

$$\frac{\mathrm{d}Q}{\mathrm{d}t} = \rho - \mu Q, \ Q_{\min} \leq Q \leq Q_{\max} \tag{A.26}$$

Following Morel (1987), Grover (1991) assumes that nutrient uptake is a Michaelis-Menten function of external nutrient concentration N and scales with the maximum nutrient uptake rate $\rho_{\max}$:

$$\rho = \begin{cases} \rho_{\max} \dfrac{N}{k_N + N}, \ Q < Q_{\max} \\ 0, \qquad\qquad\quad Q = Q_{\max} \end{cases} \tag{A.27}$$

Similar to μ_∞ and $Q_{\min}$, we calculate $\rho_{\max}$ and the half saturation constant k_N from cell volume using allometric relations for nitrogen-limited phytoplankton (Table A.2.3). Based on experimental studies (Gotham and Rhee, 1981), Grover (1991) assumes that $\rho_{\max}$ is not constant but decreases linearly with increasing Q. Thus, $\rho_{\max}$ is highest under the most extreme nutrient limitation, which is expressed by Equation (A.28):

$$\rho_{\max} = \rho_{\max}^{\text{hi}} - (\rho_{\max}^{\text{hi}} - \rho_{\max}^{\text{lo}}) \, \frac{Q - Q_{\min}}{Q_{\max} - Q_{\min}} \tag{A.28}$$

with $\rho_{\max}^{\mathrm{lo}}$ and $\rho_{\max}^{\mathrm{hi}}$ being the lower and upper bounds on $\rho_{\max}$, respectively. We assume that the allometric relation that we use for $\rho_{\max}$ (Ward et al., 2017) gives values close to $\rho_{\max}^{\mathrm{hi}}$. Ward et al. (2017) used experimental data from Marañón et al. (2013), who ensured nitrogen limitation during their measurements of $\rho_{\max}$. During nitrogen-limited conditions, $\rho_{\max}$ should approach $\rho_{\max}^{\mathrm{hi}}$ (Gotham and Rhee, 1981).

To calculate $\rho_{\max}^{\mathrm{lo}}$, we use Equation (A.26) with Equations (A.25) and (A.27):

$$\frac{\mathrm{d}Q}{\mathrm{d}t} = \rho_{\max}\,\frac{N}{k_N + N} - \mu_{\infty}(Q - Q_{\min}) \tag{A.29}$$

When $Q \approx Q_{\max}$, then $\rho_{\max} \approx \rho_{\max}^{\mathrm{lo}}$ and $\mathrm{d}Q/\mathrm{d}t \approx 0$. With these assumptions, Equation (A.29) becomes Equation (A.30):

$$\rho_{\max}^{\mathrm{lo}} \approx \mu_{\infty}(Q_{\max} - Q_{\min}) \tag{A.30}$$

Symbol	Unit	Relation	Reference
μ_{∞}	d^{-1}	$4.7 \times V^{-0.26}$	Ward et al. (2017)
$Q_{\min}$	$\mathrm{pg\,N\,cell^{-1}}$	$0.032 \times V^{0.76}$	Ward et al. (2017)
$\rho_{\max}^{\mathrm{hi}}$	$\mathrm{pg\,N\,cell^{-1}\,d^{-1}}$	$0.024 \times V^{1.10}$	Ward et al. (2017)
k_N	$\mu\mathrm{mol\,N\,l^{-1}}$	$0.17 \times V^{0.27}$	Litchman et al. (2007)
$Q_{\max}$	$\mathrm{pg\,N\,cell^{-1}}$	$0.055 \times V^{0.93}$	Marañón et al. (2013)

Table A.2.3: Allometric relations between cell volume V and nitrogen-related metabolic cell properties used in this study.

Temperature limitation

Thermal reaction norms of individual phytoplankton populations are typically left-skewed (Eppley, 1972; Moisan et al., 2002), meaning that the decrease is steeper for higher than for lower temperature values with distance from the optimum temperature T^{opt}. In our model, we use three different left-skewed temperature limitation functions, one for each functional group. All temperature limitation functions that we use have already been successfully applied in models. The parameters for each temperature limitation function are given in Table A.2.4 at the end of this section. A visualization is available in Fig. A4 in Appendix A.4.

For dinoflagellates, we apply the same temperature limitation function as Hinners et al. (2019) in their 0-dimensional life cycle model for *Apocalathium malmogiense* (Equation (A.31)). The function is based on temperature-dependence experiments (Hinners et al., 2017), which revealed an optimum temperature T^{opt1} close to 11 °C.

$$\lim_{T1} = \exp\left(-\frac{(T - T^{\mathrm{opt1}})^2}{(T_{l1} - T_{l2}\,\mathrm{sign}(T - T^{\mathrm{opt1}}))^2}\right) \tag{A.31}$$

Temperature limitation of diatoms is adopted from the diatom SRRC model (size reduction-restitution cycle) by Hense and Beckmann (2015) (Equation (A.32)). Based on observations of *Thalassiosira baltica* (Spilling, 2011), we use an initial optimum temperature of $T^{\mathrm{opt2}} = 12\,^{\circ}\mathrm{C}$.

$$\lim_{T2} = \begin{cases} \exp\left(-\left(\dfrac{|T - T^{\mathrm{opt2}}|}{\theta_1}\right)^2\right), & T \leq T^{\mathrm{opt2}} \\ \exp\left(-\left(\dfrac{|T - T^{\mathrm{opt2}}|}{\theta_2}\right)^3\right), & T > T^{\mathrm{opt2}} \end{cases} \tag{A.32}$$

For cyanobacteria, we apply a similar temperature dependence as Hense and Beckmann (2006) in their cyanobacteria life cycle model (CLC) (Equation (A.33)). Since the optimum temperatures of *Nodularia*, *Aphanizomenon*, and *Anabaena* vary between 22 and 35 °C (Uehlinger, 1981; Lehtimäki et al., 1997; Pandey, 1989; Vincent and Silvester, 1979; Seki et al., 1981; Collins and Boylen, 1982; Nalewajko and Murphy, 2001), we use the mean value of 28.5 °C as initial value for T^{opt3}.

$$\lim_{T3} = 0.022 + \frac{1}{0.25 + \exp(3/(T - T_3) - 0.5) + \exp(-(500/(T - T_3) - 25))} \tag{A.33}$$

with $T_3 = T^{\mathrm{opt3}} - 16.43\,^{\circ}\mathrm{C}$.

Table A.2.4: Parameters for the three temperature limitation functions used in this study.

Functional group	Symbol	Parameter	Value [°C]
Dinoflagellates	T^{opt1}	Initial optimum temperature	10.8
	T_{l1}	Width parameter of thermal reaction norm	7.22
	T_{l2}	Width parameter of thermal reaction norm	6.03
Diatoms	T^{opt2}	Initial optimum temperature	12
	θ_1	Temperature scale below optimum	7
	θ_2	Temperature scale above optimum	4
Cyanobacteria	T^{opt3}	Initial optimum temperature	28.5

Light limitation

Similar to temperature limitation, we use established light limitation functions that have already been applied in models. The functions are visualized in the bottom panel of Fig. A5 in Appendix A.4 for the parameters given in Table A.2.5. We assume light to be limiting during winter, while light saturation occurs during the rest of the year.

Light limitation of dinoflagellates (Equation (A.34)) is adopted from Hinners et al. (2019), who implemented a formulation from Webb et al. (1974) into their model. Since dinoflagellates bloom early in the year, their light limitation function has an additional condition: When temperature falls below the freezing point in the Gulf of Finland ($T_f = -0.33\,^{\circ}\mathrm{C}$), sea ice absorbs and reflects light, thus preventing growth ($\lim_{L1}$=0).

$$\lim_{L1} = \begin{cases} 0, & T < T_f \\ 1 - \exp\left(\dfrac{-\alpha_1 \times I}{\mu_{\mathrm{sat}}}\right), & T \geq T_f \end{cases} \tag{A.34}$$

For diatoms, we follow Warns (2013) and use the same formulation as for dinoflagellates but with parameters for *T. baltica* (Equation (A.35)). However, the condition that growth ceases below the freezing point is not included since for our parameterization, diatoms bloom later in the year than dinoflagellates (see "Deviations in spring bloom timing" in **Study I** (section 2.1)).

$$\lim_{L2} = 1 - \exp\left(\frac{-\alpha_2 \times I}{\mu_{\text{sat}}}\right) \tag{A.35}$$

We calculate light limitation of cyanobacteria (Equation (A.36)) similar to Beckmann and Hense (2004).

$$\lim_{L3} = \frac{\alpha_3 \times I}{\sqrt{\omega_{lc}^2 + \alpha_3^2 \times I^2}} \tag{A.36}$$

Table A.2.5: Parameters for the three light limitation functions used in this study.

Functional group	Symbol	Parameter	Value	Unit
Dinoflagellates	α_1	Initial slope of $\lim_{L1}$	0.0085	$\text{m}^2\,\text{W}^{-1}\,\text{d}^{-1}$
	T_f	Freezing point Gulf of Finland	-0.33	°C
Diatoms	α_2	Initial slope of $\lim_{L2}$	0.015	$\text{m}^2\,\text{W}^{-1}\,\text{d}^{-1}$
Cyanobacteria	α_3	Initial slope of $\lim_{L3}$	0.0151	$\text{m}^2\,\text{W}^{-1}\,\text{d}^{-1}$
	ω_{lc}	Maximum light capture rate	$5\ \mu_{\text{sat}}\ \lim_{T3}$	d^{-1}

A.2.3 Life cycle transitions

Dinoflagellates

To simulate the transfer between vegetative cells and resting cysts of our *Apocalathium* species, we follow Hinners et al. (2019). Resting cysts germinate after a dormancy period of several months (Kremp, 2000; Kremp and Anderson, 2000; Kremp and Parrow, 2006). As shown in Equation (A.37), we simplify this process by fixing germination of vegetative cells from cysts to the period between day 44 and day 60 of each year with a constant germination rate σ_{CV} (for all transition-related parameters, see Table A.2.6):

$$\tau_{P_2^1 P_1^1} = \begin{cases} \sigma_{CV}, & 44\,\text{d} < t < 60\,\text{d} \\ 0, & \text{else} \end{cases} \tag{A.37}$$

Cyst formation is implemented temperature-dependent with a strong gradient T_{VC2}, which is centered around a temperature of $T_{VC1} = 6\,°\text{C}$. Resurrection experiments with *A. malmogiense* revealed that the encystment rate of recent strains ($2013 \pm 0.2\,\text{yr}$) is 4.6 times lower than that of historic strains ($1910 \pm 8\,\text{yr}$) (Hinners et al., 2017). Therefore, Hinners et al. (2019) included an encystment factor X_C into their model, with $X_C = 1.0$ for recent strains and $X_C = 4.6$ for historic strains. Since our model is calibrated for present-day conditions, we use the encystment factor for recent strains. Based on these assumptions, vegetative cells transform into cysts according to Equation (A.38):

$$\tau_{P_1^1 P_2^1} = \sigma_{VC} \times X_C \times 0.5\left(1 + \tanh\left[\frac{T - T_{VC1}}{T_{VC2}}\right]\right) \tag{A.38}$$

with the basic encystment rate σ_{VC}.

Diatoms

For our diatom species of the genus *Thalassiosira*, we simulate the transfer between vegetative cells and resting spores by using the approach from Warns (2013). Resting spores form when conditions are unfavorable for growth (Drebes, 1966; Durbin, 1978; McQupoid and Hobson, 1996). Thus, we assume that growth conditions of vegetative cells determine the transfer from vegetative cells to spores and vice versa. To prevent ongoing switches between both stages, we use the average growth rate over 5 d. If the average growth rate $\overline{\mu}$ increases above the critical growth rate μ_{crit2}, spores transform into vegetative cells; if the average growth rate sinks below the critical growth rate, vegetative cells transform into spores. We define the rates for a transfer from spores to vegetative cells $\tau_{P_2^2 P_1^2}$ (Equation (A.39)) and for a transfer from vegetative cells to spores $\tau_{P_1^2 P_2^2}$ (Equation (A.40)) as

$$\tau_{P_2^2 P_1^2} = \sigma_2 \left(-0.5 \;\left(1 - \tanh\left(c\left(\overline{\mu} - \mu_{\text{crit2}}\right)\right) + 1\right)\right. \tag{A.39}$$

$$\tau_{P_1^2 P_2^2} = \sigma_2 \times 0.5 \;\left(1 - \tanh\left(c\left(\overline{\mu} - \mu_{\text{crit2}}\right)\right)\right) \tag{A.40}$$

with the maximum transition rate σ_2 and the constant c.

Cyanobacteria

We assume that the transfer from the resting stage to the vegetative stage is initiated when two conditions are met: First, resting cells need to restore their internal nitrogen and energy quotas before they can resume vegetative growth. Since we do not explicitly compute energy quotas outside the N_2-fixing stage, we parameterize energy recharge with a maturation phase that ends at a specific day each year. Thus, we follow Hinners et al. (2019) and define an annual time window during which the transfer to the vegetative stage is possible. However, the transfer is only initiated if the second condition is fulfilled as well. Similar to diatoms, the second condition assumes that growth conditions need to be favorable for vegetative cells, meaning that the vegetative growth rate must exceed a critical value. Following Hense and Beckmann (2010), we average the vegetative growth rate over a time period of 12 h to ensure a stable transfer. If the averaged growth rate $\overline{\mu}$ increases above the critical growth rate μ_{crit33}, resting cells transform into vegetative cells according to Equation (A.41):

$$\tau_{P_3^3 P_1^3} = \begin{cases} \sigma_{33}, & 149\,\text{d} < t < 180\,\text{d} \;\&\; \overline{\mu} \geq \mu_{\text{crit33}} \\ 0, & \text{else} \end{cases} \tag{A.41}$$

with the transition rate σ_{33}.

When nitrogen becomes limiting, vegetative cells transform into the N_2-fixing life cycle stage, i. e., vegetative cells with heterocysts. The corresponding transfer rate in Equation (A.42) scales with the strength of nitrogen limitation $\lim_N$:

$$\tau_{P_1^3 P_2^3} = \sigma_{31} \times 0.5\left(1 - \tanh\left(2\pi \,\lim_N - \pi\right)\right)\!), \text{ with } \lim_N = \frac{N}{k_N + N} \tag{A.42}$$

with $\lim_N$ after Monod (1949). We average nitrogen limitation over all vegetative cells to represent the general status of nitrogen availability and not the status of individual cells.

The transfer from vegetative cells to resting cells does not depend on nitrogen but on temperature and light, starting when temperature and light conditions become unfavorable for growth. We assume that vegetative cells transform into resting cells when two conditions are fulfilled (Equation (A.43)): First, the product of temperature and irradiance Θ must decrease over time, i. e., $\mathrm{d}\Theta/\mathrm{d}t < 0$. Second, the average (12 h) saturated growth rate $\overline{\mu}_{\mathrm{sat31}}$ must sink below a critical value of $\mu_{\mathrm{crit31}} = 1.95 \times \mu_{\mathrm{crit33}}$. We use a larger value for μ_{crit31} than for μ_{crit33} since we consider the saturated growth rate instead of the actual growth rate. We calculate the saturated growth rate for $Q = Q_{\max}$.

$$\tau_{P_1^3 P_3^3} = \begin{cases} 22.7273 \times \sigma_{31} \times 0.5 \left(1 - \tanh\left[2\pi \left(\dfrac{\overline{\mu}_{\mathrm{sat31}}}{\mu_{\mathrm{crit31}}}\right) - \pi)\right]\right), & \dfrac{\mathrm{d}\Theta}{\mathrm{d}t} < 0 \ \& \ \mu_{\mathrm{sat31}} < \mu_{\mathrm{crit31}} \\ 0, & \text{else} \end{cases} \tag{A.43}$$

We apply the same assumptions as above to parameterize the transfer from vegetative cells with heterocysts to resting cells. Since vegetative cells with heterocysts are not limited by dissolved inorganic nitrogen, their transfer to the resting stage depends on the average saturated growth rate. To account for the reduced growth rates of vegetative cells with heterocysts compared to vegetative cells without heterocysts, we use a transition threshold of $\mu_{\mathrm{crit32}} = \zeta \times \mu_{\mathrm{crit31}}$ with $\zeta = 0.25$. We then calculate the transition rate according to Equation (A.44):

$$\tau_{P_2^3 P_3^3} = \begin{cases} \sigma_{32}, & \dfrac{\mathrm{d}\Theta}{\mathrm{d}t} < 0 \ \& \ \overline{\mu}_{\mathrm{sat32}} < \mu_{\mathrm{crit32}} \\ 0, & \text{else} \end{cases} \tag{A.44}$$

Table A.2.6: Life cycle parameterization for the three different phytoplankton functional groups. Visually adjusted parameters are indicated by *, all other parameters were adopted from the references stated in the text.

Functional group	Symbol	Parameter	Value	Unit
Dinoflagellates	σ_{CV}	Germination rate	0.1	d^{-1}
	σ_{VC}	Basic encystment rate	0.02	d^{-1}
	X_C	Encystment factor	1.0	–
	T_{VC1}	Temp. threshold for encystment	6.0	°C
	T_{VC2}	Temp. slope for encystment	1.6	°C
Diatoms	σ_2	Maximum transition rate	0.2	d^{-1}
	μ_{crit2}	Transition threshold	0.135^*	d^{-1}
	c	Constant in Equations (A.39) and (A.40)	1^*	d
Cyanobacteria	σ_{33}	Basic transition rate RES	0.1447^*	d^{-1}
	σ_{31}	Basic transition rate VEG	0.0713^*	d^{-1}
	σ_{32}	Basic transition rate HET	0.1447^*	d^{-1}
	μ_{crit33}	Critical growth rate RES	0.35^*	d^{-1}
	μ_{crit31}	Critical growth rate VEG	0.6825^*	d^{-1}
	μ_{crit32}	Critical growth rate HET	0.1706^*	d^{-1}

A.2.4 Environmental forcing

During control simulations, we force our model with annual irradiance and temperature curves, which represent present-day conditions in the Gulf of Finland (see Fig. A3a in Appendix A.4). We created the annual temperature curve from 10 yr (2011 – 2020) of sea surface temperature data, which we downloaded from the Copernicus database (https://resources.marine.copernicus.eu/products). To relativize spatial differences and special temperature events such as heat waves, we averaged the data over time and the entire gulf area. Since the resulting annual temperature curve has different start and end temperatures, we cannot use it to force the model over several years. Instead, we use a sinusoidal fit to the data, which has the following form:

$$T = a_1 \sin\left(\frac{2\pi t}{a_2} + \frac{2\pi}{a_3}\right) + a_4 \tag{A.45}$$

The fitting parameters a_1 to a_4 are given in Table A.2.7. To create the temperature forcing for our warming simulations, we add a continuous increase of 0.3 °C per decade to the temperature curve in Equation (A.45), which corresponds to the IPCC scenario SSP3-7.0 (Allan et al., 2021, see Fig. A3b in Appendix A.4).

Contrary to the temperature curve, the irradiance curve (Equation (A.46)) is the same for control and warming simulations. We use the same function as Hinners et al. (2019), which was originally adapted from Stramska and Zuzewicz (2013). The function provides lower irradiance levels during winter and higher irradiance levels during summer:

$$I = i_1 + i_2 \cos\left(\frac{2\pi(t - 180 \times 24)}{360 \times 24}\right) \tag{A.46}$$

Table A.2.7: Parameters for the annual temperature and irradiance curves.

Forcing	Symbol	Parameter	Value	Unit
Temperature	a_1	Amplitude	10.0754	°C
	a_2	Period	8640	h
	a_3	Phase shift	-0.9138 π	h
	a_4	Mean temperature	9.76275	°C
Irradiance	i_1	Mean light intensity	142	$\mathrm{W\,m^{-2}}$
	i_2	Range of light intensity	130	$\mathrm{W\,m^{-2}}$

A.3 Supporting tables

Table A1: Minimum/reference cell volumes at 15 °C and agent resolution for the three phytoplankton functional groups in our model. Note that resolution is lower for smaller cells. In comparison, Beckmann et al. (2019) used a resolution of 10^4 cells per agent for cells with a reference volume of $\sim$3000 μm^3.

[*] *Apocalathium malmogiense* (Hinners et al., 2017)

[†] *Thalassiosira weissflogii* (Atkinson et al., 2003); cell volume of *T. weissflogii* is within the lower range of *T. baltica* (Olenina et al., 2006), for which we defined temperature and light limitation

[‡] *Aphanizomenon flos-aquae* (Foy, 1980)

Functional group	Cell volume $[\mu\text{m}^3]$	Resolution [cells/agent]
Dinoflagellates	3424^*	6.5546×10^3
Diatoms	$1533^\dagger$	1.3950×10^4
Cyanobacteria	$88^\ddagger$	2.0568×10^5

Table A2: Results for a two-sample t-test that compares the control scenarios C (control), CA (control and adaptation), and CAR (control and adaptation and resuspension) regarding bloom timing, taxa abundance, and optimum temperature T_{opt}. Shown are the value of the test statistic (t), the degrees of freedom (df), and the p-value (p).

	Variable	Functional group	t	df	p
CA vs. C	Timing	Dinoflagellates	27.8575	12	2.8312×10^{-12}
		Diatoms (spring)	18.5617	12	3.3275×10^{-10}
		Diatoms (autumn)	−10.1827	12	2.9439×10^{-7}
		Cyanobacteria	NaN	12	NaN
	Abundance	Dinoflagellates	−8.8898	12	1.2573×10^{-6}
		Diatoms (spring)	−11.4046	12	8.5076×10^{-8}
		Diatoms (autumn)	−11.2969	12	9.4484×10^{-8}
		Cyanobacteria	−9.8830	12	4.0665×10^{-7}
CA vs. CAR	Timing	Dinoflagellates	1.9853	12	0.0704
		Diatoms (spring)	−0.3868	12	0.7056
		Diatoms (autumn)	4.1449	12	0.0014
		Cyanobacteria	NaN	12	NaN
	Abundance	Dinoflagellates	−0.5094	12	0.6197
		Diatoms (spring)	−0.2146	12	0.8337
		Diatoms (autumn)	1.0628	12	0.3088
		Cyanobacteria	0.1835	12	0.8574
	T_{opt}	Dinoflagellates	−1.4280	12	0.1788
		Diatoms	−1.5746	12	0.1413
		Cyanobacteria	−2.9410	12	0.0123

Table A3: Results for a two-sample t-test that compares the warming scenarios W (warming), WA (warming and adaptation), and WAR (warming and adaptation and resuspension) regarding bloom timing, taxa abundance, and optimum temperature T_{opt}. Shown are the value of the test statistic (t), the degrees of freedom (df), and the p-value (p).

	Variable	Functional group	t	df	p
WA vs. W	Timing	Dinoflagellates	14.4770	12	5.8277×10^{-9}
		Diatoms (spring)	-5.9551	12	6.6606×10^{-5}
		Diatoms (autumn)	12.0413	12	4.6542×10^{-8}
		Cyanobacteria	NaN	12	NaN
	Abundance	Dinoflagellates	-19.0053	12	2.5282×10^{-10}
		Diatoms (spring)	-4.7051	12	5.0979×10^{-4}
		Diatoms (autumn)	15.2059	12	3.3250×10^{-9}
		Cyanobacteria	19.6682	12	1.6955×10^{-10}
WA vs. WAR	Timing	Dinoflagellates	1.7160	12	0.1118
		Diatoms (spring)	3.6154	12	0.0035
		Diatoms (autumn)	-0.4275	12	0.6766
		Cyanobacteria	NaN	12	NaN
	Abundance	Dinoflagellates	0.2738	12	0.7889
		Diatoms (spring)	-3.6167	12	0.0035
		Diatoms (autumn)	-2.6150	12	0.0226
		Cyanobacteria	-9.3889	12	7.0477×10^{-7}
	T_{opt}	Dinoflagellates	2.7320	12	0.0182
		Diatoms	0.9058	12	0.3829
		Cyanobacteria	0.9146	12	0.3784

Table A4: Results for a paired-sample t-test that compares the control scenarios C (control), CA (control and adaptation), and CAR (control and adaptation and resuspension) to the corresponding warming scenarios W (warming), WA (warming and adaptation), and WAR (warming and adaptation and resuspension) regarding bloom timing, taxa abundance, and optimum temperature T_{opt}. Shown are the value of the test statistic (t), the degrees of freedom (df), and the p-value (p). In this case, a paired-sample t-test was chosen since all control and warming simulations were performed pairwise.

	Variable	Functional group	t	df	p
C vs. W	Timing	Dinoflagellates	25.4575	6	2.4205×10^{-7}
		Diatoms (spring)	171.6014	6	2.6421×10^{-12}
		Diatoms (autumn)	-36.0199	6	3.0534×10^{-8}
		Cyanobacteria	Inf	6	0
	Abundance	Dinoflagellates	-5.6633	6	0.0013
		Diatoms (spring)	-54.6486	6	2.5208×10^{-9}
		Diatoms (autumn)	-43.1157	6	1.0419×10^{-8}
		Cyanobacteria	-103.6771	6	5.4271×10^{-11}
CA vs. WA	Timing	Dinoflagellates	5.4501	6	0.0016
		Diatoms (spring)	38.2397	6	2.1357×10^{-8}
		Diatoms (autumn)	-16.8894	6	2.7535×10^{-6}
		Cyanobacteria	Inf	6	0
	Abundance	Dinoflagellates	2.9454	6	0.0258
		Diatoms (spring)	-11.4712	6	2.6351×10^{-5}
		Diatoms (autumn)	-18.9149	6	1.4110×10^{-6}
		Cyanobacteria	-11.4535	6	2.6586×10^{-5}
	T_{opt}	Dinoflagellates	-8.3318	6	1.6229×10^{-4}
		Diatoms	-15.5590	6	4.4616×10^{-6}
		Cyanobacteria	7.5639	6	2.7733×10^{-4}
CAR vs. WAR	Timing	Dinoflagellates	8.3445	6	1.6091×10^{-4}
		Diatoms (spring)	78.9854	6	2.7729×10^{-10}
		Diatoms (autumn)	-25.1179	6	2.6219×10^{-7}
		Cyanobacteria	Inf	6	0
	Abundance	Dinoflagellates	3.7696	6	0.0093
		Diatoms (spring)	-13.7065	6	9.3734×10^{-6}
		Diatoms (autumn)	-39.6585	6	1.7177×10^{-8}
		Cyanobacteria	-42.6023	6	1.1193×10^{-8}
	T_{opt}	Dinoflagellates	-10.8952	6	3.5453×10^{-5}
		Diatoms	-34.0430	6	4.2781×10^{-8}
		Cyanobacteria	-8.4589	6	1.4912×10^{-4}

A.4 Supporting figures

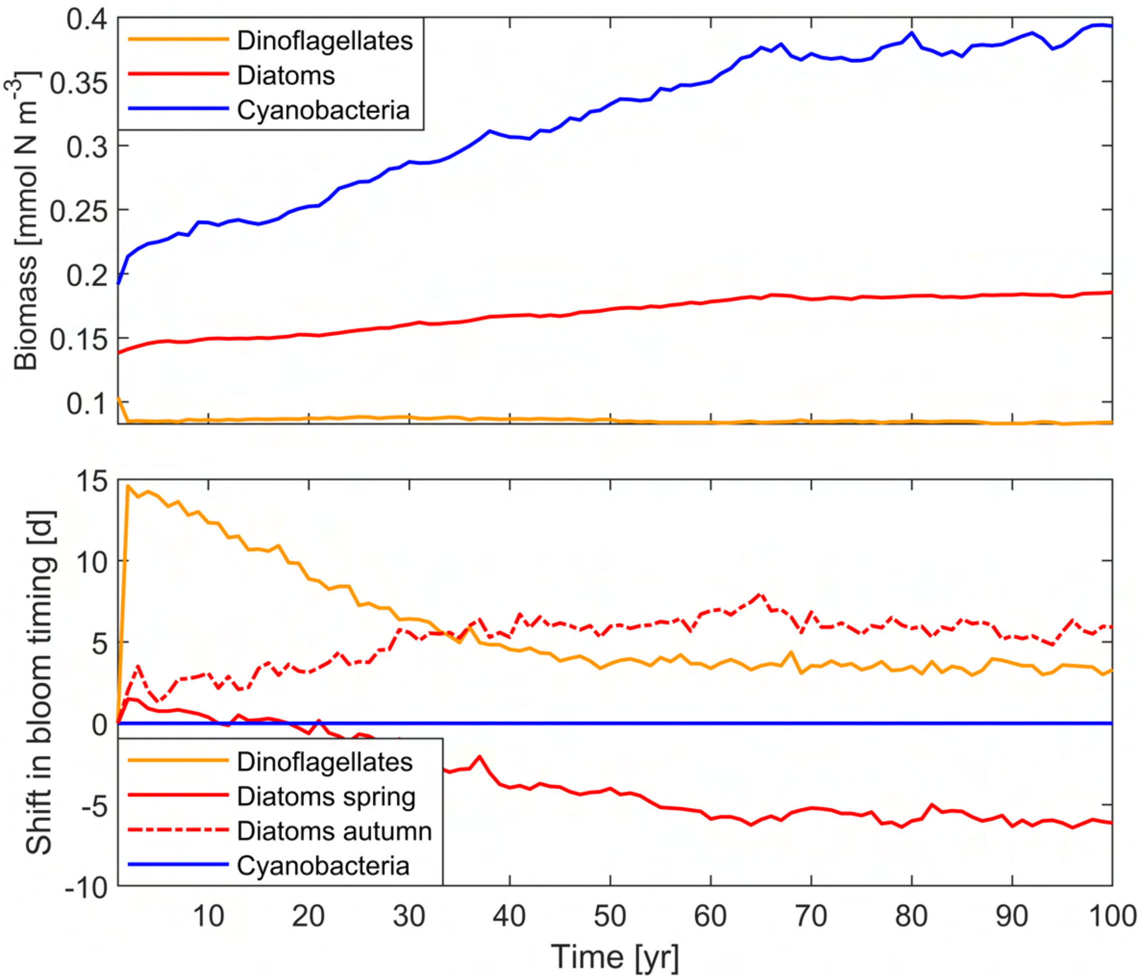

Figure A1: Temporal development of annual mean biomass and bloom timing averaged over seven different CA simulations (control and adaptation) for dinoflagellates, diatoms, and cyanobacteria. Negative changes in bloom timing indicate that the bloom occurs earlier, while positive changes mean that the bloom is shifted towards later in the year. Please note that the x-axis starts at 1 yr since annual values are shown.

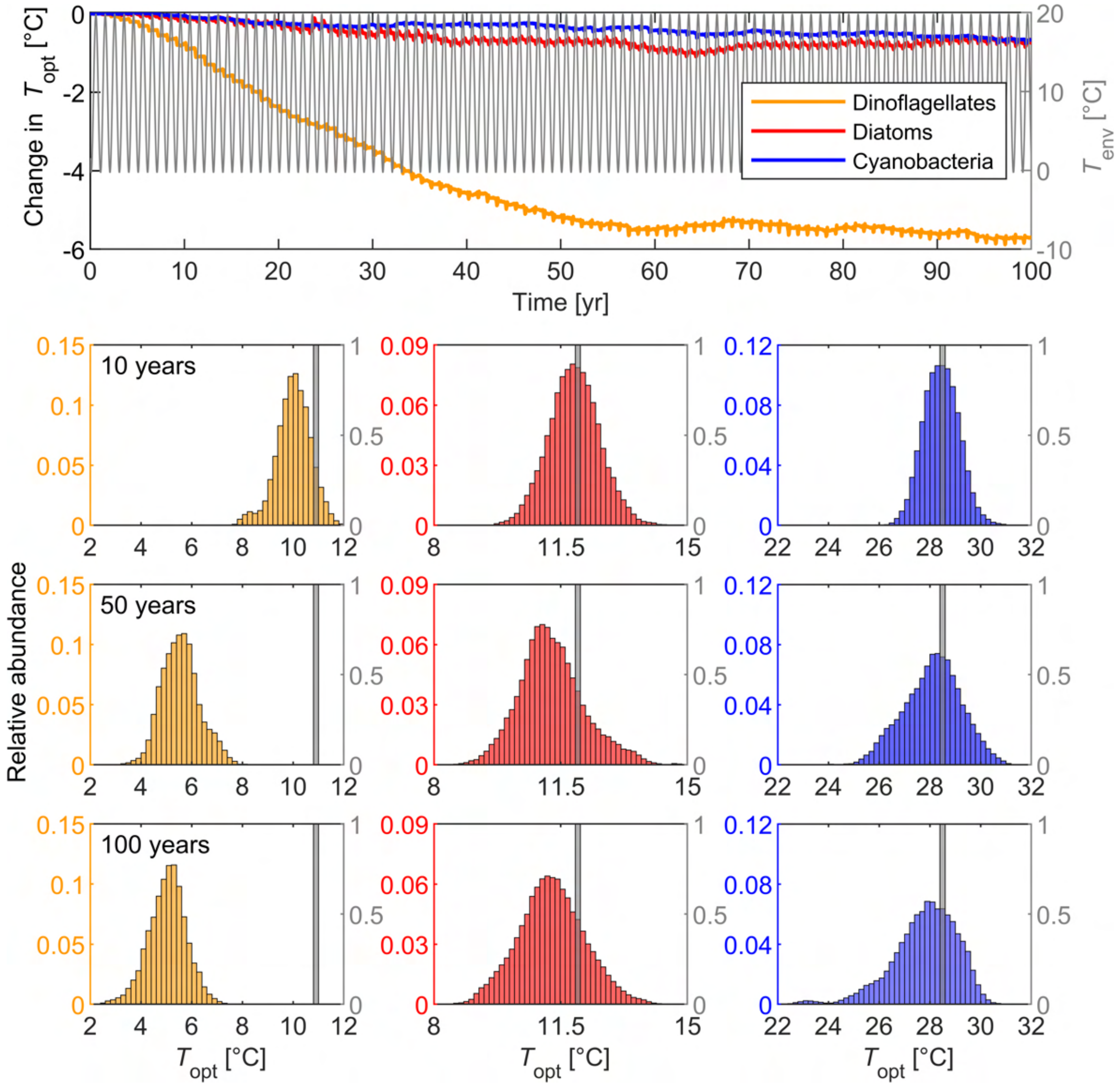

Figure A2: Temporal evolution of the mean optimum temperature (T_{opt}) for dinoflagellates, diatoms, and cyanobacteria, including T_{opt} distributions for selected years. Temporal changes in T_{opt} were averaged over seven different CA simulations (control and adaptation); T_{opt} distributions were merged from monthly histograms of the corresponding year from all seven CA simulations.

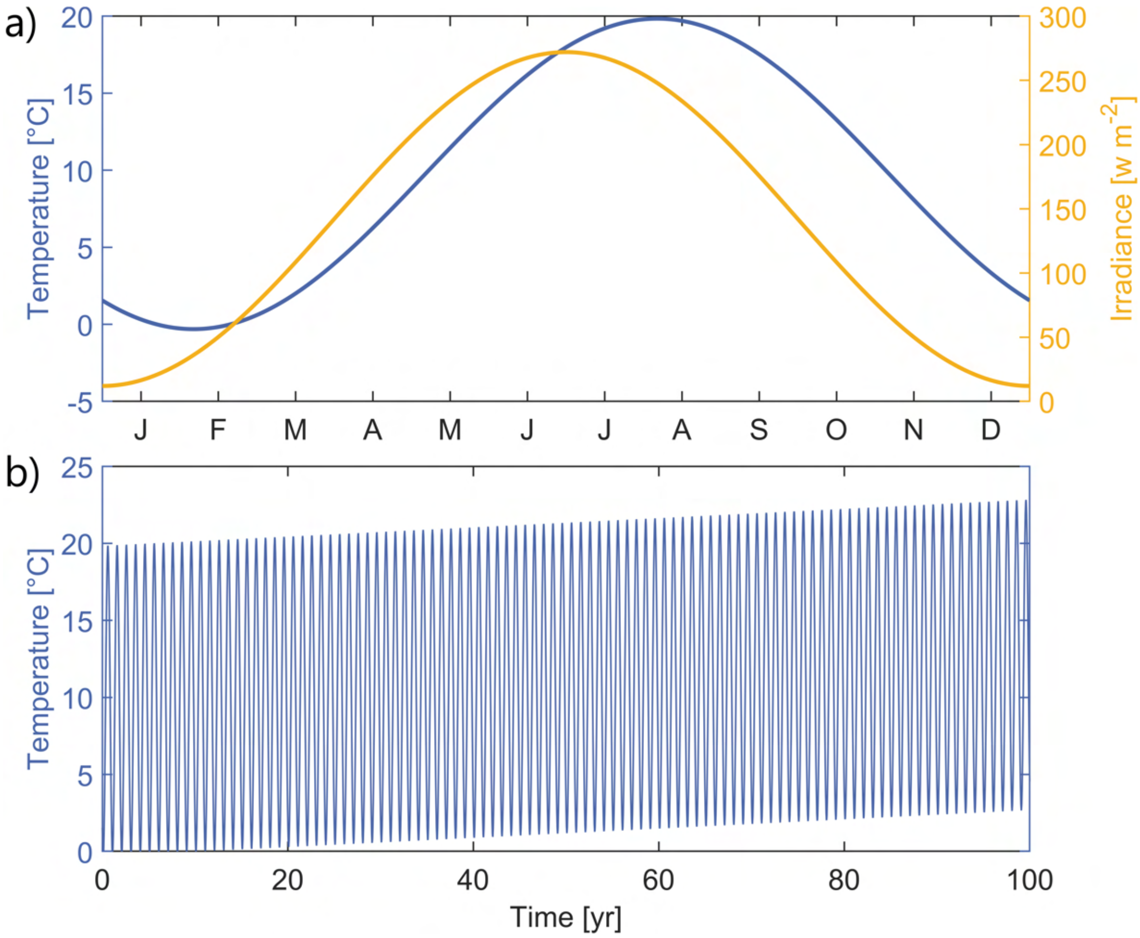

Figure A3: Environmental temperature and irradiance forcing; the corresponding equations are available in Appendix A.2.4. **(a)** Seasonal cycle of temperature and irradiance as derived from the Copernicus database (https://resources.marine.copernicus.eu/products) and from Stramska and Zuzewicz (2013); Hinners et al. (2019), respectively. **(b)** Global warming temperature forcing with a steady temperature increase of 0.3 °C per decade (IPCC scenario SSP3-7.0; Allan et al., 2021).

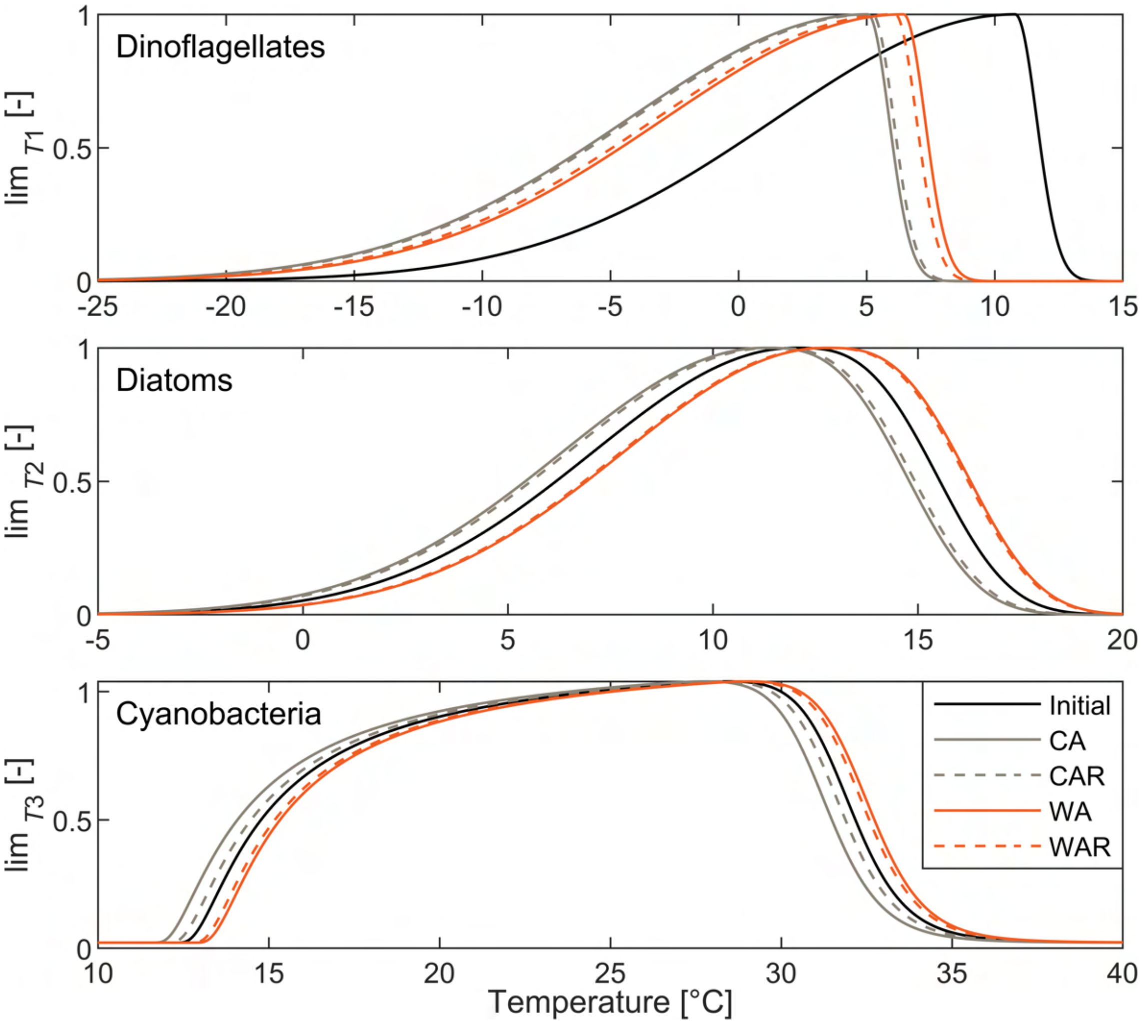

Figure A4: Temperature limitation functions for dinoflagellates (Hinners et al., 2019), diatoms (Warns, 2013), and cyanobacteria (Hense and Beckmann, 2006). Temperature limitation is shown for the initial optimum temperature, as well as for the mean optimum temperatures from the CA (control and adaptation), CAR (control and adaptation and resuspension), WA (warming and adaptation), and WAR (warming and adaptation and resuspension) scenarios. The corresponding equations are available in Appendix A.2.2. Please note that the x-axis covers a different temperature range for each functional group.

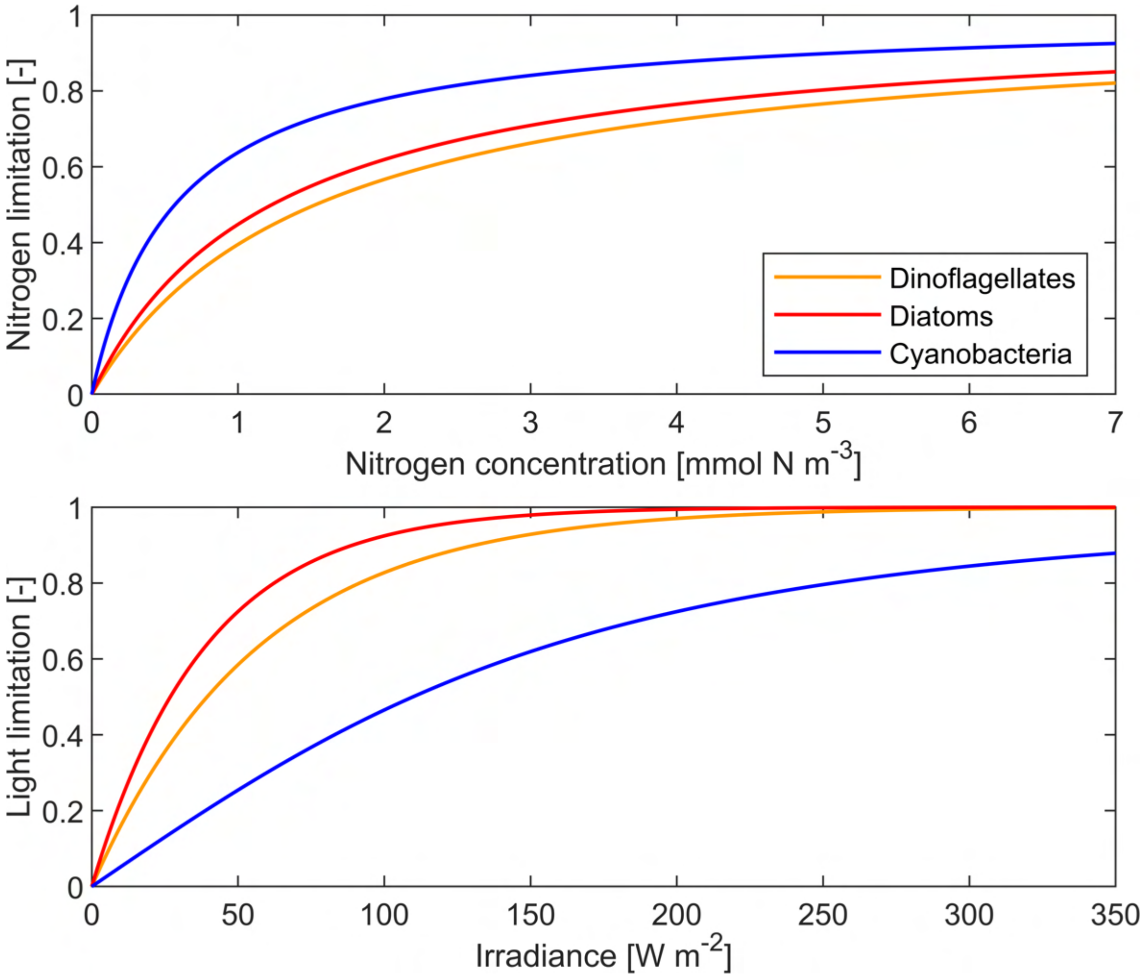

Figure A5: Nitrogen and light limitation functions for all three phytoplankton functional groups in our model. **Top:** Nitrogen limitation after Monod (1949); half saturation constants were calculated from cell volume at 15 °C following Litchman et al. (2007) (see Table A.2.3 in Appendix A.2.2). **Bottom:** Light limitation for dinoflagellates (Hinners et al., 2019), diatoms (Warns, 2013), and cyanobacteria (Hense and Beckmann, 2006) for cell volumes at 15 °C and $Q = Q_{\max}$. The corresponding equations can be found in Appendix A.2.2.

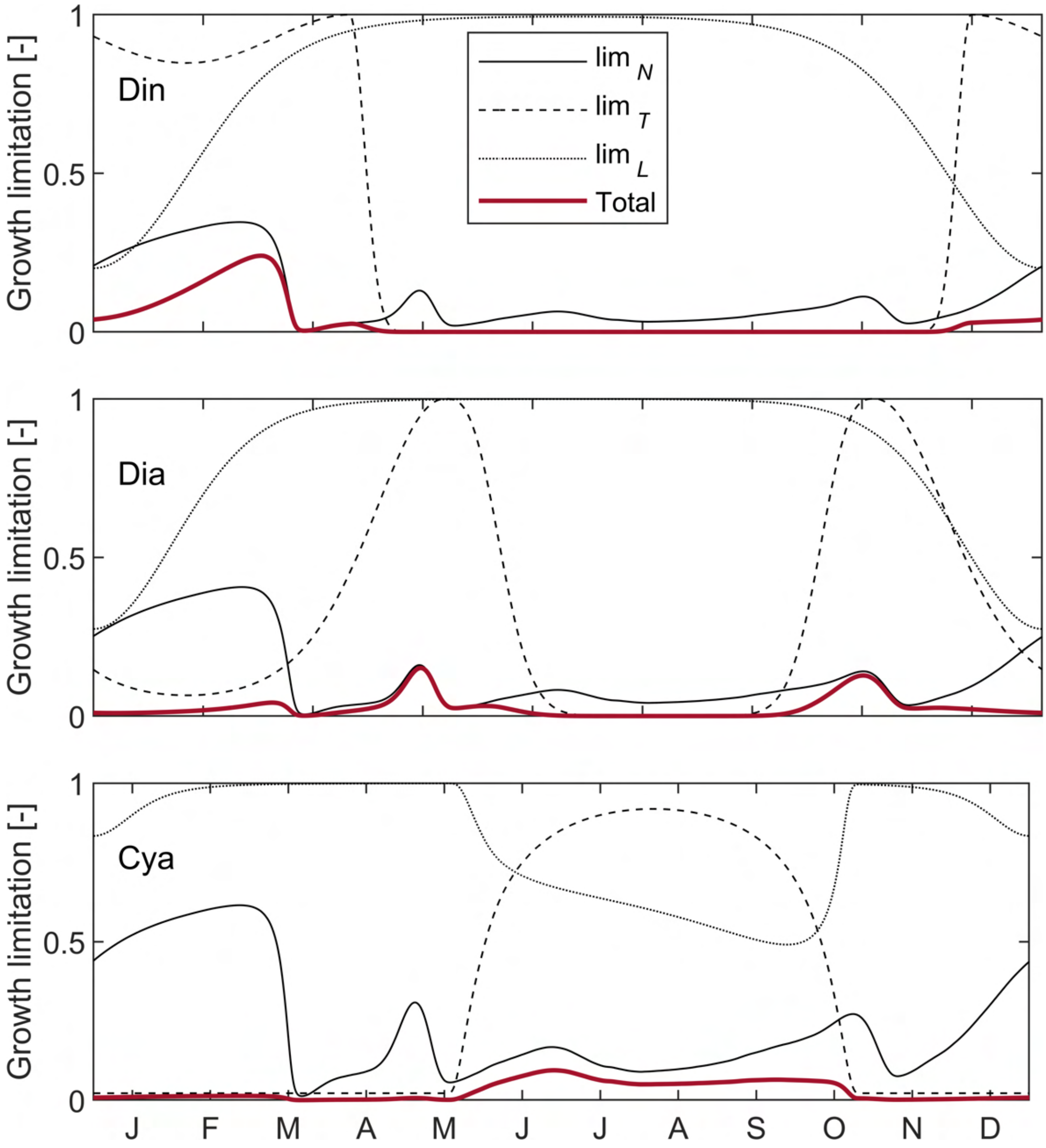

Figure A6: Growth limitation throughout the seasonal cycle calculated from the product of nitrogen limitation $\lim_N$, temperature limitation $\lim_T$, and light limitation $\lim_L$ (i.e., $\lim_N \times \lim_T \times \lim_L$). To calculate lim$_T$, we used the mean optimum temperatures from the CA scenario (control and adaptation).

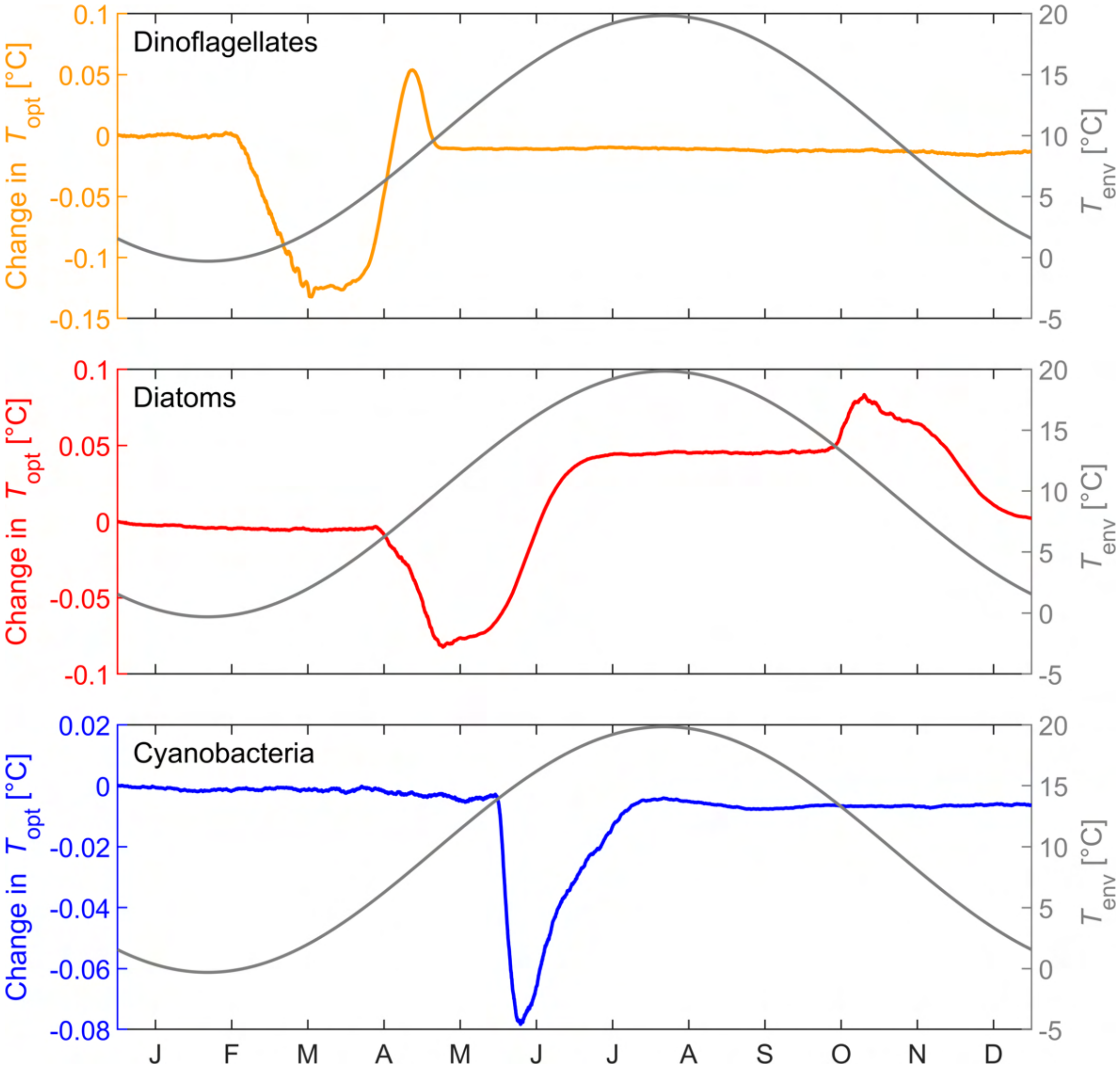

Figure A7: Seasonal changes in the mean optimum temperature (T_{opt}) for dinoflagellates, diatoms, and cyanobacteria. The displayed T_{opt} variations were averaged over the last 25 simulation years of seven different CA simulations (control and adaptation). Please note that the y-axis differs between functional groups.

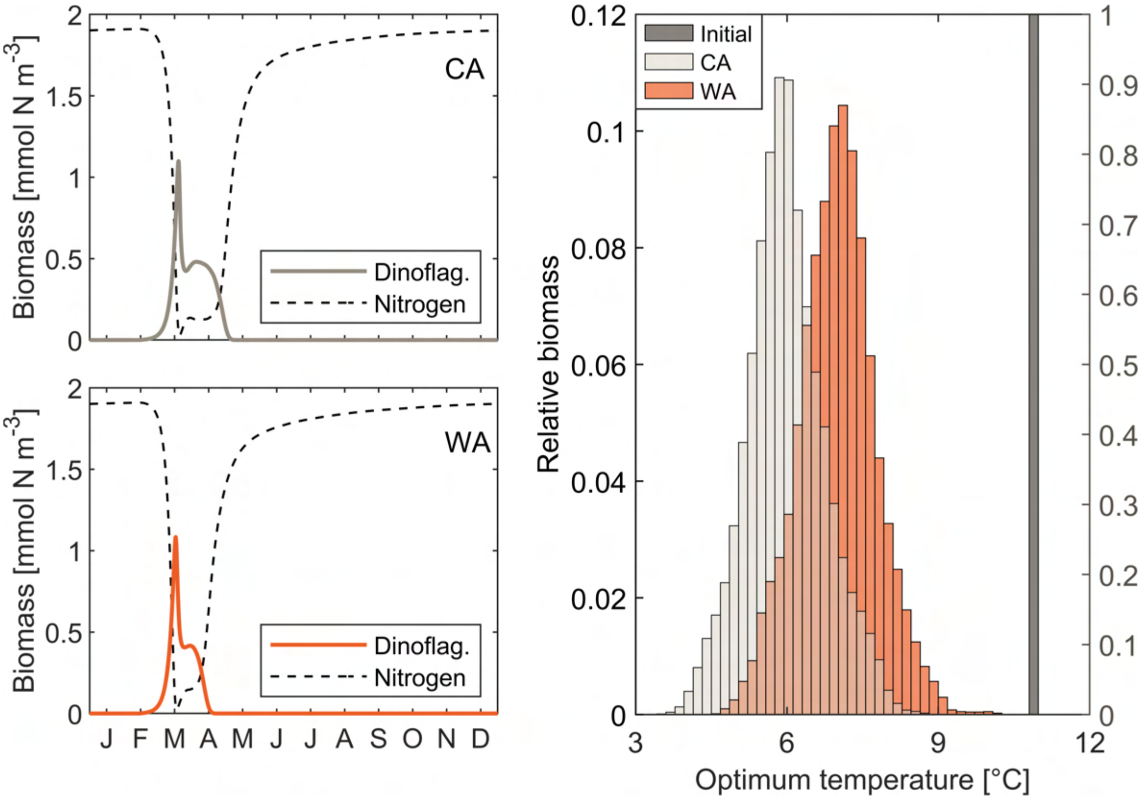

Figure A8: Results for a CA scenario (control and adaptation) and a follow-up WA scenario (warming and adaptation) with only dinoflagellates. Mass was conserved during simulations. **Left panels:** Biomass of vegetative dinoflagellate cells and nitrogen concentration during the last simulation year averaged over seven different simulations. **Right panel:** Evolutionary adaptation of the optimum temperature through mutation and selection. Shown are the initial value, the preliminary trait distribution after 100 yr of present-day seasonal forcing, and the final trait distribution after 100 yr of warming. Trait distributions were merged from monthly histograms of the corresponding year from seven different simulations. The results reveal that dinoflagellate adaptation does not change in the absence of interspecific competition. The fixed temperature threshold of encystment prohibits a shift towards later blooming. Within the remaining niche, dinoflagellate adaptation is controlled by intraspecific competition for nitrogen. In both CA and WA, the environment selects for early bloomers with comparatively low optimum temperatures, which grow first and leave less nitrogen for individuals with higher optimum temperatures.

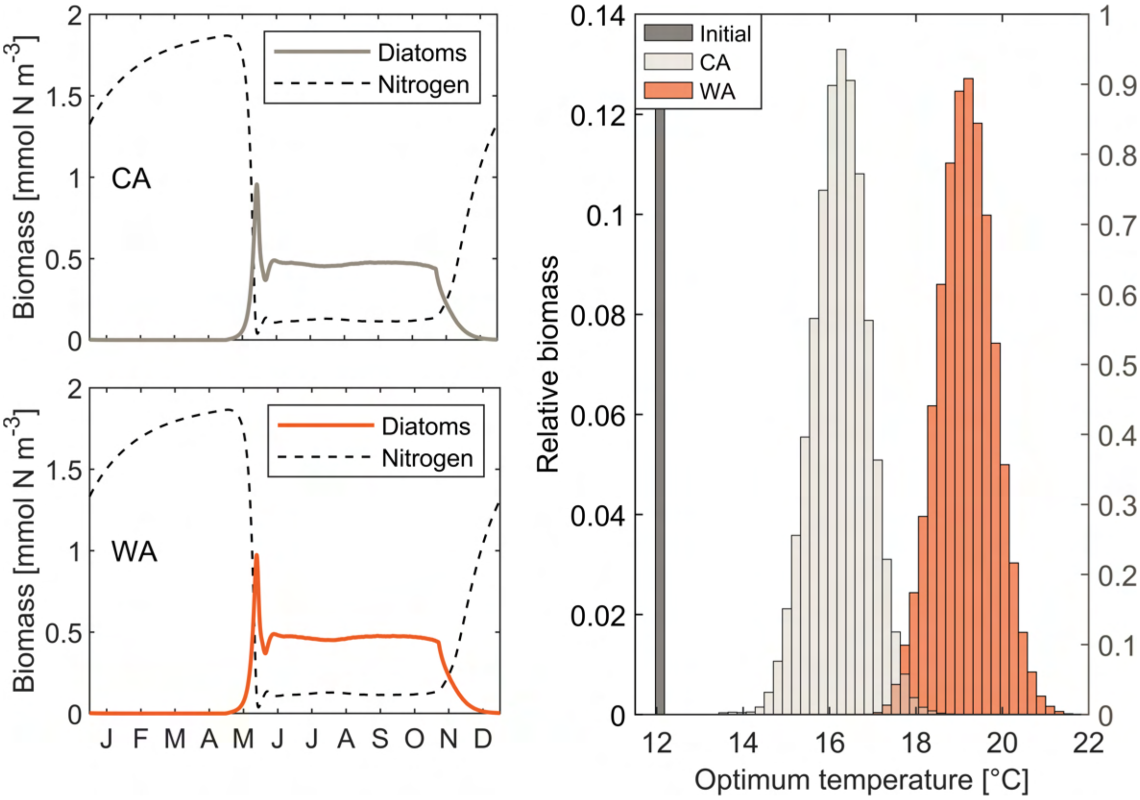

Figure A9: Results for a CA scenario (control and adaptation) and a follow-up WA scenario (warming and adaptation) with only diatoms. Mass was conserved during simulations. **Left panels:** Biomass of vegetative diatom cells and nitrogen concentration during the last simulation year averaged over seven different simulations. **Right panel:** Evolutionary adaptation of the optimum temperature through mutation and selection. Shown are the initial value, the preliminary trait distribution after 100 yr of present-day seasonal forcing, and the final trait distribution after 100 yr of warming. Trait distributions were merged from monthly histograms of the corresponding year from seven different simulations. The results reveal that in the absence of interspecific competition, diatoms merge their spring and autumn blooms into a single bloom between mid-May and mid-December. A single bloom is beneficial since it allows nitrogen to recover completely until the next blooming season. Similar to dinoflagellates, intraspecific competition selects for the first bloomers. In WA, diatoms are able to track the increase in environmental temperature, which they are not in the presence of interspecific competition. We can conclude that in our simulations, adaptation of diatoms is controlled by interspecific competition with (warmer-adapted) cyanobacteria in both steady and changing environments.

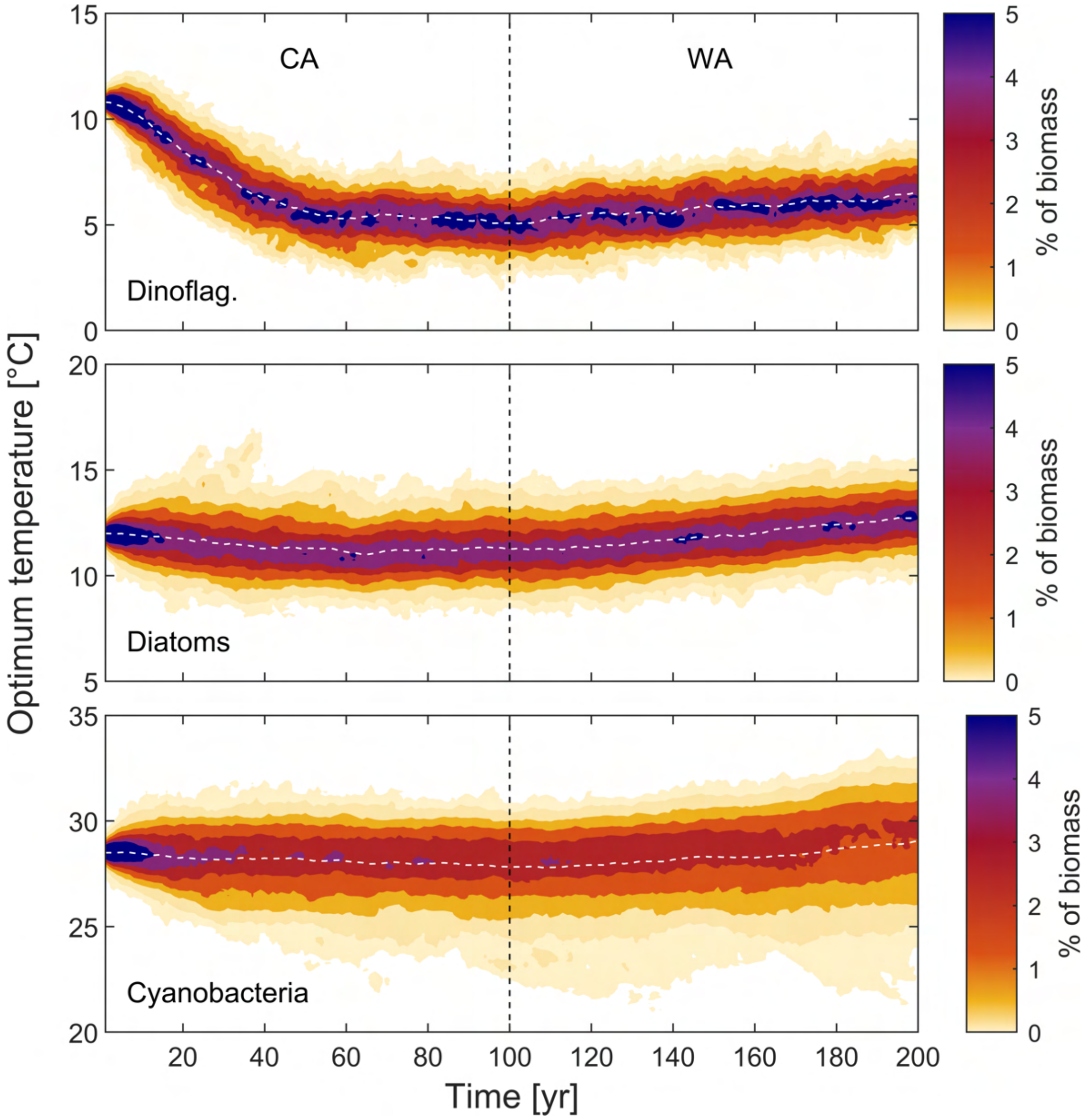

Figure A10: Temporal changes in the T_{opt} trait distributions of dinoflagellates, diatoms, and cyanobacteria throughout CA (control and adaptation) and WA (warming and adaptation). Shown are yearly trait distributions merged from monthly histograms of seven different simulations. Please note that the x-axis starts at 1 yr since annual values are shown.

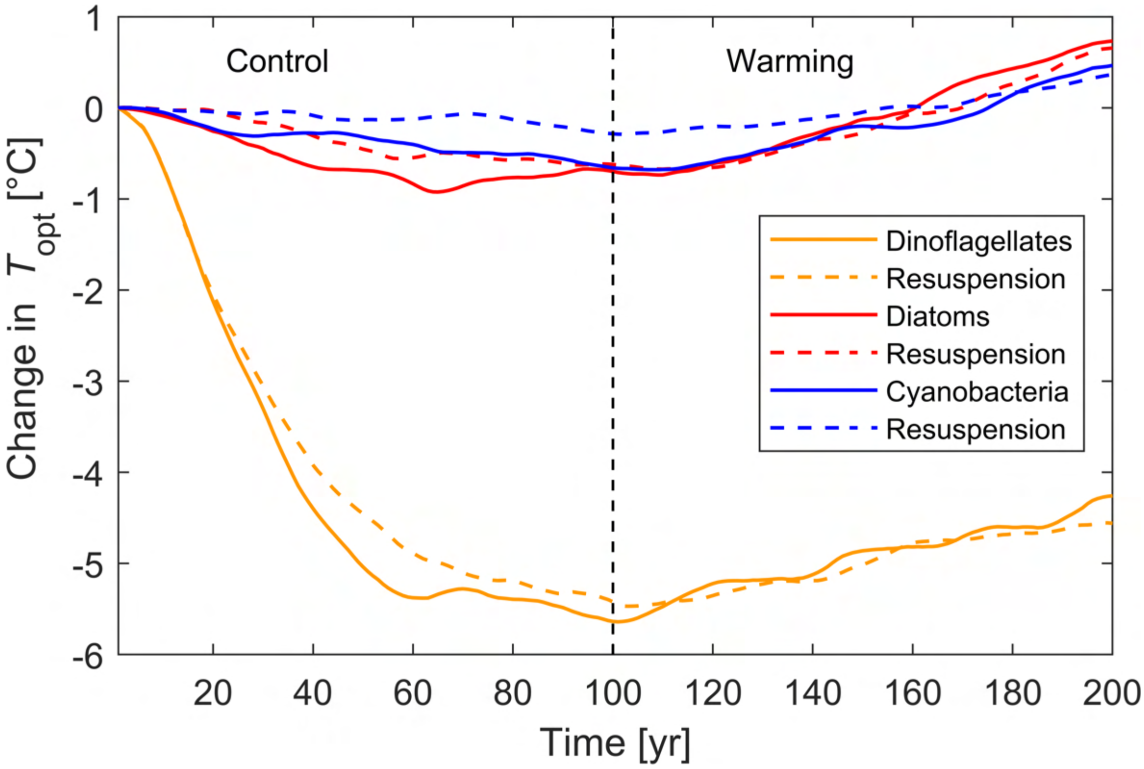

Figure A11: Temporal evolution of mean optimum temperatures with and without resuspension for dinoflagellates, diatoms, and cyanobacteria. Mean optimum temperatures were calculated from the annual averages of seven different simulations and filtered with a centered moving average using a window length of 10 yr. Please note that the x-axis starts at 1 yr since annual values are shown.

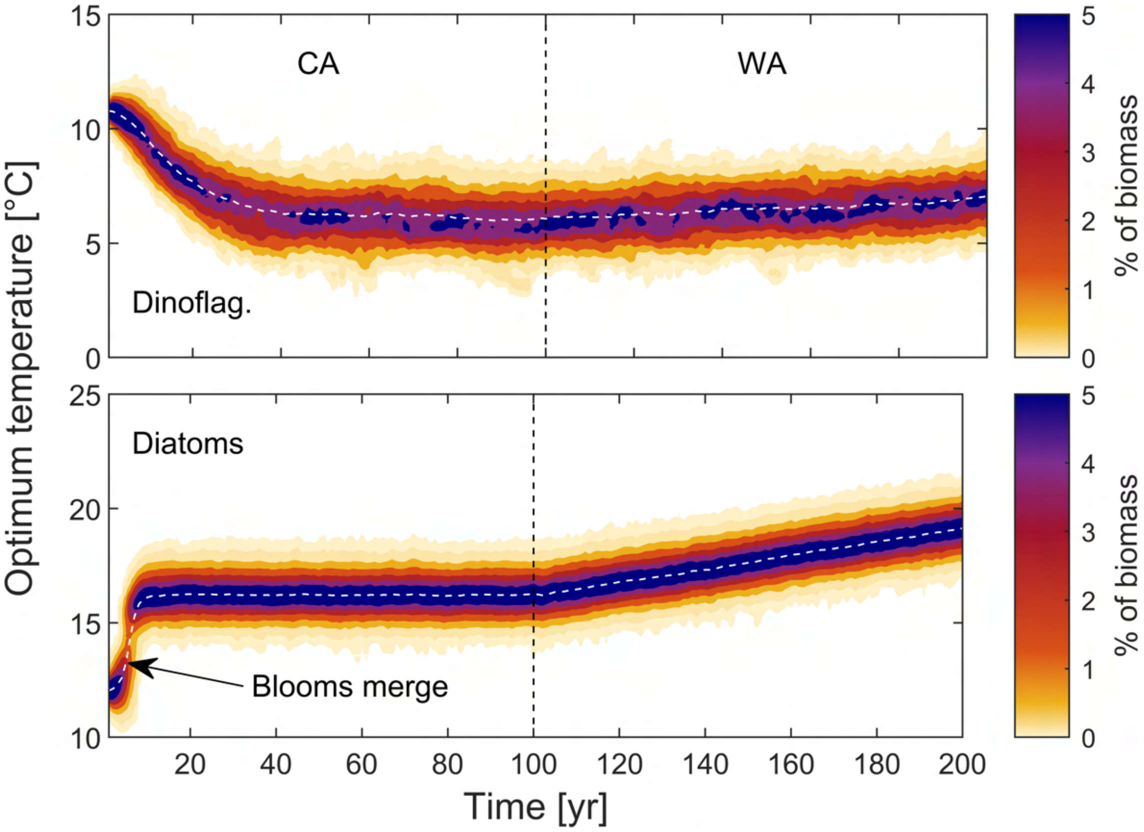

Figure A12: Temporal changes in the T_{opt} trait distributions of dinoflagellates and diatoms throughout CA (control and adaptation) and WA (warming and adaptation) in the absence of interspecific competition. Shown are annual trait distributions merged from monthly histograms of seven different simulations. Please note that the x-axis starts at 1 yr since annual values are shown. For diatoms, the spring and autumn blooms merge after 5 yr, which is also shown in the figure.

Appendix B

APPENDICES FOR STUDY II

B.1 Supporting tables

Table B1: Results of a series of t-tests comparing all model scenarios (C: control; CA: control and adaptation; W: warming; WA: warming and adaptation) with regard to zooplankton bloom timing, zooplankton peak abundance, and the time lag between the peaks of phytoplankton and zooplankton. The table presents the value of the test statistic (t), the degrees of freedom (df), and the p-value (p). Please note that we used a paired-sample t-test when comparing control and warming simulations since these were performed pairwise, and a two-sample t-test otherwise.

	Variable	t	df	p
CA vs. C	Timing	13.2463	12	1.5965×10^{-8}
	Abundance	−6.9046	12	1.6404×10^{-5}
	Time lag	6.0295	6	9.4005×10^{-4}
WA vs. W	Timing	8.1747	12	3.0117×10^{-6}
	Abundance	2.4289	12	0.0318
	Time lag	−3.4739	6	0.0132
W vs. C	Timing	27.9240	6	1.3954×10^{-7}
	Abundance	−31.5978	6	6.6762×10^{-8}
	Time lag	16.2498	6	3.4561×10^{-6}
WA vs. CA	Timing	7.3860	6	3.1602×10^{-4}
	Abundance	−4.6286	6	0.0036
	Time lag	3.9232	6	0.0078

Table B2: Results of a series of t-tests comparing all model scenarios (C: control; CA: control and adaptation; W: warming; WA: warming and adaptation) with regard to annual balances. The table presents the value of the test statistic (t), the degrees of freedom (df), and the p-value (p). Please note that we used a paired-sample t-test when comparing control and warming simulations since these were performed pairwise, and a two-sample t-test otherwise.

	Variable	t	df	p
CA vs. C	Dinoflagellates	2.1795	12	0.0499
	Diatoms	-7.7662	12	5.0873×10^{-6}
	Cyanobacteria	-6.1108	12	5.2491×10^{-5}
	Phytoplankton	-6.4065	12	3.3697×10^{-5}
	Zooplankton	-9.1802	12	8.9508×10^{-7}
	N_2 fixation	-5.8068	12	8.3836×10^{-5}
	Carbon export	-5.8882	12	7.3861×10^{-5}
	RUE	-27.2736	12	3.6372×10^{-12}
WA vs. W	Dinoflagellates	-1.9463	12	0.0754
	Diatoms	-3.0493	12	0.0101
	Cyanobacteria	-13.7101	12	1.0818×10^{-8}
	Phytoplankton	-12.5522	12	2.9249×10^{-8}
	Zooplankton	-7.3374	12	9.0067×10^{-6}
	N_2 fixation	-12.1507	12	4.2078×10^{-8}
	Carbon export	-12.8997	12	2.1524×10^{-8}
	RUE	25.0575	12	9.8930×10^{-12}
W vs. C	Dinoflagellates	18.1062	6	1.8266×10^{-6}
	Diatoms	-31.8063	6	6.4192×10^{-8}
	Cyanobacteria	-99.4698	6	6.9577×10^{-11}
	Phytoplankton	-77.4443	6	3.1205×10^{-10}
	Zooplankton	-39.0206	6	1.8926×10^{-8}
	N_2 fixation	-88.6053	6	1.3921×10^{-10}
	Carbon export	-77.9701	6	2.9965×10^{-10}
	RUE	48.8723	6	4.9211×10^{-9}
CA vs. WA	Dinoflagellates	9.4959	6	7.7730×10^{-5}
	Diatoms	-12.3243	6	1.7400×10^{-5}
	Cyanobacteria	-8.9350	6	1.0966×10^{-4}
	Phytoplankton	-9.0959	6	9.9165×10^{-5}
	Zooplankton	-5.2772	6	0.0019
	N_2 fixation	-8.2710	6	1.6905×10^{-4}
	Carbon export	-9.3836	6	8.3152×10^{-5}
	RUE	62.3327	6	1.1462×10^{-9}

B.2 Supporting figures

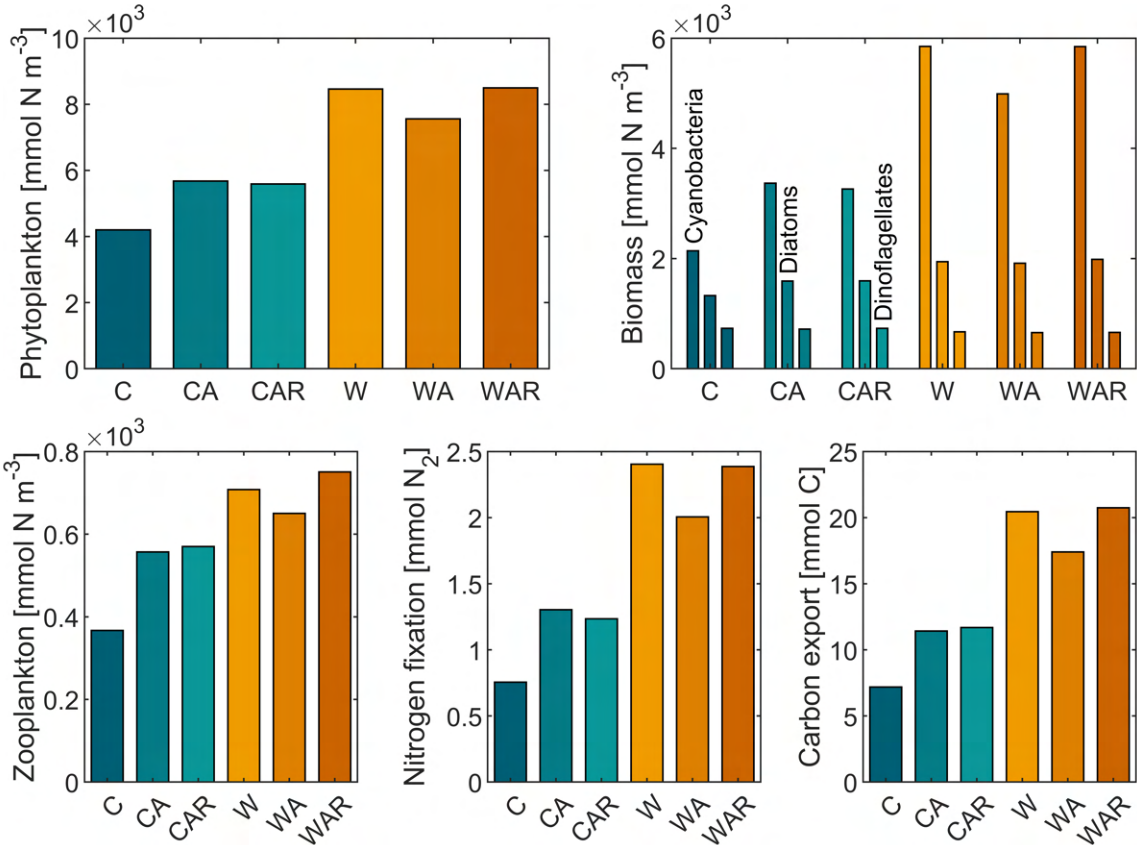

Figure B1: Annual balances for additional simulations with resuspension (C: control; CA: control and adaptation; CAR: control and adaptation and resuspension; W: warming; WA: warming and adaptation; WAR: warming and adaptation and resuspension). Carbon export is corrected for the carbon content of resuspended resting cells. Please note that we excluded resource use efficiency (RUE) from the figure since RUE simulations with resuspension are not comparable to those without.

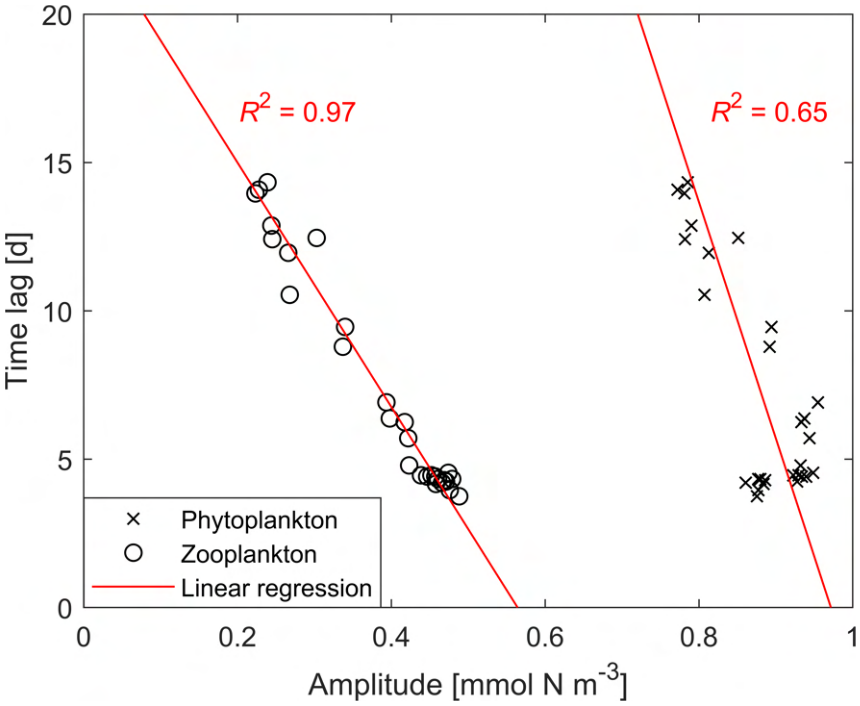

Figure B2: Time lag between phytoplankton and zooplankton blooms as a function of the peak amplitudes of phytoplankton and zooplankton, respectively. Shown are the time lags for the last simulation year of seven different simulations per model scenario, including linear regressions with both phytoplankton and zooplankton peak amplitudes and the corresponding R^2-values.

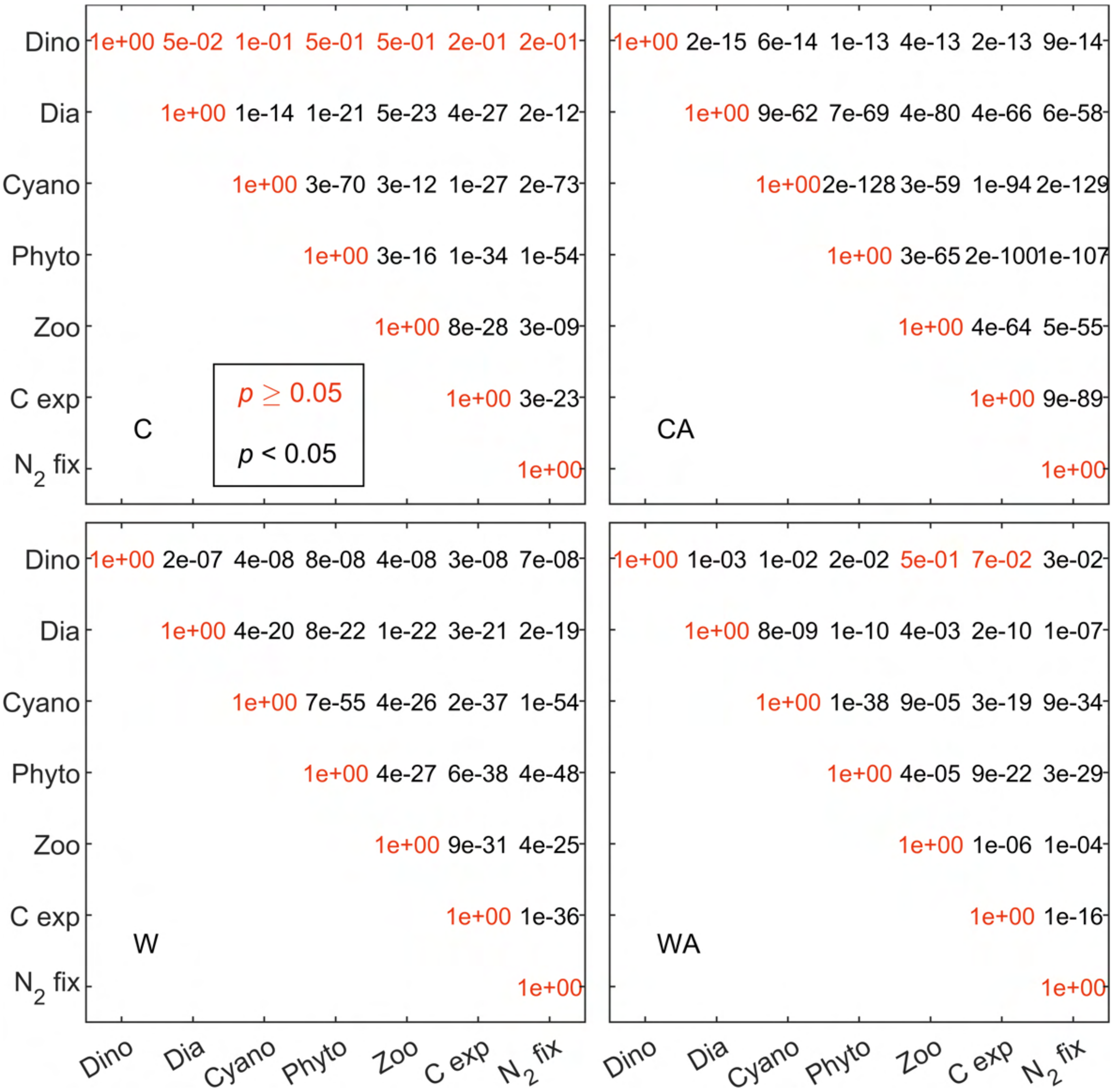

C

	Dino	Dia	Cyano	Phyto	Zoo	C exp	N_2 fix
Dino	1e+00	5e-02	1e-01	5e-01	5e-01	2e-01	2e-01
Dia		1e+00	1e-14	1e-21	5e-23	4e-27	2e-12
Cyano			1e+00	3e-70	3e-12	1e-27	2e-73
Phyto				1e+00	3e-16	1e-34	1e-54
Zoo					1e+00	8e-28	3e-09
C exp						1e+00	3e-23
N_2 fix							1e+00

CA

	Dino	Dia	Cyano	Phyto	Zoo	C exp	N_2 fix
Dino	1e+00	2e-15	6e-14	1e-13	4e-13	2e-13	9e-14
Dia		1e+00	9e-62	7e-69	4e-80	4e-66	6e-58
Cyano			1e+00	2e-128	3e-59	1e-94	2e-129
Phyto				1e+00	3e-65	2e-100	1e-107
Zoo					1e+00	4e-64	5e-55
C exp						1e+00	9e-89
N_2 fix							1e+00

W

	Dino	Dia	Cyano	Phyto	Zoo	C exp	N_2 fix
Dino	1e+00	2e-07	4e-08	8e-08	4e-08	3e-08	7e-08
Dia		1e+00	4e-20	8e-22	1e-22	3e-21	2e-19
Cyano			1e+00	7e-55	4e-26	2e-37	1e-54
Phyto				1e+00	4e-27	6e-38	4e-48
Zoo					1e+00	9e-31	4e-25
C exp						1e+00	1e-36
N_2 fix							1e+00

WA

	Dino	Dia	Cyano	Phyto	Zoo	C exp	N_2 fix
Dino	1e+00	1e-03	1e-02	2e-02	5e-01	7e-02	3e-02
Dia		1e+00	8e-09	1e-10	4e-03	2e-10	1e-07
Cyano			1e+00	1e-38	9e-05	3e-19	9e-34
Phyto				1e+00	4e-05	9e-22	3e-29
Zoo					1e+00	1e-06	1e-04
C exp						1e+00	1e-16
N_2 fix							1e+00

Figure B3: Matrices showing the p-values for the correlations in Fig. 2.2.5, section "Annual balances" in **Study II** (section 2.2). Model scenario abbreviations: C = control; CA = control and adaptation; W = warming; WA = warming and adaptation. Black numbers indicate that the corresponding correlations are statistically significant at the 0.05 level, while orange numbers indicate the opposite.

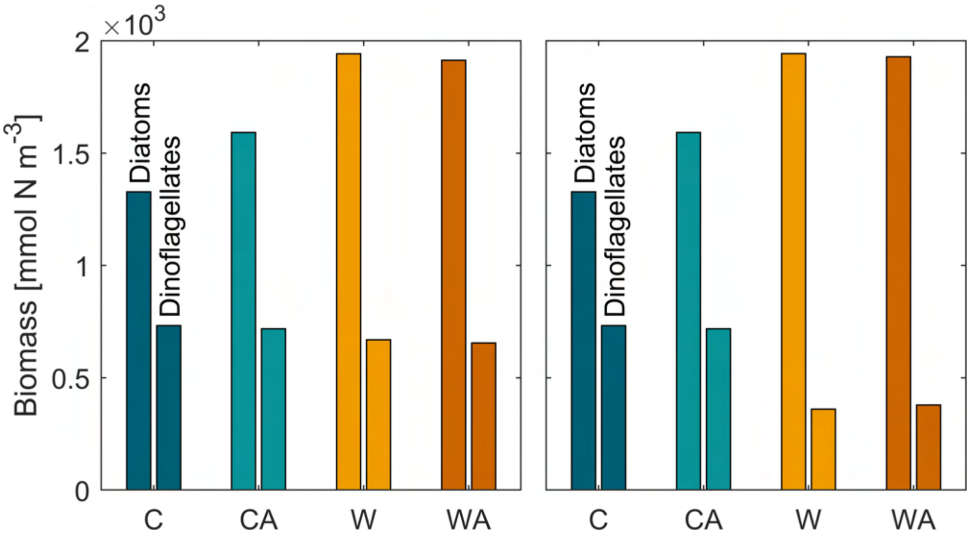

Figure B4: Annual biomasses of the cold-water dinoflagellate *Apocalathium* and the cold-water diatom *Thalassiosira* for the four different model scenarios (C: control; CA: control and adaptation; W: warming; WA: warming and adaptation). **Left:** Results for our standard simulations with a fixed encystemt rate of *Apocalathium*. **Right:** Results for additional simulations, in which we artificially decreased the encystment rate of *Apocalathium* at the rate found by Hinners et al. (2017).

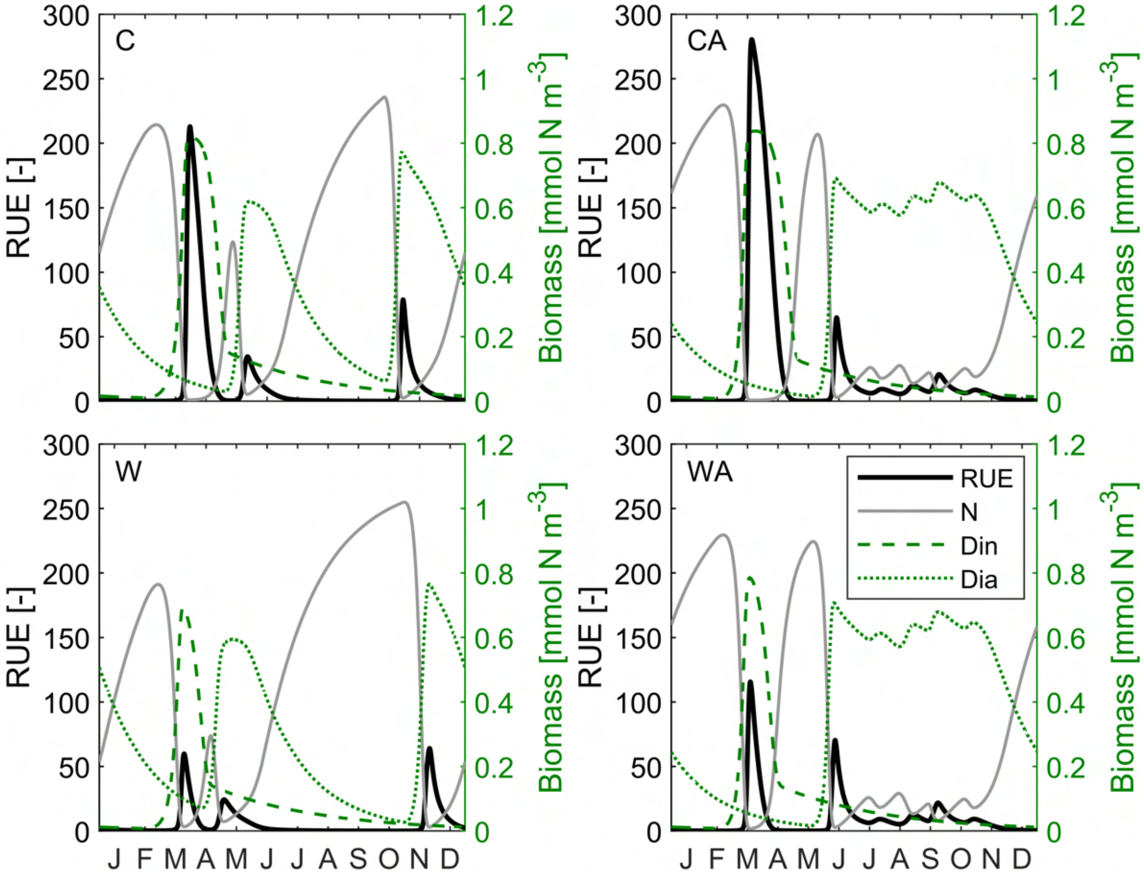

Figure B5: Resource use efficiency (RUE) of our focal dinoflagellate and diatom species of the genera *Apocalathium* and *Thalassiosira* throughout the seasonal cycle for all model scenarios (C: control; CA: control and adaptation; W: warming; WA: warming and adaptation). The figure shows results for the last simulation year, which were averaged over seven different simulations per scenario. Also shown are the nitrogen concentration (N), as well as the biomasses of *Apocalathium* (Din) and *Thalassiosira* (Dia).

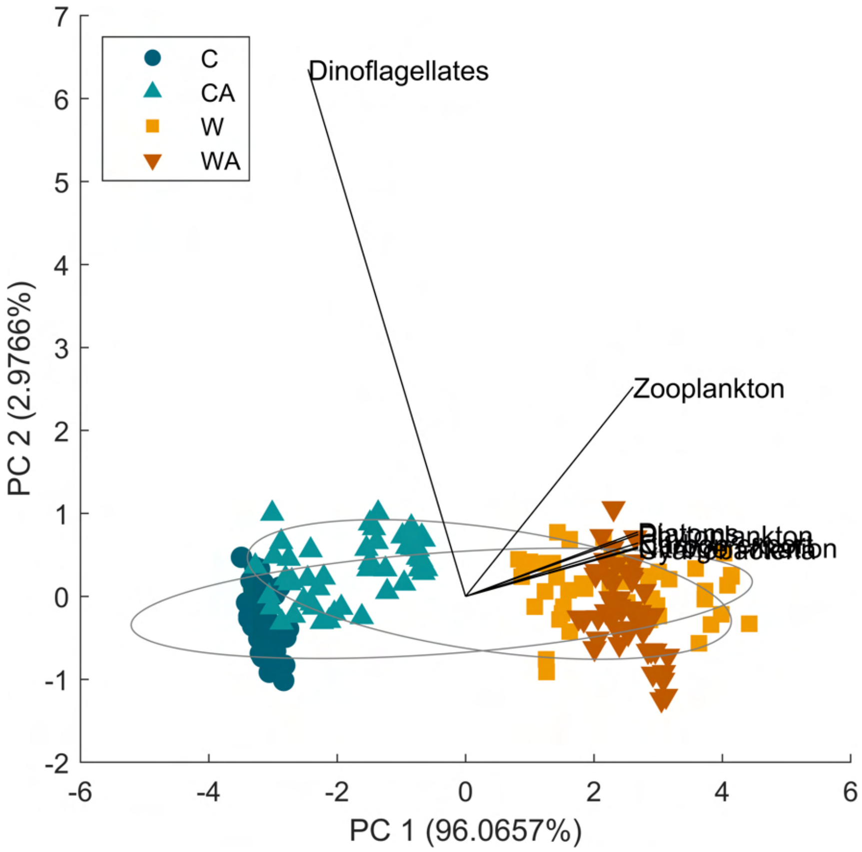

Figure B6: Results for a principal component analysis (PCA). The PCA shows that most variability in our model ecosystem can be explained by the first principal component (PC 1), which is associated with all model variables that are positively impacted by cyanobacteria. Zooplankton and especially dinoflagellates can be clearly identified as outliers.

REFERENCES

Aberle, N., Bauer, B., Lewandowska, A., Gaedke, U., and Sommer, U.: Warming induces shifts in microzooplankton phenology and reduces time-lags between phytoplankton and protozoan production, Marine Biology, 159, 2441–2453, https://doi.org/10.1007/s00227-012-1947-0, 2012.

Abrantes, F., Lebreiro, S., Rodrigues, T., Gil, I., Bartels-Jónsdóttir, H., Oliveira, P., Kissel, C., and Grimalt, J.: Shallow-marine sediment cores record climate variability and earthquake activity off Lisbon (Portugal) for the last 2000 years, Quaternary Science Reviews, 24, 2477–2494, https://doi.org/10.1016/j.quascirev.2004.04.009, 2005.

Acevedo-Trejos, E., Marañón, E., and Merico, A.: Phytoplankton size diversity and ecosystem function relationships across oceanic regions, Proceedings of the Royal Society B: Biological Sciences, 285, 20180 621, https://doi.org/10.1098/rspb.2018.0621, 2018.

Adrian, R., Wilhelm, S., and Gerten, D.: Life-history traits of lake plankton species may govern their phenological response to climate warming, Global Change Biology, 12, 652–661, https://doi.org/10.1111/j.1365-2486.2006.01125.x, 2006.

Allan, R. P., Cassou, C., Chen, D., Cherchi, A., Connors, L., Doblas-Reyes, F. J., Douville, H., Driouech, F., Edwards, T. L., Fischer, E., Flato, G. M., Forster, P., AchutaRao, K. M., Adhikary, B., Aldrian, E., and Armour, K.: Summary for policymakers, Tech. Rep. 6, IPCC, https://doi.org/10.1017/9781009157896.001, 2021.

Almén, A.-K. and Tamelander, T.: Temperature-related timing of the spring bloom and match between phytoplankton and zooplankton, Marine Biology Research, 16, 674–682, https://doi.org/10.1080/17451000.2020.1846201, 2020.

Alsos, I. G., Rijal, D. P., Ehrich, D., Karger, D. N., Yoccoz, N. G., Heintzman, P. D., Brown, A. G., Lammers, Y., Pellissier, L., Alm, T., Bråthen, K. A., Coissac, E., Merkel, M. K. F., Alberti, A., Denoeud, F., Bakke, J., and Consortium, P.: Postglacial species arrival and diversity buildup of northern ecosystems took millennia, Science Advances, 8, eabo7434, https://doi.org/10.1126/sciadv.abo7434, 2022.

Alsos, I. G., Boussange, V., Rijal, D. P., Beaulieu, M., Brown, A. G., Herzschuh, U., Svenning, J.-C., and Pellissier, L.: Using ancient sedimentary DNA to forecast ecosystem trajectories under climate change, Philosophical Transactions of the Royal Society B: Biological Sciences, 379, 20230 017, https://doi.org/10.1098/rstb.2023.0017, 2024.

Anderson, D. M., Cembella, A. D., and Hallegraeff, G. M.: Progress in understanding harmful algal blooms: Paradigm shifts and new technologies for research, monitoring, and management, Annual Review of Marine Science, 4, 143–176, https://doi.org/10.1146/annurev-marine-120308-081121, 2012.

Appleby, P. G.: Chronostratigraphic techniques in recent sediments, in: Tracking environmental change using lake sediments: Basin analysis, coring, and chronological techniques, edited by Last, W. M. and Smol, J. P., pp. 171–203, Springer Netherlands, Dordrecht, https://doi.org/10.1007/0-306-47669-X_9, 2001.

Aranguren-Gassis, M., Kremer, C. T., Klausmeier, C. A., and Litchman, E.: Nitrogen limitation inhibits marine diatom adaptation to high temperatures, Ecology Letters, 22, 1860–1869, https://doi.org/10.1111/ele.13378, 2019.

Argyle, P. A., Hinners, J., Walworth, N. G., Collins, S., Levine, N. M., and Doblin, M. A.: A high-throughput assay for quantifying phenotypic traits of microalgae, Frontiers in Microbiology, 12, 1–14, https://doi.org/10.3389/fmicb.2021.706235, 2021.

Armbrecht, L., Weber, M. E., Raymo, M. E., Peck, V. L., Williams, T., Warnock, J., Kato, Y., Hernández-Almeida, I., Hoem, F., Reilly, B., Hemming, S., Bailey, I., Martos, Y. M., Gutjahr, M., Percuoco, V., Allen, C., Brachfeld, S., Cardillo, F. G., Du, Z., Fauth, G., Fogwill, C., Garcia, M., Glüder, A., Guitard, M., Hwang, J.-H., Iizuka, M., Kenlee, B., O'Connell, S., Pérez, L. F., Ronge, T. A., Seki, O., Tauxe, L., Tripathi, S., and Zheng, X.: Ancient marine sediment DNA reveals diatom transition in Antarctica, Nature Communications, 13, 5787, https://doi.org/10.1038/s41467-022-33494-4, 2022.

Asch, R. G., Stock, C. A., and Sarmiento, J. L.: Climate change impacts on mismatches between phytoplankton blooms and fish spawning phenology, Global Change Biology, 25, 2544–2559, https://doi.org/10.1111/gcb.14650, 2019.

Atkinson, A., Siegel, V., Pakhomov, E., and Rothery, P.: Long-term decline in krill stock and increase in salps within the Southern Ocean, Nature, 432, 100–103, https://doi.org/10.1038/nature02996, 2004.

Atkinson, D., Ciotti, B. J., and Montagnes, D. J. S.: Protists decrease in size linearly with temperature: Ca. 2.5 % °C^{-1}, Proceedings of the Royal Society of London. Series B: Biological Sciences, 270, 2605–2611, https://doi.org/10.1098/rspb.2003.2538, 2003.

Azam, F. and Malfatti, F.: Microbial structuring of marine ecosystems, Nature Reviews Microbiology, 5, 782–791, https://doi.org/10.1038/nrmicro1747, 2007.

Backer, L. C. and McGillicuddy, D. J.: Harmful algal blooms: At the interface between coastal oceanography and human health, Oceanography, 19, 94–106, https://doi.org/10.5670/oceanog.2006.72, 2006.

Bálint, M., Pfenninger, M., Grossart, H.-P., Taberlet, P., Vellend, M., Leibold, M. A., Englund, G., and Bowler, D.: Environmental DNA time series in ecology, Trends in Ecology & Evolution, 33, 945–957, https://doi.org/10.1016/j.tree.2018.09.003, 2018.

Barabás, G. and D'Andrea, R.: The effect of intraspecific variation and heritability on community pattern and robustness, Ecology Letters, 19, 977–986, https://doi.org/10.1111/ele.12636, 2016.

Basu, S. and Mackey, K. R. M.: Phytoplankton as key mediators of the biological carbon pump: Their responses to a changing climate, Sustainability, 10, 869, https://doi.org/10.3390/su10030869, 2018.

Beckmann, A. and Hense, I.: Torn between extremes: The ups and downs of phytoplankton, Ocean Dynamics, 54, 581–592, https://doi.org/10.1007/s10236-004-0103-x, 2004.

Beckmann, A., Schaum, C.-E., and Hense, I.: Phytoplankton adaptation in ecosystem models, Journal of Theoretical Biology, 468, 60–71, https://doi.org/10.1016/j.jtbi.2019.01.041, 2019.

Bennington, C. C., McGraw, J. B., and Vavrek, M. C.: Ecological genetic variation in seed banks. II. Phenotypic and genetic differences between young and old subpopulations of *Luzula parviflora*, Journal of Ecology, 79, 627–643, https://doi.org/10.2307/2260658, 1991.

Blank, C. E. and Sánchez-Baracalco, P.: Timing of morphological and ecological innovations in the cyanobacteria – A key to understanding the rise in atmospheric oxygen, Geobiology, 8, 1–23, https://doi.org/10.1111/j.1472-4669.2009.00220.x, 2010.

Bopp, L., Aumont, O., Belviso, S., and Monfray, P.: Potential impact of climate change on marine dimethyl sulfide emissions, Tellus B: Chemical and Physical Meteorology, 55, 11–22, https://doi.org/10.3402/tellusb.v55i1.16359, 2003.

Bradley, R. S.: Paleoclimatology: Reconstructing climates of the Quaternary, Elsevier, Academic Press, Amsterdam ; Heidelberg, 3. edn., https://doi.org/10.1016/C2009-0-18310-1, 2015.

Brand, L. E., Campbell, L., and Bresnan, E.: *Karenia*: The biology and ecology of a toxic genus, Harmful Algae, 14, 156–178, https://doi.org/10.1016/j.hal.2011.10.020, 2012.

Breitburg, D., Levin, L. A., Oschlies, A., Grégoire, M., Chavez, F. P., Conley, D. J., Garçon, V., Gilbert, D., Gutiérrez, D., Isensee, K., Jacinto, G. S., Limburg, K. E., Montes, I., Naqvi, S. W. A., Pitcher, G. C., Rabalais, N. N., Roman, M. R., Rose, K. A., Seibel, B. A., Telszewski, M., Yasuhara, M., and Zhang, J.: Declining oxygen in the global ocean and coastal waters, Science, 359, eaam7240, https://doi.org/10.1126/science.aam7240, 2018.

Bruggeman, J. and Kooijman, S. A. L. M.: A biodiversity-inspired approach to aquatic ecosystem modeling, Limnology and Oceanography, 52, 1533–1544, https://doi.org/10.4319/lo.2007.52.4.1533, 2007.

Brumsack, H.-J.: The trace metal content of recent organic carbon-rich sediments: Implications for Cretaceous black shale formation, Palaeogeography, Palaeoclimatology, Palaeoecology, 232, 344–361, https://doi.org/10.1016/j.palaeo.2005.05.011, 2006.

Capo, E., Giguet-Covex, C., Rouillard, A., Nota, K., Heintzman, P. D., Vuillemin, A., Ariztegui, D., Arnaud, F., Belle, S., Bertilsson, S., Bigler, C., Bindler, R., Brown, A. G., Clarke, C. L., Crump, S. E., Debroas, D., Englund, G., Ficetola, G. F., Garner, R. E., Gauthier, J., Gregory-Eaves, I., Heinecke, L., Herzschuh, U., Ibrahim, A., Kisand, V., Kjær, K. H., Lammers, Y., Littlefair, J., Messager, E., Monchamp, M.-E., Olajos, F., Orsi, W., Pedersen, M. W., Rijal, D. P., Rydberg, J., Spanbauer, T., Stoof-Leichsenring, K. R., Taberlet, P., Talas, L., Thomas, C., Walsh, D. A., Wang, Y., Willerslev, E., van Woerkom, A., Zimmermann, H. H., Coolen, M. J. L., Epp, L. S., Domaizon, I., G. Alsos, I., and Parducci, L.: Lake sedimentary DNA research on past terrestrial and aquatic biodiversity: Overview and recommendations, Quaternary, 4, 1–58, https://doi.org/10.3390/quat4010006, 2021.

Catlett, D., Siegel, D., Simons, R., Guillocheau, N., Henderikx-Freitas, F., and Thomas, C.: Diagnosing seasonal to multi-decadal phytoplankton group dynamics in a highly productive coastal ecosystem, Progress in Oceanography, 197, 102 637, https://doi.org/10.1016/j.pocean.2021.102637, 2021.

Cermeño, P., Marañón, E., and Romero, O. E.: Response of marine diatom communities to late Quaternary abrupt climate changes, Journal of Plankton Research, 35, 12–21, https://doi.org/10.1093/plankt/fbs073, 2012.

Charlesworth, B.: Effective population size and patterns of molecular evolution and variation, Nature Reviews Genetics, 10, 195–205, https://doi.org/10.1038/nrg2526, 2009.

Chen, B. and Smith, S. L.: CITRATE 1.0: Phytoplankton continuous trait-distribution model with one-dimensional physical transport applied to the North Pacific, Geoscientific Model Development, 11, 467–495, https://doi.org/10.5194/gmd-11-467-2018, 2018.

Cherabier, P. and Ferrière, R.: Eco-evolutionary responses of the microbial loop to surface ocean warming and consequences for primary production, The ISME Journal, 16, 1130–1139, https://doi.org/10.1038/s41396-021-01166-8, 2022.

Chorus, I. and Welker, M., eds.: Toxic cyanobacteria in water: A guide to their public health consequences, monitoring and management, Taylor & Francis, https://doi.org/10.1201/9781003081449, 2021.

Clark, J. R., Lenton, T. M., Williams, H. T. P., and Daines, S. J.: Environmental selection and resource allocation determine spatial patterns in picophytoplankton cell size, Limnology and Oceanography, 58, 1008–1022, https://doi.org/10.4319/lo.2013.58.3.1008, 2013.

Clarke, A. D., Davis, D., Kapustin, V. N., Eisele, F., Chen, G., Paluch, I., Lenschow, D., Bandy, A. R., Thornton, D., Moore, K., Mauldin, L., Tanner, D., Litchy, M., Carroll, M. A., Collins, J., and Albercook, G.: Particle nucleation in the tropical boundary layer and its coupling to marine sulfur sources, Science, 282, 89–92, https://doi.org/10.1126/science.282.5386.89, 1998.

Clarke, C. L., Edwards, M. E., Brown, A. G., Gielly, L., Lammers, Y., Heintzman, P. D., Ancin-Murguzur, F. J., Bråthen, K.-A., Goslar, T., and Alsos, I. G.: Holocene floristic diversity and richness in Northeast Norway revealed by sedimentary ancient DNA (sedaDNA) and pollen, Boreas, 48, 299–316, https://doi.org/10.1111/bor.12357, 2019.

Cléroux, C., Cortijo, E., Anand, P., Labeyrie, L., Bassinot, F., Caillon, N., and Duplessy, J.-C.: Mg/Ca and Sr/Ca ratios in planktonic foraminifera: Proxies for upper water column temperature reconstruction, Paleoceanography, 23, 1–16, https://doi.org/10.1029/2007PA001505, 2008.

Collins, C. D. and Boylen, C. W.: Physiological responses of *Anabaena variabilis* (cyanophyceae) to instantaneous exposure to various combinations of light intensity and temperature, Journal of Phycology, 18, 206–211, https://doi.org/10.1111/j.1529-8817.1982.tb03175.x, 1982.

Collins, S.: Competition limits adaptation and productivity in a photosynthetic alga at elevated CO_2, Proceedings of the Royal Society B: Biological Sciences, 278, 247–255, https://doi.org/10.1098/rspb.2010.1173, 2011.

Collins, S. and Bell, G.: Phenotypic consequences of 1,000 generations of selection at elevated CO_2 in a green alga, Nature, 431, 566–569, https://doi.org/10.1038/nature02945, 2004.

Collins, S., Boyd, P. W., and Doblin, M. A.: Evolution, microbes, and changing ocean conditions, Annual Review of Marine Science, 12, 181–208, https://doi.org/10.1146/annurev-marine-010318-095311, 2020.

Conley, D. J., Humborg, C., Rahm, L., Savchuk, O. P., and Wulff, F.: Hypoxia in the Baltic Sea and basin-scale changes in phosphorus biogeochemistry, Environmental Science & Technology, 36, 5315–5320, https://doi.org/10.1021/es025763w, 2002.

Coolen, M. J. L.: 7000 Years of *Emiliania huxleyi* viruses in the Black Sea, Science, 333, 451–452, https://doi.org/10.1126/science.1200072, 2011.

Coolen, M. J. L., Saenz, J. P., Giosan, L., Trowbridge, N. Y., Dimitrov, P., Dimitrov, D., and Eglinton, T. I.: DNA and lipid molecular stratigraphic records of haptophyte succession in the Black Sea during the Holocene, Earth and Planetary Science Letters, 284, 610–621, https://doi.org/10.1016/j.epsl.2009.05.029, 2009.

Coolen, M. J. L., Orsi, W. D., Balkema, C., Quince, C., Harris, K., Sylva, S. P., Filipova-Marinova, M., and Giosan, L.: Evolution of the plankton paleome in the Black Sea from the Deglacial to Anthropocene, Proceedings of the National Academy of Sciences, 110, 8609–8614, https://doi.org/10.1073/pnas.1219283110, 2013.

Cropp, R., Norbury, J., and Braddock, R.: Dimethylsulphide, clouds, and phytoplankton: Insights from a simple plankton ecosystem feedback model, Global Biogeochemical Cycles, 21, 1–17, https://doi.org/10.1029/2006GB002812, 2007.

Daewel, U. and Schrum, C.: Simulating long-term dynamics of the coupled North Sea and Baltic Sea ecosystem with ECOSMO II: Model description and validation, Journal of Marine Systems, 119-120, 30–49, https://doi.org/10.1016/j.jmarsys.2013.03.008, 2013.

Daines, S. J., Clark, J. R., and Lenton, T. M.: Multiple environmental controls on phytoplankton growth strategies determine adaptive responses of the N : P ratio, Ecology Letters, 17, 414–425, https://doi.org/10.1111/ele.12239, 2014.

Dam, H. G.: Evolutionary adaptation of marine zooplankton to global change, Annual Review of Marine Science, 5, 349–370, https://doi.org/10.1146/annurev-marine-121211-172229, 2013.

De Mazancourt, C., Johnson, E., and Barraclough, T. G.: Biodiversity inhibits species' evolutionary responses to changing environments, Ecology Letters, 11, 380–388, https://doi.org/10.1111/j.1461-0248.2008.01152.x, 2008.

Delebecq, G., Schmidt, S., Ehrhold, A., Latimier, M., and Siano, R.: Revival of ancient marine dinoflagellates using molecular biostimulation, Journal of Phycology, 56, 1077–1089, https://doi.org/10.1111/jpy.13010, 2020.

Dellwig, O., Wegwerth, A., Schnetger, B., Schulz, H., and Arz, H. W.: Dissimilar behaviors of the geochemical twins W and Mo in hypoxic-euxinic marine basins, Earth-Science Reviews, 193, 1–23, https://doi.org/10.1016/j.earscirev.2019.03.017, 2019.

Denman, K. L.: A model simulation of the adaptive evolution through mutation of the coccolithophore *Emiliania huxleyi* based on a published laboratory study, Frontiers in Marine Science, 3, 1–13, https://doi.org/10.3389/fmars.2016.00286, 2017.

DeVries, T., Primeau, F., and Deutsch, C.: The sequestration efficiency of the biological pump, Geophysical Research Letters, 39, 1–5, https://doi.org/10.1029/2012GL051963, 2012.

Dommain, R., Andama, M., McDonough, M. M., Prado, N. A., Goldhammer, T., Potts, R., Maldonado, J. E., Nkurunungi, J. B., and Campana, M. G.: The challenges of reconstructing tropical biodiversity with sedimentary ancient DNA: A 2200-year-long metagenomic record from Bwindi Impenetrable Forest, Uganda, Frontiers in Ecology and Evolution, 8, 1–26, https://doi.org/10.3389/fevo.2020.00218, 2020.

Drebes, G.: On the life history of the marine plankton diatom *Stephanopyxis palmeriana*, Helgoländer Wissenschaftliche Meeresuntersuchungen, 13, 101–114, https://doi.org/10.1007/BF01612659, 1966.

Droop, M. R.: Some thoughts on nutrient limitation in algae, Journal of Phycology, 9, 264–272, https://doi.org/10.1111/j.1529-8817.1973.tb04092.x, 1973.

Durbin, E. G.: Aspects of the biology of resting spores of *Thalassiosira nordenskioeldii* and *Detonula confervacea*, Marine Biology, 45, 31–37, https://doi.org/10.1007/BF00388975, 1978.

Dutkiewicz, S., Morris, J. J., Follows, M. J., Scott, J., Levitan, O., Dyhrman, S. T., and Berman-Frank, I.: Impact of ocean acidification on the structure of future phytoplankton communities, Nature Climate Change, 5, 1002–1006, https://doi.org/10.1038/nclimate2722, 2015.

Dutkiewicz, S., Cermeno, P., Jahn, O., Follows, M. J., Hickman, A. E., Taniguchi, D. A. A., and Ward, B. A.: Dimensions of marine phytoplankton diversity, Biogeosciences, 17, 609–634, https://doi.org/10.5194/bg-17-609-2020, 2020.

Dutz, J., Mohrholz, V., and van Beusekom, J. E. E.: Life cycle and spring phenology of *Temora longicornis* in the Baltic Sea, Marine Ecology Progress Series, 406, 223–238, https://doi.org/10.3354/meps08545, 2010.

Dzierzbicka-Głowacka, L., Janecki, M., Nowicki, A., and Jakacki, J.: Activation of the operational ecohydrodynamic model (3D CEMBS) – The ecosystem module, Oceanologia, 55, 543–572, https://doi.org/10.5697/oc.55-3.543, 2013.

Edwards, M. and Richardson, A. J.: Impact of climate change on marine pelagic phenology and trophic mismatch, Nature, 430, 881–884, https://doi.org/10.1038/nature02808, 2004.

Edwards, M., Beaugrand, G., Hays, G. C., Koslow, J. A., and Richardson, A. J.: Multi-decadal oceanic ecological datasets and their application in marine policy and management, Trends in Ecology & Evolution, 25, 602–610, https://doi.org/10.1016/j.tree.2010.07.007, 2010.

Eilola, K., Meier, H. E. M., and Almroth, E.: On the dynamics of oxygen, phosphorus and cyanobacteria in the Baltic Sea; A model study, Journal of Marine Systems, 75, 163–184, https://doi.org/10.1016/j.jmarsys.2008.08.009, 2009.

Eilola, K., Gustafsson, B., Kuznetsov, I., Meier, H., Neumann, T., and Savchuk, O.: Evaluation of biogeochemical cycles in an ensemble of three state-of-the-art numerical models of the Baltic Sea, Journal of Marine Systems, 88, 267–284, https://doi.org/10.1016/j.jmarsys.2011.05.004, 2011.

Elena, S. F. and Lenski, R. E.: Evolution experiments with microorganisms: The dynamics and genetic bases of adaptation, Nature Reviews Genetics, 4, 457–469, https://doi.org/10.1038/nrg1088, 2003.

Ellegaard, M., Dale, B., Mertens, K. N., Pospelova, V., and Ribeiro, S.: Dinoflagellate cysts as proxies for Holocene environmental change in estuaries: Diversity, abundance and morphology, in: Applications of paleoenvironmental techniques in estuarine studies, edited by Weckström, K., Saunders, K. M., Gell, P. A., and Skilbeck, C. G., pp. 295–312, Springer Netherlands, Dordrecht, https://doi.org/10.1007/978-94-024-0990-1_12, 2017.

Ellegaard, M., Clokie, M. R. J., Czypionka, T., Frisch, D., Godhe, A., Kremp, A., Letarov, A., McGenity, T. J., Ribeiro, S., and John Anderson, N.: Dead or alive: Sediment DNA archives as tools for tracking aquatic evolution and adaptation, Communications Biology, 3, 1–11, https://doi.org/10.1038/s42003-020-0899-z, 2020.

Elliott, J. A., Thackeray, S. J., Huntingford, C., and Jones, R. G.: Combining a regional climate model with a phytoplankton community model to predict future changes in phytoplankton in lakes, Freshwater Biology, 50, 1404–1411, https://doi.org/10.1111/j.1365-2427.2005.01409.x, 2005.

Eppley, R. W.: Temperature and phytoplankton growth in the sea, Fishery Bulletin, 70, 1063–1085, 1972.

Everson, I.: Krill biology, ecology and fisheries, Blackwell Science Oxford, UK, 2000.

Eyring, V., Bony, S., Meehl, G. A., Senior, C. A., Stevens, B., Stouffer, R. J., and Taylor, K. E.: Overview of the Coupled Model Intercomparison Project Phase 6 (CMIP6) experimental design and organization, Geoscientific Model Development, 9, 1937–1958, https://doi.org/10.5194/gmd-9-1937-2016, 2016.

Fasham, M. J. R., Ducklow, H. W., and McKelvie, S. M.: A nitrogen-based model of plankton dynamics in the oceanic mixed layer, Journal of Marine Research, 48, 591–639, 1990.

Feike, M., Heerkloss, R., Rieling, T., and Schubert, H.: Studies on the zooplankton community of a shallow lagoon of the Southern Baltic Sea: Long-term trends, seasonal changes, and relations with physical and chemical parameters, Hydrobiologia, 577, 95–106, https://doi.org/10.1007/s10750-006-0420-9, 2007.

Fenchel, T.: Marine plankton food chains, Annual Review of Ecology and Systematics, 19, 19–38, https://doi.org/10.1146/annurev.es.19.110188.000315, 1988.

Field, C. B., Behrenfeld, M. J., Randerson, J. T., and Falkowski, P.: Primary production of the biosphere: Integrating terrestrial and oceanic components, Science, 281, 237–240, https://doi.org/10.1126/science.281.5374.237, 1998.

Finni, T., Kononen, K., Olsonen, R., and Wallström, K.: The history of cyanobacterial blooms in the Baltic Sea, AMBIO: A Journal of the Human Environment, 30, 172–178, https://doi.org/10.1579/0044-7447-30.4.172, 2001.

Follows, M. J., Dutkiewicz, S., Grant, S., and Chisholm, S. W.: Emergent biogeography of microbial communities in a model ocean, Science, 315, 1843–1846, https://doi.org/10.1126/science.1138544, 2007.

Fossheim, M., Primicerio, R., Johannesen, E., Ingvaldsen, R. B., Aschan, M. M., and Dolgov, A. V.: Recent warming leads to a rapid borealization of fish communities in the Arctic, Nature Climate Change, 5, 673–677, https://doi.org/10.1038/nclimate2647, 2015.

Foy, R.: The influence of surface to volume ratio on the growth rates of planktonic blue-green algae, British Phycological Journal, 15, 279–289, https://doi.org/10.1080/00071618000650281, 1980.

Fransner, F., Gustafsson, E., Tedesco, L., Vichi, M., Hordoir, R., Roquet, F., Spilling, K., Kuznetsov, I., Eilola, K., Mörth, C.-M., Humborg, C., and Nycander, J.: Non-Redfieldian dynamics explain seasonal pCO_2 drawdown in the Gulf of Bothnia, Journal of Geophysical Research: Oceans, 123, 166–188, https://doi.org/10.1002/2017JC013019, 2018.

Frederiksen, M., Elston, D. A., Edwards, M., Mann, A. D., and Wanless, S.: Mechanisms of long-term decline in size of lesser sandeels in the North Sea explored using a growth and phenology model, Marine Ecology Progress Series, 432, 137–147, https://doi.org/10.3354/meps09177, 2011.

Gibbs, S. J., Bown, P. R., Ward, B. A., Alvarez, S. A., Kim, H., Archontikis, O. A., Sauterey, B., Poulton, A. J., Wilson, J., and Ridgwell, A.: Algal plankton turn to hunting to survive and recover from end-Cretaceous impact darkness, Science Advances, 6, eabc9123, https://doi.org/10.1126/sciadv.abc9123, 2020.

Glibert, P. M., Burkholder, J. M., and Kana, T. M.: Recent insights about relationships between nutrient availability, forms, and stoichiometry, and the distribution, ecophysiology, and food web effects of pelagic and benthic *Prorocentrum* species, Harmful Algae, 14, 231–259, https://doi.org/10.1016/j.hal.2011.10.023, 2012.

Glibert, P. M., Icarus Allen, J., Artioli, Y., Beusen, A., Bouwman, L., Harle, J., Holmes, R., and Holt, J.: Vulnerability of coastal ecosystems to changes in harmful algal bloom distribution in response to climate change: Projections based on model analysis, Global Change Biology, 20, 3845–3858, https://doi.org/10.1111/gcb.12662, 2014.

Gobler, C. J., Doherty, O. M., Hattenrath-Lehmann, T. K., Griffith, A. W., Kang, Y., and Litaker, R. W.: Ocean warming since 1982 has expanded the niche of toxic algal blooms in the North Atlantic and North Pacific oceans, Proceedings of the National Academy of Sciences, 114, 4975–4980, https://doi.org/10.1073/pnas.1619575114, 2017.

Godhe, A., Asplund, M. E., Härnström, K., Saravanan, V., Tyagi, A., and Karunasagar, I.: Quantification of diatom and dinoflagellate biomasses in coastal marine seawater samples by real-time PCR, Applied and Environmental Microbiology, 74, 7174–7182, https://doi.org/10.1128/AEM.01298-08, 2008.

Goñi, M. A., Yunker, M. B., Macdonald, R. W., and Eglinton, T. I.: Distribution and sources of organic biomarkers in arctic sediments from the Mackenzie River and Beaufort Shelf, Marine Chemistry, 71, 23–51, https://doi.org/10.1016/S0304-4203(00)00037-2, 2000.

Gotham, I. J. and Rhee, G.-Y.: Comparative kinetic studies of phosphate-limited growth and phosphate uptake in phytoplankton in continuous culture, Journal of Phycology, 17, 257–265, https://doi.org/10.1111/j.1529-8817.1981.tb00848.x, 1981.

Grover, J. P.: Resource competition in a variable environment: Phytoplankton growing according to the Variable-Internal-Stores Model, The American Naturalist, 138, 811–835, https://doi.org/10.1086/285254, 1991.

Gustafsson, B. G., Schenk, F., Blenckner, T., Eilola, K., Meier, H. E. M., Müller-Karulis, B., Neumann, T., Ruoho-Airola, T., Savchuk, O. P., and Zorita, E.: Reconstructing the development of Baltic Sea eutrophication 1850–2006, AMBIO, 41, 534–548, https://doi.org/10.1007/s13280-012-0318-x, 2012.

Gustafsson, E., Savchuk, O. P., Gustafsson, B. G., and Müller-Karulis, B.: Key processes in the coupled carbon, nitrogen, and phosphorus cycling of the Baltic Sea, Biogeochemistry, 134, 301–317, https://doi.org/10.1007/s10533-017-0361-6, 2017.

Hain, M., Sigman, D., and Haug, G.: 8.18 - The biological pump in the past, in: Treatise on geochemistry, edited by Holland, H. D. and Turekian, K. K., pp. 485–517, Elsevier, Oxford, 2. edn., https://doi.org/10.1016/B978-0-08-095975-7.00618-5, 2014.

Hairston Jr, N. G. and De Stasio Jr, B. T.: Rate of evolution slowed by a dormant propagule pool, Nature, 336, 239–242, https://doi.org/10.1038/336239a0, 1988.

Hajdas, I., Ascough, P., Garnett, M. H., Fallon, S. J., Pearson, C. L., Quarta, G., Spalding, K. L., Yamaguchi, H., and Yoneda, M.: Radiocarbon dating, Nature Reviews Methods Primers, 1, 1–26, https://doi.org/10.1038/s43586-021-00058-7, 2021.

Hallegraeff, G. M.: Ocean climate change, phytoplankton community responses, and harmful algal blooms: A formidable predictive challenge, Journal of Phycology, 46, 220–235, https://doi.org/10.1111/j.1529-8817.2010.00815.x, 2010.

Hancock, G., Leslie, C., Everett, S., Tims, S., Brunskill, G., and Haese, R.: Plutonium as a chronomarker in Australian and New Zealand sediments: A comparison with ^{137}Cs, Journal of Environmental Radioactivity, 102, 919–929, https://doi.org/10.1016/j.jenvrad.2009.09.008, 2011.

Härnström, K., Ellegaard, M., Andersen, T. J., and Godhe, A.: Hundred years of genetic structure in a sediment revived diatom population, Proceedings of the National Academy of Sciences, 108, 4252–4257, https://doi.org/10.1073/pnas.1013528108, 2011.

Hattich, G. S. I., Jokinen, S., Sildever, S., Gareis, M., Heikkinen, J., Junghardt, N., Segovia, M., Machado, M., and Sjöqvist, C.: Temperature optima of a natural diatom population increases as global warming proceeds, Nature Climate Change, 14, 518–525, https://doi.org/10.1038/s41558-024-01981-9, 2024.

Heil, C. A., Glibert, P. M., and Fan, C.: *Prorocentrum minimum* (Pavillard) Schiller: A review of a harmful algal bloom species of growing worldwide importance, Harmful Algae, 4, 449–470, https://doi.org/10.1016/j.hal.2004.08.003, 2005.

Heiskanen, A.-S.: Factors governing sedimentation and pelagic nutrient cycles in the northern Baltic Sea, no. 8 in Monographs of the boreal environment research, Finnish Environment Institute, Helsinki, 1998.

Heneghan, R. F., Everett, J. D., Blanchard, J. L., Sykes, P., and Richardson, A. J.: Climate-driven zooplankton shifts cause large-scale declines in food quality for fish, Nature Climate Change, 13, 470–477, https://doi.org/10.1038/s41558-023-01630-7, 2023.

Hense, I.: Regulative feedback mechanisms in cyanobacteria-driven systems: A model study, Marine Ecology Progress Series, 339, 41–47, https://doi.org/10.3354/meps339041, 2007.

Hense, I. and Beckmann, A.: Towards a model of cyanobacteria life cycle—Effects of growing and resting stages on bloom formation of N_2-fixing species, Ecological Modelling, 195, 205–218, https://doi.org/10.1016/j.ecolmodel.2005.11.018, 2006.

Hense, I. and Beckmann, A.: The representation of cyanobacteria life cycle processes in aquatic ecosystem models, Ecological Modelling, 221, 2330–2338, https://doi.org/10.1016/j.ecolmodel.2010.06.014, 2010.

Hense, I. and Beckmann, A.: A theoretical investigation of the diatom cell size reduction–restitution cycle, Ecological Modelling, 317, 66–82, https://doi.org/10.1016/j.ecolmodel.2015.09.003, 2015.

Hense, I., Meier, H. E. M., and Sonntag, S.: Projected climate change impact on Baltic Sea cyanobacteria, Climatic Change, 119, 391–406, https://doi.org/10.1007/s10584-013-0702-y, 2013.

Henson, S. A., Laufkötter, C., Leung, S., Giering, S. L. C., Palevsky, H. I., and Cavan, E. L.: Uncertain response of ocean biological carbon export in a changing world, Nature Geoscience, 15, 248–254, https://doi.org/10.1038/s41561-022-00927-0, 2022.

Hillaire-Marcel, C. and De Vernal, A., eds.: Proxies in late Cenozoic paleoceanography, Elsevier, Amsterdam, Boston, Heidelberg, London, 2007.

Hinners, J., Hofmeister, R., and Hense, I.: Modeling the role of pH on Baltic Sea cyanobacteria, Life, 5, 1204–1217, https://doi.org/10.3390/life5021204, 2015.

Hinners, J., Kremp, A., and Hense, I.: Evolution in temperature-dependent phytoplankton traits revealed from a sediment archive: Do reaction norms tell the whole story?, Proceedings of the Royal Society B: Biological Sciences, 284, 20171 888, https://doi.org/10.1098/rspb.2017.1888, 2017.

Hinners, J., Hense, I., and Kremp, A.: Modelling phytoplankton adaptation to global warming based on resurrection experiments, Ecological Modelling, 400, 27–33, https://doi.org/10.1016/j.ecolmodel.2019.03.006, 2019.

Hinners, J., Argyle, P. A., Walworth, N. G., Doblin, M. A., Levine, N. M., and Collins, S.: Multi-trait diversification in marine diatoms in constant and warmed environments, Proceedings of the Royal Society B: Biological Sciences, 291, 20232 564, https://doi.org/10.1098/rspb.2023.2564, 2024.

Hirschhorn, J. N. and Daly, M. J.: Genome-wide association studies for common diseases and complex traits, Nature Reviews Genetics, 6, 95–108, https://doi.org/10.1038/nrg1521, 2005.

Hjerne, O., Hajdu, S., Larsson, U., Downing, A. S., and Winder, M.: Climate driven changes in timing, composition and magnitude of the Baltic Sea phytoplankton spring bloom, Frontiers in Marine Science, 6, 1–15, https://doi.org/10.3389/fmars.2019.00482, 2019.

Hochfeld, I. and Hinners, J.: Evolutionary adaptation to steady or changing environments affects competitive outcomes in marine phytoplankton, Limnology and Oceanography, 69, 1172–1186, https://doi.org/10.1002/lno.12559, 2024.

Hoegh-Guldberg, O. and Bruno, J. F.: The impact of climate change on the world's marine ecosystems, Science, 328, 1523–1528, https://doi.org/10.1126/science.1189930, 2010.

Hollingsworth, A.: Validation and diagnosis of atmospheric models, Dynamics of Atmospheres and Oceans, 20, 227–246, https://doi.org/10.1016/0377-0265(94)90019-1, 1994.

Hollowed, A. B., Barange, M., Beamish, R. J., Brander, K., Cochrane, K., Drinkwater, K., Foreman, M. G. G., Hare, J. A., Holt, J., Ito, S.-i., Kim, S., King, J. R., Loeng, H., MacKenzie, B. R., Mueter, F. J., Okey, T. A., Peck, M. A., Radchenko, V. I., Rice, J. C., Schirripa, M. J., Yatsu, A., and Yamanaka, Y.: Projected impacts of climate change on marine fish and fisheries, ICES Journal of Marine Science, 70, 1023–1037, https://doi.org/10.1093/icesjms/fst081, 2013.

Howarth, R. W. and Marino, R.: Nitrogen as the limiting nutrient for eutrophication in coastal marine ecosystems: Evolving views over three decades, Limnology and Oceanography, 51, 364–376, https://doi.org/10.4319/lo.2006.51.1_part_2.0364, 2006.

Hutchins, D. A. and Fu, F.: Microorganisms and ocean global change, Nature Microbiology, 2, 1–11, https://doi.org/10.1038/nmicrobiol.2017.58, 2017.

Hutchins, D. A., Walworth, N. G., Webb, E. A., Saito, M. A., Moran, D., McIlvin, M. R., Gale, J., and Fu, F.-X.: Irreversibly increased nitrogen fixation in *Trichodesmium* experimentally adapted to elevated carbon dioxide, Nature Communications, 6, 8155, https://doi.org/10.1038/ncomms9155, 2015.

Hutchinson, P. A. and Webster, I. T.: On the distribution of blue-green algae in lakes: Wind-tunnel tank experiments, Limnology and Oceanography, 39, 374–382, https://doi.org/10.4319/lo.1994.39.2.0374, 1994.

Intergovernmental Panel on Climate Change (IPCC): Climate Change 2022 – Impacts, Adaptation and Vulnerability: Working Group II Contribution to the Sixth Assessment Report of the Intergovernmental Panel on Climate Change, Cambridge University Press, 1. edn., https://doi.org/10.1017/9781009325844, 2022.

Irwin, A. J., Finkel, Z. V., Müller-Karger, F. E., and Troccoli Ghinaglia, L.: Phytoplankton adapt to changing ocean environments, Proceedings of the National Academy of Sciences, 112, 5762–5766, https://doi.org/10.1073/pnas.1414752112, 2015.

Isanta-Navarro, J., Hairston, N. G., Beninde, J., Meyer, A., Straile, D., Möst, M., and Martin-Creuzburg, D.: Reversed evolution of grazer resistance to cyanobacteria, Nature Communications, 12, 1945, https://doi.org/10.1038/s41467-021-22226-9, 2021.

Jin, P. and Agustí, S.: Fast adaptation of tropical diatoms to increased warming with trade-offs, Scientific Reports, 8, 17 771, https://doi.org/10.1038/s41598-018-36091-y, 2018.

Jung, H.-C. and Moon, B.-K.: Impacts of albedo and wind stress changes due to phytoplankton on ocean temperature in a coupled global ocean-biogeochemistry model, Journal of the Korean earth science society, 40, 392–405, https://doi.org/10.5467/JKESS.2019.40.4.392, 2019.

Kaiser, J., van der Meer, M. T., and Arz, H. W.: Long-chain alkenones in Baltic Sea surface sediments: New insights, Organic Geochemistry, 112, 93–104, https://doi.org/10.1016/j.orggeochem.2017.07.002, 2017.

Karlsson, K. M., Kankaanpää, H., Huttunen, M., and Meriluoto, J.: First observation of microcystin-LR in pelagic cyanobacterial blooms in the northern Baltic Sea, Harmful Algae, 4, 163–166, https://doi.org/10.1016/j.hal.2004.02.002, 2005.

Keller, M. D., Bellows, W. K., and Guillard, R. R. L.: Dimethyl sulfide production in marine phytoplankton, in: Biogenic sulfur in the environment, vol. 393 of *ACS Symposium Series*, pp. 167–182, American Chemical Society, https://doi.org/10.1021/bk-1989-0393.ch011, 1989.

Kerfoot, W. C. and Weider, L. J.: Experimental paleoecology (resurrection ecology): Chasing Van Valen's Red Queen hypothesis, Limnology and Oceanography, 49, 1300–1316, https://doi.org/10.4319/lo.2004.49.4_part_2.1300, 2004.

Khatiwala, S., Tanhua, T., Mikaloff Fletcher, S., Gerber, M., Doney, S. C., Graven, H. D., Gruber, N., McKinley, G. A., Murata, A., Ríos, A. F., and Sabine, C. L.: Global ocean storage of anthropogenic carbon, Biogeosciences, 10, 2169–2191, https://doi.org/10.5194/bg-10-2169-2013, 2013.

Kjær, K. H., Winther Pedersen, M., De Sanctis, B., De Cahsan, B., Korneliussen, T. S., Michelsen, C. S., Sand, K. K., Jelavić, S., Ruter, A. H., Schmidt, A. M. A., Kjeldsen, K. K., Tesakov, A. S., Snowball, I., Gosse, J. C., Alsos, I. G., Wang, Y., Dockter, C., Rasmussen, M., Jørgensen, M. E., Skadhauge, B., Prohaska, A., Kristensen, J. r., Bjerager, M., Allentoft, M. E., Coissac, E., Rouillard, A., Simakova, A., Fernandez-Guerra, A., Bowler, C., Macias-Fauria, M., Vinner, L., Welch, J. J., Hidy, A. J., Sikora, M., Collins, M. J., Durbin, R., Larsen, N. K., and Willerslev, E.: A 2-million-year-old ecosystem in Greenland uncovered by environmental DNA, Nature, 612, 283–291, https://doi.org/10.1038/s41586-022-05453-y, 2022.

Klais, R., Tamminen, T., Kremp, A., Spilling, K., and Olli, K.: Decadal-scale changes of dinoflagellates and diatoms in the anomalous Baltic Sea spring bloom, PLOS ONE, 6, e21 567, https://doi.org/10.1371/journal.pone.0021567, 2011.

Klausmeier, C. A., Kremer, C. T., and Koffel, T.: Trait-based ecological and eco-evolutionary theory, in: Theoretical ecology: Concepts and applications, Oxford University Press, https://doi.org/10.1093/oso/9780198824282.003.0011, 2020a.

Klausmeier, C. A., Osmond, M. M., Kremer, C. T., and Litchman, E.: Ecological limits to evolutionary rescue, Philosophical Transactions of the Royal Society B: Biological Sciences, 375, 20190 453, https://doi.org/10.1098/rstb.2019.0453, 2020b.

Korkonen, S. T., Ojala, A., Kosonen, E. M., and Weckström, J. B.: Seasonality of chrysophyte cyst and diatom assemblages in varved Lake Nautajärvi–Implications for palaeolimnological studies, Journal of Limnology, 76, 366–379, https://doi.org/10.4081/jlimnol.2017.1473, 2017.

Krasovec, M., Sanchez-Brosseau, S., and Piganeau, G.: First estimation of the spontaneous mutation rate in diatoms, Genome Biology and Evolution, 11, 1829–1837, https://doi.org/10.1093/gbe/evz130, 2019.

Kremer, C. T. and Klausmeier, C. A.: Species packing in eco-evolutionary models of seasonally fluctuating environments, Ecology Letters, 20, 1158–1168, https://doi.org/10.1111/ele.12813, 2017.

Kremp, A.: Morphology and germination pattern of the resting cyst of *Peridiniella catenata* (dinophyceae) from the Baltic Sea, Phycologia, 39, 183–186, https://doi.org/10.2216/i0031-8884-39-3-183.1, 2000.

Kremp, A. and Anderson, D. M.: Factors regulating germination of resting cysts of the spring bloom dinoflagellate *Scrippsiella hangoei* from the northern Baltic Sea, Journal of Plankton Research, 22, 1311–1327, https://doi.org/10.1093/plankt/22.7.1311, 2000.

Kremp, A. and Parrow, M. W.: Evidence for asexual resting cysts in the life cycle of the marine peridinoid dinoflagellate, *Scrippsiella hangoei*, Journal of Phycology, 42, 400–409, https://doi.org/10.1111/j.1529-8817.2006.00205.x, 2006.

Kremp, A., Rengefors, K., and Montresorc, M.: Species specific encystment patterns in three Baltic cold-water dinoflagellates: The role of multiple cues in resting cyst formation, Limnology and Oceanography, 54, 1125–1138, https://doi.org/10.4319/lo.2009.54.4.1125, 2009.

Kremp, A., Oja, J., LeTortorec, A. H., Hakanen, P., Tahvanainen, P., Tuimala, J., and Suikkanen, S.: Diverse seed banks favour adaptation of microalgal populations to future climate conditions, Environmental Microbiology, 18, 679–691, https://doi.org/10.1111/1462-2920.13070, 2016.

Kremp, A., Hinners, J., Klais, R., Leppänen, A.-P., and Kallio, A.: Patterns of vertical cyst distribution and survival in 100-year-old sediment archives of three spring dinoflagellate species from the Northern Baltic Sea, European Journal of Phycology, 53, 135–145, https://doi.org/10.1080/09670262.2017.1386330, 2018.

Krishna, S., Peterson, V., Listmann, L., and Hinners, J.: Interactive effects of viral lysis and warming in a coastal ocean identified from an idealized ecosystem model, Ecological Modelling, 487, 110 550, https://doi.org/10.1016/j.ecolmodel.2023.110550, 2024.

Lässig, M., Mustonen, V., and Walczak, A. M.: Predicting evolution, Nature Ecology & Evolution, 1, 1–9, https://doi.org/10.1038/s41559-017-0077, 2017.

Laufkötter, C., Vogt, M., Gruber, N., Aita-Noguchi, M., Aumont, O., Bopp, L., Buitenhuis, E., Doney, S. C., Dunne, J., Hashioka, T., Hauck, J., Hirata, T., John, J., Le Quéré, C., Lima, I. D., Nakano, H., Seferian, R., Totterdell, I., Vichi, M., and Völker, C.: Drivers and uncertainties of future global marine primary production in marine ecosystem models, Biogeosciences, 12, 6955–6984, https://doi.org/10.5194/bg-12-6955-2015, 2015.

Laufkötter, C., Vogt, M., Gruber, N., Aumont, O., Bopp, L., Doney, S. C., Dunne, J. P., Hauck, J., John, J. G., Lima, I. D., Seferian, R., and Völker, C.: Projected decreases in future marine export production: The role of the carbon flux through the upper ocean ecosystem, Biogeosciences, 13, 4023–4047, https://doi.org/10.5194/bg-13-4023-2016, 2016.

Lawrence, D., Fiegna, F., Behrends, V., Bundy, J. G., Phillimore, A. B., Bell, T., and Barraclough, T. G.: Species interactions alter evolutionary responses to a novel environment, PLOS Biology, 10, e1001 330, https://doi.org/10.1371/journal.pbio.1001330, 2012.

Le Gland, G., Vallina, S. M., Smith, S. L., and Cermeño, P.: SPEAD 1.0 – Simulating Plankton Evolution with Adaptive Dynamics in a two-trait continuous fitness landscape applied to the Sargasso Sea, Geoscientific Model Development, 14, 1949–1985, https://doi.org/10.5194/gmd-14-1949-2021, 2021.

Lear, C. H., Rosenthal, Y., and Slowey, N.: Benthic foraminiferal Mg/Ca-paleothermometry: A revised core-top calibration, Geochimica et Cosmochimica Acta, 66, 3375–3387, https://doi.org/10.1016/S0016-7037(02)00941-9, 2002.

Lee, S., Hofmeister, R., and Hense, I.: The role of life cycle processes on phytoplankton spring bloom composition: A modelling study applied to the Gulf of Finland, Journal of Marine Systems, 178, 75–85, https://doi.org/10.1016/j.jmarsys.2017.10.010, 2018.

Lehtimäki, J., Moisander, P., Sivonen, K., and Kononen, K.: Growth, nitrogen fixation, and nodularin production by two Baltic Sea cyanobacteria, Applied and Environmental Microbiology, 63, 1647–1656, https://doi.org/10.1128/aem.63.5.1647-1656.1997, 1997.

Lenski, R. E. and Travisano, M.: Dynamics of adaptation and diversification: A 10,000-generation experiment with bacterial populations., Proceedings of the National Academy of Sciences, 91, 6808–6814, https://doi.org/10.1073/pnas.91.15.6808, 1994.

Lenton, T. M., Held, H., Kriegler, E., Hall, J. W., Lucht, W., Rahmstorf, S., and Schellnhuber, H. J.: Tipping elements in the Earth's climate system, Proceedings of the National Academy of Sciences, 105, 1786–1793, https://doi.org/10.1073/pnas.0705414105, 2008.

Leterme, S. C., Edwards, M., Seuront, L., Attrill, M. J., Reid, P. C., and John, A. W. G.: Decadal basin-scale changes in diatoms, dinoflagellates, and phytoplankton color across the North Atlantic, Limnology and Oceanography, 50, 1244–1253, https://doi.org/10.4319/lo.2005.50.4.1244, 2005.

Levins, R.: Theory of fitness in a heterogeneous environment. I. The fitness set and adaptive function, The American Naturalist, 96, 361–373, https://doi.org/10.1086/282245, 1962.

Limoges, A., Van Nieuwenhove, N., Head, M. J., Mertens, K. N., Pospelova, V., and Rochon, A.: A review of rare and less well known extant marine organic-walled dinoflagellate cyst taxa of the orders Gonyaulacales and Suessiales from the Northern Hemisphere, Marine Micropaleontology, 159, 101 801, https://doi.org/10.1016/j.marmicro.2019.101801, 2020.

Listmann, L., LeRoch, M., Schlüter, L., Thomas, M. K., and Reusch, T. B. H.: Swift thermal reaction norm evolution in a key marine phytoplankton species, Evolutionary Applications, 9, 1156–1164, https://doi.org/10.1111/eva.12362, 2016.

Listmann, L., Hattich, G. S. I., Matthiessen, B., and Reusch, T. B. H.: Eco-evolutionary interaction in competing phytoplankton: Nutrient driven genotype sorting likely explains dominance shift and species responses to CO_2, Frontiers in Marine Science, 7, 1–13, https://doi.org/10.3389/fmars.2020.00634, 2020.

Litchman, E., Klausmeier, C. A., Schofield, O. M., and Falkowski, P. G.: The role of functional traits and trade-offs in structuring phytoplankton communities: Scaling from cellular to ecosystem level, Ecology Letters, 10, 1170–1181, https://doi.org/10.1111/j.1461-0248.2007.01117.x, 2007.

Litchman, E., de Tezanos Pinto, P., Edwards, K. F., Klausmeier, C. A., Kremer, C. T., and Thomas, M. K.: Global biogeochemical impacts of phytoplankton: A trait-based perspective, Journal of Ecology, 103, 1384–1396, https://doi.org/10.1111/1365-2745.12438, 2015.

Long, A. M., Jurgensen, S. K., Petchel, A. R., Savoie, E. R., and Brum, J. R.: Microbial ecology of oxygen minimum zones amidst ocean deoxygenation, Frontiers in Microbiology, 12, 748 961, https://doi.org/10.3389/fmicb.2021.748961, 2021.

Lowe, D. J. and Alloway, B. V.: Tephrochronology, in: Encyclopedia of scientific dating methods, pp. 783–799, Springer, Dordrecht, https://doi.org/10.1007/978-94-007-6304-3_19, 2015.

Manizza, M., Le Quéré, C., Watson, A. J., and Buitenhuis, E. T.: Bio-optical feedbacks among phytoplankton, upper ocean physics and sea-ice in a global model, Geophysical Research Letters, 32, 1–4, https://doi.org/10.1029/2004GL020778, 2005.

Manizza, M., Le Quéré, C., Watson, A. J., and Buitenhuis, E. T.: Ocean biogeochemical response to phytoplankton-light feedback in a global model, Journal of Geophysical Research: Oceans, 113, 1–13, https://doi.org/10.1029/2007JC004478, 2008.

Marañón, E., Cermeño, P., López-Sandoval, D. C., Rodríguez-Ramos, T., Sobrino, C., Huete-Ortega, M., Blanco, J. M., and Rodríguez, J.: Unimodal size scaling of phytoplankton growth and the size dependence of nutrient uptake and use, Ecology Letters, 16, 371–379, https://doi.org/10.1111/ele.12052, 2013.

Margalef, R., Estrada, M., and Blasco, D.: Functional morphology of organisms involved in red tides, as adapted to decaying turbulence, Developments in marine biology, 1, 89–94, 1979.

María Trigueros, J. and Orive, E.: Seasonal variations of diatoms and dinoflagellates in a shallow, temperate estuary, with emphasis on neritic assemblages, Hydrobiologia, 444, 119–133, https://doi.org/10.1023/A:1017563031810, 2001.

Maslin, M., Pike, J., Stickley, C., and Ettwein, V.: Evidence of Holocene climate variability in marine sediments, in: Global change in the Holocene, Routledge, 2005.

Matul, A., Spielhagen, R. F., Kazarina, G., Kruglikova, S., Dmitrenko, O., and Mohan, R.: Warm-water events in the eastern Fram Strait during the last 2000 years as revealed by different microfossil groups, Polar Research, 37, 1540 243, https://doi.org/10.1080/17518369.2018.1540243, 2018.

McGraw, J. B., Vavrek, M. C., and Bennington, C. C.: Ecological genetic variation in seed banks I. Establishment of a time transect, Journal of Ecology, 79, 617–625, https://doi.org/10.2307/2260657, 1991.

McQupoid, M. R. and Hobson, L. A.: Diatom resting stages, Journal of Phycology, 32, 889–902, https://doi.org/10.1111/j.0022-3646.1996.00889.x, 1996.

Medlin, L., Sáez, A., and Young, J.: A molecular clock for coccolithophores and implications for selectivity of phytoplankton extinctions across the K/T boundary, Marine Micropaleontology, 67, 69–86, https://doi.org/10.1016/j.marmicro.2007.08.007, 2008.

Meier, H. E. M., Eilola, K., and Almroth, E.: Climate-related changes in marine ecosystems simulated with a 3-dimensional coupled physical-biogeochemical model of the Baltic Sea, Climate Research, 48, 31–55, https://doi.org/10.3354/cr00968, 2011.

Meier, H. E. M., Hordoir, R., Andersson, H. C., Dieterich, C., Eilola, K., Gustafsson, B. G., Höglund, A., and Schimanke, S.: Modeling the combined impact of changing climate and changing nutrient loads on the Baltic Sea environment in an ensemble of transient simulations for 1961–2099, Climate Dynamics, 39, 2421–2441, https://doi.org/10.1007/s00382-012-1339-7, 2012a.

Meier, H. E. M., Müller-Karulis, B., Andersson, H. C., Dieterich, C., Eilola, K., Gustafsson, B. G., Höglund, A., Hordoir, R., Kuznetsov, I., Neumann, T., Ranjbar, Z., Savchuk, O. P., and Schimanke, S.: Impact of climate change on ecological quality indicators and biogeochemical fluxes in the Baltic Sea: A multi-model ensemble study, AMBIO, 41, 558–573, https://doi.org/10.1007/s13280-012-0320-3, 2012b.

Meier, H. E. M., Andersson, H. C., Arheimer, B., Donnelly, C., Eilola, K., Gustafsson, B. G., Kotwicki, L., Neset, T.-S., Niiranen, S., Piwowarczyk, J., Savchuk, O. P., Schenk, F., Węsławski, J. M., and Zorita, E.: Ensemble modeling of the Baltic Sea ecosystem to provide scenarios for management, AMBIO, 43, 37–48, https://doi.org/10.1007/s13280-013-0475-6, 2014.

Mejbel, H. S., Dodsworth, W., Baud, A., Gregory-Eaves, I., and Pick, F. R.: Comparing quantitative methods for analyzing sediment DNA records of cyanobacteria in experimental and reference lakes, Frontiers in Microbiology, 12, 1–17, https://doi.org/10.3389/fmicb.2021.669910, 2021.

Merico, A., Bruggeman, J., and Wirtz, K.: A trait-based approach for downscaling complexity in plankton ecosystem models, Ecological Modelling, 220, 3001–3010, https://doi.org/10.1016/j.ecolmodel.2009.05.005, 2009.

Merico, A., Brandt, G., Smith, S. L., and Oliver, M.: Sustaining diversity in trait-based models of phytoplankton communities, Frontiers in Ecology and Evolution, 2, 1–8, https://doi.org/10.3389/fevo.2014.00059, 2014.

Mitchell, D., Willerslev, E., and Hansen, A.: Damage and repair of ancient DNA, Mutation Research/Fundamental and Molecular Mechanisms of Mutagenesis, 571, 265–276, https://doi.org/10.1016/j.mrfmmm.2004.06.060, 2005.

Moisan, J. R., Moisan, T. A., and Abbott, M. R.: Modelling the effect of temperature on the maximum growth rates of phytoplankton populations, Ecological Modelling, 153, 197–215, https://doi.org/10.1016/S0304-3800(02)00008-X, 2002.

Monchamp, M.-E., Walser, J.-C., Pomati, F., and Spaak, P.: Sedimentary DNA reveals cyanobacterial community diversity over 200 years in two perialpine lakes, Applied and Environmental Microbiology, 82, 6472–6482, https://doi.org/10.1128/AEM.02174-16, 2016.

Monod, J.: The growth of bacterial cultures, Annu. Rev. Microbiol., 3, 371–394, 1949.

Morel, F. M. M.: Kinetics of nutrient uptake and growth in phytoplankton, Journal of Phycology, 23, 137–150, https://doi.org/10.1111/j.0022-3646.1987.00137.x, 1987.

Moreno-Ostos, E., Cruz-Pizarro, L., Basanta, A., and George, D. G.: The influence of wind-induced mixing on the vertical distribution of buoyant and sinking phytoplankton species, Aquatic Ecology, 43, 271–284, https://doi.org/10.1007/s10452-008-9167-x, 2009.

Munkes, B., Löptien, U., and Dietze, H.: Cyanobacteria blooms in the Baltic Sea: A review of models and facts, Biogeosciences, 18, 2347–2378, https://doi.org/10.5194/bg-18-2347-2021, 2021.

Nalewajko, C. and Murphy, T. P.: Effects of temperature, and availability of nitrogen and phosphorus on the abundance of *Anabaena* and *Microcystis* in Lake Biwa, Japan: An experimental approach, Limnology, 2, 45–48, https://doi.org/10.1007/s102010170015, 2001.

Neumann, T.: Climate-change effects on the Baltic Sea ecosystem: A model study, Journal of Marine Systems, 81, 213–224, https://doi.org/10.1016/j.jmarsys.2009.12.001, 2010.

Neumann, T., Fennel, W., and Kremp, C.: Experimental simulations with an ecosystem model of the Baltic Sea: A nutrient load reduction experiment, Global Biogeochemical Cycles, 16, 7–1–7–19, https://doi.org/10.1029/2001GB001450, 2002.

Neumann, T., Radtke, H., Cahill, B., Schmidt, M., and Rehder, G.: Non-Redfieldian carbon model for the Baltic Sea (ERGOM version 1.2) – Implementation and budget estimates, Geoscientific Model Development, 15, 8473–8540, https://doi.org/10.5194/gmd-15-8473-2022, 2022.

Northfield, T. D. and Ives, A. R.: Coevolution and the effects of climate change on interacting species, PLOS Biology, 11, e1001 685, https://doi.org/10.1371/journal.pbio.1001685, 2013.

O'Donnell, D. R., Hamman, C. R., Johnson, E. C., Kremer, C. T., Klausmeier, C. A., and Litchman, E.: Rapid thermal adaptation in a marine diatom reveals constraints and trade-offs, Global Change Biology, 24, 4554–4565, https://doi.org/10.1111/gcb.14360, 2018.

Oke, P., Larnicol, G., Fujii, Y., Smith, G., Lea, D., Guinehut, S., Remy, E., Balmaseda, M. A., Rykova, T., Surcel-Colan, D., Martin, M., Sellar, A., Mulet, S., and Turpin, V.: Assessing the impact of observations on ocean forecasts and reanalyses: Part 1, Global studies, Journal of Operational Oceanography, 8, s49–s62, https://doi.org/10.1080/1755876X.2015.1022067, 2015a.

Oke, P., Larnicol, G., Jones, E., Kourafalou, V., Sperrevik, A., Carse, F., Tanajura, C., Mourre, B., Tonani, M., Brassington, G., Henaff, M. L., Jr., G. H., Atlas, R., Moore, A., Edwards, C., Martin, M., Sellar, A., Alvarez, A., Mey, P. D., and Iskandarani, M.: Assessing the impact of observations on ocean forecasts and reanalyses: Part 2, Regional applications, Journal of Operational Oceanography, 8, s63–s79, https://doi.org/10.1080/1755876X.2015.1022080, 2015b.

Olenina, I., Hajdu, S., Edler, L., Andersson, A., Wasmund, N., Busch, S., Göbel, J., Gromisz, S., Huseby, S., Huttunen, M., Jaanus, A., Kokkonen, P., Ledaine, I., and Niemkiewicz, E.: Biovolumes and size-classes of phytoplankton in the Baltic Sea, Baltic Sea Environmental Proceedings, p. 144, 2006.

Østman, B., Hintze, A., and Adami, C.: Impact of epistasis and pleiotropy on evolutionary adaptation, Proceedings of the Royal Society B: Biological Sciences, 279, 247–256, https://doi.org/10.1098/rspb.2011.0870, 2012.

Paerl, H. W. and Paul, V. J.: Climate change: Links to global expansion of harmful cyanobacteria, Water Research, 46, 1349–1363, https://doi.org/10.1016/j.watres.2011.08.002, 2012.

Paerl, H. W., Xu, H., Hall, N. S., Rossignol, K. L., Joyner, A. R., Zhu, G., and Qin, B.: Nutrient limitation dynamics examined on a multi-annual scale in Lake Taihu, China: Implications for controlling eutrophication and harmful algal blooms, Journal of Freshwater Ecology, 30, 5–24, https://doi.org/10.1080/02705060.2014.994047, 2015.

Pandey, R. K.: Induction of akinete formation in *Nodularia spumigena* by temperature, Journal of Basic Microbiology, 29, 477–480, https://doi.org/10.1002/jobm.3620290721, 1989.

Park, J.-Y., Kug, J.-S., Bader, J., Rolph, R., and Kwon, M.: Amplified Arctic warming by phytoplankton under greenhouse warming, Proceedings of the National Academy of Sciences, 112, 5921–5926, https://doi.org/10.1073/pnas.1416884112, 2015.

Pauwels, K., De Meester, L., Put, S., Decaestecker, E., Decaestecker, E., and Stoks, R.: Rapid evolution of phenoloxidase expression, a component of innate immune function, in a natural population of *Daphnia magna*, Limnology and Oceanography, 55, 1408–1413, https://doi.org/10.4319/lo.2010.55.3.1408, 2010.

Pecl, G. T., Araújo, M. B., Bell, J. D., Blanchard, J., Bonebrake, T. C., Chen, I.-C., Clark, T. D., Colwell, R. K., Danielsen, F., Evengård, B., Falconi, L., Ferrier, S., Frusher, S., Garcia, R. A., Griffis, R. B., Hobday, A. J., Janion-Scheepers, C., Jarzyna, M. A., Jennings, S., Lenoir, J., Linnetved, H. I., Martin, V. Y., McCormack, P. C., McDonald, J., Mitchell, N. J., Mustonen, T., Pandolfi, J. M., Pettorelli, N., Popova, E., Robinson, S. A., Scheffers, B. R., Shaw, J. D., Sorte, C. J. B., Strugnell, J. M., Sunday, J. M., Tuanmu, M.-N., Vergés, A., Villanueva, C., Wernberg, T., Wapstra, E., and Williams, S. E.: Biodiversity redistribution under climate change: Impacts on ecosystems and human well-being, Science, 355, eaai9214, https://doi.org/10.1126/science.aai9214, 2017.

Peer, A. C. and Miller, T. J.: Climate change, migration phenology, and fisheries management interact with unanticipated consequences, North American Journal of Fisheries Management, 34, 94–110, https://doi.org/10.1080/02755947.2013.847877, 2014.

Peterson, J., Griffis, R., Alaska, G. o., Zador, S. G., Sigler, M. F., Joyce, J. E., Current, C., Hunsicker, M., Bograd, S., Crozier, L. G., McClatchie, S., Morris Jr., J. A., Peterson, W. T., Price, C., Islands, P., Woodworth-Jefcoats, P. A., Mexico, G. o., Karnauskas, M., Muñoz, R., Schueller, A., Kevin Craig, J., Atlantic, S. U., Bacheler, N., Burton, M. L., Gore, K., Kellison, T., Morris Jr., J. A., Muñoz, R., Price, C., Atlantic, N. U., Hare, J. A., Friedland, K. D., and Miller, T. J.: Climate change impacts on fisheries and aquaculture of the United States, in: Climate change impacts on fisheries and aquaculture, pp. 159–218, John Wiley & Sons, Ltd, https://doi.org/10.1002/9781119154051.ch8, 2017.

Poloczanska, E. S., Brown, C. J., Sydeman, W. J., Kiessling, W., Schoeman, D. S., Moore, P. J., Brander, K., Bruno, J. F., Buckley, L. B., Burrows, M. T., Duarte, C. M., Halpern, B. S., Holding, J., Kappel, C. V., O'Connor, M. I., Pandolfi, J. M., Parmesan, C., Schwing, F., Thompson, S. A., and Richardson, A. J.: Global imprint of climate change on marine life, Nature Climate Change, 3, 919–925, https://doi.org/10.1038/nclimate1958, 2013.

Poutanen, E.-L. and Nikkilä, K.: Carotenoid pigments as tracers of cyanobacterial blooms in recent and post-glacial sediments of the Baltic Sea, AMBIO: A Journal of the Human Environment, 30, 179–183, https://doi.org/10.1579/0044-7447-30.4.179, 2001.

Prahl, F. G., Muehlhausen, L. A., and Zahnle, D. L.: Further evaluation of long-chain alkenones as indicators of paleoceanographic conditions, Geochimica et Cosmochimica Acta, 52, 2303–2310, https://doi.org/10.1016/0016-7037(88)90132-9, 1988.

Prentice, I. C., Williams, S., and Friedlingstein, P.: Biosphere feedbacks and climate change, Grantham Institute Briefing paper no. 12, Imperial College London, pp. 1–19, 2015.

Ptacnik, R., Solimini, A. G., Andersen, T., Tamminen, T., Brettum, P., Lepistö, L., Willén, E., and Rekolainen, S.: Diversity predicts stability and resource use efficiency in natural phytoplankton communities, Proceedings of the National Academy of Sciences, 105, 5134–5138, https://doi.org/10.1073/pnas.0708328105, 2008.

Quesada, A., Moreno, E., Carrasco, D., Paniagua, T., Wormer, L., Hoyos, C. d., and Sukenik, A.: Toxicity of *Aphanizomenon ovalisporum* (cyanobacteria) in a Spanish water reservoir, European Journal of Phycology, 41, 39–45, https://doi.org/10.1080/09670260500480926, 2006.

Redfield, A. C.: On the proportions of organic derivatives in sea water and their relation to the composition of plankton, vol. 1, University Press of Liverpool, 1934.

Reid, K. and Croxall, J. P.: Environmental response of upper trophic-level predators reveals a system change in an Antarctic marine ecosystem, Proceedings of the Royal Society of London. Series B: Biological Sciences, 268, 377–384, https://doi.org/10.1098/rspb.2000.1371, 2001.

Renaud, P. E., Løkken, T. S., Jørgensen, L. L., Berge, J., and Johnson, B. J.: Macroalgal detritus and food-web subsidies along an Arctic fjord depth-gradient, Frontiers in Marine Science, 2, 1–15, https://doi.org/10.3389/fmars.2015.00031, 2015.

Rengefors, K., Kremp, A., Reusch, T. B., and Wood, A. M.: Genetic diversity and evolution in eukaryotic phytoplankton: Revelations from population genetic studies, Journal of Plankton Research, 39, 165–179, https://doi.org/10.1093/plankt/fbw098, 2017.

Repavich, W. M., Sonzogni, W. C., Standridge, J. H., Wedepohl, R. E., and Meisner, L. F.: Cyanobacteria (blue-green algae) in wisconsin waters: Acute and chronic toxicity, Water Research, 24, 225–231, https://doi.org/10.1016/0043-1354(90)90107-H, 1990.

Reusch, T. B. H., Dierking, J., Andersson, H. C., Bonsdorff, E., Carstensen, J., Casini, M., Czajkowski, M., Hasler, B., Hinsby, K., Hyytiäinen, K., Johannesson, K., Jomaa, S., Jormalainen, V., Kuosa, H., Kurland, S., Laikre, L., MacKenzie, B. R., Margonski, P., Melzner, F., Oesterwind, D., Ojaveer, H., Refsgaard, J. C., Sandström, A., Schwarz, G., Tonderski, K., Winder, M., and Zandersen, M.: The Baltic Sea as a time machine for the future coastal ocean, Science Advances, 4, eaar8195, https://doi.org/10.1126/sciadv.aar8195, 2018.

Ribeiro, S., Berge, T., Lundholm, N., and Ellegaard, M.: Hundred years of environmental change and phytoplankton ecophysiological variability archived in coastal sediments, PLOS ONE, 8, e61 184, https://doi.org/10.1371/journal.pone.0061184, 2013.

Richardson, A. J.: In hot water: Zooplankton and climate change, ICES Journal of Marine Science, 65, 279–295, https://doi.org/10.1093/icesjms/fsn028, 2008.

Richardson, A. J. and Schoeman, D. S.: Climate impact on plankton ecosystems in the Northeast Atlantic, Science, 305, 1609–1612, https://doi.org/10.1126/science.1100958, 2004.

Rockström, J., Steffen, W., Noone, K., Persson, r., Chapin, F. S., Lambin, E. F., Lenton, T. M., Scheffer, M., Folke, C., Schellnhuber, H. J., Nykvist, B., de Wit, C. A., Hughes, T., van der Leeuw, S., Rodhe, H., Sörlin, S., Snyder, P. K., Costanza, R., Svedin, U., Falkenmark, M., Karlberg, L., Corell, R. W., Fabry, V. J., Hansen, J., Walker, B., Liverman, D., Richardson, K., Crutzen, P., and Foley, J. A.: A safe operating space for humanity, Nature, 461, 472–475, https://doi.org/10.1038/461472a, 2009.

Rosell-Melé, A.: Interhemispheric appraisal of the value of alkenone indices as temperature and salinity proxies in high-latitude locations, Paleoceanography, 13, 694–703, https://doi.org/10.1029/98PA02355, 1998.

Rutgersson, A., Jaagus, J., Schenk, F., and Stendel, M.: Observed changes and variability of atmospheric parameters in the Baltic Sea region during the last 200 years, Climate Research, 61, 177–190, https://doi.org/10.3354/cr01244, 2014.

Sallon, S., Solowey, E., Cohen, Y., Korchinsky, R., Egli, M., Woodhatch, I., Simchoni, O., and Kislev, M.: Germination, genetics, and growth of an ancient date seed, Science, 320, 1464–1464, https://doi.org/10.1126/science.1153600, 2008.

Sanyal, A., Larsson, J., van Wirdum, F., Andrén, T., Moros, M., Lönn, M., and Andrén, E.: Not dead yet: Diatom resting spores can survive in nature for several millennia, American Journal of Botany, 109, 67–82, https://doi.org/10.1002/ajb2.1780, 2022.

Sathyendranath, S., Gouveia, A. D., Shetye, S. R., Ravindran, P., and Platt, T.: Biological control of surface temperature in the Arabian Sea, Nature, 349, 54–56, https://doi.org/10.1038/349054a0, 1991.

Sauterey, B. and Ward, B. A.: Environmental control of marine phytoplankton stoichiometry in the North Atlantic Ocean, Proceedings of the National Academy of Sciences, 119, e2114602 118, https://doi.org/10.1073/pnas.2114602118, 2022.

Sauterey, B., Ward, B., Rault, J., Bowler, C., and Claessen, D.: The implications of eco-evolutionary processes for the emergence of marine plankton community biogeography, The American Naturalist, 190, 116–130, https://doi.org/10.1086/692067, 2017.

Savchuk, O. P.: Nutrient biogeochemical cycles in the Gulf of Riga: Scaling up field studies with a mathematical model, Journal of Marine Systems, 32, 253–280, https://doi.org/10.1016/S0924-7963(02)00039-8, 2002.

Schabhüttl, S., Hingsamer, P., Weigelhofer, G., Hein, T., Weigert, A., and Striebel, M.: Temperature and species richness effects in phytoplankton communities, Oecologia, 171, 527–536, https://doi.org/10.1007/s00442-012-2419-4, 2013.

Schartau, M. and Oschlies, A.: Simultaneous data-based optimization of a 1D-ecosystem model at three locations in the North Atlantic: Part I - Method and parameter estimates, Journal of Marine Research, 61, 765–793, 2003.

Schaum, C. E. and Collins, S.: Plasticity predicts evolution in a marine alga, Proceedings of the Royal Society B: Biological Sciences, 281, 20141 486, https://doi.org/10.1098/rspb.2014.1486, 2014.

Schouten, S., Hopmans, E. C., and Sinninghe Damsté, J. S.: The organic geochemistry of glycerol dialkyl glycerol tetraether lipids: A review, Organic Geochemistry, 54, 19–61, https://doi.org/10.1016/j.orggeochem.2012.09.006, 2013.

Séférian, R., Bopp, L., Gehlen, M., Swingedouw, D., Mignot, J., Guilyardi, E., and Servonnat, J.: Multiyear predictability of tropical marine productivity, Proceedings of the National Academy of Sciences, 111, 11 646–11 651, https://doi.org/10.1073/pnas.1315855111, 2014.

Séférian, R., Berthet, S., Yool, A., Palmiéri, J., Bopp, L., Tagliabue, A., Kwiatkowski, L., Aumont, O., Christian, J., Dunne, J., Gehlen, M., Ilyina, T., John, J. G., Li, H., Long, M. C., Luo, J. Y., Nakano, H., Romanou, A., Schwinger, J., Stock, C., Santana-Falcón, Y., Takano, Y., Tjiputra, J., Tsujino, H., Watanabe, M., Wu, T., Wu, F., and Yamamoto, A.: Tracking improvement in simulated marine biogeochemistry between CMIP5 and CMIP6, Current Climate Change Reports, 6, 95–119, https://doi.org/10.1007/s40641-020-00160-0, 2020.

Seki, H., Ozawa, H., and Ichimura, S.: Temperature dependence of filament length of *Anabaena spiroides* Klebahn var. *crassa* Lemm., Hydrobiologia, 83, 419–423, https://doi.org/10.1007/BF02187039, 1981.

Simó, R.: Production of atmospheric sulfur by oceanic plankton: Biogeochemical, ecological and evolutionary links, Trends in Ecology & Evolution, 16, 287–294, https://doi.org/10.1016/S0169-5347(01)02152-8, 2001.

Smith, S. L., Vallina, S. M., and Merico, A.: Phytoplankton size-diversity mediates an emergent trade-off in ecosystem functioning for rare versus frequent disturbances, Scientific Reports, 6, 34 170, https://doi.org/10.1038/srep34170, 2016.

Sommer, U., Paul, C., and Moustaka-Gouni, M.: Warming and ocean acidification effects on phytoplankton – From species shifts to size shifts within species in a mesocosm experiment, PLOS ONE, 10, 1–17, https://doi.org/10.1371/journal.pone.0125239, 2015.

Sonntag, S. and Hense, I.: Phytoplankton behavior affects ocean mixed layer dynamics through biological-physical feedback mechanisms, Geophysical Research Letters, 38, 1–6, https://doi.org/10.1029/2011GL048205, 2011.

Spilling, K.: Optimizing lipid production by planktonic algae: LIPIDO, 2011.

Spilling, K., Kremp, A., Klais, R., Olli, K., and Tamminen, T.: Spring bloom community change modifies carbon pathways and C : N : P : Chl a stoichiometry of coastal material fluxes, Biogeosciences, 11, 7275–7289, https://doi.org/10.5194/bg-11-7275-2014, 2014.

Spilling, K., Olli, K., Lehtoranta, J., Kremp, A., Tedesco, L., Tamelander, T., Klais, R., Peltonen, H., and Tamminen, T.: Shifting diatom—dinoflagellate dominance during spring bloom in the Baltic Sea and its potential effects on biogeochemical cycling, Frontiers in Marine Science, 5, 1–17, https://doi.org/10.3389/fmars.2018.00327, 2018.

Stal, L. J., Albertano, P., Bergman, B., Bröckel, K. v., Gallon, J. R., Hayes, P. K., Sivonen, K., and Walsby, A. E.: BASIC: Baltic Sea cyanobacteria. An investigation of the structure and dynamics of water blooms of cyanobacteria in the Baltic Sea—Responses to a changing environment, Continental Shelf Research, 23, 1695–1714, https://doi.org/10.1016/j.csr.2003.06.001, 2003.

Stephens, N., Flynn, K. J., and Gallon, J. R.: Interrelationships between the pathways of inorganic nitrogen assimilation in the cyanobacterium *Gloeothece* can be described using a mechanistic mathematical model, The New Phytologist, 160, 545–555, https://doi.org/10.1046/j.1469-8137.2003.00901.x, 2003.

Stramska, M. and Zuzewicz, A.: Influence of the parametrization of water optical properties on the modelled sea surface temperature in the Baltic Sea, Oceanologia, 55, 53–76, https://doi.org/10.5697/oc.55-1.053, 2013.

Suikkanen, S., Laamanen, M., and Huttunen, M.: Long-term changes in summer phytoplankton communities of the open northern Baltic Sea, Estuarine, Coastal and Shelf Science, 71, 580–592, https://doi.org/10.1016/j.ecss.2006.09.004, 2007.

Sundqvist, L., Godhe, A., Jonsson, P. R., and Sefbom, J.: The anchoring effect—Long-term dormancy and genetic population structure, The ISME Journal, 12, 2929–2941, https://doi.org/10.1038/s41396-018-0216-8, 2018.

Tallberg, P. and Heiskanen, A.-S.: Species-specific phytoplankton sedimentation in relation to primary production along an inshore—offshore gradient in the Baltic Sea, Journal of Plankton Research, 20, 2053–2070, https://doi.org/10.1093/plankt/20.11.2053, 1998.

Tamelander, T., Spilling, K., and Winder, M.: Organic matter export to the seafloor in the Baltic Sea: Drivers of change and future projections, Ambio, 46, 842–851, https://doi.org/10.1007/s13280-017-0930-x, 2017.

Thamm, R., Schernewski, G., Wasmund, N., and Neumann, T.: Spatial phytoplankton pattern in the Baltic Sea, in: Baltic Sea typology, vol. 4 of *Coastline Reports*, pp. 85–109, EUCC-The Coastal Union, 2004.

Toggweiler, J. R., Gnanadesikan, A., Carson, S., Murnane, R., and Sarmiento, J. L.: Representation of the carbon cycle in box models and GCMs: 1. Solubility pump, Global Biogeochemical Cycles, 17, https://doi.org/10.1029/2001GB001401, 2003.

Tonani, M., Balmaseda, M., Bertino, L., Blockley, E., Brassington, G., Davidson, F., Drillet, Y., Hogan, P., Kuragano, T., Lee, T., Mehra, A., Paranathara, F., Tanajura, C. A., and Wang, H.: Status and future of global and regional ocean prediction systems, Journal of Operational Oceanography, 8, s201–s220, https://doi.org/10.1080/1755876X.2015.1049892, 2015.

Tyler, A. L., Asselbergs, F. W., Williams, S. M., and Moore, J. H.: Shadows of complexity: What biological networks reveal about epistasis and pleiotropy, BioEssays, 31, 220–227, https://doi.org/10.1002/bies.200800022, 2009.

Uehlinger, U.: Experimental studies of the autoecology of *Aphanizomenon flos-aquae*, Archiv für Hydrobiologie, 60, 260–288, 1981.

Uffelmann, E., Huang, Q. Q., Munung, N. S., de Vries, J., Okada, Y., Martin, A. R., Martin, H. C., Lappalainen, T., and Posthuma, D.: Genome-wide association studies, Nature Reviews Methods Primers, 1, 1–21, https://doi.org/10.1038/s43586-021-00056-9, 2021.

Vahtera, E., Conley, D. J., Gustafsson, B. G., Kuosa, H., Pitkänen, H., Savchuk, O. P., Tamminen, T., Viitasalo, M., Voss, M., Wasmund, N., and Wulff, F.: Internal ecosystem feedbacks enhance nitrogen-fixing cyanobacteria blooms and complicate management in the Baltic Sea, AMBIO: A Journal of the Human Environment, 36, 186–194, https://doi.org/10.1579/0044-7447(2007)36[186:IEFENC]2.0.CO;2, 2007.

Valente, A., Sathyendranath, S., Brotas, V., Groom, S., Grant, M., Taberner, M., Antoine, D., Arnone, R., Balch, W. M., Barker, K., Barlow, R., Bélanger, S., Berthon, J.-F., Beşiktepe, c., Brando, V., Canuti, E., Chavez, F., Claustre, H., Crout, R., Frouin, R., García-Soto, C., Gibb, S. W., Gould, R., Hooker, S., Kahru, M., Klein, H., Kratzer, S., Loisel, H., McKee, D., Mitchell, B. G., Moisan, T., Muller-Karger, F., O'Dowd, L., Ondrusek, M., Poulton, A. J., Repecaud, M., Smyth, T., Sosik, H. M., Twardowski, M., Voss, K., Werdell, J., Wernand, M., and Zibordi, G.: A compilation of global bio-optical in situ data for ocean-colour satellite applications, Earth System Science Data, 8, 235–252, https://doi.org/10.5194/essd-8-235-2016, 2016.

van Beusekom, J. E. E., Mengedoht, D., Augustin, C. B., Schilling, M., and Boersma, M.: Phytoplankton, protozooplankton and nutrient dynamics in the Bornholm Basin (Baltic Sea) in 2002–2003 during the German GLOBEC Project, International Journal of Earth Sciences, 98, 251–260, https://doi.org/10.1007/s00531-007-0231-x, 2009.

Van Nieuwenhove, N., Head, M. J., Limoges, A., Pospelova, V., Mertens, K. N., Matthiessen, J., De Schepper, S., de Vernal, A., Eynaud, F., Londeix, L., Marret, F., Penaud, A., Radi, T., and Rochon, A.: An overview and brief description of common marine organic-walled dinoflagellate cyst taxa occurring in surface sediments of the Northern Hemisphere, Marine Micropaleontology, 159, 101 814, https://doi.org/10.1016/j.marmicro.2019.101814, 2020.

Vasselon, V., Bouchez, A., Rimet, F., Jacquet, S., Trobajo, R., Corniquel, M., Tapolczai, K., and Domaizon, I.: Avoiding quantification bias in metabarcoding: Application of a cell biovolume correction factor in diatom molecular biomonitoring, Methods in Ecology and Evolution, 9, 1060–1069, https://doi.org/10.1111/2041-210X.12960, 2018.

Vichi, M., Ruardij, P., and Baretta, J. W.: Link or sink: A modelling interpretation of the open Baltic biogeochemistry, Biogeosciences, 1, 79–100, https://doi.org/10.5194/bg-1-79-2004, 2004.

Vincent, W. and Silvester, W.: Growth of blue-green algae in the Manukau (New Zealand) oxidation ponds—I. Growth potential of oxidation pond water and comparative optima for blue-green and green algal growth, Water Research, 13, 711–716, https://doi.org/10.1016/0043-1354(79)90234-3, 1979.

Visscher, P. M., Wray, N. R., Zhang, Q., Sklar, P., McCarthy, M. I., Brown, M. A., and Yang, J.: 10 years of GWAS discovery: Biology, function, and translation, The American Journal of Human Genetics, 101, 5–22, http://dx.doi.org/10.1016/j.ajhg.2017.06.005, 2017.

Wakeham, S. G. and Canuel, E. A.: Degradation and preservation of organic matter in marine sediments, in: Marine organic matter: Biomarkers, isotopes and DNA, edited by Volkman, J. K., pp. 295–321, Springer Berlin Heidelberg, Berlin, Heidelberg, https://doi.org/10.1007/698_2_009, 2006.

Walsby, A. E., Hayes, P. K., and Boje, R.: The gas vesicles, buoyancy and vertical distribution of cyanobacteria in the Baltic Sea, European Journal of Phycology, 30, 87–94, https://doi.org/10.1080/09670269500650851, 1995.

Walworth, N. G., Zakem, E. J., Dunne, J. P., Collins, S., and Levine, N. M.: Microbial evolutionary strategies in a dynamic ocean, Proceedings of the National Academy of Sciences, 117, 5943–5948, https://doi.org/10.1073/pnas.1919332117, 2020.

Ward, B. A., Dutkiewicz, S., Jahn, O., and Follows, M. J.: A size-structured food-web model for the global ocean, Limnology and Oceanography, 57, 1877–1891, https://doi.org/10.4319/lo.2012.57.6.1877, 2012.

Ward, B. A., Marañón, E., Sauterey, B., Rault, J., and Claessen, D.: The size dependence of phytoplankton growth rates: A trade-off between nutrient uptake and metabolism, The American Naturalist, 189, 170–177, https://doi.org/10.1086/689992, 2017.

Ward, B. A., Collins, S., Dutkiewicz, S., Gibbs, S., Bown, P., Ridgwell, A., Sauterey, B., Wilson, J. D., and Oschlies, A.: Considering the role of adaptive evolution in models of the ocean and climate system, Journal of Advances in Modeling Earth Systems, 11, 3343–3361, https://doi.org/10.1029/2018MS001452, 2019.

Warns, A.: Modelling the life cycle of cold-water dinoflagellates and diatoms—Dynamics on seasonal and interannual time scales, Ph.D. thesis, Universität Hamburg, Hamburg, 2013.

Wasmund, N., Voss, M., and Lochte, K.: Evidence of nitrogen fixation by non-heterocystous cyanobacteria in the Baltic Sea and re-calculation of a budget of nitrogen fixation, Marine Ecology Progress Series, 214, 1–14, https://doi.org/10.3354/meps214001, 2001.

Wasmund, N., Nausch, G., Gerth, M., Busch, S., Burmeister, C., Hansen, R., and Sadkowiak, B.: Extension of the growing season of phytoplankton in the western Baltic Sea in response to climate change, Marine Ecology Progress Series, 622, 1–16, https://doi.org/10.3354/meps12994, 2019.

Weatherdon, L. V., Magnan, A. K., Rogers, A. D., Sumaila, U. R., and Cheung, W. W. L.: Observed and projected impacts of climate change on marine fisheries, aquaculture, coastal tourism, and human health: An update, Frontiers in Marine Science, 3, 1–21, https://doi.org/10.3389/fmars.2016.00048, 2016.

Webb, W. L., Newton, M., and Starr, D.: Carbon dioxide exchange of *Alnus rubra*, Oecologia, 17, 281–291, https://doi.org/10.1007/BF00345747, 1974.

Weckström, K.: Assessing recent eutrophication in coastal waters of the Gulf of Finland (Baltic Sea) using subfossil diatoms, Journal of Paleolimnology, 35, 571–592, https://doi.org/10.1007/s10933-005-5264-1, 2006.

Weitz, J. S., Stock, C. A., Wilhelm, S. W., Bourouiba, L., Coleman, M. L., Buchan, A., Follows, M. J., Fuhrman, J. A., Jover, L. F., Lennon, J. T., Middelboe, M., Sonderegger, D. L., Suttle, C. A., Taylor, B. P., Frede Thingstad, T., Wilson, W. H., and Eric Wommack, K.: A multitrophic model to quantify the effects of marine viruses on microbial food webs and ecosystem processes, The ISME Journal, 9, 1352–1364, https://doi.org/10.1038/ismej.2014.220, 2015.

Wersebe, M. J. and Weider, L. J.: Resurrection genomics provides molecular and phenotypic evidence of rapid adaptation to salinization in a keystone aquatic species, Proceedings of the National Academy of Sciences, 120, e2217276 120, https://doi.org/10.1073/pnas.2217276120, 2023.

Willerslev, E., Hansen, A. J., Binladen, J., Brand, T. B., Gilbert, M. T. P., Shapiro, B., Bunce, M., Wiuf, C., Gilichinsky, D. A., and Cooper, A.: Diverse plant and animal genetic records from Holocene and Pleistocene sediments, Science, 300, 791–795, https://doi.org/10.1126/science.1084114, 2003.

Winder, M. and Schindler, D. E.: Climate change uncouples trophic interactions in an aquatic ecosystem, Ecology, 85, 2100–2106, https://doi.org/10.1890/04-0151, 2004a.

Winder, M. and Schindler, D. E.: Climatic effects on the phenology of lake processes, Global Change Biology, 10, 1844–1856, https://doi.org/10.1111/j.1365-2486.2004.00849.x, 2004b.

Winder, M. and Sommer, U.: Phytoplankton response to a changing climate, Hydrobiologia, 698, 5–16, https://doi.org/10.1007/s10750-012-1149-2, 2012.

Wingenter, O. W., Haase, K. B., Zeigler, M., Blake, D. R., Rowland, F. S., Sive, B. C., Paulino, A., Thyrhaug, R., Larsen, A., Schulz, K., Meyerhöfer, M., and Riebesell, U.: Unexpected consequences of increasing CO_2 and ocean acidity on marine production of DMS and CH2ClI: Potential climate impacts, Geophysical Research Letters, 34, 1–5, https://doi.org/10.1029/2006GL028139, 2007.

Wood, S. M., Kremp, A., Savela, H., Akter, S., Vartti, V.-P., Saarni, S., and Suikkanen, S.: Cyanobacterial akinete distribution, viability, and cyanotoxin records in sediment archives from the Northern Baltic Sea, Frontiers in Microbiology, 12, 1–16, https://doi.org/10.3389/fmicb.2021.681881, 2021.

Worden, A. Z., Follows, M. J., Giovannoni, S. J., Wilken, S., Zimmerman, A. E., and Keeling, P. J.: Rethinking the marine carbon cycle: Factoring in the multifarious lifestyles of microbes, Science, 347, 1257 594, https://doi.org/10.1126/science.1257594, 2015.

Yvon-Durocher, G., Allen, A. P., Cellamare, M., Dossena, M., Gaston, K. J., Leitao, M., Montoya, J. M., Reuman, D. C., Woodward, G., and Trimmer, M.: Five years of experimental warming increases the biodiversity and productivity of phytoplankton, PLOS Biology, 13, 1–22, https://doi.org/10.1371/journal.pbio.1002324, 2015.

Zimmermann, H. H., Stoof-Leichsenring, K. R., Dinkel, V., Harms, L., Schulte, L., Hütt, M.-T., Nürnberg, D., Tiedemann, R., and Herzschuh, U.: Marine ecosystem shifts with deglacial sea-ice loss inferred from ancient DNA shotgun sequencing, Nature Communications, 14, 1650, https://doi.org/10.1038/s41467-023-36845-x, 2023.

Zonneveld, K. A. F., Versteegh, G. J. M., Kasten, S., Eglinton, T. I., Emeis, K.-C., Huguet, C., Koch, B. P., de Lange, G. J., de Leeuw, J. W., Middelburg, J. J., Mollenhauer, G., Prahl, F. G., Rethemeyer, J., and Wakeham, S. G.: Selective preservation of organic matter in marine environments; processes and impact on the sedimentary record, Biogeosciences, 7, 483–511, https://doi.org/10.5194/bg-7-483-2010, 2010.

Eidesstattliche Versicherung

Hiermit erkläre ich an Eides statt, dass ich die vorliegende Dissertationsschrift selbst verfasst und keine anderen als die angegebenen Quellen und Hilfsmittel benutzt habe.

I hereby declare upon oath that I have written the present dissertation independently and have not used further resources and aids than those stated.

Hamburg, 03.06.2024